Controlling Selectivity in Cross-Coupling Reactions with Ester Electrophiles

by Jeanne Masson-Makdissi

Thesis Supervisor: Stephen G. Newman

A thesis submitted to the
Faculty of Graduate and Postdoctoral Studies
in partial fulfillment of the requirements for the
Master's degree in Chemistry

Department of Chemistry and Biomolecular Sciences

Faculty of Science

University of Ottawa

Abstract

First popularized in the 1970s, transition metal-catalyzed cross-couplings now constitute staple reactions for the formation of carbon-carbon and carbon-heteroatom bonds. Recent endeavours in the field have been invested towards expanding the range of compatible coupling partners, with the aim of accessing complex molecules from simple, widely available starting materials. Notably, esters represent an attractive class of alternative coupling partners compared to traditional aryl halides, due to their ubiquity and robustness. Moreover, different cleavage modes can be accessed with esters. Which bond cleavage occurs is highly dependent on which catalyst is used, providing an opportunity to quickly access diverse products from a common precursor. Chapter 1 of this thesis provides a literature overview of cross-couplings with carboxylic acid derivatives to contextualize our contributions described in Chapter 2 and 3.

Chapter 2 describes the Pd-catalyzed cross-coupling of phenyl esters with alkyl boranes. Two reaction modes are enabled, namely C(acyl)–O bond activation with carbonyl-retention and C(acyl)–O bond activation with decarbonylation. As such, both alkyl ketones and alkylated arenes are accessed selectively by simple changes in the catalytic system. The disclosed reaction is applied to the diversification of bioactive molecules and discussed in light of recent mechanistic studies of related transformations.

In Chapter 3, the first additive-free Ni-catalyzed amidation and transesterification of methyl esters are disclosed. In both transformations, a simple Ni catalyst enables widely available methyl or ethyl esters to be converted into value-added products, producing methanol as the only stoichiometric waste by-product. The Ni-catalyzed amidation protocol strongly contrasts wasteful yet common methods used to convert methyl esters into amides, involving wasteful hydrolysis and coupling with stoichiometric activating agents.

Acknowledgements

First, I would like to thank my research supervisor Dr. Newman. Steve, thank you for making time whenever I had questions, for always encouraging me to take every opportunity that there was, and for sharing your undeniable passion for chemistry with all of us. I've had a fantastic time working in your lab. I am grateful for everything that you taught me and that you made me achieve.

I cannot fail to mention the former and current members of the Newman lab. My experience here has been all the more enjoyable because of them. Wanying and Kaylie, thank you for mentoring me during my undergraduate studies and for giving a good model on how to complete a successful Master's degree. I am very grateful that we are still in touch to this day. I would also like to thank Taoufik, whom I had the chance to collaborate with on the project described in Chapter 3. Your perseverance and hard work do not go unnoticed. Jay, thanks for helping me out with columns and for sharing your ridiculously spicy (but oh so good) food. See you in Toronto for our next coffee break! Ryan, thanks for being a genius, and for always being willing to help when I need it. Eric "I.", my friend, my unofficial Goldfish provider, I will miss you. I wish you the best of luck for the rest of your Master's - I do not doubt your ability to achieve great things. Saeed, thank you for being a great friend, a good listener, and a surprisingly patient shopping buddy. You truly have a golden heart, and your determination will get you far. Sam, I am so proud of us for keeping up with the gym plan. I wish you the best for your M. Sc. in Chemical Engineering! I've also had a great time mentoring Émile during his Honours project, and I wish him success in his future endeavours. Kendra, I can relate to you in many aspects (especially with your love of cats). I wish you success in your future studies; I'm sure you'll do more than a great job at whatever you decide to do. Lars, my favorite column buddy, I didn't mind sharing a fumehood with you at all! You have such

a positive outlook on life, and your happiness is contagious. Yanlong, thanks for always being so nice, and for introducing me to the good old prep TLC. I wish that I can become as efficient as you in the lab one day! There is also another bunch of awesome people that I met along the way: Imane (thank you for all those funny moments in Summer 2015), Annika, Bharath, Sara, Claudia, Mohanad, Mads, Niraj, Hamdi, Thomas, Jacob, Eric S., Garrett, Omid, and Prakash.

Although they are not in our group, I would also like to thank three other persons that have made several impromptu appearances in our lab: Alexandre Sicard, Alexandra Rochon, and Christopher Godwin. Alex S., thank you for the funny lunch conversations and for sharing your awesome ligands with us. Keep on living the #fancylife. Alexe R., I admire your ability to make time to help others; whether that is helping your mom with her kindergarten class, preparing the "mini-cours", or tutoring (or bringing me Cliff bars from Costco nearly every month!), I honestly don't understand how you manage to do it all. Finally, Chris, I admit it: Yes, I will miss your slightly inappropriate comments, and yes, I do believe that you will be a great teacher one day.

Last, but not least, I cannot thank my family enough. Papa, Myra, I am incredibly grateful for everything that you did (and still do) for me. Thank you for providing me comfort, love, and support through it all. Étienne, Karen, I could not hope for a better brother and sister. And, of course, I cannot forget to thank the star of the house, Betty Shaw.

Table of Contents

List of Tables

List of Figures

List of Schemes

Statement of Contribution

The project described in Chapter 2 was done in collaboration with Dr. Jaya K. Vandavasi. Jaya performed some of the late-stage optimization experiments and helped with the purification and characterization of compounds. This work has been published in a peer-reviewed journal (1).

Chapter 3 regards the Ni-catalyzed coupling of methyl esters. A Ph. D. candidate, Taoufik Ben Halima, optimized the amidation reaction. I contributed to the design and experimentation for the scope and application examples. This work was recently accepted in a peer-reviewed journal (2). A provisional patent related to this work has also been filed (3).

The transesterification project originated from the work described above. Undergraduate student, Émile Pinault-Masson, worked on this as part of his Honours project under my supervision from September 2017 to April 2018. I took over the project in June 2018. All experiments presented herein were designed and performed by me unless otherwise specified.

1) "*Switchable Selectivity in Pd-Catalyzed Alkylative Cross-Couplings of Esters*," Masson-Makdissi, J.; Vandavasi, J. K.; Newman, S. G. *Org. Lett.* **2018**, *20*, 4094–4098.
2) "*Nickel-Catalyzed Amidation of Methyl Esters*," Ben Halima, T.; Masson-Makdissi, J.; Newman, S. G. *Angew. Chem. Int. Ed.* **2018**, *57*, 12925–12929.
3) "*Synthesis of Amides from Esters,"* Newman, S. G.; Ben Halima, T.; Masson-Makdissi, J *US Provisional Patent application*, **2018**, S/N 62/624,286.

Abbreviations

$\Delta G^{\ddagger}$	activation energy
9-BBN	9-borabicyclo(3.3.1)nonane
Ac	acetyl
aq.	aqueous
Ar	aryl
BA	Brönsted acid
BDE	bond dissociation energy
Bn	benzyl
Boc	tert-butyloxycarbonyl
Bu	butyl
calcd	calculated
cat.	catalytic or catalyst
cod	1,5-cyclooctadiene
Cp	cyclopentadienyl
CPME	cyclopentyl methyl ether
CuTC	copper(I) thiophene-2-carboxylate
Cy	cyclohexyl
Cyp	cyclopentyl
d	doublet
dba	dibenzylideneacetone
dcype	1,2-bis(dicyclohexylphosphino)ethane
dcypt	3,4-bis(dicyclohexylphosphino)thiophene
DFT	density functional theory
DMAP	4-dimethylaminopyridine
DMF	dimethylformamide

DMSO	dimethylsulfoxide
dppp	1,3-bis(diphenylphosphino)propane
E or E^+	electrophile
e.e.	enantiomeric excess
e.r.	enantiomeric ratio
EDC	N-(3-dimethylaminopropyl)-N′-ethylcarbodiimide
EDG	electron-donating group
EI	electron impact
equiv	equivalent
ESI	electrospray ionization
Et	ethyl
EWG	electron-withdrawing group
FID	flame ionization detector
g	gram(s)
GC	gas chromatography
h	hour(s)
HATU	hexafluorophosphate azabenzotriazole tetramethyl uranium
HRMS	high resolution mass spectrometry
HTPS	high throughput screening
Hz	hertz
i	iso
ICy	1,3-bis(1-adamantyl)imidazol-2-ylidene
IMes	1,3-bis(2,4,6-trimethylphenyl)imidazol-2-ylidene
IPent	1,3-bis(2,6-di-3-pentylphenyl)imidazol-2-ylidene
^{i}Pr or *i*-Pr	iso-propyl
IPr	1,3-bis(2,4,6-trimethylphenyl)-1,3-dihydro-2H-imidazol-2-ylidene
IR	infrared

J	coupling constant
L	generic ligand
LA	Lewis acid
LED	light emitting diode
LHMDS	lithium bis(trimethylsilyl)amide
M	generic metal, or molecular ion, or molar
m	meta or multiplet
m/z	mass over charge
mCPBA	meta-chloroperbenzoic acid
Me	methyl
mg	milligram(s)
min	minute(s)
mL	milliliter(s)
mol	mole(s)
mp	melting point
MS	mass spectrometry
nep	neopentyl glycolato
NHC	N-heterocyclic carbene
NMP	1-methyl-2-pyrrolidone
NMR	nuclear magnetic resonance
Nu	nucleophile
o	ortho
p	para
Pent	pentyl
Ph	phenyl
phen	phenanthroline
pin	pinacolato

PMHS	poly(methylhydrosiloxane)
ppm	parts per million
q	quartet
Q-TOF	quadrupole time of flight
quin	quintet
R	generic chemical group
r. t.	room temperature
SIMes	1,3-Bis(2,4,6-trimethylphenyl)-4,5-dihydroimidazolidene
SIPr	1,3-bis(2,6-diisopropylphenyl)-4,5-dihydroimidazolidene
S_NAr	nucleophilic aromatic substitution
t	triplet
T. or temp.	temperature
TBS	tert-butyldimethylsilyl
^{t}Bu or *t*-Bu	tert-butyl
THF	tetrahydrofuran
TLC	thin layer chromatography
TMS	trimethylsilyl
Ts	tosyl
UV	ultraviolet
X	generic halogen/heteroatom
Y	generic halogen/heteroatom

Chapter 1. Cross-Couplings of Esters: An Introduction

1.1. Transition metal-catalyzed cross-coupling reactions[1]

The synthesis of pharmaceuticals, agrochemicals, and many other routinely used compounds rely on the formation of carbon-carbon or carbon-heteroatom bonds. Despite the exhaustive list of existing chemical reactions that can form these bonds, there is still much room for improvement. More specifically, with current environmental concerns, chemists are seeking to develop reactions that utilize simple, abundant starting materials, ideally obtainable from renewable resources, while minimizing waste production. The development of new and improved transition metal-catalyzed processes, as opposed to those relying on activation with stoichiometric agents, represents a promising way to achieve these goals.

1.1.1. Cross-coupling reactions: General information

Before the widespread use of cross-coupling reactions, functionalization of aromatic rings was severely limited in comparison to what is now accessible via transition metal catalysis. Traditional synthetic methods rely primarily on electrophilic aromatic substitutions and nucleophilic aromatic substitutions. Both methods have significant scope limitations. In an electrophilic aromatic substitution reaction (Scheme 1), the aromatic ring plays the role of the nucleophile. Since arenes are poor nucleophiles, the electrophile scope is limited to highly electrophilic species such as carbocations (Friedel-Crafts acylation or alkylation) or heteroatom-based cation (nitronium, or halonium).

[1] Hartwig, J. F. (2010) *Organotransition Metal Chemistry: From Bonding to Catalysis*. Mill Valley, California: University Science Books.

Scheme 1. Electrophilic aromatic substitution

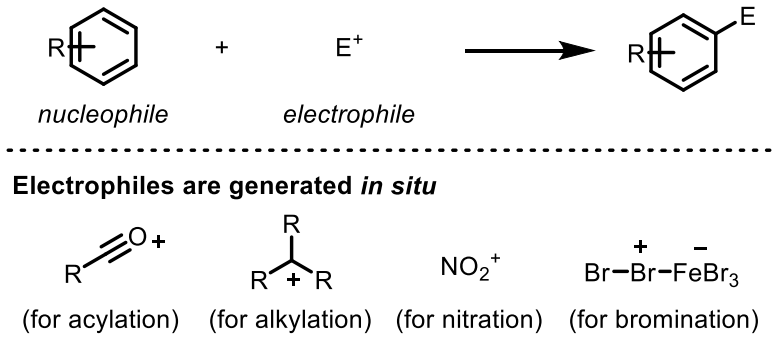

In nucleophilic aromatic substitutions (S_NAr), the aromatic ring takes on the role of the electrophile. Consequently, the aromatic ring typically requires the presence of an electron-withdrawing group. This method also has a narrow range of compatible nucleophiles and is mostly limited to the formation of carbon-heteroatom bonds.

By contrast, cross-coupling reactions were able to significantly broaden the reaction scope because they operate via a distinct mechanism that does not require the use of activated arenes. Transition metal catalysts can enable breakage of a C(sp^2)–X bond without interfering with the aromaticity of the ring via oxidative addition. A simplified mechanism for a general Pd-catalyzed cross-coupling reaction is provided in Scheme 2. A cross-coupling reaction usually consists of three main elementary steps. The first step is the oxidative addition of a low-valent metal such as $L_nPd(0)$ into the C–X bond. Then, Pd intermediate **1.2** can undergo transmetalation with a given organometallic reagent R'MX. Lastly, reductive elimination of Pd intermediate **1.3** occurs to provide the final product R–R' and regenerate Pd(0).

Scheme 2. Mechanism of a general cross-coupling reaction

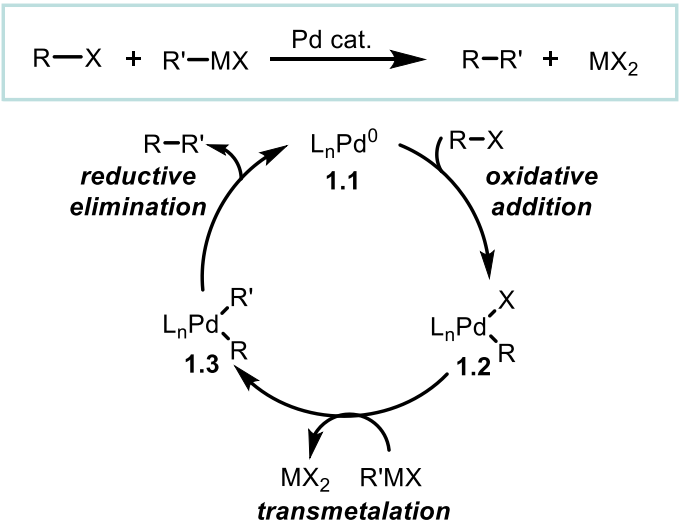

In homogeneous catalysis, ligands (L) are utilized to solubilize the metal catalyst species and to modify the electronic properties of the catalyst, and they play a crucial role in enabling discrete reactivities. Ligands have an immediate influence on the reaction efficiency and are, consequently, one of the primary variables that chemists screen when developing new catalytic reactions. Accordingly, a good understanding of how ligands can affect each elementary step of a cross-coupling reaction is important.

Oxidative addition

In this step, a transition metal catalyst inserts itself into a C–X bond, and its oxidation state increases by 2. Since oxidative addition involves oxidation of the metal, this step is favoured by electron-rich metal centers. The electron-donating properties of the metal catalyst are mostly dictated by the following factors: the nature of the metal, the oxidation state of the metal and the nature of the bound ligands. Oxidative addition is usually more facile with less electronegative transition metals; accordingly, Ni(0) tends to be better at oxidative addition than Pd(0).[2] Oxidative addition is also favoured with low-valent

[2] (a) Tasker, S. Z.; Standley, E. A.; Jamison, T. F. *Nature* **2014**, *509*, 299–309; (b)

transition metals. For instance, oxidative addition with Pd(0) usually occurs readily, but not with Pd(II) as this would result in the formation of a highly oxidized Pd(IV) species.[3] Last, but not least, the ligands can also tune the electron-donating properties of the metal.[4] Electron-rich ligands, such as alkylphosphines or N-heterocyclic carbenes (NHC),[5] are strong σ-donors and thus facilitate the oxidative addition step (Figure 1). The steric properties of ligands also greatly affect the rate of oxidative addition. Oxidative addition is more facile with less hindered metal centers. As such, less sterically hindered ligands are good. However, highly hindered ligands can favour ligand dissociation, and the resulting monoligated metal species is better at oxidative addition.[6]

Figure 1. N-heterocyclic carbenes and alkyl phosphines

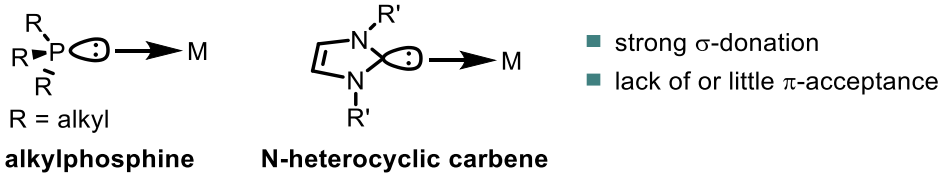

Another factor that inherently affects the rate of oxidative addition is the nature of the bond that is to be broken. The stronger the bond, the slower the oxidative addition. For aryl halides, the trend for the rate of oxidative addition is as follows: Ar–I > Ar–Br > Ar–Cl. To this trend, we can add less traditional coupling partners that will be central to the projects described in Chapter 2 & 3 of this thesis (Figure 2). Oxidative addition into the C(acyl)–O bond of these esters is even more challenging.

---

[3] Oxidative addition of Pd(II) to Pd(IV) is generally unfavourable but possible in some cases, such as the Catellani reaction. For a review of the latter reaction, see: Della Cá, N.; Fontana, M.; Motti, E.; Catellani, M. *Acc. Chem. Res.* **2016**, *49*, 1389−1400.

[4] Clarke, M. L.; Frew, J. J. R. *Organomet. Chem.* **2009**, *35*, 19–46.

[5] (a) Fortman, G. C.; Nolan, S. P. *Chem. Soc. Rev.* **2011**, *40*, 5151-5169; (b)

[6] (a) Christmann, U.; Vilar, R. *Angew. Chem. Int. Ed.* **2005**, *44*, 366–374; (b) Fleckenstein, C. A.; Plenio, H. *Chem. Soc. Rev.* **2010**, *39*, 694–711.

Figure 2. Oxidative addition rates based on nature of the C–Y bond

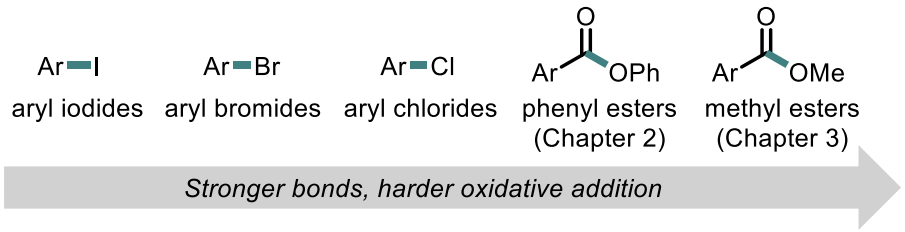

Transmetalation or ligand exchange

Transmetalation is the step where the transition metal exchanges one of its X ligand for an R′ group of an organometallic reagent R′MX. Many organometallic reagents of varying mildness can be employed. Grignard reagents were the first organometallic reagents to be used in a cross-coupling reaction (Kumada-Corriu cross-coupling).[7] The reaction scope is limited when using Grignard reagents though due to the low functional group tolerance arising from the high reactivity of those nucleophiles. The chemoselectivity issues associated with the Kumada-Corriu coupling drove chemists to develop new cross-coupling reactions involving milder nucleophilic coupling partners (Scheme 3). Notably, the use of the following nucleophiles of increased mildness was enabled: organozinc species (Negishi cross-coupling),[8] organostannanes (Stille cross-coupling),[9] organoboron reagents (Suzuki-Miyaura cross-coupling)[10] and organosilicon compounds (Hiyama cross-coupling).[11] Both organoboron and organosilicon compounds are very mild coupling partners that generally need to be activated *in situ* via the use of base/water or fluoride sources.

[7] Tamao, K.; Sumitani, K.; Kumada, M. *J. Am. Chem. Soc.* **1972**, *94*, 4374–4376; (b) Corriu, R. J. P.; Masse, J. P. *J. Chem. Soc., Chem. Comm.* **1972**, 144a.
[8] Negishi, E. -I.; King, A. O.; Okukado, N. *J. Org. Chem.* **1977**, *42*, 1821–1823.
[9] Milstein, D.; Stille, J. K. *J. Am. Chem. Soc.* **1978**, *100*, 3636-3638.
[10] Miyaura, N.; Yamada, K.; Suzuki, A. *Tetrahedron Lett.* **1979**, *20*, 3437-3440.
[11] Hatanaka, Y.; Hiyama, T. *J. Org. Chem.* **1988**, *53*, 918–920.

Scheme 3. Evolution of the nucleophilic coupling partner in cross-couplings

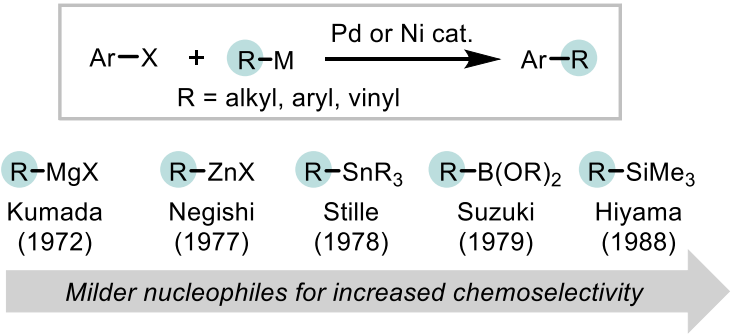

From the cross-couplings shown above (Scheme 3), the Suzuki-Miyaura cross-coupling is probably the one that has had the greatest impact on modern synthetic chemistry. For instance, it is used industrially for the multi-ton synthesis of precursors of Valsartan (a drug used to lower blood pressure) and Boscalid (fungicide from BASF), namely 2-cyano-4′-methylbiphenyl **1.6** and 4-chloro-2′-nitrobiphenyl **1.9**, respectively (Scheme 4).[12]

It is important to note that other nucleophiles than organometallic reagents can be used in cross-coupling reactions. In these cases, 'transmetalation' would not be the correct term. For examples, alkenes (Mizoroki-Heck coupling)[13] undergo an *insertion* step instead of *transmetalation*. Moreover, cross-coupling reactions are not limited to C–C bond formation. For example, amines can be used (Buchwald-Hartwig amination);[14] these undergo *ligand exchange*. Other types of cross-couplings involving carbon-heteroatom

[12] Calderazzo, F.; Catellani, M.; Chiusoli, G. P. "Carbon-Carbon Bond Formation." *Metal-catalysis in Industrial Organic Processes.* Chiusoli, G. P.; Maitlis, P. M. Cambridge: *The Royal Society of Chemistry*, 2006. 163–200.
[13] (a) Heck, R. F.; Nolley, J. P. *J. Org. Chem.* **1972**, *37*, 2320–2322; (b) Mizoroki, T.; Mori, K.; Ozaki, A. *Bull. Chem. Soc. Jap.* **1971**, *44*, 581.
[14] Ruiz-Castillo, P.; Buchwald, S. L. *Chem. Rev.* **2016**, *116*, 12564–12649.

bond formation include phosphorylation (Hirao cross-coupling),[15] borylation (Miyaura borylation),[16] silylation,[17] and etherification[18] processes.

Scheme 4. Industrial applications of the Suzuki-Miyaura cross-coupling

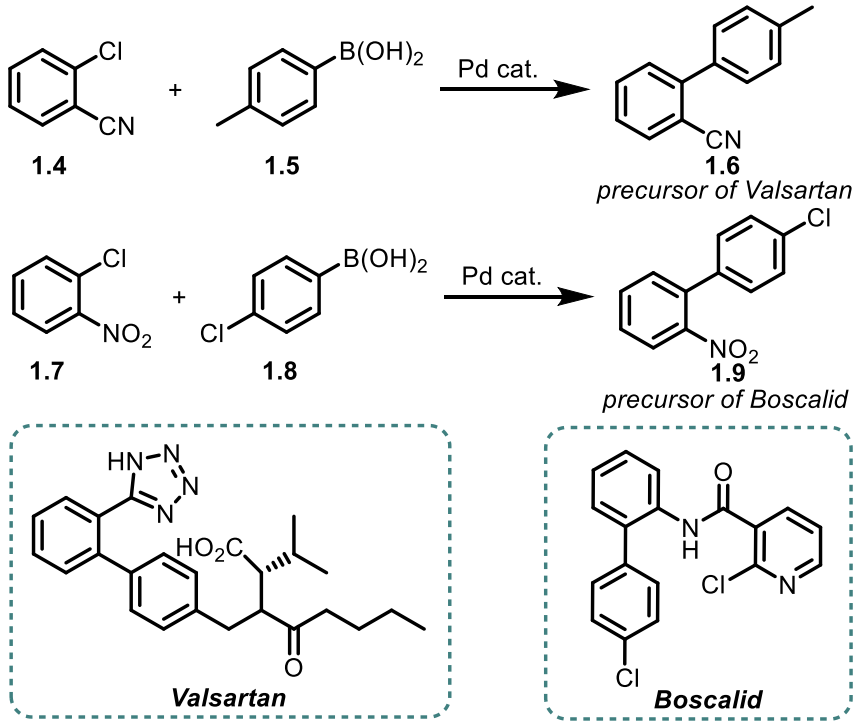

Reductive elimination

Reductive elimination is the microscopic reverse of oxidative addition. Upon reductive elimination, the oxidation state of the metal goes down by 2. Electron-poor metals thus facilitate it. More electronegative transition metals (e.g. Pd over Ni) and the use of electron-deficient ligands can accelerate this step.[19]

[15] Hirao, T.; Masunaga, T.; Ohshiro, Y.; Agawa, T. *Synthesis* **1981**, *1981*, 56–57.
[16] Ishiyama, T.; Murata, M.; Miyaura, N. *J. Org. Chem.* **1995**, *60*, 7508–7510.
[17] Matsumoto, H.; Nagashima, S.; Yoshihiro, K.; Nagai, Y. *J. Organomet. Chem.* **1975**, *85*, C1–C3.
[18] Burgos, C. H.; Barder, T. E.; Huang, X.; Buchwald, S. L. *Angew. Chem. Int. Ed.* **2006**, *45*, 4321–4326.
[19] Korenaga, T.; Abe, K.; Ko, A.; Maenishi, R.; Sakai, T. *Organometallics* **2010**, *29*, 4025–4035.

Reductive elimination requires the two bonds to be *cis* to each other for the metal to reductively eliminate the desired product.[20] *Trans* metal species thus need to undergo *trans*-to-*cis* isomerization before reductive elimination. On the other hand, bidentate phosphine ligands force a *cis* configuration, and therefore, no *trans*-to-*cis* isomerization is required. Moreover, as a rule of thumb, the larger the bite angle, the faster the reductive elimination.[21]

Scheme 5. Trans-to-cis isomerization before reductive elimination

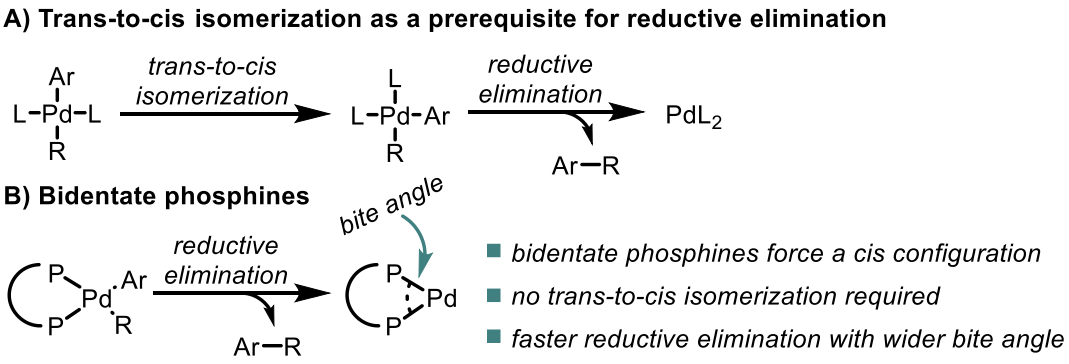

1.1.2. Expanding the electrophile scope

In a traditional cross-coupling reaction, an organohalide is used as the electrophilic partner. However, in recent years, the scope of electrophiles has greatly expanded beyond organohalides. One of the goals of expanding the electrophile scope in cross-coupling reactions is to overcome the problem of chemical accessibility. Too often, reaction routes are opted out solely because the starting materials are not available or too elaborate/expensive to synthesize. Because there is not a single ideal universal electrophile, enlarging the range of viable substrates that can be utilized in cross-couplings is truly the key to solving the problem.

[20]Gillie, A.; Stille, J. K. *J. Am. Chem. Soc.* **1980**, *102*, 4933-4941.
[21] Brown, J. M.; Guiry, P. J. *Inorg. Chim. Acta* **1994**, *220*, 249–259.

During the expansion of the nucleophile scope in cross-coupling reactions, a shift towards milder coupling partners was observed. Similarly, academic chemists are now emphasizing research efforts towards activation of more and more robust substrates for the electrophile scope. This becomes particularly valuable when the synthesis of complex molecules is sought, wherein activation of a robust functionality can be used for late-stage functionalization (Scheme 6). Ideally, the C–Y bond will be inert towards the reagents used in the early steps of multi-step synthesis, and it can then be cleaved towards the end of the multi-step synthesis via a reaction with an appropriate catalyst. By contrast, many methods for late-stage functionalization rely on protection/deprotection sequences, which have poorer atom- and step-economy.

Scheme 6. Catalysis in late-stage functionalization

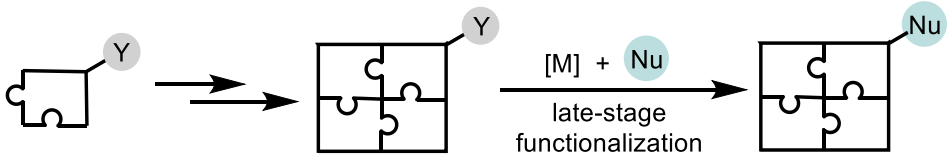

Some examples of typically inert functionalities that can be cleaved via catalysis are provided in Figure 3. For example, aryl fluorides[22] and anisole derivatives[23] have been successfully activated. The cross-coupling of robust carboxylic acid derivatives like esters and amides has also been enabled.[24]

[22] Amii, H.; Uneyama, K. *Chem. Rev.* **2009**, *109*, 2119–2183.
[23] Tobisu, M.; Chatani, N. *Acc. Chem. Res.* **2015**, *48*, 1717–1726.
[24] For recent reviews, see: (a) Takise, R.; Muto, K.; Yamaguchi, J. *Chem. Soc. Rev.* **2017**, *46*, 5864–5888; (b) Guo, L.; Rueping, M. *Acc. Chem. Res.* **2018**, *51*, 1185–1195.

Figure 3. Robust functionalities that can be activated via transition metal catalysis

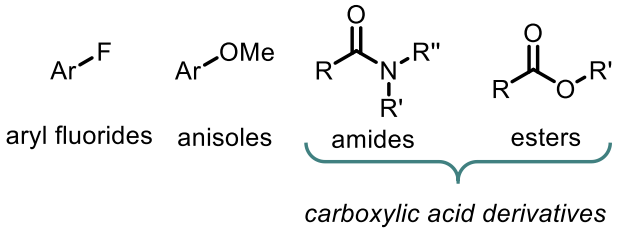

Our group and many others have become interested in utilizing carboxylic acid derivatives as coupling partners. The use of the latter substrates is desirable in many aspects. They are widely abundant and are thus generally quite cheap. Most interestingly, two types of cross-coupling adduct can be obtained with these substrates as outlined in Scheme 7. Both carbonyl-containing adducts (type A) and decarbonylated products (type B) can be obtained. Which type of products forms depends on the catalyst system used.

Scheme 7. Product types in cross-couplings of carboxylic acid derivatives

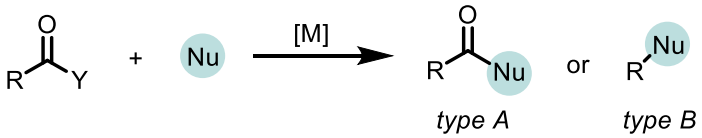

1.2. Cross-coupling reactions of carboxylic acid derivatives

1.2.1. Availability of carboxylic acids and derivatives thereof

Regarding substrate availability, carboxylic acid derivatives are not necessarily better nor worse than the traditional aryl halide coupling partners, but they are highly complementary. One aspect where the advantage of using carboxylic acid derivatives becomes evident is when dealing with heteroaryl substrates. A lot of heteroaryl carboxylic acids—especially esters—are widely available because malonates and their derivatives are often used in heterocycle synthesis. Scheme 8 provides two examples of such heterocyclization.

Scheme 8. Heterocycle synthesis using malonate derivatives

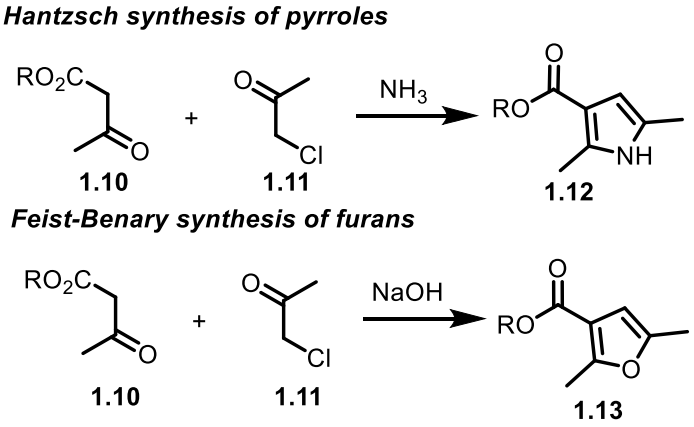

By contrast, the availability of heteroaryl halides is a bit more restrained due to polyhalogenation and regioselectivity issues arising during their synthesis; for instance, the halogenation of nitrogen-bearing 6-membered heteroaromatic compounds (e.g. pyridine) is particularly difficult. Given the relevance of heterocycles in the pharmaceutical industry, developing cross-couplings using readily available heteroaromatic carboxylates constitutes an important goal.

1.2.2. Cross-coupling reactions of activated carboxylic acid derivatives

During the evolution of the nucleophilic coupling partner, a shift towards less reactive organometallic reagents was observed (from Grignard reagents to organoboron reagents). Similarly, throughout the years, the activation of more and more robust carboxylic acid derivatives was introduced for the electrophile scope. This section will cover cross-couplings of acyl chlorides, acid anhydrides, twisted amides, thioesters, and activated esters. Then, section 1.2.3 will focus on cross-couplings of aryl esters.

Acyl chlorides

In 1978, Stille disclosed one of the earliest examples of cross-couplings with a carboxylic acid derivative, by successfully coupling acyl chlorides with organotin reagents to form ketones via Pd catalysis (Scheme 9).[25]

Scheme 9. Stille coupling of acyl chlorides

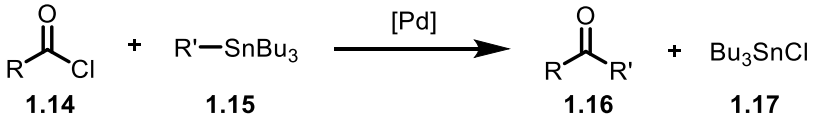

Notwithstanding the importance of this coupling reaction, acyl chlorides represent a strongly activated class of carboxylic acid derivatives. These are known to react with Grignard reagents in the absence of any transition metal catalyst, where over-addition can be controlled via the use of chelating agents (Scheme 10).[26] The chelating agent **1.20** also decreases the reactivity of the Grignard reagent, resulting in enhanced functional group tolerance.

Scheme 10. Transition metal-free chemoselective coupling of acyl chlorides with Grignard reagents

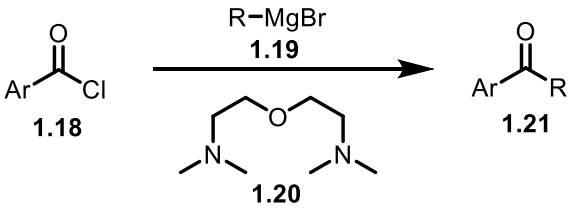

[25] The first cross-coupling of organotin compounds with aryl halides was disclosed by Migita. Stille later developed the acyl chloride variant: (a) Kosugi, M. Sasazawa, K.; Shimizu, Y.; Migita, T. *Chem. Lett.* **1977**, 301; (b) Milstein, D.; Stille, J. K. *J. Am. Chem. Soc.* **1978**, *100*, 3636–3638.

[26] Wang, X.-j.; Zhang, L.; Sun, X.; Xu, Y.; Krishnamurthy, D.; Senanayake, C. H. *Org. Lett.* **2005**, *7*, 5593–5595.

Acid anhydrides

Acid anhydrides, while more robust than acyl chlorides, are also a reactive class of carboxylic acid derivatives. The first report utilizing acid anhydrides as cross-coupling partners was disclosed in 1998 by the group of de Vries (Scheme 11).[27] Therein, a Pd-catalyzed decarbonylative Heck-type cross-coupling reaction of acid anhydrides is described. Remarkably, very low catalyst loadings could be used.

Scheme 11. Pd-catalyzed decarbonylative Heck-type coupling of acid anhydrides

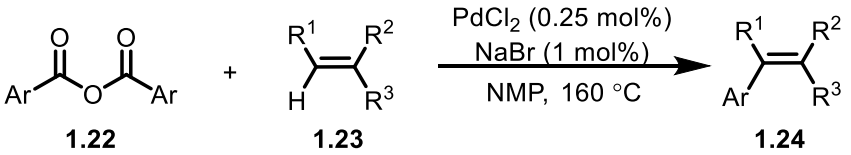

The Gooβen lab later disclosed a Pd-catalyzed Suzuki-Miyaura decarbonylative couplings of acid anhydrides (Scheme 12A).[28] They also extended it to the coupling of the free carboxylic acids, which can be converted to acid anhydrides *in situ* with the use of stoichiometric pivalic anhydride (Scheme 12B).

Scheme 12. Suzuki-Miyaura couplings of acid anhydrides

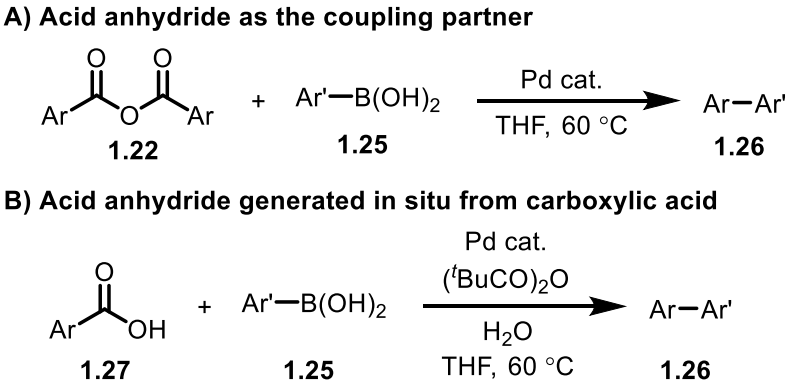

[27] Stephan, M. S.; Teunissen, A. J. J. M.; Verzijl, G. K. M.; de Vries, J. G. *Angew. Chem. Int. Ed.* **1998**, *37*, 662–664.

[28] Gooβen, L. J.; Ghosh, K. *Angew. Chem. Int. Ed.* **2001**, *40*, 3458–3460.

Other notable contributions of cross-couplings with acid anhydrides have been made.[29] As has been mentioned previously, acid anhydrides are quite reactive; thus, they are not amenable to late-stage functionalization. Moreover, using acid anhydrides is poorly atom-economical since there are formally two equivalents of the aryl group in the anhydride, yet only one gets transferred.

Twisted amides

Amides are generally perceived as very stable moieties. The lone pair of nitrogen can be easily delocalized through resonance (Figure 4); with increased double bond character, the C–N becomes harder to break. In reality, the stability of an amide is highly dependent on the nature of the N-substituents. Any substituent that will reduce the resonance will significantly decrease the stability of the amide.

Figure 4. Resonance structure of amides

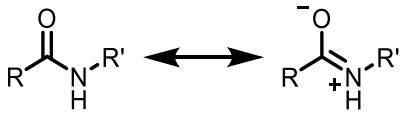

The principle of amide bond destabilization can be exploited to facilitate oxidative addition of the metal into the C–N bond. These destabilized or so-called twisted amides have largely dominated the field of C–N bond activation of amides. Three examples of such amides are outlined in Figure 5.

[29] (a) Jin, W.; Yu, Z.; He W.; Ye, W.; Xiao, W.-J. *Org. Lett.* **2009**, *11*, 1317–1320; (b) Chen, Q.; Fan, X.-H.; Zhangab, L.-P.; Yang, L.-M. *RSC Adv.* **2014**, *4*, 53885–53890; (c) O'Brien, E. M.; Bercot, E. A.; Rovis, T. *J. Am. Chem. Soc*. **2003**, *125*, 10498–10499.

Figure 5. Destabilized amides used in cross-couplings[30]

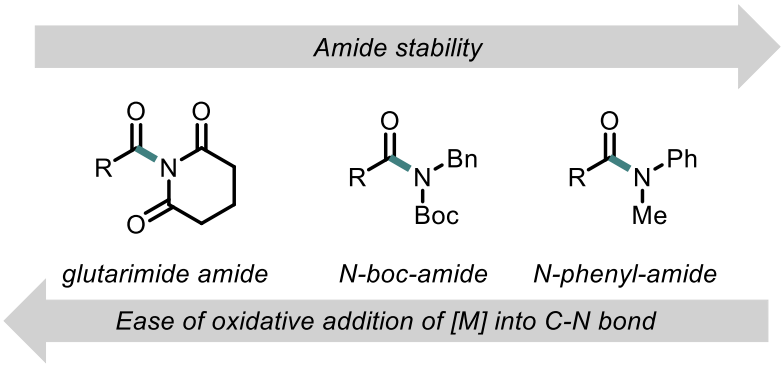

Glutarimide amides are quite peculiar amides. In fact, in their preferred conformation, the glutarimide ring lies almost perpendicular to the acyclic amide functionality. Consequently, the lone pair on the nitrogen atom is not properly aligned for conjugation with the carbonyl π system, and thus there is little to no resonance stabilization. Moreover, these amides are highly electron deficient. For these reasons, glutarimide amides are significantly easier to cleave by transition metal catalysis relative to other amides.

The Szostak lab reported the first cross-coupling reaction using glutarimide amides as coupling partners in 2015.[31] They disclosed that glutarimide amides could be coupled with boronic acids via Pd-catalysis to afford aryl ketones (Scheme 13). Their protocol required stoichiometric boric acid, but they later demonstrated that the use of Pd(IPr)(cinnamyl)Cl catalyst enabled efficient couplings in the absence of boric acid.[32] Following the seminal report by the Szostak lab, a versatile range of coupling reactions with glutarimide amides have been disclosed.[33]

[30] Stability trends as reported in: Ji, C.-L.; Hong, X. *J. Am. Chem. Soc*. **2017**, *139*, 15522−15529.
[31] Meng, G.; Szostak, M. *Org. Lett.* **2015**, *17*, 4364−4367.
[32] Lei, P.; Meng, G.; Szostak, M. *ACS Catal.* **2017**, *7*, 1960–1965.
[33] For a recent review, see: Meng, G.; Szostak, M. *Eur. J. Org. Chem.* **2018**, 2352–2365.

Scheme 13. Pd-catalyzed Suzuki-Miyaura cross-couplings of glutarimide amides

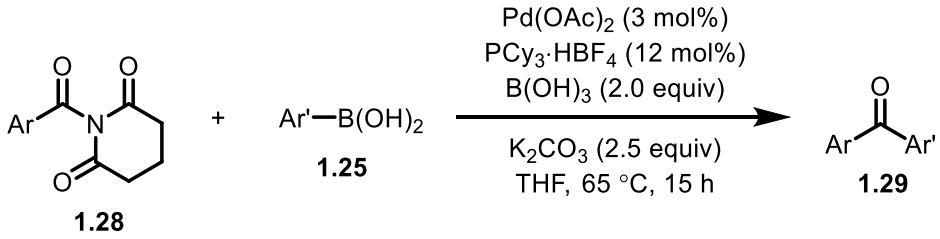

N-Boc- and N-tosyl-amides have also been used as coupling partners in cross-coupling reactions, primarily by the Garg group.[34] Although these types of substrates are considerably less activated than the glutarimide amides, they are also reactive towards transition metals for the same reason: electron-deficiency and disruption of the amide resonance. Notably, the coupling of even less activated amides (**1.30**) with alcohols has been enabled by the Garg lab (Scheme 14).[35]

Scheme 14. Ni-catalyzed esterification of N-phenyl amides

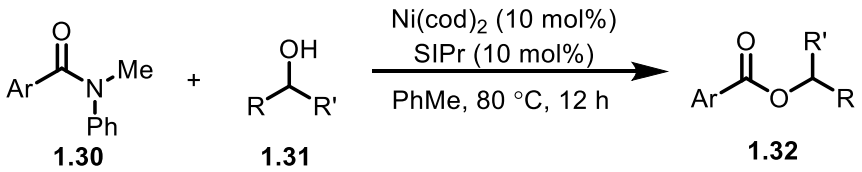

Activated esters

Esters have also been used in cross-coupling reactions, although initial reports were using significantly activated ester substrates.

[34] (a) Weires, N. A.; Baker, E. L.; Garg, N. K. *Nat. Chem.* **2016**, *8*, 75–79; (b) Simmons, B. J.; Weires, N. A.; Dander, J. E.; Garg, N. K. *ACS Catal.* **2016**, *6*, 3176–3179; (c) Medina, J. M.; Moreno, J.; Racine, S.; Du, S.; Garg, N. K. *Angew. Chem. Int. Ed.* **2017**, *56*, 6567–6571; (d) Hie, L.; Baker, E. L.; Anthony, S. M.; Desrosiers, J.-N.; Senanayake, C.; Garg, N. K. *Angew. Chem. Int. Ed.* **2016**, *55*, 15129–15132; (e) Dander, J. E.; Baker, E. L.; Garg, N. K. *Chem. Sci.* **2017**, *8*, 6433–6438; (f) Boit, T. B.; Weires, N. A.; Kim, J.; Garg, N. K. *ACS Catal.* **2018**, *8*, 1003−1008.

[35] (a) Hie, L.; Fine Nathel, N. F.; Shah, T. K.; Baker, E. L.; Hong, X.; Yang, Y.-F.; Liu, P.; Houk, K. N.; Garg, N. K. *Nature* **2015**, *524*, 79–83; (b) Dander, J. E.; Weires, N. A.; Garg, N. K. *Org. Lett.* **2016**, *18*, 3934–3936.

In 2002, Gooβen reported the Pd-catalyzed Mizoroki-Heck coupling of para-nitrophenyl esters **1.33** (Scheme 15).[36]

Scheme 15. Mizoroki-Heck cross-coupling of p-nitrophenyl esters

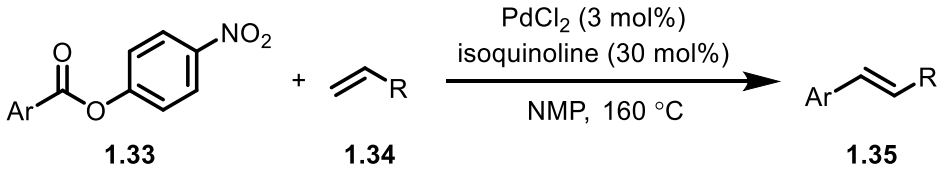

1.33 **1.34** **1.35**

In 2004, Chatani disclosed a Suzuki-Miyaura type coupling of 2-pyridyl ester **1.29** to yield diaryl ketones (Scheme 16).[37] The coordination of the nitrogen atom of the pyridine ring to the metal center was found to be critical for the reaction efficiency.

Scheme 16. Suzuki-Miyaura cross-coupling of 2-pyridyl esters

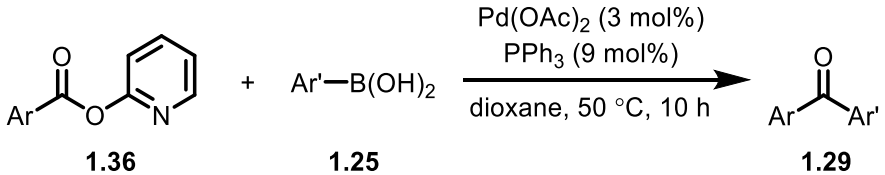

1.36 **1.25** **1.29**

Both Gooβen's and Chatani's reports utilize electron-deficient aryl esters, which drastically facilitates the oxidative addition step as compared to the use of simple phenyl esters. Gooβen has also disclosed a decarbonylative Mizoroki-Heck protocol for the coupling of enol esters **1.37** (Scheme 17).[38] In this case, the leaving group is an enol that can then tautomerize to a stable ketone.

[36] Paetzold, J.; Gooßen, L. J. *Angew. Chem. Int. Ed.* **2002**, *41*, 1237–1241.
[37] Tatamidani, H.; Kakiuchi, F.; Chatani, N. *Org. Lett.* **2004**, *6*, 3597–3599.
[38] Paetzold, J.; Gooßen, L. J. *Angew. Chem. Int. Ed.* **2004**, *43*, 1095 –1095.

Scheme 17. Mizoroki-Heck coupling of enol esters

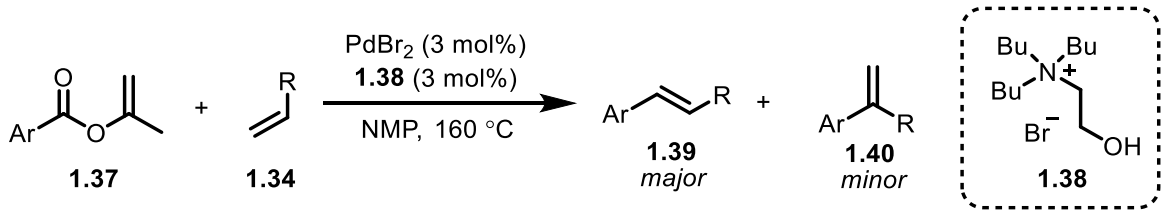

Thioesters

In 1998, Fukuyama et al. developed a cross-coupling method to couple thioesters with organozinc compounds (Scheme 18A).[39] In 2000, Liebeskind and Srogl disclosed a Suzuki-Miyaura variant (Scheme 18B).[40] Palladium catalyzes this reaction, and the CuTC is proposed to mediate the transmetalation step.

Scheme 18. Cross-couplings of thioesters

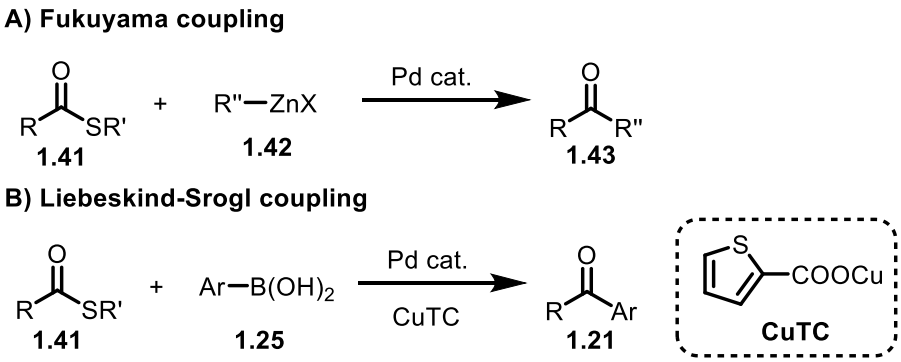

Thioesters are quite robust compounds; yet, they are more reactive than the corresponding ester substrates. This can be explained by the larger atomic radius of sulfur compared to that of oxygen. Because of this, the sulfur atom can better stabilize a negative charge, making thiols better leaving groups than alcohols. Moreover, the larger atomic

[39] Tokuyama, H.; Yokoshima, S.; Yamashita, T.; Lin, S.-C.; Li, L.; Fukuyama, T. *J. Braz. Chem. Soc.* **1998**, *9*, 381–387.

[40] Liebeskind, L. S.; Srogl, J. *J. Am. Chem. Soc.* **2000**, *122*, 11260–11261.

radius of sulfur makes C(acyl)–S bonds inherently longer (and weaker) then C(acyl)–O bonds, facilitating oxidative addition.

1.2.3. Cross-coupling of aryl esters

In contrast to the activated esters mentioned in the above section, unactivated aryl esters such as aryl pivalates and phenyl esters represent more challenging substrates to couple via transition metal catalysis. Wanying Zhang, a former M. Sc. candidate in our group, performed decomposition studies to predict the robustness of phenyl esters as opposed to other activated carboxylic acid derivatives.[41] The extrapolated trend is illustrated in Scheme 19. The increased robustness of phenyl esters makes them attractive coupling partners that could find potential applications in the synthesis of complex molecules.

Scheme 19. Robustness of phenyl esters compared to other carboxylic acid derivatives

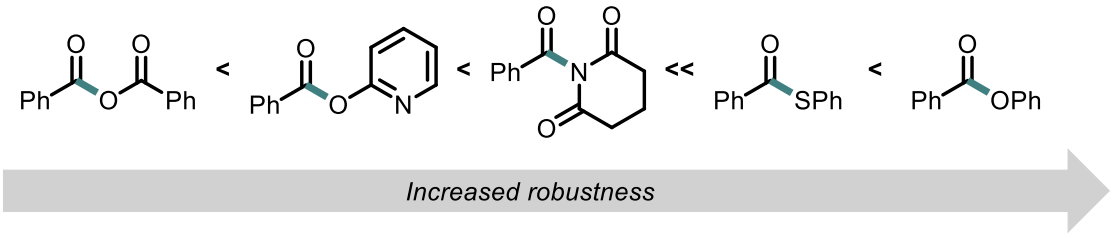

Moreover, different cleavage modes are accessible with aryl esters (Scheme 20). As with other carboxylic acid derivatives, C(acyl)–O bond activation can occur, either with retention of the carbonyl moiety (path a) or with decarbonylation (path b). Alternatively, activation of the stronger C(aryl)–O bond can also be a proficient pathway (path c).

[41] The carboxylic acids were subjected to both methanolysis and amidation. The recovery of the starting material was tracked over time. These results have been published in the following report:

Scheme 20. Different cleavage modes of aryl esters

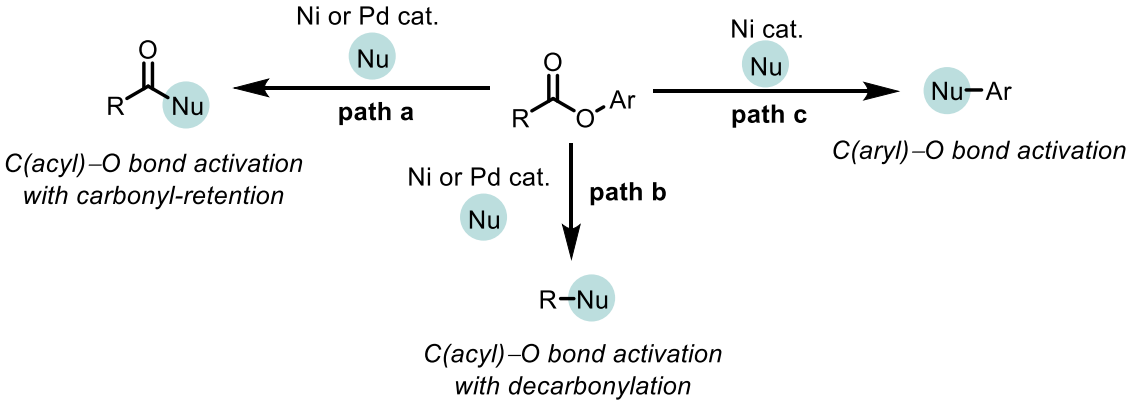

Aryl pivalates

Aryl pivalates are a unique class of esters because they typically undergo cleavage of the robust C(aryl)–O bond as opposed to the weaker C(acyl)–O bond (Scheme 21). This is in no small part due to the steric bulk of the *tert*-butyl functionality; this will be explained in more details in section 1.3. Aryl pivalates thus tend to be cleaved in the same way that aryl sulfonates do; both substrates are phenol derivatives that can be utilized as efficient cross-coupling partners. Aryl pivalates offer the added benefit of being less prone to hydrolysis.

Scheme 21. Cleavage mode of aryl pivalates versus aryl sulfonates and aromatic aryl esters

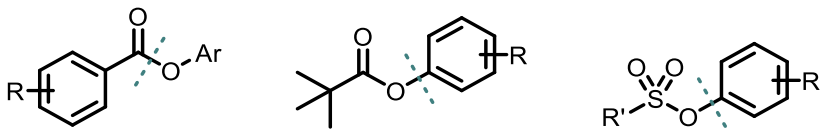

Seminal reports of cross-couplings with aryl pivalates were disclosed in 2008 by the Garg and Shi groups, independently (Scheme 22).[42] Later, other couplings of aryl pivalates

[42] (a) Quasdorf, K. W.; Tian, X.; Garg, N. K. *J. Am. Chem. Soc.* **2008**, *130*, 14422–14423; (b) Guan, B.-T.; Wang, Y.; Li, B.-J.; Yu, D.-G.; Shi, Z.-J. *J. Am. Chem. Soc.* **2008**, *130*, 14468–14470.

utilizing different Ni catalysts afforded the product arising from C(aryl)–O bond cleavage, suggesting that selectivity was in part substrate-controlled.[43] Nonetheless, in Shi's report, C(aryl)–O activation is achieved favourably over C(acyl)–O bond cleavage with aryl esters other than just aryl pivalates, suggesting the Ni-PCy_3 catalyst was particularly effective at enabling this reaction mode. Later, DFT studies revealed how this catalyst could enable selective C(aryl)–O bond cleavage, despite the increased weakness of the C(acyl)–O bond. This will be discussed in section 1.3.

Scheme 22. Seminal cross-coupling reactions using aryl pivalates

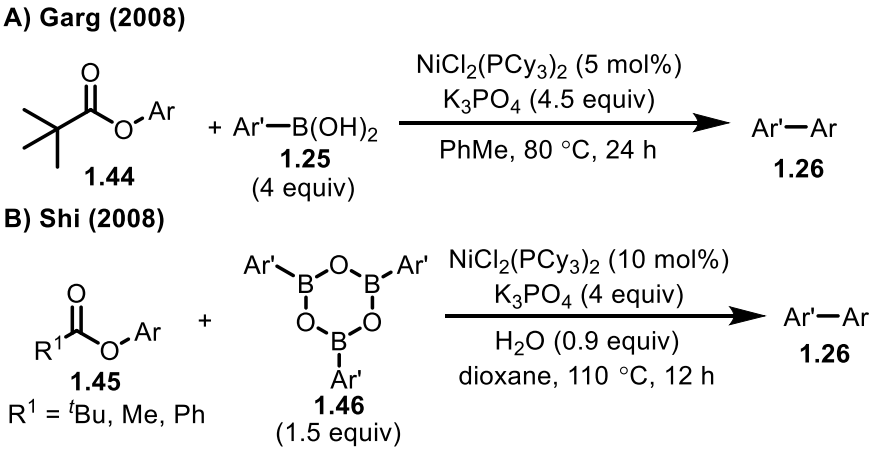

Phenyl esters

It had long been suggested that Ni(0) catalysts could oxidatively add into phenyl esters in stoichiometric studies performed by the Yamamoto laboratory in 1976.[44] However, it took more than 35 years before the development of a catalytic reaction with phenyl esters. The seminal catalytic report was disclosed in 2012 by the Itami lab (Scheme 23).[45] Therein,

[43] (a) Li, B.-J.; Xu, L.; Wu, Z.-H.; Guan, B.-T.; Sun, C.-L.; Wang, B.-Q.; Shi, Z.-J. *J. Am. Chem. Soc.* **2009**, *131*, 14656–14657; (b) Guo, L.; Hsiao, C.-C.; Yue, H.; Liu, X.; Rueping, M. *ACS Catal.* **2016**, *6*, 4438−4442; (c) Li, B.-J.; Li, Y.-Z.; Lu, X.-Y.; Liu, J.; Guan, B.-T.; Shi, Z.-J. *Angew. Chem. Int. Ed.* **2008**, *47*, 10124 –10127; (d) Muto, K.; Yamaguchi, J.; Itami, K. *J. Am. Chem.Soc.* **2012**, *134*, 169−172; (e) Xi, X.; Chen, T.; Zhanga, J.-S.; Han, L.-B. *Chem. Commun.* **2018**, *54*, 1521–1524; (f) Shimasaki, T.; Tobisu, M.; Chatani, N. *Angew. Chem. Int. Ed.* **2010**, *49*, 2929–2932.

[44] Ishizu, J.; Yamamoto, T.; Yamamoto, A. *Chem. Lett.* **1976**, 1091.

[45] Muto, K.; Yamaguchi, J.; Itami, K. *J. Am. Chem. Soc.* **2012**, *134*, 13573–13576.

they disclosed the Ni-catalyzed decarbonylative coupling of phenyl esters with oxazole and thiazole derivatives **1.48**.

Scheme 23. Ni-catalyzed coupling of phenyl esters with oxazole and thiazole derivatives

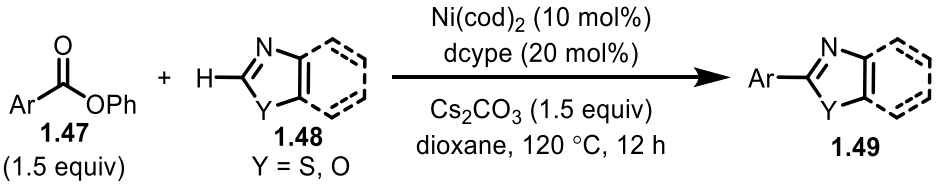

Later, in 2015, the Love and Itami labs independently reported the first Suzuki-Miyaura cross-coupling of phenyl esters.[46] In both reports, the decarbonylated adduct is obtained selectively. The phenyl esters scope was broader in Itami's report (Scheme 24A), whereas Love's was limited to pyridine phenyl esters **1.50** (Scheme 24B).

Scheme 24. Decarbonylative Suzuki-Miyaura couplings of phenyl esters

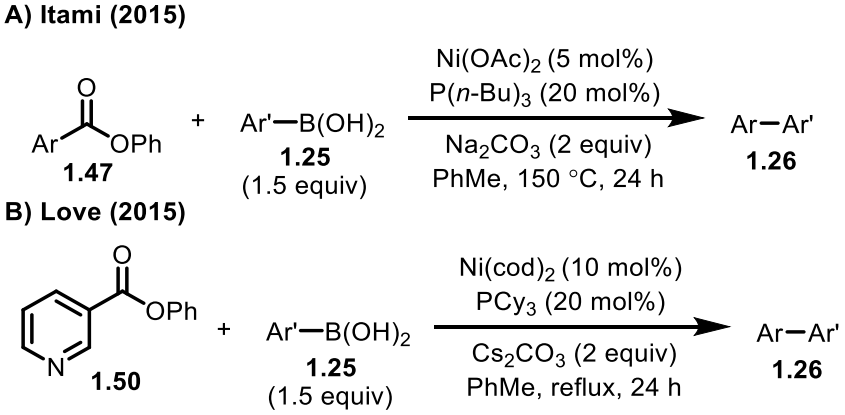

Our group later disclosed that carbonyl-retentive Suzuki-Miyaura couplings of phenyl esters could also be achieved via the use of a Pd-IPr catalyst to afford biaryl ketones (Scheme 25).[47]

---

[46] (a) Muto, K.; Yamaguchi, J.; Musaev, D. G.; Itami, K. *Nat. Commun.* **2015**, *6*, 7508-7515; (b) LaBerge, N. A.; Love, J. A. *Eur. J. Org. Chem.* **2015**, *2015*, 5546–5553.

[47] Ben Halima, T.; Zhang, W.; Yalaoui, I.; Hong, X.; Yang, Y.-F.; Houk, K. N.; Newman, S. G. *J. Am. Chem. Soc.* **2017**, *139*, 1311–1318.

Scheme 25. Carbonyl-retentive Suzuki-Miyaura coupling of phenyl esters

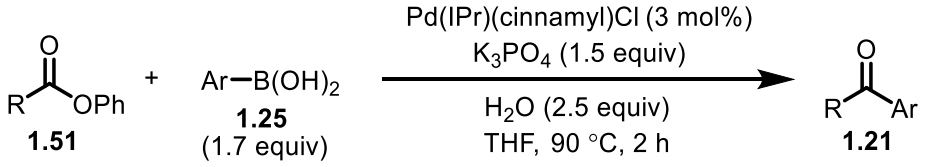

Many other nucleophiles have been successfully coupled to phenyl esters. Scheme 26 summarizes the different types of couplings that have been enabled with these electrophiles.[48] Notably, the field of cross-coupling with phenyl esters has largely been dominated by decarbonylative couplings rather than carbonyl-retentive ones.

[48] (a) Muto, K.; Hatakeyama, T.; Itami, K.; Yamaguchi, J. *Org. Lett.* **2016**, *18*, 5106–5109; (b) Okita, T.; Kumazawa, K.; Muto, K.; Itami, K.; Yamaguchi, J. *Chem. Lett.* **2017**, *46*, 218–220; (c) Pu, X.; Hu, J.; Zhao, Y.; Shi, Z. *ACS Catal.* **2016**, *6*, 6692–6698; (d) Guo, L.; Chatupheeraphat, A.; Rueping, M. *Angew. Chem. Int. Ed.* **2016**, *55*, 11810–11813; (e) Guo, L.; Rueping, M. *Chem. Eur. J.* **2016**, *22*, 16787–16790; (f) Yue, H.; Guo, L.; Liao, H.-H.; Cai, Y.; Zhu, C.; Rueping, M. *Angew.Chem. Int. Ed*. **2017**, *56*,4282–4285; (g) Yue, H.; Guo, L.; Lee, S.-C.; Liu, X.; Rueping, M. *Angew. Chem. Int. Ed.* **2017**, *56*, 3972–3976; (h) Chatupheeraphat, A.; Liao, H.-H.; Lee, S.-C.; Rueping, M. *Org. Lett.* **2017**, *19*, 4255–4258; (i) Liu, X.; Jia, J.; Rueping, M. *ACS Catal.* **2017**, *7*, 4491–4496; (j) Lee, S.-C.; Liao, H.-H.; Chatupheeraphat, A.; Rueping, M. *Chem. Eur. J.* **2018**, *24*, 3608–3612; (k) Takise, R.; Isshiki, R.; Muto, K.; Itami, K.; Yamaguchi, J. *J. Am. Chem. Soc.* **2017**, *139*, 3340–3343; (l) Yue, H.; Zhu, C.; Rueping, M. *Org. Lett.* **2018**, *20*, 385–388; (m) Ben Halima, T.; Vanadavasi, J. K.; Shkoor, M.; Newman, S. G. *ACS Catal.* **2017**, *7*, 2176–2180.

Scheme 26. Reported couplings of phenyl esters

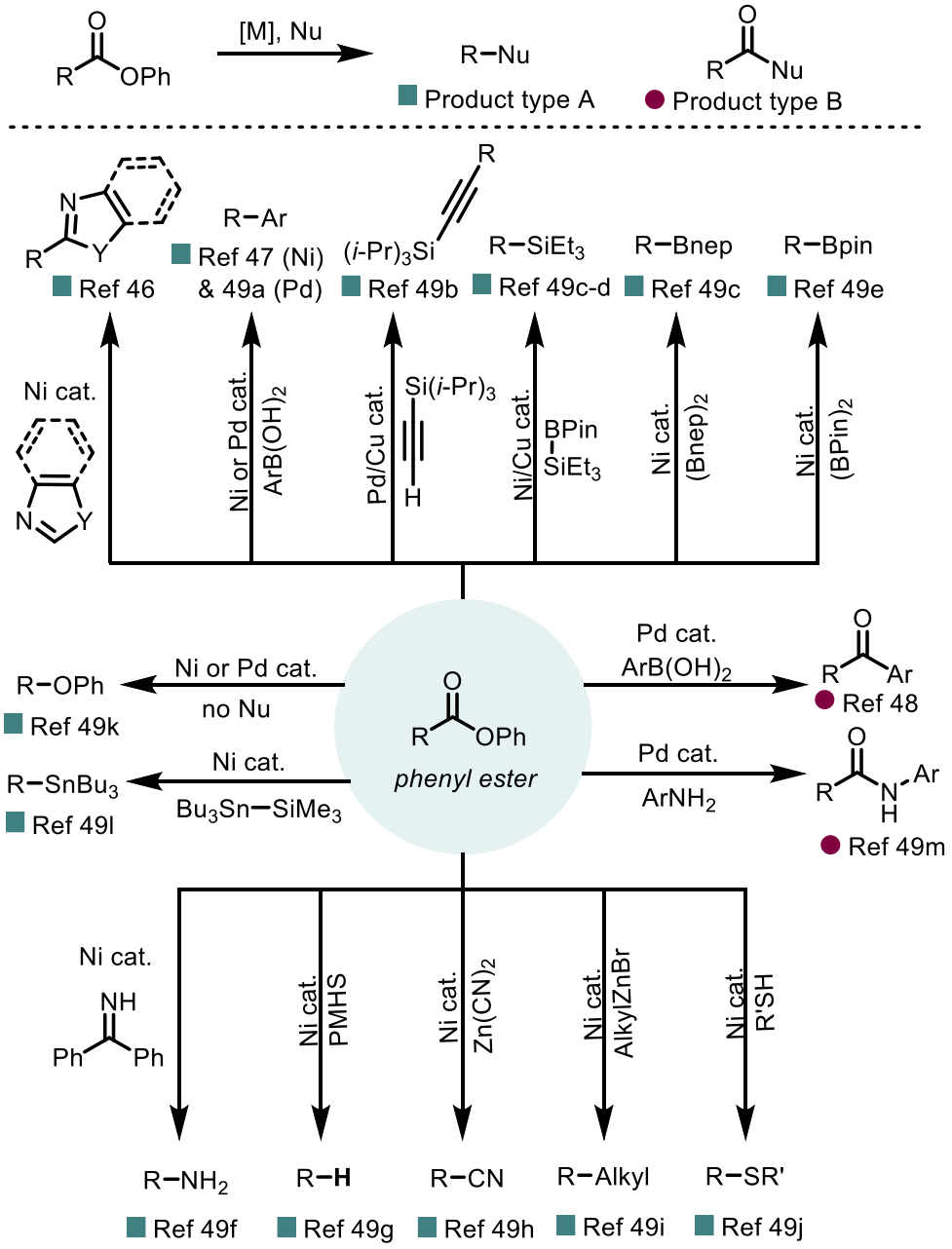

1.3. Cross-couplings of aryl esters: Mechanistic insights

With three accessible cleavage modes, aryl esters constitute a highly versatile class of coupling partner. Understanding how selectivity can be controlled in these couplings is

crucial in order to exploit the potential of these substrates in cross-coupling reactions. In recent years, good mechanistic reports related to this topic have been disclosed.[49] These reports will be the foundation of the discussion presented in this section.

1.3.1. Switchable selectivity of aryl esters

As mentioned previously, both the C(aryl)–O bond activation and C(acyl)–O bond cleavage have been shown to be accessible with aryl esters. The Shi lab demonstrated the efficacy of Ni-PCy_3 to enable selective C(aryl)–O bond cleavage of aryl esters (Scheme 27). On the other hand, Ni-dcype preferentially mediates C(acyl)–O bond cleavage.

Scheme 27. C(aryl)- vs. C(acyl)-O bond cleavage of aryl esters

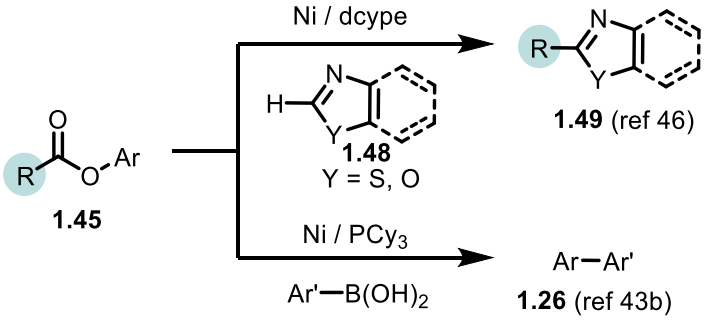

In 2014, the Houk lab performed intensive DFT calculations to elucidate the origin of this diverging chemoselectivity.[49a] In the case of the Ni-dcype catalyst, the overall energy barrier for oxidative addition into the C(acyl)–O bond was found to be 12.6 kcal/mol lower than that required to insert the Ni-dcype catalyst into the C(aryl)–O bond.

Figure 6 shows a simplified energy diagram for the oxidative addition steps with the Ni-PCy_3 catalyst. Initial calculations for the oxidative addition of Ni-PCy_3 found a 28.5 kcal/mol activation energy barrier (**TS1.1**).

[49] (a) Hong, X.; Liang, Y.; Houk, K. N. *J. Am. Chem. Soc.* **2014**, *136*, 2017–2025; (b) Ben Halima, T.; Zhang, W.; Yalaoui, I.; Hong, X.; Yang, Y.-F.; Houk, K. N.; Newman, S. G. *J. Am. Chem. Soc.* **2017**, *139*, 1311–1318; (c) Hie, L.; Fine Nathel, N. F.; Shah, T. K.; Baker, E. L.; Hong, X.; Yang, Y.-F.; Liu, P.; Houk, K. N.; Garg, N. K. *Nature* **2015**, *524*, 79–83; (d) Chatupheeraphat, A.; Liao, H.-H.; Srimontree, W.; Guo, L.; Minenkov, Y.; Poater, A.; Cavallo, L.; Rueping, M. *J. Am. Chem. Soc.* **2018**, *140*, 3724–3735.

Figure 6. Energy diagram for oxidative addition of Ni-PCy_3 in C(acyl)- vs. C(aryl)-O bond of phenyl benzoate

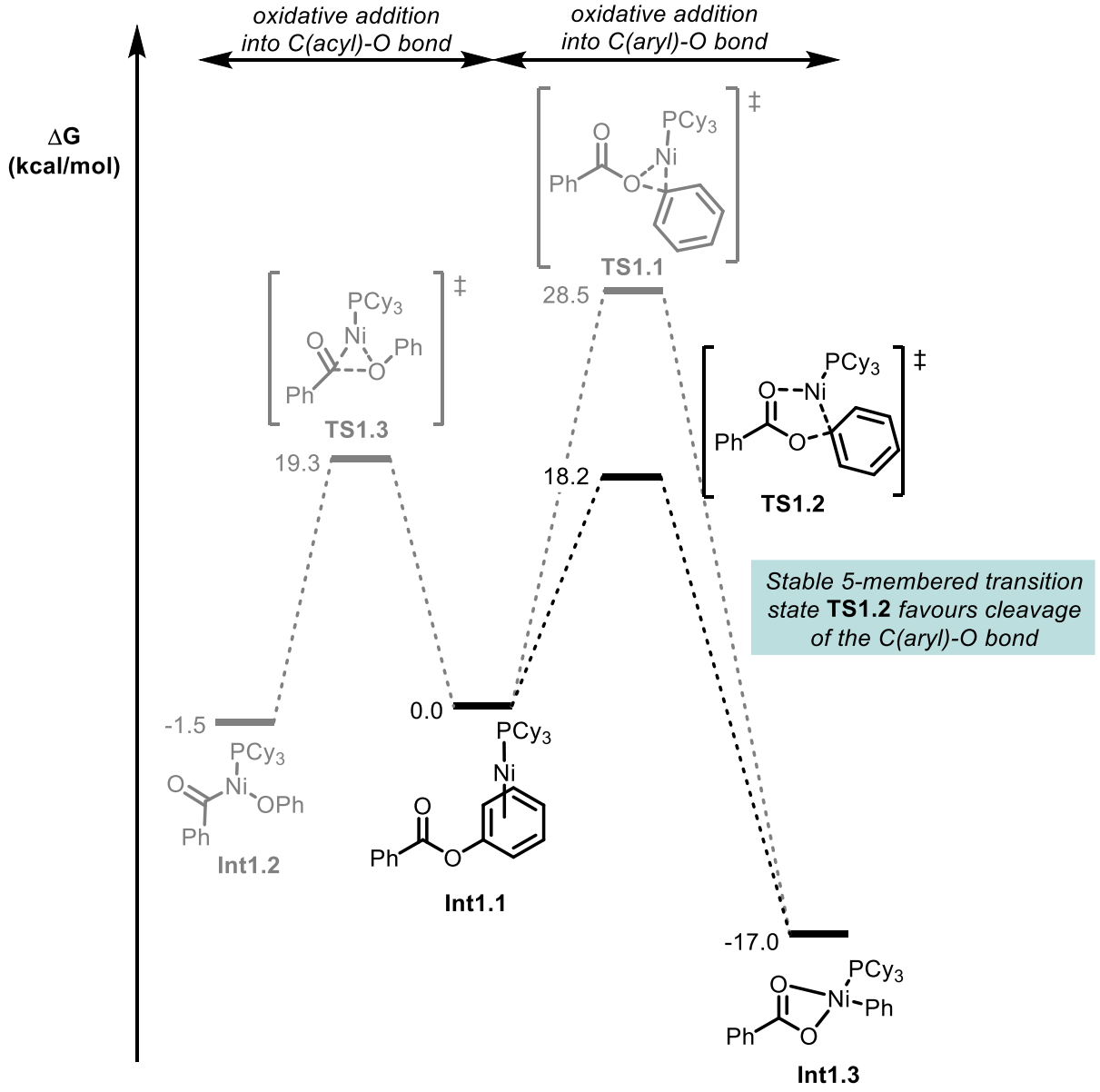

However, a highly stabilizing interaction between the oxygen atom of the carbonyl and the monoligated Ni in transition state **TS1.2** lowers this barrier by 10.3 kcal/mol. Consequently, the activation energy required for oxidative addition into the C(aryl)–O bond is 1.1 kcal/mol lower than that needed for C(acyl)–O bond activation.

In summary, bidentate phosphines seem to favour cleavage of the weakest C(acyl)–O bond. By contrast, activation of the stronger C(aryl)–O bond can be accessed if monodentate phosphine PCy_3 is used. In this case, it is proposed that oxidative addition into the strong C(aryl)–O bond is favoured due to the formation of a stable 5-membered transition state (see Figure 6, **TS1.2**).

1.3.2. Substrate-dependent selectivity: The special case of aryl pivalates

In section 1.3.1, it was shown that ligand-controlled switchable selectivity is possible with aryl esters. However, in some instances, selectivity is mostly substrate-dependent. For instance, Ni-dcype catalyst favours the cleavage of the C(acyl)–O bond for most aryl esters (Scheme 28a).[45] However, with the same catalyst, aryl pivalates undergo formal cleavage of the C(aryl)–O bond instead (Scheme 28b).[50]

Scheme 28. Ni-dcype catalyst for couplings with aryl esters vs. aryl pivalates

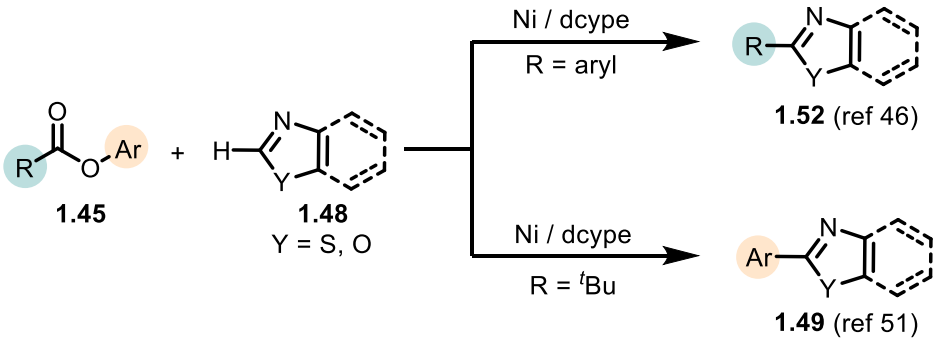

The Houk lab performed DFT calculations aimed at understanding why C(aryl)–O cleavage is favoured aryl pivalates.[49a] As was the case with phenyl esters, the calculated activation energy to oxidatively insert Ni-dcype into the C(acyl)-O bond of aryl pivalates is significantly lower than that required for insertion into the C(aryl)-O bond (Figure 7). Despite this significant difference in activation energy, the product arising from cleavage of the stronger C(aryl)-O bond is observed exclusively.

[50] Muto, K.; Yamaguchi, J.; Itami, K. *J. Am. Chem. Soc.* **2012**, *134*, 169–172.

Figure 7. Energy diagram for the oxidative addition of Ni-dcype into C(aryl)- vs. C(acyl)-O bond of phenyl pivalate

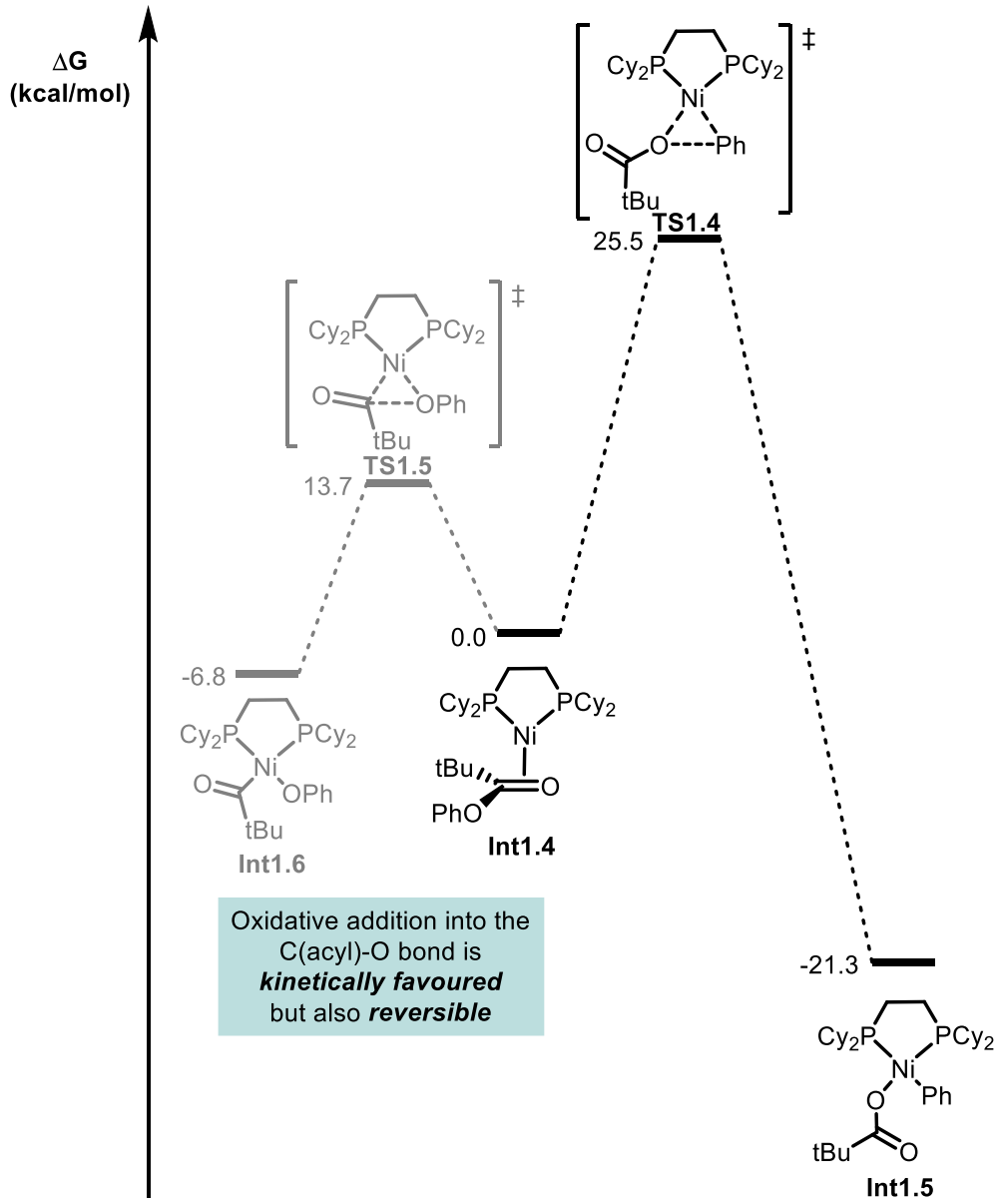

This unusual selectivity is suggested to be possible because oxidative addition into the C(acyl)–O bond is reversible. The species **Int1.6** formed after oxidative addition of Ni into the C(acyl)–O bond is relatively high in energy. Thus reductive elimination to go back to **Int1.4** requires only 20.5 kcal/mol of energy. Moreover, the subsequent steps after the formation of **Int1.6** have high energy barriers, whereas the steps following the formation

of **Int1.5** require less energy (Scheme 29). To be exact, the overall energy barrier to get product **1.55** from **Int1.6** is 10 kcal/mol higher than the subsequent steps required to form product **1.54** from **Int1.5**.

Scheme 29. Overall energy barriers for the C(aryl)- vs. C(acyl)-O bond activation pathways of phenyl pivalate

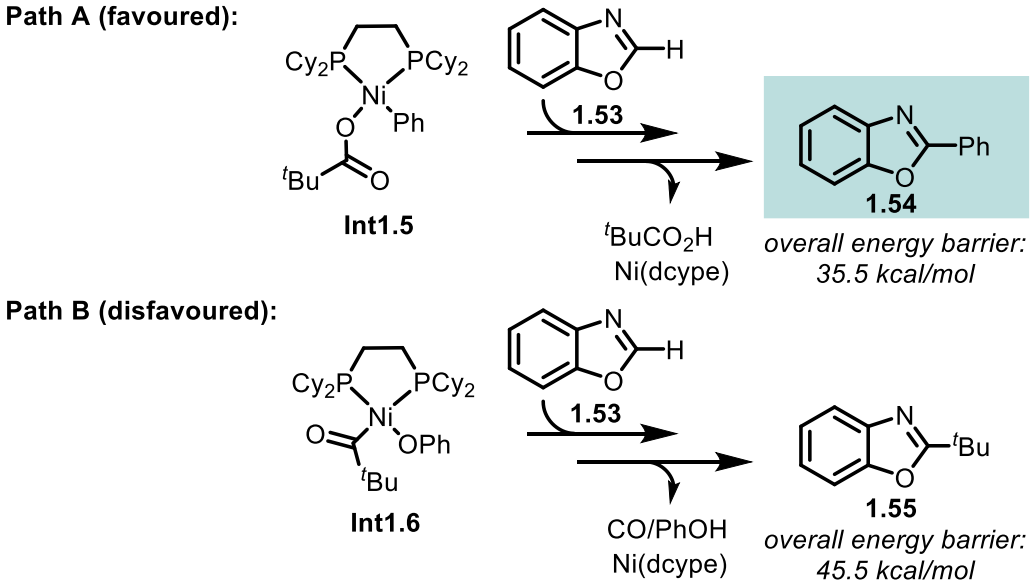

Notably, decarbonylation of **Int1.6** to form the highly unstable intermediate **Int1.7** is endergonic by 23.2 kcal/mol (Scheme 30). The instability of **Int1.7** can be explained by the lack of stabilizing d_{Ni}-π^* interaction and by the steric repulsion between the cyclohexyl groups of the bidentate phosphine ligand and the tert-butyl group.

Scheme 30. Thermodynamically unfavourable decarbonylation of aryl pivalates

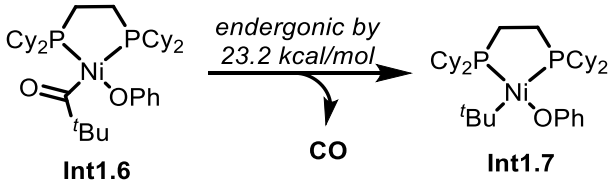

In brief, even though the C(acyl)–O bond of aryl pivalates is weaker than the C(aryl)–O bond, the product arising from formal cleavage of the C(aryl)–O bond is observed exclusively. It has been proposed by the Houk lab that oxidative into both the C(acyl)–O

and C(aryl)–O bond is feasible, but the former is reversible while the latter is not. Moreover, decarbonylation from the Ni intermediate **Int1.6**, obtained after oxidative addition into the C(acyl)–O bond, has been calculated to be prohibitive; therefore, no product arising from C(acyl)–O bond cleavage is observed.

1.3.3. Carbonyl-retentive vs. decarbonylative couplings

Depending on the type of catalyst and nucleophile used, the decarbonylative or carbonyl-retentive reaction mode can be enabled. Recent work from our group demonstrated that a palladium catalyst with a bulky NHC ligand could favor the carbonyl-retentive mode in Suzuki-Miyaura type couplings.[49b] DFT calculations were performed in collaboration with the Houk lab to gain a better understanding of the reaction selectivity. The activation barrier for decarbonylation from Pd intermediate **Int1.10** was found to be 17.4 kcal/mol higher than for direct reductive elimination. Not only that, but decarbonylation is also endergonic by 6.3 kcal/mol. Thus, decarbonylation is disfavoured both thermodynamically and kinetically. This preference was attributed to the bulkiness of the NHC which substantially hinders decarbonylation while favouring reductive elimination.

Significant energy barriers for decarbonylation barriers were also calculated for similar Ni-NHC catalysts in other reports (Scheme 31).[49c] Reductive elimination of ester **1.57** from **Int1.13** was found to require 16.6 kcal/mol less energy than that required for decarbonylation. Similarly, the activation energy for reductive elimination to afford amide **1.58** was found to be favourable over decarbonylation by 18.2 kcal/mol.

Figure 8. Select DFT calculations for the carbonyl-retentive Suzuki-Miyaura couplings of phenyl esters

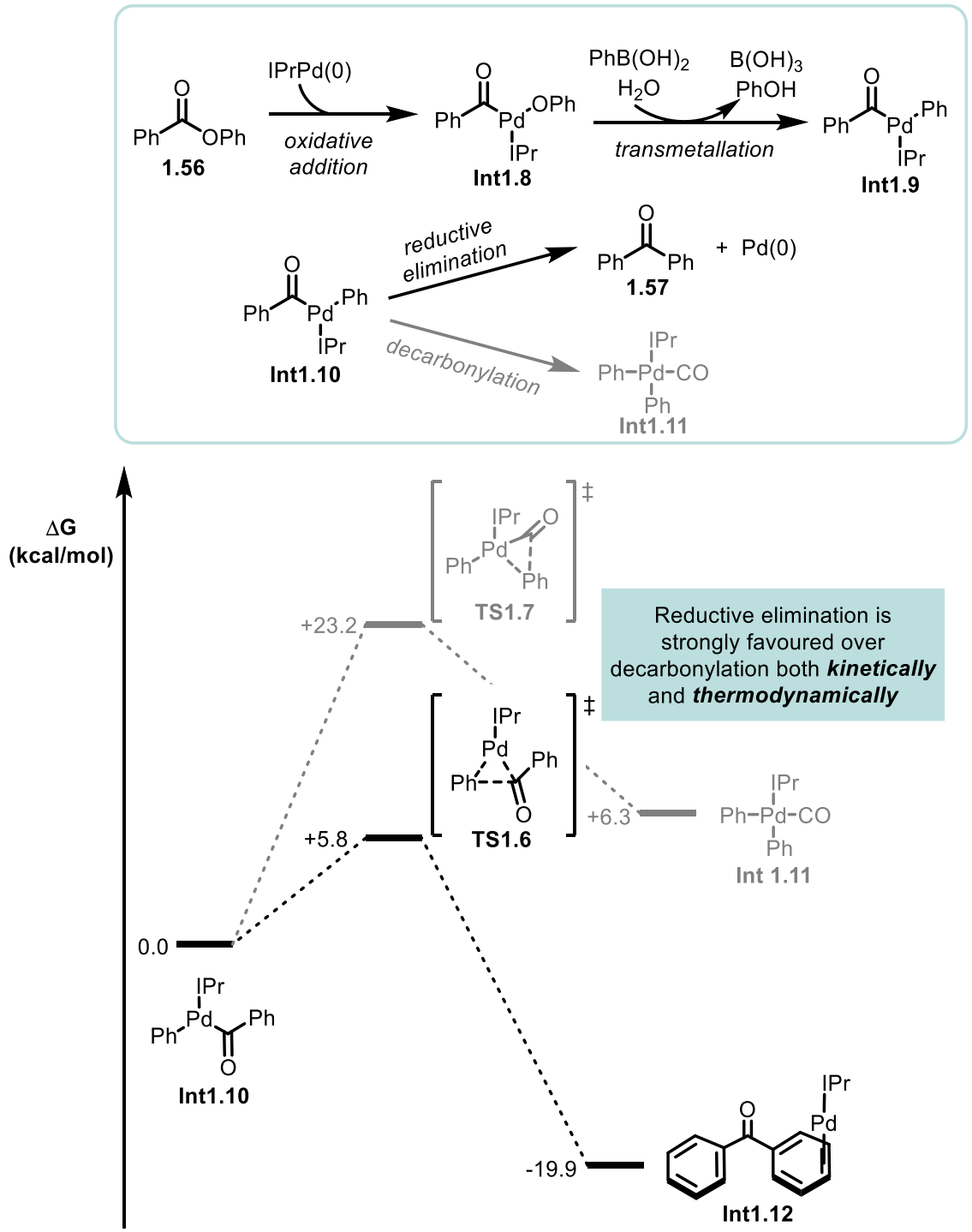

Scheme 31. Reductive elimination vs. decarbonylation of Ni-SIPr species

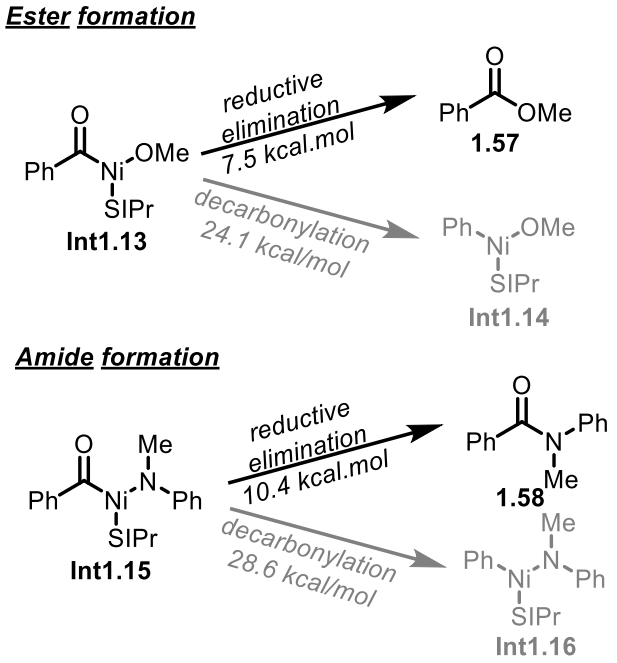

1.3.4. C(aryl)–C(acyl) activation

Most decarbonylative couplings of phenyl esters are proposed to occur via oxidative addition into the C(acyl)–O bond, followed by decarbonylation (Scheme 32A). An alternative hypothesis involves oxidative addition into the C(aryl)–C(acyl) bond, which leads to the formation of the same product (Scheme 32B).

Scheme 32. Plausible mechanisms for the formation of decarbonylated adducts

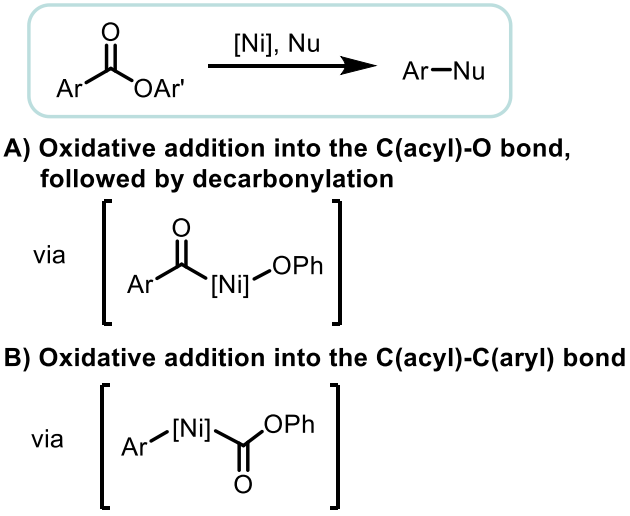

In a recent report by the Rueping lab, oxidative addition of Ni-dcype into the C(acyl)–C(aryl) bond of phenyl 1-naphthoate was calculated to be favoured by 2.3 kcal/mol over oxidative addition into the C(acyl)–O bond (Figure 9).[49d] Further experimental mechanistic studies might be needed to corroborate one of the two proposals.

Figure 9. Transition state energies for oxidative addition of Ni-dcype

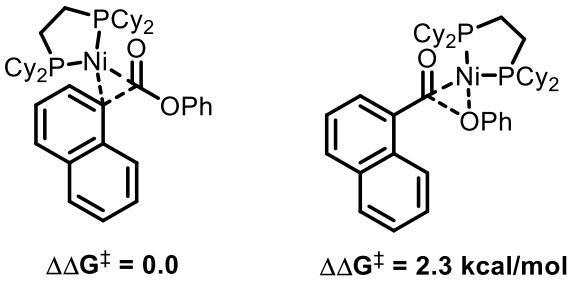

1.4. Research goals

Aryl esters have recently emerged as powerful coupling partners in cross-coupling reactions. In addition to their ubiquity and robustness, aryl esters exhibit three possible cleavage modes. The C(acyl)–O bond activation pathway can be enabled with or without carbonyl loss, and C(aryl)–O bond cleavage is also accessible with these electrophiles. Those three reaction modes have been demonstrated independently (see section 1.2.3). Mechanistic studies have helped to rationalize the diverging selectivity and offered some insights as to how ligands can influence which reaction pathway is favoured (see section 1.3).

In Chapter 2, this mechanistic information will be used to develop an unprecedented Pd-catalyzed alkylative Suzuki-Miyaura cross-coupling of phenyl esters. We will extend upon the concept of catalyst-controlled selectivity by providing a cohesive report on how both carbonyl-retentive and decarbonylative couplings can be achieved with these coupling partners.

Phenyl esters represent robust functionalities, especially in contrast to other carboxylic acid derivatives used in the field such as acid anhydrides or glutarimide amides. However, the use of widely abundant methyl and ethyl esters would be of highest practicality. Their use in cross-coupling chemistry remains underdeveloped, however, due to the relative inertness of methyl esters. The activation of methyl esters via transition metal catalysis will be further pursued in Chapter 3 in the context of esterification and amidation reactions.

Scheme 33. Summary of research projects

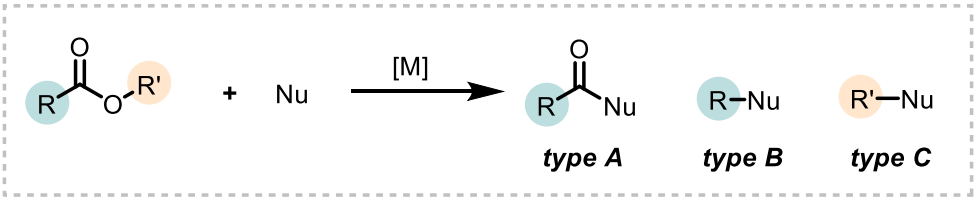

Chapter 2

R' = Ph

Nu = alkyl boranes

Products: type A & type B

Chapter 3

R' = Me

Nu = alcohols, amines

Products: type A

Chapter 2. Switchable Selectivity in Alkylative Cross-Couplings of Phenyl Esters

2.1. Background

A lot of research efforts are being devoted to broadening the scope of the electrophilic partner in cross-coupling reactions. During the general expansion of the electrophile scope, there has been an evident shift towards activation of stronger and stronger bonds, which reflects the movement towards milder and milder nucleophiles observed during the expansion of the nucleophilic coupling partner scope. This, in turn, has the potential to greatly simplify synthesis of complex molecules by obviating the need of protecting groups or the use of stoichiometric activating agents.

In particular, esters are highly desirable substrates to couple due to their abundancy and low cost. Moreover, three different cleavage modes are accessible with aryl esters, making them versatile coupling partners. Most of the progress in cross-couplings of esters has focused on the formation of $C(sp^2)$–$C(sp^2)$ bonds or carbon-heteroatom bonds, while alkylative couplings of esters have remained scarce. Due to the prevalence of $C(sp^2)$–$C(sp^3)$ bonds in relevant pharmaceutical molecules, the development of such couplings represents an important goal. The cross-coupling of phenyl esters **2.1** with an alkyl organometallic reagent **2.2** could be a viable route to synthesize alkyl ketones **2.3** and alkylated arenes **2.4**, provided that selectivity could be achieved (Scheme 34).

Scheme 34. Proposed alkylative cross-coupling of esters

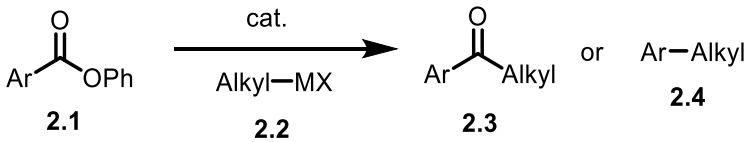

To contextualize the importance of such a transformation, traditional methods used to synthesize alkyl ketones and alkylated arenes will be reviewed in Section 2.1.1. Then, Section 2.1.2 will discuss alkylative cross-coupling methods that have been developed for the synthesis of these compounds. Finally, our research goals and contributions will be described in Section 2.1.3.

2.1.1. Traditional methods to synthesize alkyl ketones and alkylated arenes

Friedel-Crafts acylations and alkylations are classical reactions used to synthesize ketones and alkylated arenes, respectively (Scheme 35). In this reaction, a strong Lewis acid such as $AlCl_3$, catalyzes the coupling of acyl chloride **2.6** or alkyl chloride **2.9** with arene **2.5**, generating an acylated or alkylated arene (**2.7** or **2.10**) and strong acid by-product **2.8**.

Scheme 35. Friedel-Crafts reactions

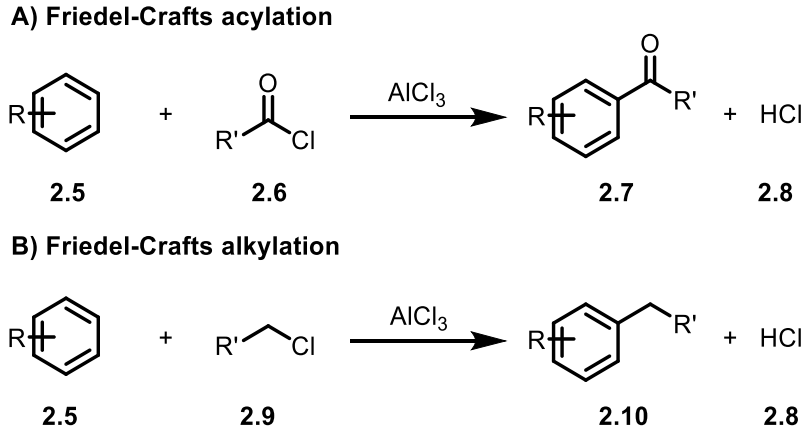

In both transformations, the strong acid by-product renders these reactions incompatible with acid-sensitive moieties. Moreover, the substrate scope is mostly limited to electron-rich arenes, and regioselectivity issues are common. A specific issue for Friedel-Crafts alkylations is the risk of overalkylation.

Another common way to prepare aryl alkyl ketones is via the addition of organometallic reagents to Weinreb amides (Scheme 36).[51] After the first addition of organometallic reagent **2.12** to the Weinreb amide **2.11**, a stable 5-membered intermediate **Int2.1** is formed, which does not collapse until the workup to afford the corresponding ketone **2.13**. By contrast, the addition of an alkyl Grignard or alkyl organolithium reagent to a "regular" amide or ester often cannot be controlled for the formation of the corresponding ketone. Instead, over-addition onto the more electrophilic ketone intermediate occurs, yielding an alcohol product.

Scheme 36. Aryl alkyl ketones via Weinreb amides

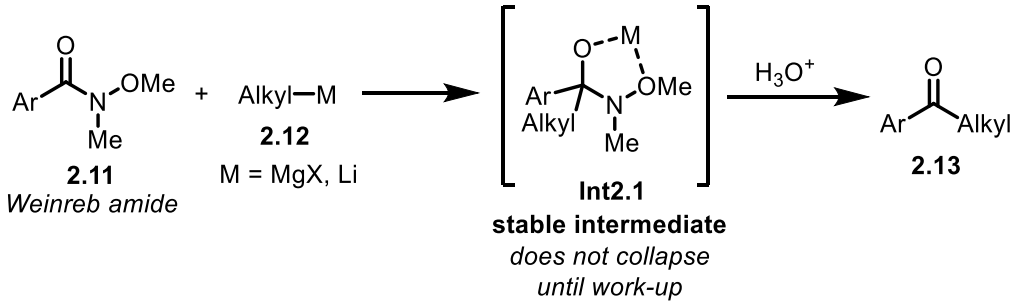

Alternatively, aryl alkyl ketones can be prepared via the addition of Grignard reagents onto acyl chlorides (see Chapter 1, Scheme 10). In this case, over-addition can be avoided via the use of appropriate chelating agents.

On the other hand, protocols for synthesis of alkylated arenes are scarcer. The regioselectivity and overalkylation issues associated with the Friedel-Crafts alkylation method significantly narrow the scope of products that can be accessed. By contrast, cross-coupling reactions represent the reliable reactions to afford these $C(sp^2)$–$C(sp^3)$ linkages.

[51] Nahm, S.; Weinreb, S. M. *Tetrahedron Lett.* **1981**, *22*, 3815–3818.

2.1.2. Alkylative cross-couplings

Alkylative cross-coupling reactions have greatly simplified the formation of $C(sp^2)$–$C(sp^3)$ bonds. In contrast to the Friedel-Crafts alkylation method, alkylative cross-couplings are more selective and generally encompass a much broader scope. Nonetheless, many challenges are associated with using alkyl organometallic reagents. First, the latter are generally slower to transmetallate than their aryl counterparts. With a slower transmetallation step, the organometallic reagent or the metal species is more susceptible to undergo other competitive decomposition pathways. Secondly, alkyl metal species are prone to β-hydride eliminate. β-Hydride elimination can be a productive step in some coupling reactions (e.g. Mizoroki-Heck cross-coupling), but it needs to be prevented if the formation of $C(sp^2)$–$C(sp^3)$ bonds is desired.

In Scheme 37, a general catalytic cycle for an alkylative cross-coupling is illustrated in black. Similarly to arylative couplings, it comprises three main steps: 1) oxidative addition, 2) transmetallation, and 3) reductive elimination. However, alkylative cross-couplings have distinct side-reactions (shown in lighter gray). Pd intermediate **Int2.3**, instead of undergoing reductive elimination, can β-hydride eliminate. β-Hydride elimination is a reversible step; thus, the olefin can re-insert into the M–H bond of **Int2.4** to give **Int2.5**. However, this can also lead to the formation of isomerized product **2.19**. Another possible pathway after β-hydride elimination is subsequent reductive elimination, which leads to the formation of reduced product **2.18**.

Scheme 37. General catalytic cycle for a Pd-catalyzed alkylative cross-coupling

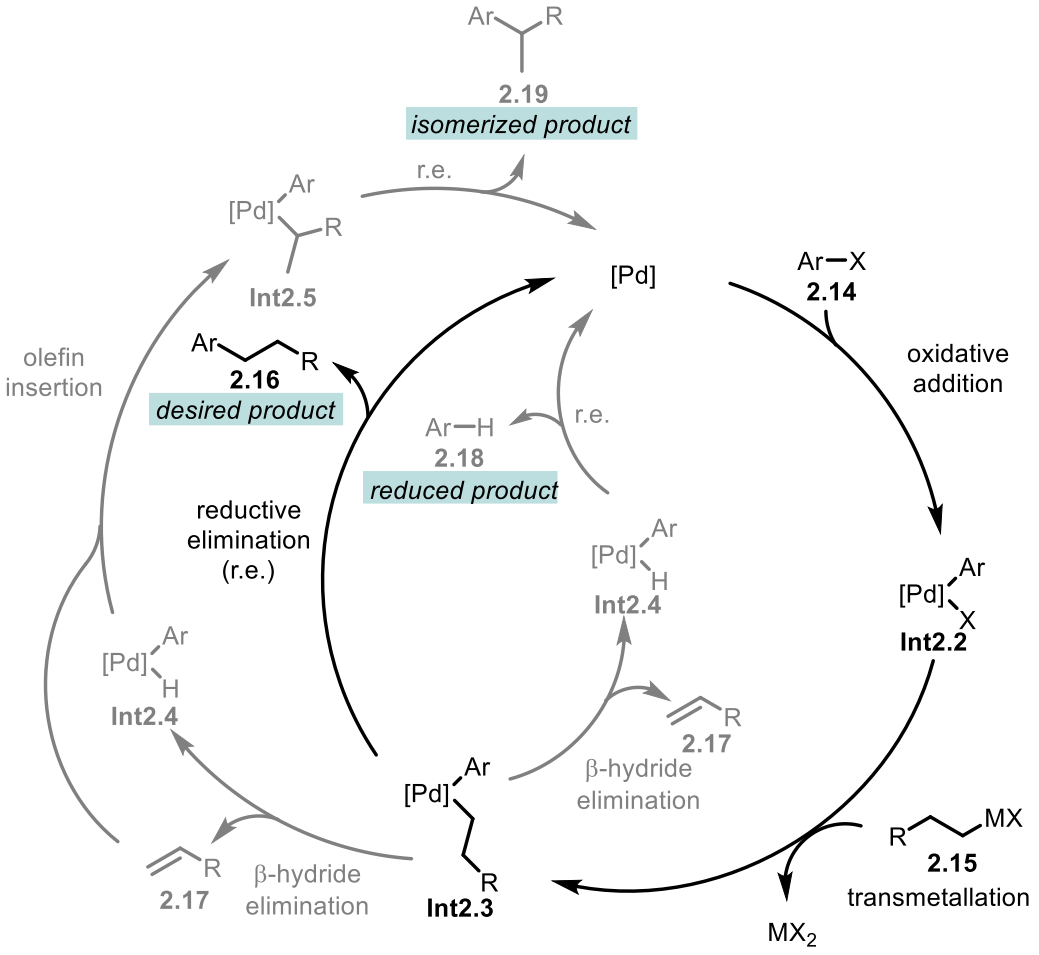

To prevent β-hydride elimination, a better understanding of the details of β-hydride elimination is necessary. Before β-hydride elimination, a vacant coordination site *cis* to the alkyl group is usually required (Scheme 38).[52] This free coordination site allows initial agostic interaction between the metal center and the β-hydrogen. In this interaction, the β C–H bond donates electron density to the metal, and the metal also backbonds into the σ* of the C–H bond. This weakens the bond and eventually leads to β-hydride elimination.

[52] For DFT studies supporting this statement, see: Carrizo, E. D. S.; Bickelhaupt, F. M.; Fernández, I. *Chem. Eur. J.* **2015**, *21*, 14362–14369.

Scheme 38. A free coordination site is a pre-requisite for β-hydride elimination

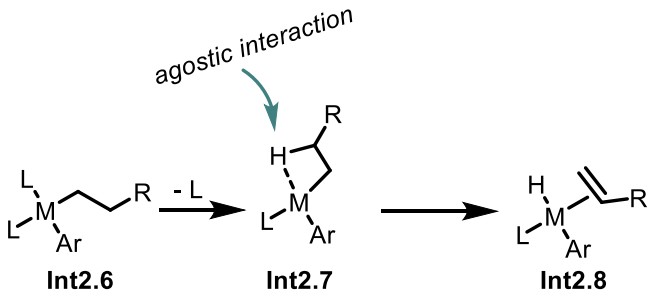

Thus, strategies to avoid β-hydride elimination in cross-couplings generally rely on preventing any vacant coordination site and speeding up reductive elimination. The use of bidentate ligands is usually preferred in alkylative couplings since they tend to dissociate less readily than monodentate ligands, and they force the alkyl and aryl ligands in a *cis*-configuration, speeding up reductive elimination.[53] The use of halide salt additives has also been reported to inhibit β-hydride elimination by occupying free coordination sites on the metal center.[54]

The use of alkyl zinc nucleophiles in Negishi cross-coupling has been thoroughly studied.[55] By contrast, the development of cross-coupling with alkyl boron reagents is less developed.[56] Notably, B-alkyl-9-BBN reagents have had more success than the corresponding alkyl boronic acids in $C(sp^2)$–$C(sp^3)$ couplings. The former nucleophiles can be easily prepared via hydroboration of alkenes with 9-BBN dimer (Scheme 39). Due to the bulkiness of the 9-BBN fragment, the anti-Markovnikov addition occurs selectively.

[53] Hamann, B. C.; Hartwig, J. F. *J. Am. Chem. Soc.* **1997**, *119*, 12382–12383.
[54] (a) Wang, Z.; Lu, X. *J. Org. Chem.* **1996**, *61*, 2254–2255; (b) Wang, Z.; Zhang, Z.; Lu, X. *Organometallics* **2000**, *19*, 775–780.
[55] For a recent review on Negishi couplings, see: Haas, D.; Hammann, J. M.; Greiner, R.; Knochel, P. *ACS Catal.* **2016**, *6*, 1540−1552.
[56] For review on organoboron reagents, see: (a) Lennox, A. J. J.; Lloyd-Jones, G. C. *Chem. Soc. Rev.* **2014**, *43*, 412–443; (b) Doucet, H. *Eur. J. Org. Chem.* **2008**, 2013–2030.

Scheme 39. Hydroboration for the synthesis of B-alkyl-9-BBN reagents

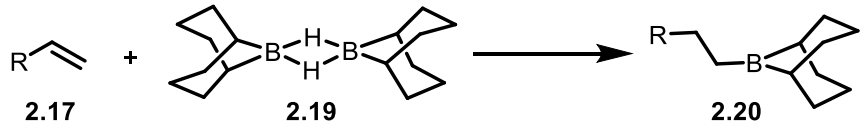

Most alkylative cross-couplings are performed with organohalides or pseudohalides such as triflates as the electrophilic partners. Using carboxylic acid derivatives as coupling partners, by contrast, can provide the usual alkylated products *and* alkyl ketones. For instance, cross-couplings of alkyl zinc nucleophiles with acid chlorides,[57] anhydrides,[58] or thioesters[59] have all been reported to yield alkyl ketone products. More recently, the Garg group demonstrated that N-tosyl amides were suitable coupling partners (Scheme 40A).[60] The Molander lab also showed that twisted amide **2.20** could be coupled with organotrifluoroborate salts **2.21** to afford dialkyl ketones **2.22** via Ni-photoredox catalysis (Scheme 40A).[61]

Scheme 40. Recent carbonyl-retentive alkylative cross-couplings

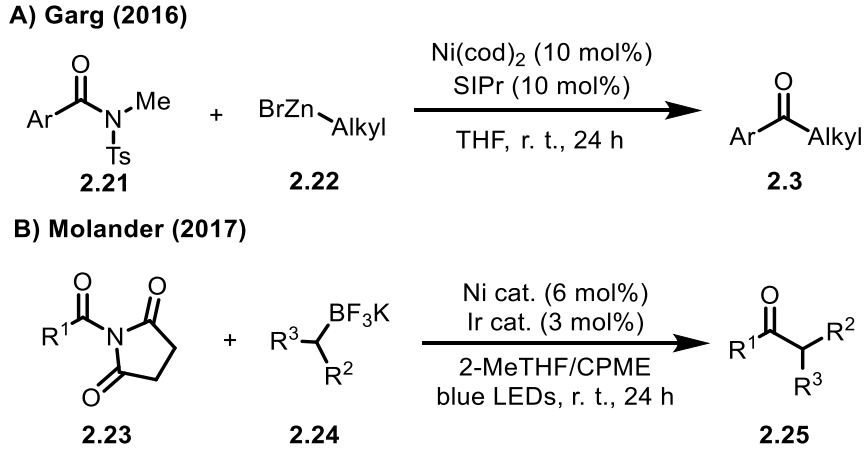

[57] Grey, R. A. *J. Org. Chem.* **1984**, *49*, 2288–2289.
[58] Bercot, E. A.; Rovis, T. *J. Am. Chem. Soc.* **2005**, *127*, 247-254.
[59] Mori, Y.; Seki, M. *Adv. Synth. Catal.* **2007**, *349*, 2027–2038.
[60] Simmons, B. J. ; Weires, N. A.; Dander, J. E.; Garg, N. K. *ACS Catal.* **2016**, *6*, 3176–3179.
[61] Amani, J.; Alam, R.; Badir, S.; Molander, G. A. *Org. Lett.* **2017**, *19*, 2426–2429.

Decarbonylative alkylative couplings have also been reported. In 2017, the Rueping lab disclosed that phenyl esters could undergo decarbonylative couplings with alkylzinc bromides with a Ni-dcype catalyst (Scheme 41A).[62] With the same catalyst, they were also able to couple aryl pivalates (Scheme 41B).

Scheme 41. Rueping's alkylative couplings of phenyl esters and aryl pivalates

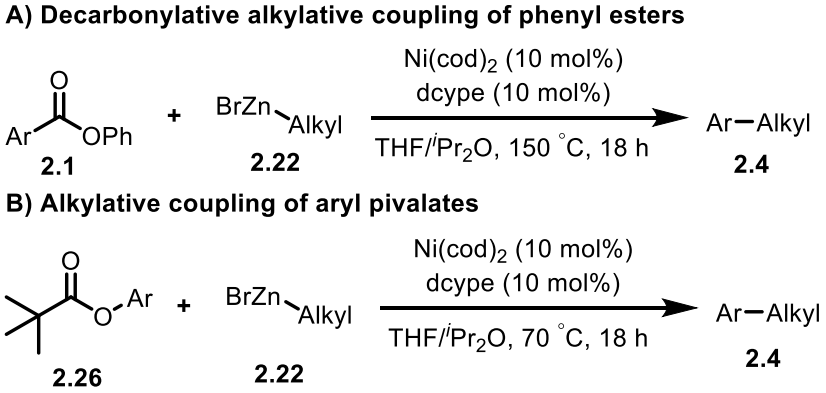

In 2016, Baran and co-workers reported the cross-coupling of redox-active aliphatic esters **2.27** with dialkylzinc reagents **2.28** to form C(sp^3)–C(sp^3) bonds (Scheme 42).[63] It should be noted that this coupling reaction is mechanistically distinct from other couplings of esters and amides, and therefore hardly comparable. The mechanism is radical-based: instead of cleavage of the C(acyl)–O bond, homolytic cleavage of the N–O bond of the redox-active ester **2.27** occurs first, followed by decarboxylation.

Scheme 42. Baran's coupling of redox-active esters with alkyl zinc reagents

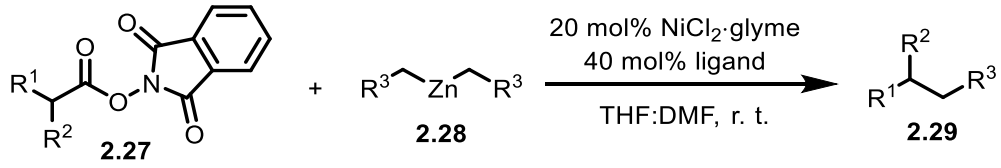

[62] Liu, X.; Jia, J.; Rueping, M. *ACS Catal.* **2017**, *7*, 4491–4496.

[63] Qin, T.; Cornella, J.; Li, C.; Malins, L. R.; Edwards, J. T.; Kawamura, S.; Maxwell, B. D.; Eastgate, M. D.; Baran, P. S. *Science* **2016**, *352*, 801–805.

Lastly, in 2016, the Rueping lab disclosed that aryl pivalates could be coupled with mild B-alkyl-B-9BBN reagents (Scheme 43).

Scheme 43. Rueping's coupling of aryl pivalates and alkyl boranes

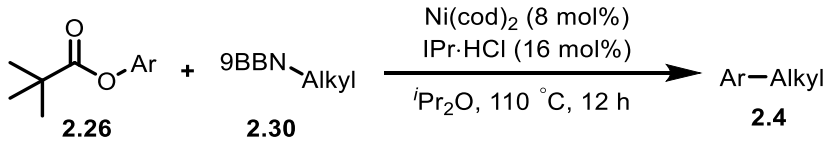

2.1.3. Research goals

Despite the significant progress made in cross-couplings of carboxylic acid derivatives, reports of alkylative cross-couplings have remained scarce, especially with simple phenyl esters. Notably, the disclosed alkylative protocols have mostly focused on the use of alkyl zinc nucleophiles; by contrast, the couplings with alkyl boron reagents could offer increased functional group tolerance. Therefore, we decided to dedicate our research efforts toward the development of a catalytic reaction to couple phenyl esters and alkyl boranes. To increase the impact of our work, we wanted to selectively enable two reaction modes instead of just one. While it is now well known that different cleavage modes are accessible with phenyl esters, selective catalytic reactions with the latter substrates have mostly been disclosed independently. The Rueping lab recently showed in one cohesive report how two reaction modes could be enabled when coupling esters with alkyl zinc nucleophiles, although the selectivity therein was *substrate-controlled* (Scheme 44A). Our goal was to disclose a cohesive report showing *catalyst-controlled* selectivity in the cross-couplings of phenyl esters with alkyl boranes to enable both the carbonyl-retentive and decarbonylative reaction mode (Scheme 44B). To do so, we used mechanistic groundwork of the field (Chapter 1, Section 1.3) to design new selective reactions rationally. This coupling would represent a valuable contribution from a practical point of view since it would allow easy access to complex alkyl ketones and alkylated arenes in a more selective fashion than what can be achieved with traditional Friedel-Crafts

reactions. As for the "bigger picture" aspect, the ability to utilize the same starting materials to attain diverse products selectively is a powerful strategy.

Scheme 44. Cohesive reports showing two reaction modes of phenyl esters

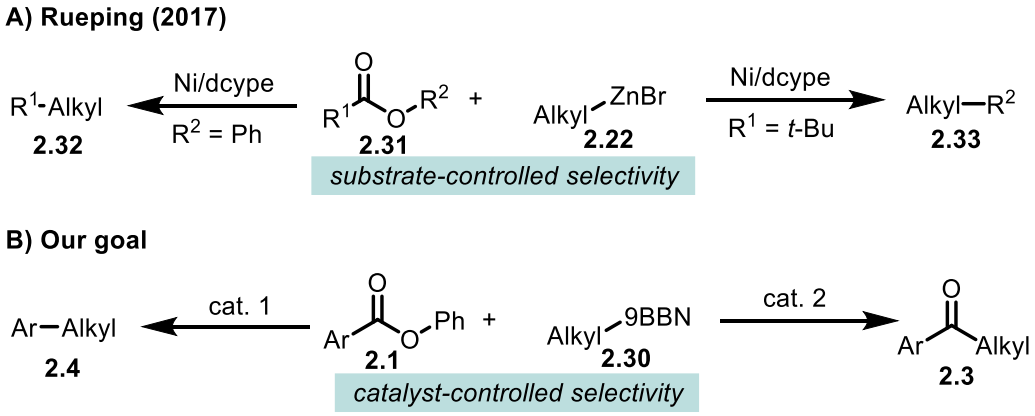

2.2. Results and discussion[64]

2.2.1. Optimization of the carbonyl-retentive couplings

Our group previously demonstrated that Suzuki-Miyaura cross-couplings of esters could occur with carbonyl retention to afford ketones selectively.[65] A critical feature that enabled this reaction mode was the use of a bulky NHC ligand that strongly disfavoured decarbonylation and, in parallel, facilitated reductive elimination. Following this work, the Szostak group was also able to access carbonyl-retentive pathways with similar Pd-NHC catalysts.[66]

---

[64] The results presented in this chapter have been published in a peer-reviewed journal: Masson-Makdissi, J.; Vandavasi, J. K.; Newman, S. G. *Org. Lett.* **2018**, *20*, 4094–4098. This project was done in collaboration with Dr. Jaya Kishore Vandavasi, who isolated the following compounds: **2.54**, **2.62**, **2.64**, **2.66**, **2.68**, and **2.81**.

[65] Ben Halima, T.; Zhang, W.; Yalaoui, I.; Hong, X.; Yang, Y.-F.; Houk, K. N.; Newman, S. G. *J. Am. Chem. Soc.* **2017**, *139*, 1311–1318.

[66] (a) Shi, S.; Lei, P.; Szostak, M. *Organometallics* **2017**, *36*, 3784–3789; (b) Lei, P.; Meng, G.; Shi, S.; Ling, Y.; An, J.; Szostak, R.; Szostak, M. *Chem. Sci.* **2017**, *8*, 6525–6530.

Based on the sound evidence that Pd-NHC catalysts can selectively enable carbonyl-retentive couplings of esters, we initially screened different Pd sources and NHC ligands (Table 1). Different palladium precursors were tested with IPr·HCl as the ligand. Common Pd precursors such as $Pd(OAc)_2$ and $Pd_2(dba)_3$ were inefficient for this coupling reaction (entry 1 and 2). $[Pd(cinnamyl)Cl]_2$ was a more suitable Pd source compared to palladium acetate but still provided a poor yield of **2.36** (entry 3). Except for $Pd_2(dba)_3$, we hypothesized that the reduction of Pd(II) to form the active catalyst Pd(0) might be challenging under the reaction conditions. For this reason, we next screened unique Pd(II) sources that are known to spontaneously reductively eliminate in the presence of a phosphine or NHC ligand to afford Pd(0). Pd(cp)(cinnamyl) and $Pd(COD)(CH_2TMS)_2$ both increased the yield by more than 3-fold (entry 4 and 5).

With an efficient palladium source identified, we then screened a variety of NHC ligands. IMes·HCl, IPent·HCl, and ICy·HCl all gave less than 10% yield (entries 7-9), while SIMes·HCl gave a moderate 39% yield of **2.36** (entry 6). Both SIPr·HCl and IPr·HCl were found to be strongly superior ligands for this coupling reaction (entries 4-5 and entries 10-11). Moreover, a Pd complex with pre-complexed IPr, Pd(IPr)(cinnamyl)Cl provided a satisfactory yield of 75%.

Table 1. Screening of Pd sources and NHC ligands

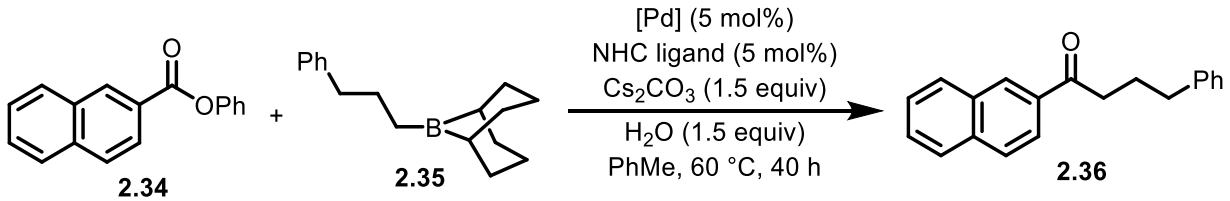

2.34 **2.35** **2.36**

Entry	Pd source	NHC ligand	%Yield of 2.36[a]
1	$Pd(OAc)_2$	IPr·HCl	0
2	$Pd_2(dba)_3$	IPr·HCl	< 5

3	[Pd(cinnamyl)Cl]$_2$	IPr·HCl	16
4	Pd(cod)(CH$_2$TMS)$_2$	IPr·HCl	70
5	Pd(cp)(cinnamyl)	IPr·HCl	54
6	Pd(cp)(cinnamyl)	SIMes·HCl	39
7	Pd(cp)(cinnamyl)	IMes·HCl	9
8	Pd(cp)(cinnamyl)	IPent·HCl	7
9	Pd(cp)(cinnamyl)	ICy·HCl	0
10	Pd(cp)(cinnamyl)	SIPr·HCl	62
11	Pd(cod)(CH$_2$TMS)$_2$	SIPr·HCl	65
12	Pd(IPr)(cinnamyl)Cl	-	75

General conditions: Ester **2.34** (24.8 mg, 0.10 mmol), alkyl-9BBN **2.35** (0.30 mL, 0.50 M in THF, 0.15 mmol), [Pd] (5 mol%), ligand (5 mol%), Cs_2CO_3 (48.9 mg, 0.15 mmol), degassed H_2O (2.7 μL, 0.15 mmol), PhMe (0.60 mL), at 60 °C for 40 h, under inert atmosphere (set-up outside of the glovebox). [a]Yields calculated by ^{1}H NMR with 1,3,5-trimethoxybenzene as the internal standard.

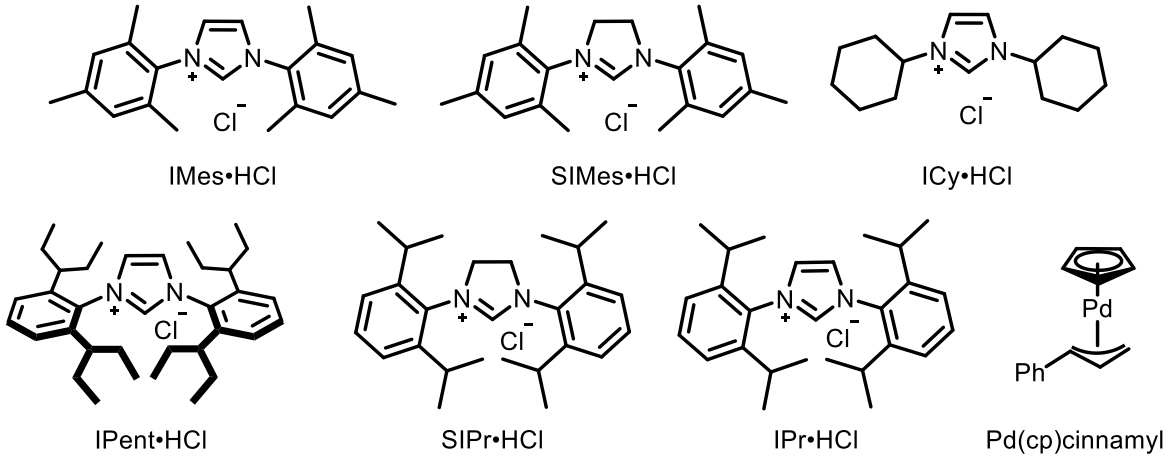

During the optimization, it was realized that the product and recovered starting material did not account for all the mass-balance. The formation of an unusual by-product was observed: butyl 2-naphthoate **2.37** (Scheme 45).

Scheme 45. Identification of an unusual by-product

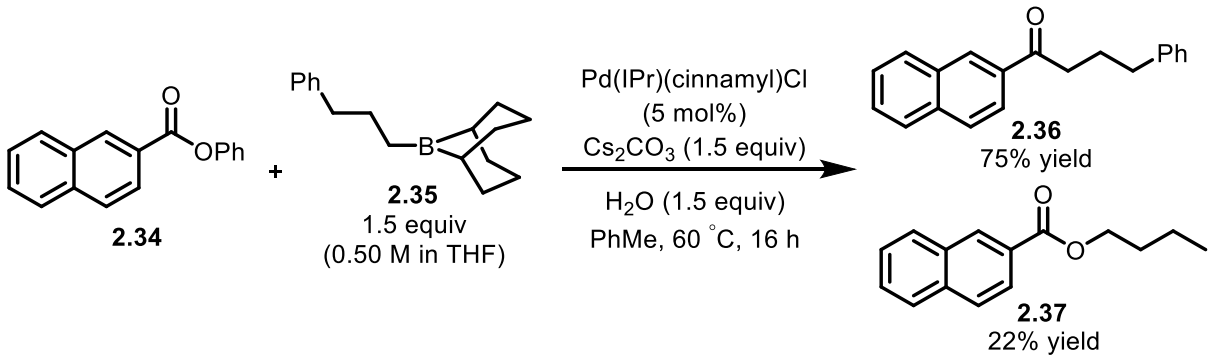

The formation of by-product **2.37** suggests that butanol is formed during the reaction. It is unclear, however, how the butanol formed. Plausibly, formal reductive cleavage of THF with the 9BBN hydride would result in formation of a source of butanol/butoxide (Scheme 46). However, this reduction should be mediated by the base since 9BBN hydride, by itself, can be stored as a solution in THF. Fortunately, removing THF from the reaction conditions suppressed the formation of by-product **2.37**.

Scheme 46. Formal reductive cleavage of THF

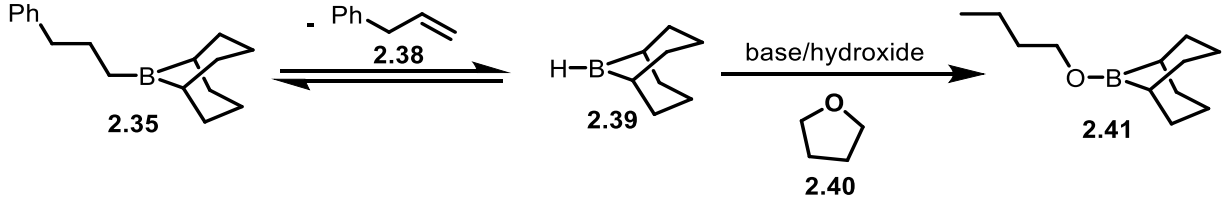

The base plays an important role in most cross-coupling reactions. Its main role in Suzuki-Miyaura couplings is to facilitate an otherwise challenging transmetalation. As can be seen in Table 2, the presence of a base was necessary in our reaction; no conversion was observed in its absence (entry 1). Sodium phenoxide and potassium fluoride were not suitable bases/additives (entries 2-3). By contrast, both potassium hydroxide and potassium phosphate promoted the reaction efficiently (entries 4-5). Cesium carbonate provided the desired product **2.36** in 74% yield (entry 6), and further addition of 1.5 equivalents of water reached near quantitative yield (entry 7).

Table 2. Screening of bases

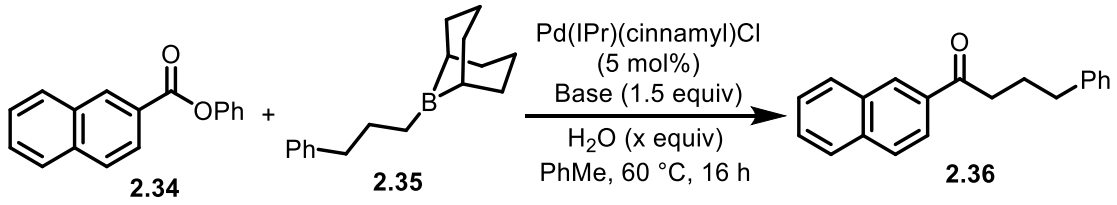

Entry	Base	Equiv of H_2O	%Yield of 2.36[a]
1	no base	0	0
2	NaOPh	0	0
3	KF	0	0
4	KOH	0	69
5	K_3PO_4	0	68
6	Cs_2CO_3	0	74
7	Cs_2CO_3	1.5	96

General conditions: Ester **2.34** (24.8 mg, 0.10 mmol), alkyl-9BBN **2.35** (0.30 mL, 0.50 M in PhMe, 0.15 mmol), Pd(IPr)(cinnamyl)Cl (3.3 mg, 5 mol%), base (0.15 mmol), additive (0.15 mmol), PhMe (0.60 mL) at 60 °C for 16 h, under inert atmosphere (set-up inside of the glovebox). [a]Yields are calculated by ^{1}H NMR with 1,3,5-trimethoxybenzene as the internal standard.

As for the temperature, we found 60 °C to be optimal (Table 3, entry 1). The use of higher temperatures resulted in lower yields and decomposition of the ester starting material (entries 2-3). Lower temperatures (< 60 °C) also gave lower yields (Table 4), but no decomposition of the starting material occurred in these cases.

Table 3. Effect of the temperature

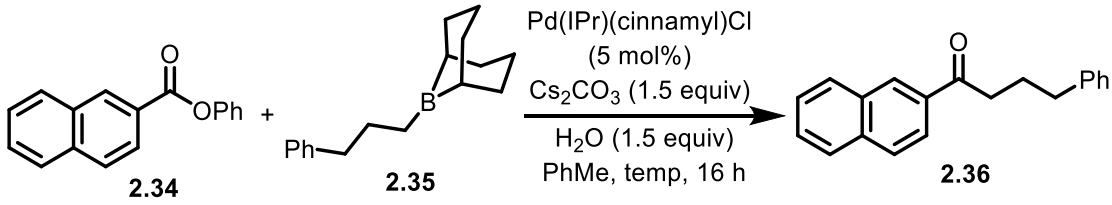

Entry	Temperature (°C)	%Yield of 2.36[a]
1	60	96
2	80	77
3	100	57

General conditions: Ester **2.34** (24.8 mg, 0.10 mmol), alkyl-9BBN **2.35** (0.30 mL, 0.50 M in PhMe, 0.15 mmol), Pd(IPr)(cinnamyl)Cl (3.3 mg, 5 mol%), Cs_2CO_3 (48.9 mg, 0.15 mmol), degassed H_2O (2.7 μL, 0.15 mmol), PhMe (0.60 mL) at the indicated temperature for 16 h, under inert atmosphere (set-up inside of the glovebox). [a]Yields are calculated by ^1H NMR with 1,3,5-trimethoxybenzene as the internal standard.

With the optimized conditions at hand (Table 3, entry 1), we tried scaling up from 0.10 mmol to 0.20 mmol before starting to evaluate the reaction scope. The reaction could be run on 0.20 mmol without any complication; the only modification necessary was to change the concentration from 0.11 M to 0.22 M in order to increase conversion.

Lastly, we were curious to probe whether Pd(IPr)(η^3-1-*t*-Bu-indenyl)Cl would be a superior catalyst to Pd(IPr)(cinnamyl)Cl since the former Pd catalyst had been shown to effectively promote the coupling of phenyl esters and aryl boronic acids at room temperature.[67] The results are listed in Table 4. At lower temperatures, the Pd(IPr)(η^3-1-*t*-Bu-indenyl)Cl catalyst was notably better than Pd(IPr)(cinnamyl)Cl. For instance, at 40 °C, Pd(IPr)(η^3-1-*t*-Bu-indenyl)Cl gave 87% yield of **2.36** whereas Pd(IPr)(cinnamyl)Cl gave 67% yield (entries 2-3). The Pd(IPr)(η^3-1-*t*-Bu-indenyl)Cl catalyst could even reach

[67] Lei, P.; Meng, G.; Shi, S.; Ling, Y.; An, J.; Szostak, R.; Szostak M. *Chem Sci.* **2017**, *8*, 6525–6530.

high yields at room temperature (entry 1). However, at 60 °C, there was not a significant difference between the efficiency of the two catalysts (entries 4-5).

Table 4. Pd(IPr)(η³-1-*t*-Bu-indenyl)Cl vs Pd(IPr)(cinnamyl)Cl

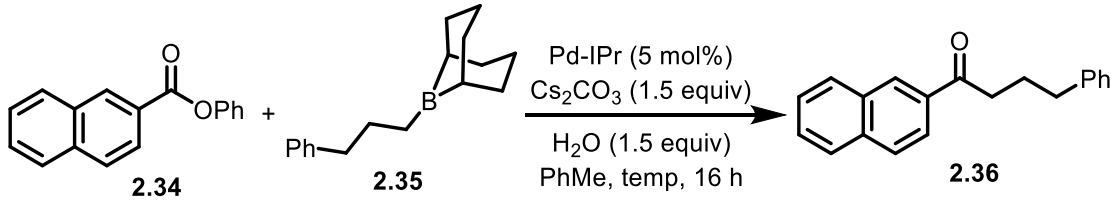

2.34 **2.35** **2.36**

Entry	Pd-IPr precatalyst	Temperature (°C)	%Yield of 2.36[a]
1	Pd(IPr)(η³-1-*t*-Bu-indenyl)Cl	22	76
2	Pd(IPr)(η³-1-*t*-Bu-indenyl)Cl	40	87
3	Pd(IPr)(cinnamyl)Cl	40	67
4	Pd(IPr)(η³-1-*t*-Bu-indenyl)Cl	60	82
5	Pd(IPr)(cinnamyl)Cl	60	89

General conditions: Ester **2.34** (49.7 mg, 0.20 mmol), alkyl-9BBN **2.35** (0.60 mL, 0.50 M in PhMe, 0.30 mmol), [Pd] (5 mol%), Cs_2CO_3 (97.7 mg, 0.30 mmol), degassed H_2O (5.4 μL, 0.30 mmol), PhMe (0.30 mL), at the indicated temperature for 16 h, under inert atmosphere (set-up inside of the glovebox). [a]Yields are calculated by ^1H NMR with 1,3,5-trimethoxybenzene as the internal standard.

The two catalysts were then tried with phenyl nicotinate with the aim of identifying which catalyst would perform best with a troublesome substrate (Table 5). At 60 °C, the Pd(IPr)(cinnamyl)Cl catalyst gave a slightly higher yield than when Pd(IPr)(η³-1-*t*-Bu-indenyl)Cl was used (entries 3-4). At lower temperatures, the Pd(IPr)(η³-1-*t*-Bu-indenyl)Cl catalyst gave even lower yields (entries 1-2). Even though the difference in yields between the two catalysts was not that significant, we decided to keep Pd(IPr)(cinnamyl)Cl as our catalyst since it is more readily available.

Table 5. Optimization with phenyl nicotinate

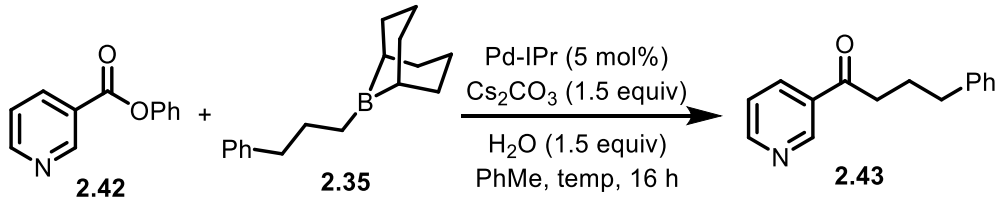

2.42 2.35 2.43

Entry	Pd-IPr pre-complex	Temperature (°C)	%Yield of 2.43[a]
1	Pd(IPr)(η^3-1-*t*-Bu-indenyl)Cl	22	19
2	Pd(IPr)(η^3-1-*t*-Bu-indenyl)Cl	40	23
3	Pd(IPr)(η^3-1-*t*-Bu-indenyl)Cl	60	28
4	Pd(IPr)(cinnamyl)Cl	60	34

General conditions: Ester **2.42** (39.8 mg, 0.20 mmol), alkyl-9BBN **2.35** (0.60 mL, 0.50 M in PhMe, 0.30 mmol), [Pd] (5 mol%), Cs_2CO_3 (97.7 mg, 0.30 mmol), degassed H_2O (5.4 μL, 0.30 mmol), PhMe (0.30 mL), at the indicated temperature for 16 h, under inert atmosphere (set-up inside of the glovebox). [a]Yields are calculated by ^1H NMR with 1,3,5-trimethoxybenzene as the internal standard.

With the optimized reaction conditions at hand (Scheme 47), we next turned our attention to the reaction scope.

Scheme 47. Optimized conditions for the alkylative coupling of phenyl esters

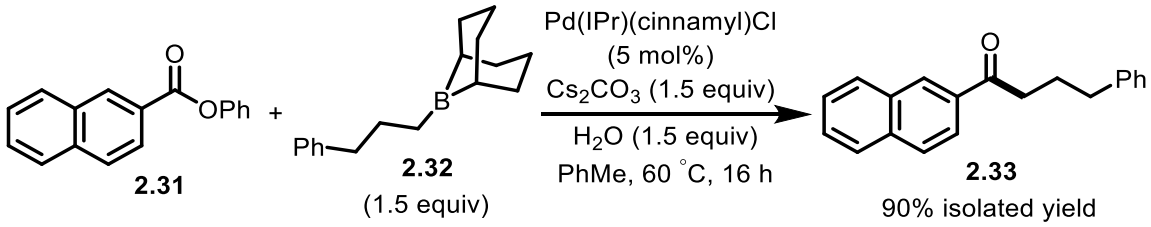

2.31 2.32 (1.5 equiv) 2.33 90% isolated yield

2.2.2. Reaction scope of the carbonyl-retentive couplings

Different aromatic and heteroaromatic esters were tested with the alkyl-B-9BBN reagent derived from allylbenzene **2.35**. Isolated yields are presented in Table 6. Electron-neutral aromatic esters provided high yields (entries 1 and 2), while electron-deficient aromatic

esters gave slightly lower yields (entries 3 and 4). Several heteroaromatics were tolerated on the ester substrates, including benzofuran (entry 5), furan (entries 6 and 7), and quinoline (entry 8).

Table 6. Scope of the ester in the carbonyl-retentive couplings

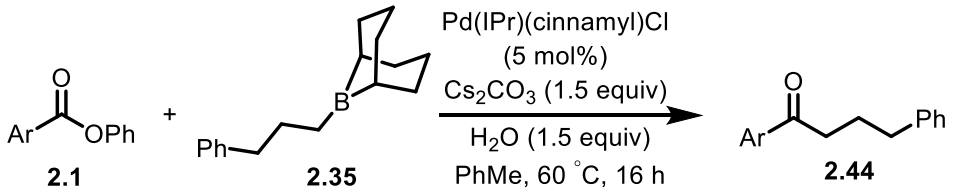

Entry	Ester starting material	Ketone product	%Yield[a]
1	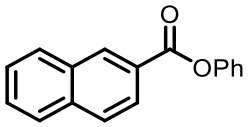 2.34	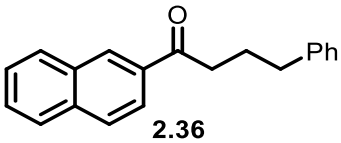 2.36	90
2	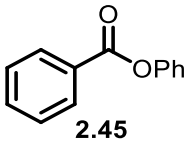 2.45	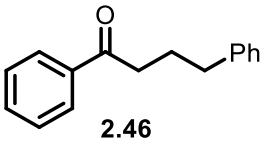 2.46	92
3	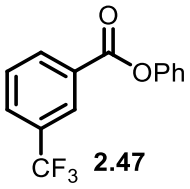 2.47	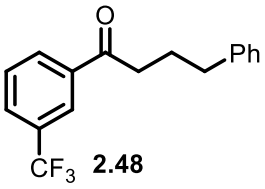 2.48	64
4	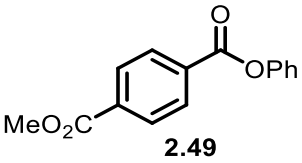 2.49	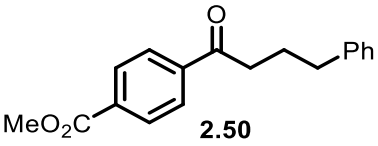 2.50	68
5	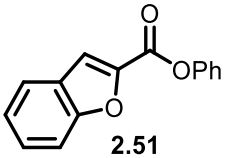 2.51	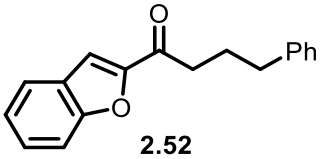 2.52	89
6	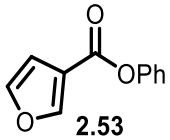 2.53	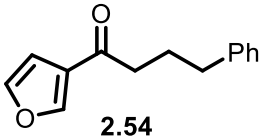 2.54	74

7	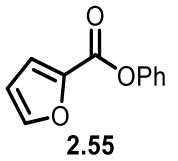 2.55	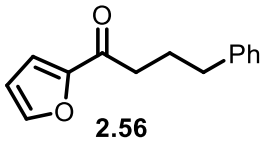 2.56	98
8	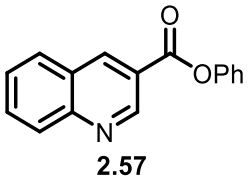 2.57	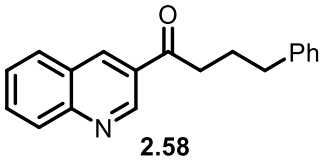 2.58	73

General conditions: Ester (0.20 mmol), alkyl-9BBN **2.35** (0.60 mL, 0.50 M in PhMe, 0.30 mmol), Pd(IPr)(cinnamyl)Cl (3.3 mg, 5 mol%), Cs_2CO_3 (97.7 mg, 0.30 mmol), degassed H_2O (5.4 μL, 0.30 mmol), PhMe (0.30 mL), at 60 °C for 16 h, under inert atmosphere (set-up inside of the glovebox). [a]Isolated yields.

Next, we briefly evaluated the scope of the alkyl-B-9BBN reagent (Table 7). The alkyl-B-9BBN derived from allylbenzene gave high conversion (entry 1); a fluorinated analog was also compatible but provided a lower yield (entry 2). An alkyl borane derived from 4-methoxystyrene was a suitable substrate as well (entry 3). Alkyl boranes with aliphatic chains bearing a TMS group (entry 4) or a cyclohexyl group (entry 5) also provided good yields of the ketone products.

Table 7. Alkyl-B-9BBN scope in the carbonyl-retentive couplings

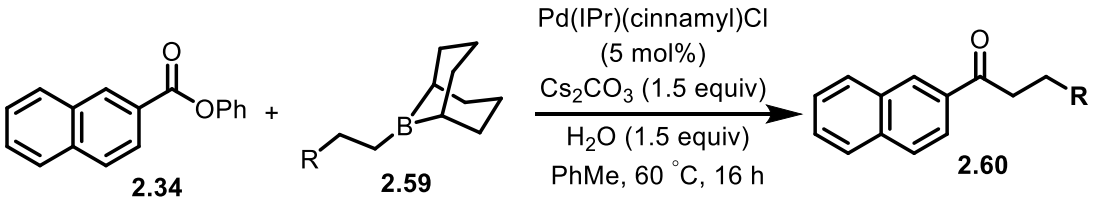

Entry	Alkyl borane	Ketone product	%Yield[a]
1	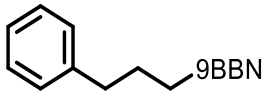 2.35	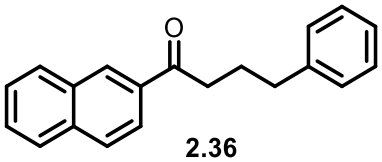 2.36	90

2	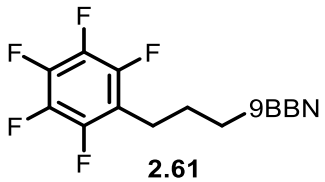 **2.61**	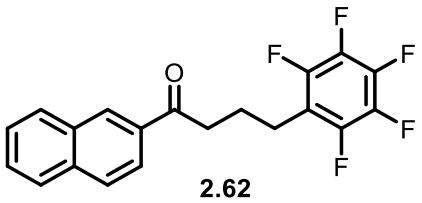 **2.62**	59
3	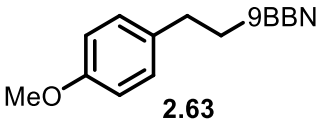 **2.63**	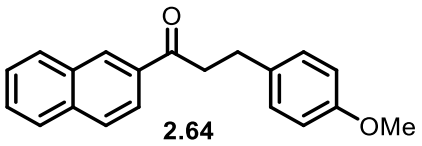 **2.64**	81
4	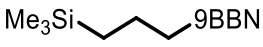 **2.65**	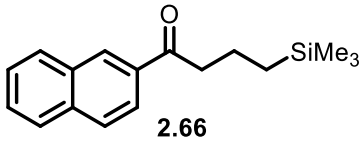 **2.66**	80
5	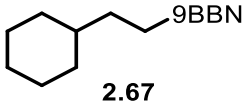 **2.67**	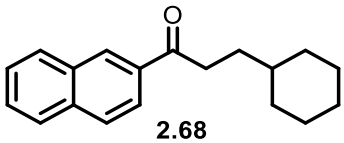 **2.68**	73

General conditions: Ester **2.34** (49.7 mg, 0.20 mmol), alkyl-9BBN **2.59** (0.60 mL, 0.50 M in PhMe, 0.30 mmol), Pd(IPr)(cinnamyl)Cl (3.3 mg, 5 mol%), Cs_2CO_3 (97.7 mg, 0.30 mmol), degassed H_2O (5.4 μL, 0.30 mmol), PhMe (0.30 mL), at 60 °C for 16 h, under inert atmosphere (set-up inside of the glovebox). [a]Isolated yields.

2.2.3. Optimization of the decarbonylative couplings

After enabling the carbonyl-retentive reaction mode, we probed whether we could also develop a decarbonylative alkylative pathway. It was anticipated that this reaction pathway would be more challenging to optimize due to β-hydride elimination. By contrast, in the carbonyl-retentive pathway, β-hydride elimination was not much of a concern. Plausibly, the bulky NHC ligand, while preventing decarbonylation, also prevents β-hydride elimination.

Preventing β-hydride elimination under decarbonylative conditions is a complex issue. This is because an open coordination site on the metal is required to enable decarbonylation, but an open coordination site should be avoided if beta-hydride elimination is undesired (Scheme 48). We hypothesized that the optimal ligand that could

access decarbonylative alkylative couplings would be labile enough to allow decarbonylation, but robust enough to prevent beta-hydride elimination.

Scheme 48. Risk of β-hydride elimination under decarbonylative conditions

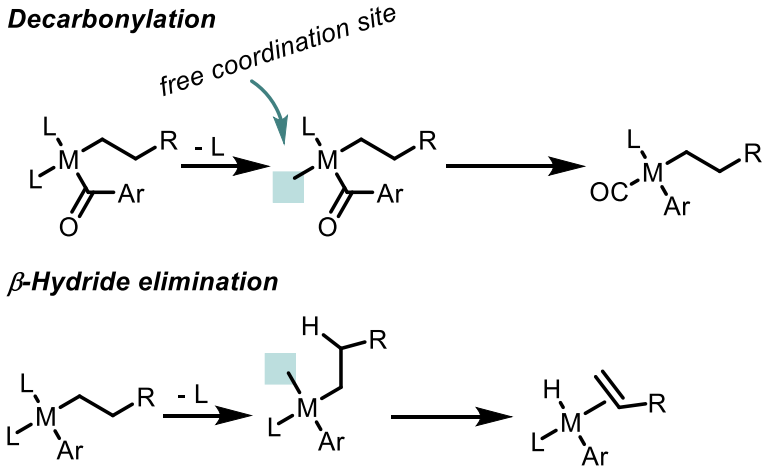

Because β-hydride elimination was anticipated to be a major side-reaction, 2-phenylnaphthoate **2.34** was chosen as the model substrate since its reduced product, naphthalene, is easily observable and quantifiable by the GC/FID. At the outset of our investigation, initial experiments were carried out in the high-throughput screening facility. A 48-well plate was designed using knowledge from previous literature reports disclosing similar types of couplings (Figure 10).

The main variable of the plate was the ligand. A wide array of monodentate and bidentate phosphine ligands were selected, as well as a tridentate phosphine and two NHC ligands. Most ligands were chosen based on literature reports of similar coupling reactions (e.g. dcype, ICy). Some ligands were also selected from what was available in our ligand library (e.g. P(*i*-Bu)$_3$, L1). Since both Pd- and Ni-catalyzed decarbonylative couplings have been reported with phenyl esters, all the ligands were tried with both Ni and Pd pre-catalysts.

Figure 10. 48 well plate for the decarbonylative couplings[68]

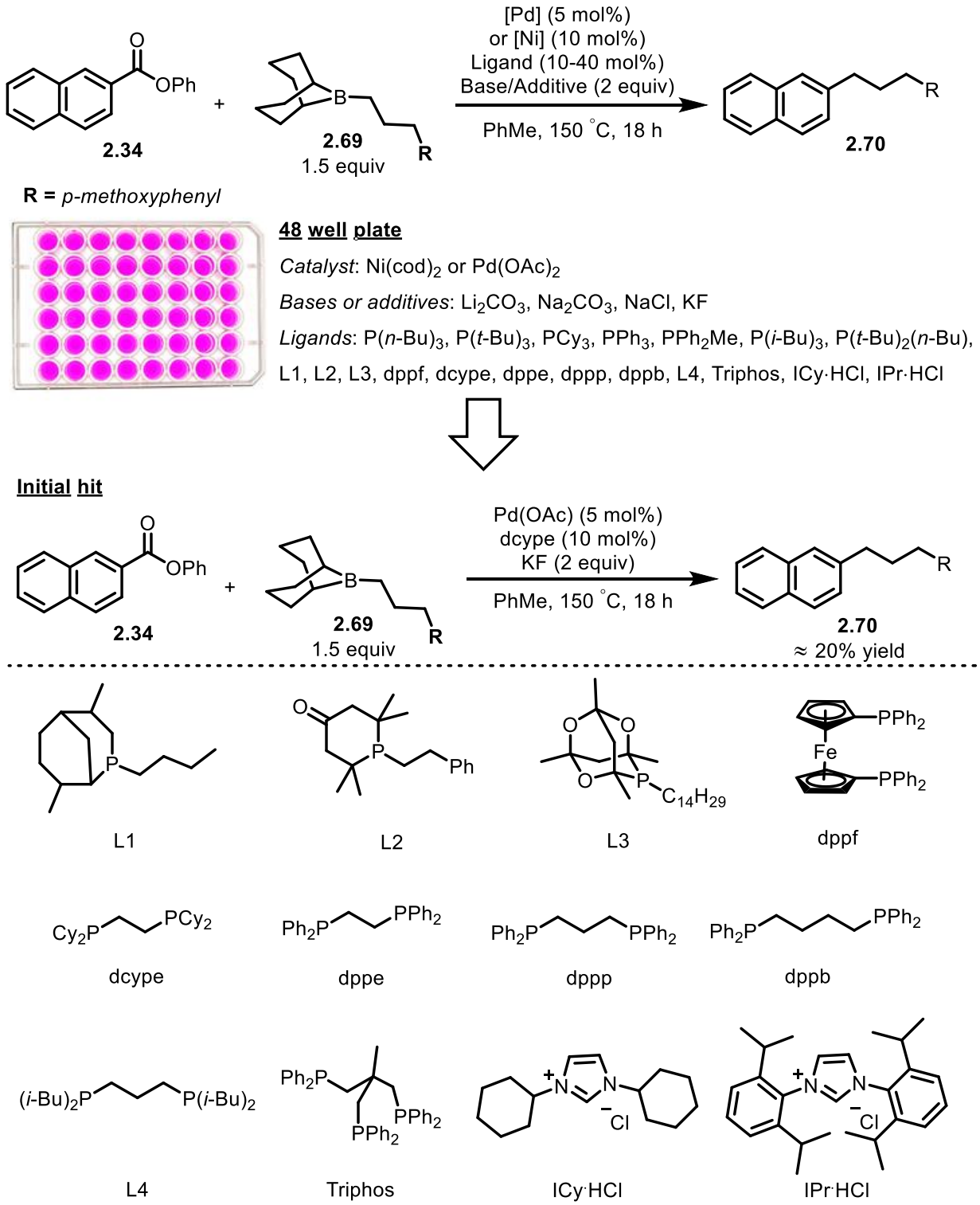

[68] The picture of the 48 well plate was taken from: https://www.mattek.com/store/p48g-1-5-6-f-case/

An initial hit was obtained with $Pd(OAc)_2$, dcype and KF as an additive, providing an approximate yield of 20%. It was later realized that the type of vial used had a considerable effect on conversion. When the same reaction was performed in an 8 mL reaction vial instead of in the small 1 mL glass vial, product **2.70** was obtained in 67% yield. It is plausible that the larger head-space is required to favour CO extrusion.

Several different Pd precursors were then screened (Table 8). No improvement in yield was observed when $[Pd(allyl)Cl]_2$ was used the Pd precatalyst (entries 1 and 2). On the other hand, when using Pd(II) precursors that are known to rapidly form Pd(0) in the presence of a phosphine ligand, the yield increased by roughly 10% (entries 3 and 4). A pre-complexed $Pd(dcype)Cl_2$ performed equally as well (entry 5). Running the reaction at 150 °C instead of 160 °C also provided satisfactory conversion (entry 6). The 5 mol% of free dcype ligand is not necessary but slightly beneficial (entry 7). Entries 8-10 describe the fine-tuning optimization when scaling up from 0.10 mmol to 0.20 mmol. A lower yield was initially obtained when scaling up (entry 8), and the rest of the mass-balance was unreacted ester starting material. Increasing the reaction concentration solved the issue (entry 9). It is worth mentioning that all these reactions were set-up outside of the glovebox, where the reactions vials were degassed with an argon balloon. Performing the whole set-up in the glovebox gave near quantitative yield (entry 10).

Table 8. Screening of Pd precursors for the decarbonylative couplings

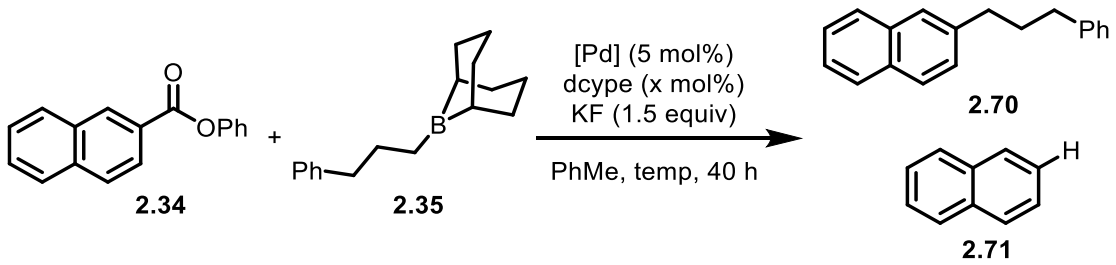

Entry	Pd pre-catalyst	x	Temp (°C)	%Yield of 2.70[a]	%Yield of 2.71[b]
1	$Pd(OAc)_2$	10	160	72	8
2	$[Pd(allyl)Cl]_2$	10	160	70	11
3	Pd(Cp)(allyl)	10	160	83	11
4	$Pd(COD)(CH_2TMS)_2$	10	160	80	5
5	$Pd(dcype)Cl_2$	5	160	84	10
6	$Pd(dcype)Cl_2$	5	150	78	5
7	$Pd(dcype)Cl_2$	0	150	71	7
8[c]	$Pd(dcype)Cl_2$	5	160	56	8
9[d]	$Pd(dcype)Cl_2$	5	160	80	9
10[e]	$Pd(dcype)Cl_2$	5	160	98	< 2

General conditions: Ester **2.34** (24.8 mg, 0.10 mmol), alkyl-9BBN **2.35** (0.30 mL, 0.50 M in PhMe, 0.15 mmol), [Pd] (5 mol%), dcype (x mol%), KF (8.7 mg, 0.15 mmol), PhMe (0.60 mL) at the indicated temperature for 16 h, under inert atmosphere (set-up outside of the glovebox). [a]Yields were calculated by ^1H NMR with 1,3,5-trimethoxybenzene as the internal standard. [b]Yields were calculated with a GC/FID calibration curve. [c]Run on 0.20 mmol scale. [d]Run on 0.20 mmol scale, with increased concentration (0.22 M). [e]Run on 0.20 mmol scale, at 0.22 M, and set-up inside of the glovebox.

After optimization, an irreproducibility issue occurred. After some troubleshooting, we identified the problem as being the new batch of $Pd(dcype)Cl_2$ from Aldrich. Although there was no clear impurity by ^{31}P and ^1H NMR, the Pd catalyst was not performing like the previous batch, giving < 20% yield of **2.70** and a lot of naphthalene **2.71** when using

the conditions described in Table 8 (entry 10). We thus decided to use $Pd(OAc)_2$ (5 mol%), and dcype (10 mol%) for the reaction scope, which provided consistent and reliable yields.

Table 9 shows selected optimization data that gives valuable information about the disclosed reaction. In contrast to the carbonyl-retentive coupling protocol, some reasonable conversion could be obtained in the absence of any base or additive (entry 1). However, potassium fluoride as an additive not only increases conversion but also gives significantly better selectivity for the desired product **2.70** over the reduced product **2.71** (entry 2). Increasing the temperature from 130 °C to 160 °C provided a significant increase in yield (entry 3). Interestingly, when using $Ni(cod)_2$ instead of $Pd(OAc)_2$, the formation of the reduced product **2.71** is favoured, providing a very low yield of the desired product **2.70** (entry 4).

Table 9. Selected optimization for the decarbonylative couplings

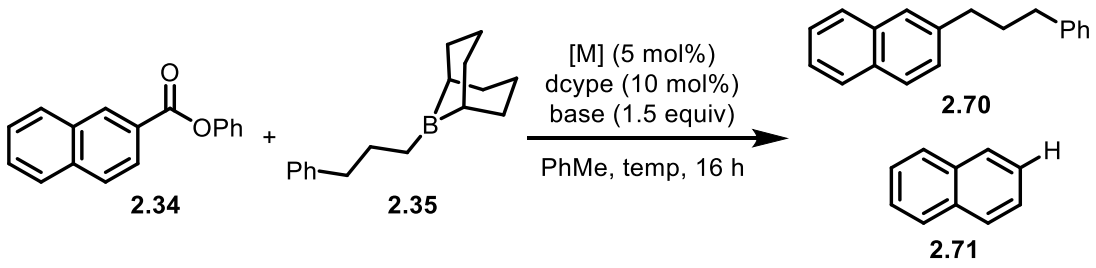

Entry	Metal source	Base	Temp (°C)	%Yield of 2.70[a]	%Yield of 2.71[b]
1	$Pd(OAc)_2$	none	130	58	21
2	$Pd(OAc)_2$	KF	130	66	7
3	$Pd(OAc)_2$	KF	160	82	13
4[c]	$Ni(cod)_2$	KF	160	12	60

General conditions: Ester **2.34** (24.8 mg, 0.10 mmol), alkyl-9BBN **2.35** (0.30 mL, 0.50 M in PhMe, 0.15 mmol), [M] (5 mol%), dcype (4.2 mg, 10 mol%), KF (8.7 mg, 0.15 mmol), PhMe (0.60 mL) at the indicated temperature for 16 h, under inert atmosphere (set-up inside of the glovebox). [a]Yields were calculated by ^1H NMR with 1,3,5-trimethoxybenzene as the internal standard. [b]Yields were calculated with a GC/FID calibration curve. [c]10 mol% $Ni(cod)_2$ was used with 20 mol% dcype.

2.2.4. Reaction scope of the decarbonylative couplings

Eight different esters were successfully coupled to afford the corresponding alkylated arenes (Table 12). Electron neutral and electron poor aromatic esters provided good yields (entries 1-3), while electron-rich esters offered excellent yields (entries 4 and 5). Pleasingly, our coupling reaction was also compatible with esters bearing pyrazine or pyridine motifs (entries 6-8).

Table 10. Ester scope for the decarbonylative couplings

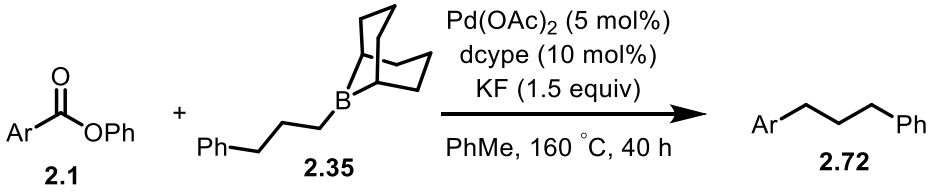

Entry	Ester starting material	Decarbonylated product	%Yield[a]
1	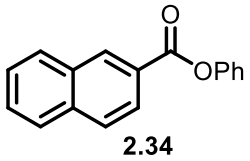 2.34	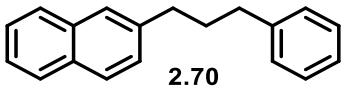 2.70	78
2	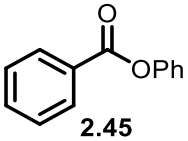 2.45	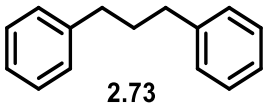 2.73	64[b]
3	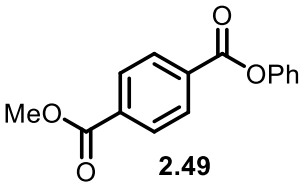 2.49	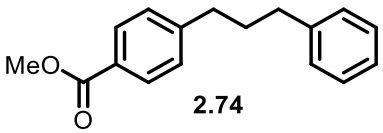 2.74	65
4	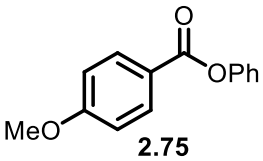 2.75	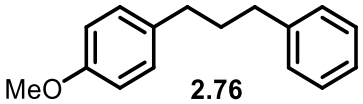 2.76	80

5	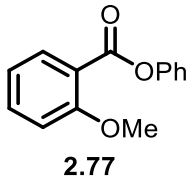 **2.77**	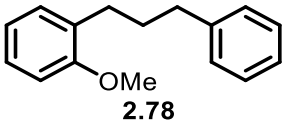 **2.78**	91
6	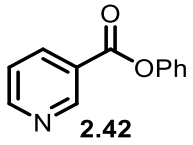 **2.42**	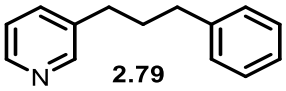 **2.79**	61
7	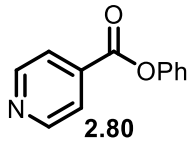 **2.80**	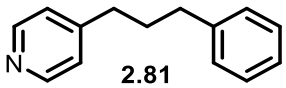 **2.81**	87
8	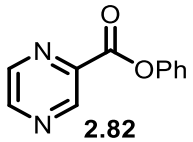 **2.82**	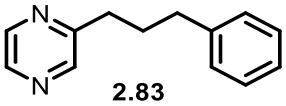 **2.83**	52[b]

General conditions: Ester (0.20 mmol), alkyl-9BBN **2.35** (0.60 mL, 0.50 M in PhMe, 0.30 mmol), $Pd(OAc)_2$ (2.2 mg, 5 mol%), dcype (8.4 mg, 10 mol%), KF (17.4 mg, 0.30 mmol), PhMe (0.30 mL), at 160 °C for 40 h, under inert atmosphere (set-up inside of the glovebox). [a]Isolated yields. [b]$Pd(COD)(CH_2TMS)_2$ (3.9 mg, 5 mol%) was used in place of $Pd(OAc)_2$.

It should be noted that, while most substrates didn't require more than 16 hours to react fully, other esters beneficiated from the longer reaction time. For example, ester **2.77** (see Table 10, entry 5) gave 87% yield of **2.78** after 16 h, while a quantitative yield was obtained after 40 h.[69] Thus, a reaction time of 40 hours was used for the scope to ensure that all the substrates would reach full completion.

Next, the scope of the B-alkyl-B-9BBN reagents was briefly explored (Table 11). Alkyl boranes derived from allylbenzene (**2.32**) and safrole (**2.81**) worked very well (entries 1 and 2). Notably, alkyl borane **2.83** having a benzylic β-hydrogen could also be coupled

[69] Yields of **2.74** were calculated by ^1H NMR with 1,3,5-trimethoxybenzene as the internal standard.

successfully (entry 3). Aliphatic boranes were compatible coupling partners as well, affording moderate yields of the decarbonylated adducts (entries 4 and 5).

Table 11. Alkyl-9BBN scope for the decarbonylative couplings

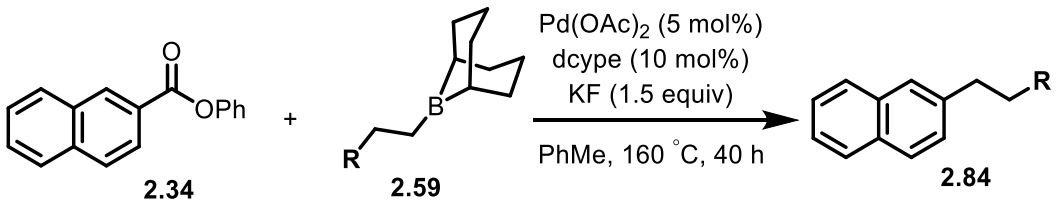

Entry	Alkyl borane	Decarbonylated product	%Yield[a]
1	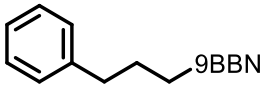 9BBN **2.35**	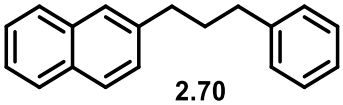 **2.70**	78
2	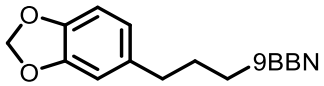 9BBN **2.85**	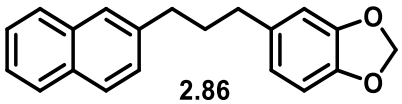 **2.86**	78
3	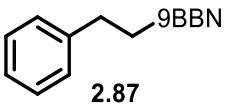 9BBN **2.87**	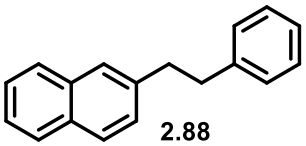 **2.88**	54
4	$H_3C(CH_2)_{10}$ 9BBN **2.89**	$(CH_2)_{10}CH_3$ **2.90**	63
5	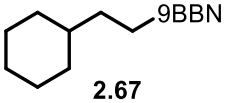 9BBN **2.67**	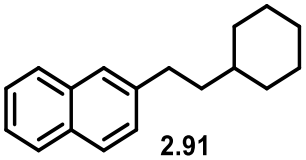 **2.91**	48[b]

General conditions: Ester **2.34** (0.20 mmol), alkyl-9BBN (0.60 mL, 0.50 M in PhMe, 0.30 mmol), $Pd(OAc)_2$ (2.2 mg, 5 mol%), dcype (8.4 mg, 10 mol%), KF (17.4 mg, 0.30 mmol), PhMe (0.30 mL), at 160 °C for 40 h, under inert atmosphere (set-up inside of the glovebox). [a]Isolated yields. [b]$Pd(COD)(CH_2TMS)_2$ (3.9 mg, 5 mol%) was used in place of $Pad(OAc)_2$.

For all scope examples, full conversion was reached, and the rest of the mass-balance was accounted by the formation of the undesired reduced by-product. As with all newly

disclosed catalytic reactions, our system has some limitations. While the Pd-dcype catalyst was able to favour reductive elimination over β-hydride elimination for many substrates, some esters gave the reduced product predominantly. Some failed substrates are illustrated in Figure 11. In these cases, β-hydride elimination was the major pathway, and less than 30% yield of the desired product was obtained.

Figure 11. Unsuccessful esters in the decarbonylative couplings

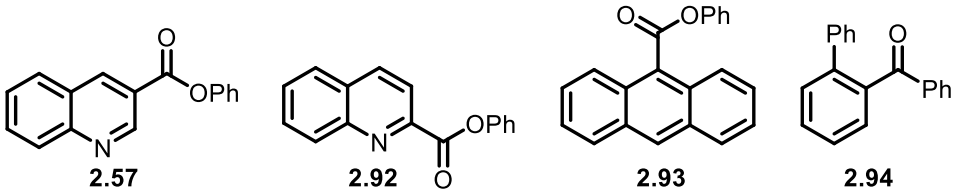

Ester **2.95** and ester **2.51** also failed due to β-hydride elimination, but unusual by-products were observed in these cases (Scheme 49). Formal dimerization of the reduced products occurred. Such oxidative couplings have been documented before by the Itami lab with oxazole and thiazole derivatives but not with simple furans or thiophenes.[70]

[70] Amaike, K.; Muto, K.; Yamaguchi, J.; Itami, K. *J. Am. Chem. Soc.* **2012**, *134*, 13573−13576.

Scheme 49. Unusual by-products from the decarbonylative couplings

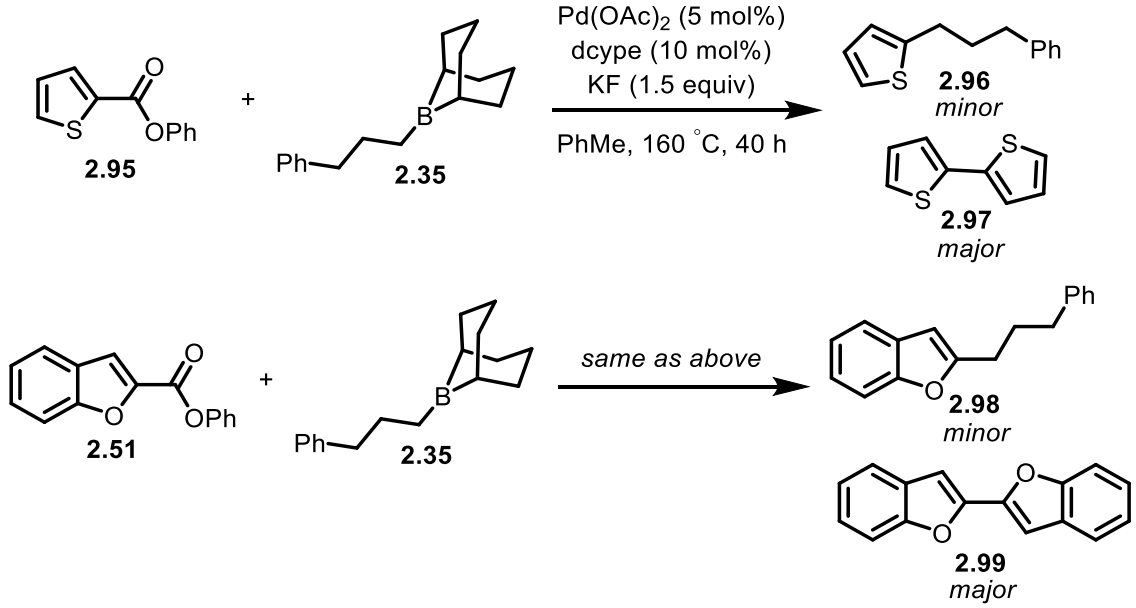

2.2.5. Derivatization of bioactive molecules

To further showcase the practicality of enabling two different reaction modes from a single starting material, the diversification of bioactive molecules was performed. First, the phenyl esters of repaglinide (antidiabetic drug) and probenecid (medecine used to treat gout and hyperuricemia) were synthesized (see Figure 12 for chemical structures of repaglinide and probenecid).

Figure 12. Chemical structures of repaglinide and probenecid

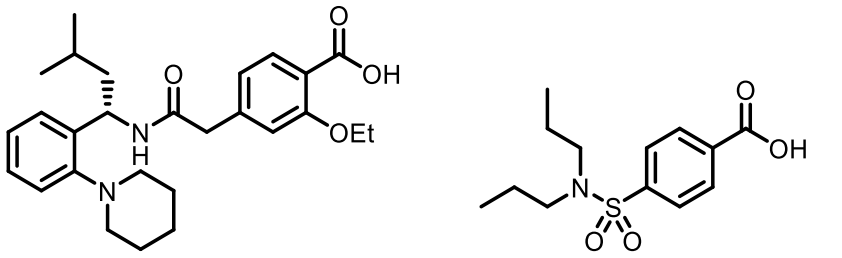

repaglinide
antidiabetic drug

probenecid
drug for gout and hyperuricemia

The repaglinide phenyl ester **2.100** was first derivatized (Scheme 50). The carbonyl-retentive reaction worked moderately well, necessitating a higher Pd loading of 10 mol%

to afford 45% yield of **2.101**, along with recovered unreacted phenyl ester starting material **2.100**. Plausibly, the oxidative addition of Pd into the phenyl ester is hindered by the ortho-methoxy group both in terms of electronic and steric effects. The decarbonylative coupling worked more efficiently. Safrole-derived B-alkyl-9-BBN **2.85** was used instead of the allylbenzene-derived one, merely to simplify subsequent purification. Formation of the reduced product accounted for the rest of the mass-balance in this case.

Scheme 50. Derivatization of repaglinide[a]

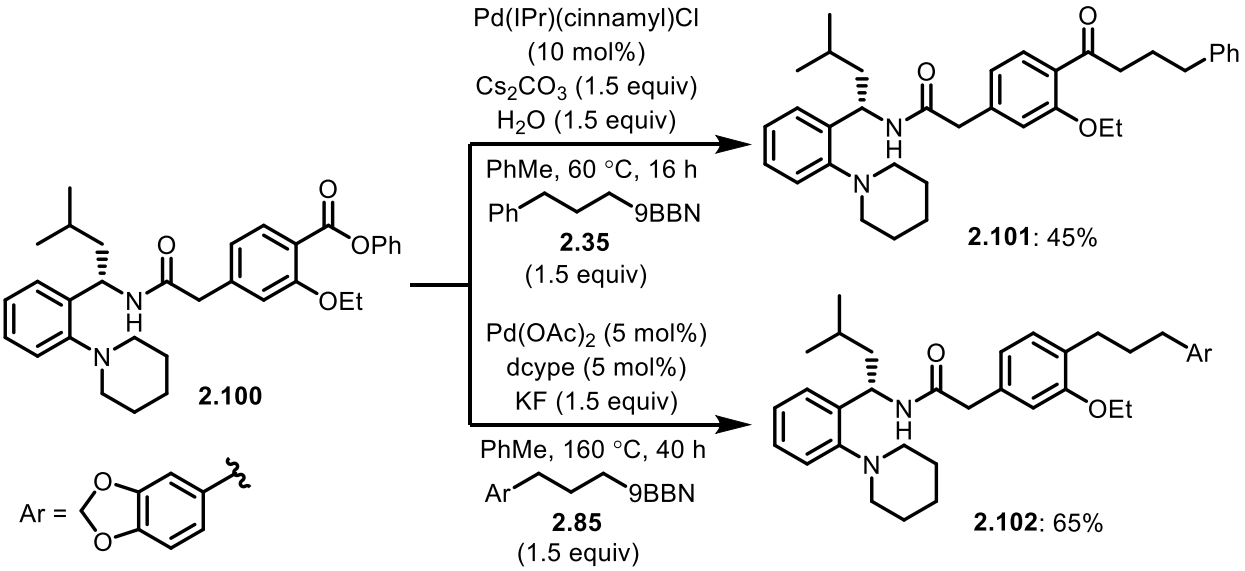

Next, we aimed at applying our two coupling reactions for the diversification of probenecid phenyl ester **2.103** (Scheme 51). To demonstrate that our coupling reaction was scalable, we performed these reactions on a 3 mmol scale. We were also able to reduce the [Pd] loading to 3 mol%. The carbonyl-retentive mode gave an excellent yield of the corresponding ketone derivative **2.104**. The decarbonylative coupling could also be enabled, providing product **2.105** in 69% yield. Some product was lost during the

challenging purification process, while the rest of the mass-balance was the reduced product arising from β-hydride elimination.

Scheme 51. Scaled-up cross-coupling reactions with probenecid phenyl ester

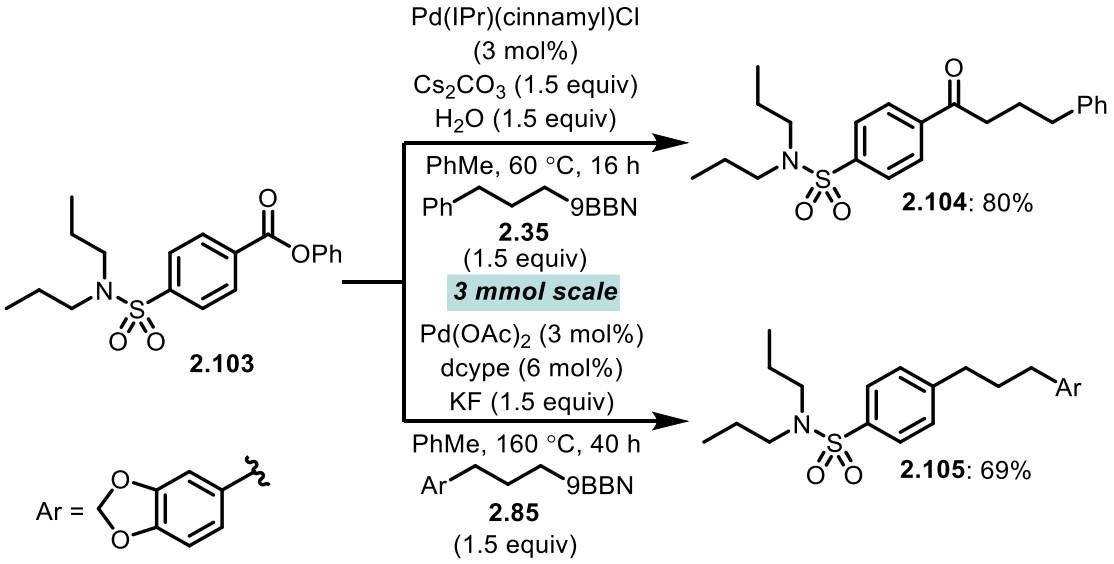

2.2.6. Mechanistic insights and discussion

In brief, we demonstrated that both a carbonyl-retentive and a decarbonylative reaction mode could be enabled when coupling phenyl esters and alkyl boranes, with a selectivity likely controlled by the catalyst. However, there is a significant temperature gap between the two optimized couplings. Thus, to corroborate that the selectivity control is not temperature-dependent, we ran some cross-experiments (Scheme 52). When the Pd-IPr catalyst was used at 160 °C, no trace of decarbonylated product **2.70** was observed (full recovery of starting material **2.34**), suggesting that this catalyst is uniquely effective for carbonyl-retentive couplings but unsuitable for decarbonylative couplings. Interestingly, no ketone **2.36** was observed either, probably because the catalyst decomposes at this elevated temperature. Similarly, when the Pd-dcype catalyst was employed at 60 °C, no product was observed along with full recovery of the starting material **2.34**. This indicates

that the Pd-dcype catalyst is inefficient at promoting carbonyl-retentive reaction mode, and high-temperature is probably required for decarbonylation.

Scheme 52. Cross-experiments

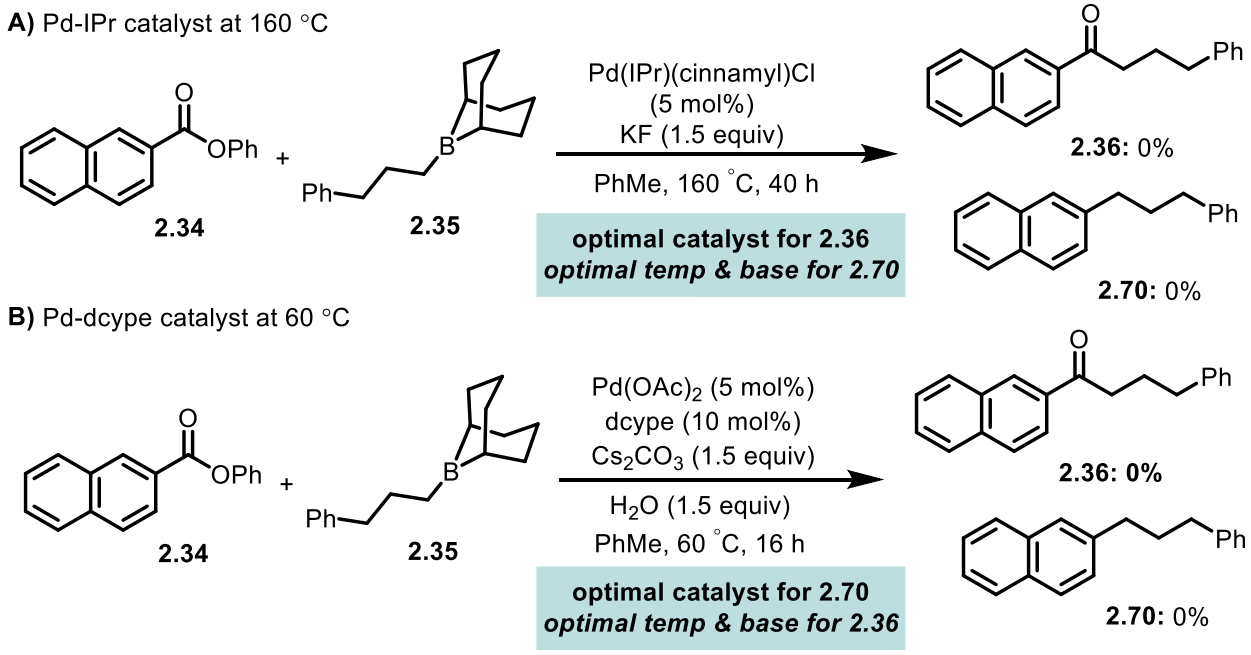

Throughout this project, three major products were observed and quantified, namely alkyl ketones **2.107**, alkylated arenes **2.108** and reduced arenes **2.18**. Possible mechanisms to explain the formation of these three products are illustrated in a common catalytic cycle in Scheme 53. Before entering the catalytic cycle, reduction of the Pd(II) pre-catalyst to Pd(0) is required. Then, it is likely that all mechanisms begin with oxidative addition of Pd(0) into the weak C(acyl)–O bond of the phenyl ester as has been proposed and experimentally proven in related couplings.[65,71]

[71] (a) Hong, X.; Liang, Y.; Houk, K. N. *J. Am. Chem. Soc.* **2014**, *136*, 2017–2025; (b) Hie, L.; Fine Nathel, N. F.; Shah, T. K.; Baker, E. L.; Hong, X.; Yang, Y.-F.; Liu, P.; Houk, K. N.; Garg, N. K. *Nature* **2015**, *524*, 79–83; (c) Pu, X.; Hu, J.; Zhao, Y.; Shi, Z. *ACS Catal.* **2016**, *6*, 6692−6698.

Scheme 53. Proposed mechanism

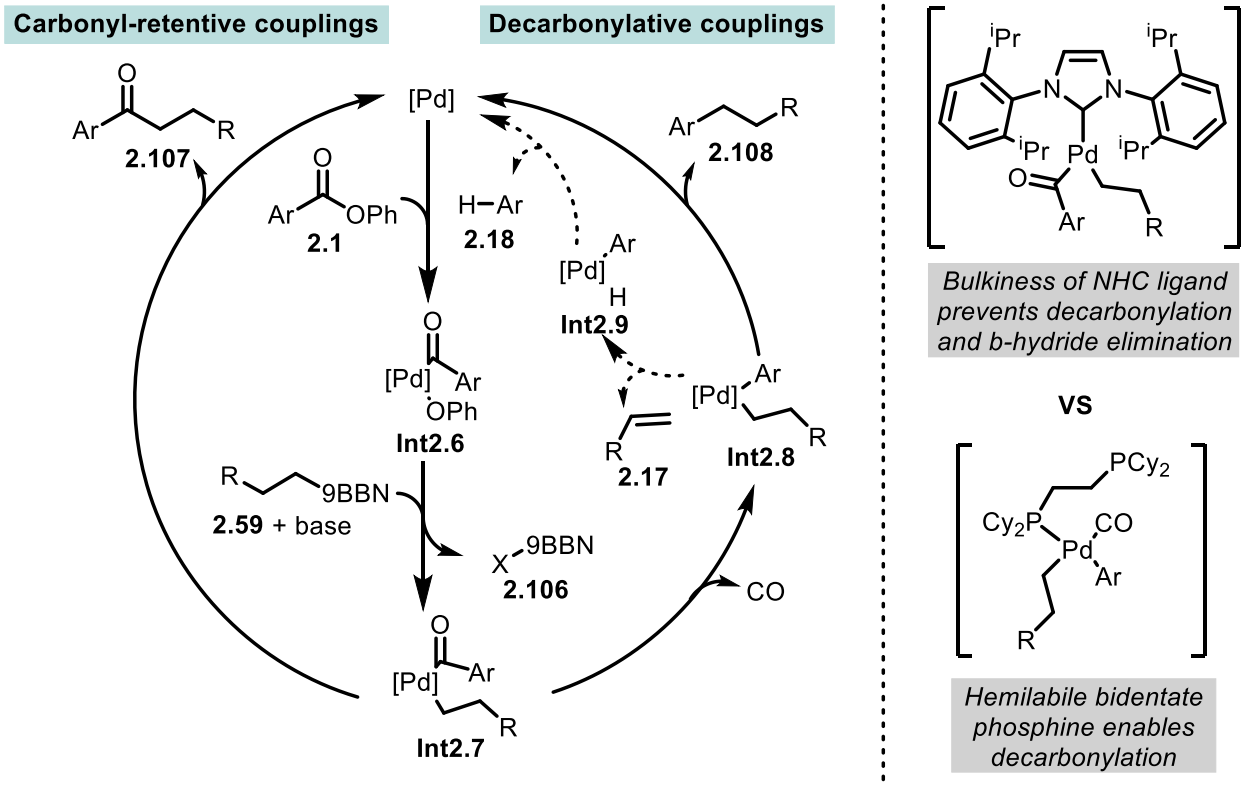

The resulting Pd-acyl intermediate **Int2.6** can then undergo transmetalation with the organoboron species to form **Int2.7**. Additives such as KF or Cs_2CO_3/H_2O can facilitate this step.[72] Following transmetalation, either direct reductive elimination to afford ketone product **2.107** or decarbonylation to form Pd intermediate **Int2.8** can occur. Which pathway occurs will depend on both the nature of the ligand. As we saw previously, Pd-IPr favours the carbonyl-retentive mode, wherein the steric bulk of the NHC ligand slows down decarbonylation and favours reductive elimination.[73] In contrast, at elevated temperatures with Pd-dcype as the catalyst, decarbonylation is favoured over reductive

[72] Amatore and Jutand performed extensive mechanistic studies on the role of hydroxide and fluoride ions in Pd-catalyzed Suzuki-Miyaura reactions. See: (a) Amatore, C.; Jutand, A.; Le Duc, G. *Chem. Eur. J.* **2011**, *17*, 2492–2503; (b) Amatore, C.; Jutand, A.; Le Duc, G. *Angew. Chem.* **2012**, *124*, 1408–1411.

[73] For DFT studies on the Pd-IPr catalyst in a carbonyl-retentive coupling reaction, see: Ben Halima, T.; Zhang, W.; Yalaoui, I.; Hong, X.; Yang, Y.-F.; Houk, K. N.; Newman, S. G. *J. Am. Chem. Soc.* **2017**, *139*, 1311–1318.

elimination. The hemi-labile nature of the bidentate phosphine is key to enable decarbonylation.[74] After CO extrusion, Pd intermediate **Int2.8** can undergo reductive elimination to form alkylated arene **2.108**. Alternatively, β-hydride elimination can occur to form Pd intermediate **Int2.9**; subsequent reductive elimination would then give the reduced product **2.18**.

2.3. Summary and future work

Aryl esters exhibit promising properties in cross-coupling reactions. Three activation modes have been independently reported with these electrophiles, and DFT calculations from the Houk group have helped to rationalize the selectivity preference of certain catalysts.

Alkylative couplings with phenyl esters lacked in the field. In response to this, we developed an alkylative Suzuki-Miyaura coupling protocol with phenyl esters. We used the mechanistic groundwork from Houk to quickly identify efficient catalysts that could selectively enable both the carbonyl-retentive and decarbonylative reaction modes. Our optimized conditions are summarized in Scheme 54. The developed coupling reactions allowed access to various (hetero)aryl alkyl ketones and alkylated (hetero)aromatic compounds.

[74] Several reports suggest dissociation of one of the phosphine arms of dcype prior to decarbonylation. See: (a) Hong, X.; Liang, Y.; Houk, K. N. *J. Am. Chem. Soc.* **2014**, *136*, 2017−2025; (b) Lu, Q.; Yu, H.; Fu, Y. *J. Am. Chem. Soc.* **2014**, *136*, 8252−8260.

Scheme 54. Pd-catalyzed alkylative cross-couplings of phenyl esters

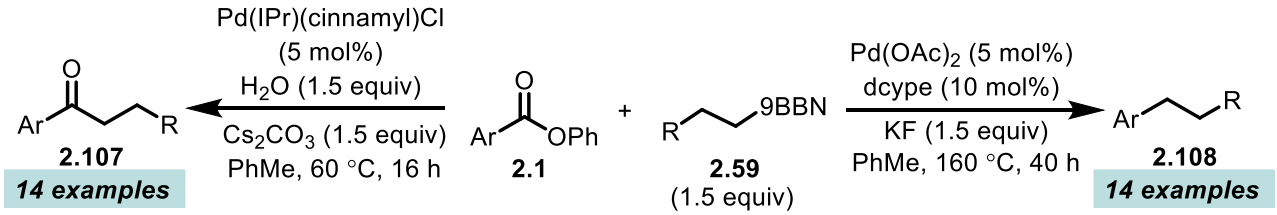

During the preparation of our manuscript, the Rueping lab disclosed very similar research,[75] which unfortunately partly compromised the novelty of our work. In their report, they also described cross-couplings of phenyl esters with alkyl boranes, and they enabled both the carbonyl-retentive and decarbonylative reaction modes as well (Scheme 55). However, Ni catalysis was used in their case.

Scheme 55. Rueping's Ni-catalyzed cross-coupling of esters with alkyl boranes

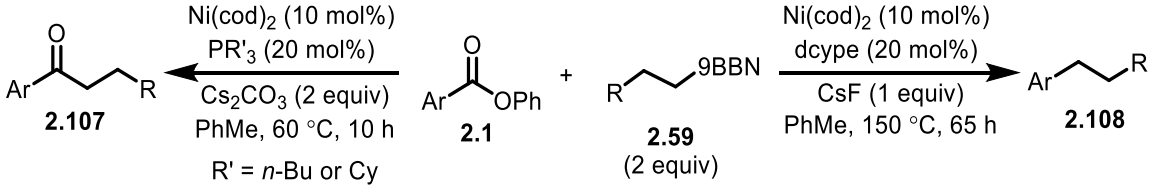

Interestingly, they found that $Ni(cod)_2$ with dcype as a ligand was an efficient catalyst to promote the decarbonylative reaction mode, whereas we found this catalyst to predominantly give the undesired reduced product during our optimization. The fact that they used a different model substrate than us for their optimization partly explains why they found Ni to be more efficient than Pd. They used benzofuran-2-carboxylic acid phenyl ester **2.51** as a model substrate, and this substrate failed with the Pd-dcype catalyst system (Table 12, entry 1). Their catalyst works efficiently for (benzo)furan and (benzo)thiophene esters, while Pd-dcype is inefficient with these substrates (Table 12, entries 1 and 2). On the other hand, our catalyst could tolerate N-containing

[75] Chatupheeraphat, A.; Liao, H.-H.; Srimontree, W.; Guo, L.; Minenkov, Y.; Poater, A.; Cavallo, L.; Rueping, M. *J. Am. Chem. Soc.* **2018**, *140*, 3724–3735.

heteroaromatic esters, which were notably absent from Rueping's reaction scope (entries 3 and 4). Both catalyst systems work well with electron-poor or electron-neutral aromatic esters, although, in Rueping's system, an excess of dcype ligand needs to be used to achieve moderately low to good yields (entries 5 and 6). Notably, the Pd-dcype catalyst seems to be better at couplings of electron-rich aromatic esters (entries 7 and 8). Another advantage that our decarbonylative protocol offers over theirs is that B-alkyl-9-BBN with benzylic β-hydrogens can be employed.

Table 12. Comparing our decarbonylative coupling to Rueping's

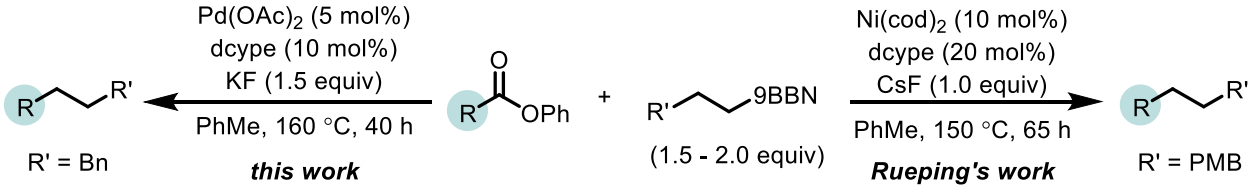

Entry	Ester starting material	Rueping: Ni-dcype	This work: Pd-dcype
	Thiophene or furan esters	*Yes*	*No*
1	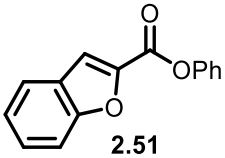 **2.51**	95% yield	< 20% yield
2	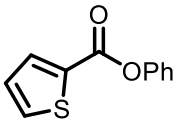 **2.95**	83% yield	< 20% yield
	Pyridine or pyridine esters	*No*	*Yes*
3	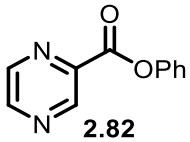 **2.82**	-	52% yield
4	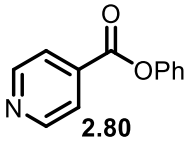 **2.80**	-	87% yield

	Electron-poor or -neutral	*Yes*	*Yes*
5	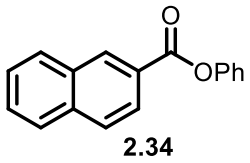 **2.34**	73% yield[a]	78% yield
6	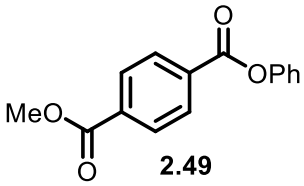 **2.49**	43% yield[a]	65% yield
	Electron-rich	*No*	*Yes*
7	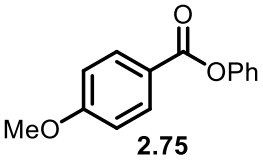 **2.75**	37% yield[a]	80% yield
8	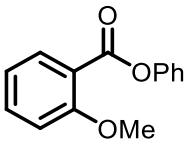 **2.77**	-	91% yield

[a] 40 mol% dcype was used.

In Rueping's paper, the issue of β-hydride elimination is not clearly addressed, and it is unclear whether low yields are associated with high recovery of starting material or formation of the reduced product. It would be valuable to gain more mechanistic understanding about why some ester substrates are more prone to β-hydride elimination with Ni than with Pd whereas the opposite is true for other substrates.

For the carbonyl reaction mode, our reaction scope was very similar to theirs. Simple arenes and furan esters worked very efficiently. Thiophene esters could be coupled more successfully with their Ni-PCy_3 system, while our Pd-IPr catalyst could be used for the coupling of quinoline ester **2.57** and alkyl boranes with benzylic β-hydrogens.

In brief, from a practical aspect, our coupling conditions are highly complementary to Rueping's protocol regarding the scope. Some of their scope limitations can be overcome using our catalytic system, and vice-versa. Moreover, our Pd-catalyzed carbonyl-retentive and decarbonylative couplings are not as sensitive to air and moisture so the use of a glovebox is not necessary; good yields can also be obtained when the reactions are set-up on the bench.

To conclude, we developed the first carbonyl-retentive and decarbonylative Pd-catalyzed alkylative Suzuki-Miyaura couplings of phenyl esters. The ability to access diverse products from a common starting material is a powerful strategy that can be applied to the quick diversification of relevant bioactive molecules. From a fundamental perspective, our work is interesting because it utilized recent mechanistic work in the field which allowed us to quickly identify an efficient catalyst to enable these transformations. This concept could be extended further for the development of new couplings of phenyl esters with other nucleophiles.

1.3. Experimental

1.3.1. General considerations

General experimental details: Unless otherwise indicated, reactions were conducted under an atmosphere of argon in 8 mL screw-capped vials that were oven dried (120 °C). Column chromatography was performed manually using Silicycle F60 40−63 μm silica gel. Analytical thin layer chromatography (TLC) was conducted with aluminum-backed EMD Millipore Silica Gel 60 F254 pre-coated plates. Visualization of developed plates was performed under UV light (254 nm) or using $KMnO_4$.

General instrumentation: ^{1}H NMR and ^{13}C NMR were recorded on a Bruker AVANCE 400 MHz spectrometer. ^{1}H NMR spectra were internally referenced to the residual

solvent signal (e.g., $CDCl_3$ = 7.27 ppm). ^{13}C NMR spectra were internally referenced to the residual solvent signal (e.g., $CDCl_3$ = 77.16 ppm). Data for ^1H NMR are reported as follows: chemical shift (δ ppm), multiplicity (s = singlet, d = doublet, t = triplet, q = quartet, quin = quintet, m = multiplet), coupling constant (Hz), integration. NMR yields for optimization studies were obtained by ^1H NMR analysis of the crude reaction mixture using 1,3,5-trimethoxybenzene as an internal standard. IR spectra were obtained using a Nicolet 6700 FT-IR spectrometer with a diamond ATR crystal (ThermoScientific) and are reported in terms of frequency of absorption (cm−1). Melting point ranges were determined on a Canlab GallenKamp Melting Point Apparatus. GC yields for optimization studies were obtained via a 5-point calibration curve using FID analysis on an Agilent Technologies 7890B GC with 30 m × 0.25 mm HP-5 column. Accurate mass data (EI) was obtained from an Agilent 5977A GC/MSD using MassWorks 4.0 from CERNO Bioscience. HRMS data was obtained from a Micromass Q-TOF 2 quadrupole – time-of-flight mass spectrometer with ESI source.

Materials: Organic solvents were purified by rigorous degassing with nitrogen before passing through a PureSolv solvent purification system, and low water content was confirmed by Karl Fischer titration (< 25 ppm for all solvents). Unless otherwise noted, reagents were used as received. $Pd(OAc)_2$ was purchased from Strem Chemicals. $[Pd(cinnamyl)Cl]_2$, dcype, Cs_2CO_3, KF were purchased from Sigma-Aldrich. Pd(IPr)(cinnamyl)Cl was synthesized according to the literature. Probenecid and repaglinide were purchased from Combi-Blocks. All esters were synthesized, except phenyl benzoate **2.45**, which was obtained commercially from Alfa Aesar. Esters **2.47**,[76]

[76] Ben Halima, T.; Vandavasi, J. K.; Shkoor, M.; Newman, S. G. *ACS Catal.* **2017**, *7*, 2176−2180.

2.49,[76] **2.53**,[77] **2.75**,[77] **2.42**,[78] **2.80**,[78] and **2.82**[78] were synthesized according to literature procedures.

Figure 13. Esters synthesized according to literature procedures

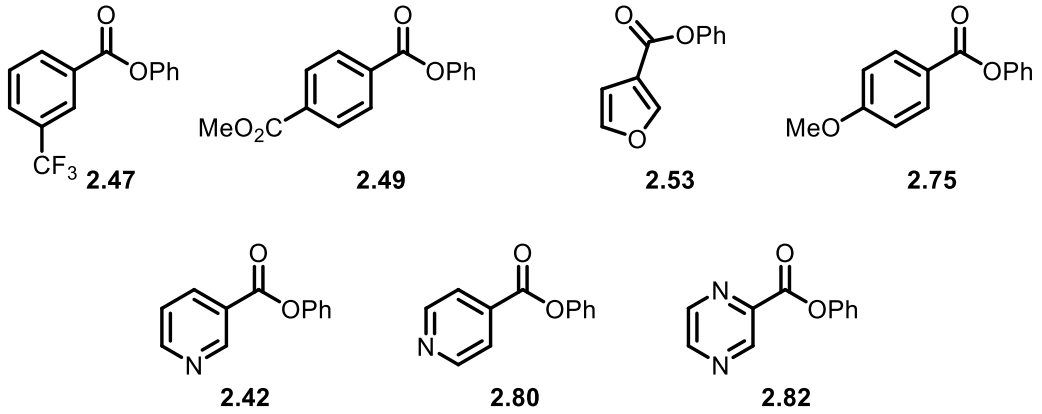

1.3.2. Synthesis of the starting materials

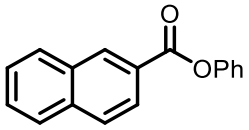

Phenyl 2-naphthoate (2.34) was synthesized from the corresponding acyl chloride. A 50 mL round-bottomed flask was equipped with a stir bar, phenol (471 mg, 5.00 mmol), DMAP (31 mg, 0.25 mmol), and 2-naphthoyl chloride (1.05 g, 5.50 mmol). The flask was closed with a rubber septum and degassed with argon. Toluene (17 mL) was added, followed by dropwise addition of triethylamine (0.77 mL, 5.5 mmol). The reaction was stirred at room temperature overnight. After, the solution was quenched with a saturated aqueous solution of sodium bicarbonate (20 mL). The mixture was transferred into a separatory funnel, and the flask was further rinsed with ethyl acetate (20 mL). The

[77] Ben Halima, T.; Zhang, W.; Yalaoui, I.; Hong, X.; Yang, Y.-F.; Houk, K. N.; Newman, S. G. *J. Am. Chem. Soc.* **2017**, *139*, 1311–1318.
[78] LaBerge, N. A.; Love, J. A. *Eur. J. Org. Chem.* **2015**, *2015*, 5546–5553.

organic phase was then washed with a 1 M aqueous solution of NaOH (20 mL), followed by a wash with brine (20 mL). The organic phase was then dried over Na_2SO_4, filtered, and concentrated *in vacuo*. The crude mixture was then subjected to manual column chromatography (gradient: 10 to 20% EtOAc in hexanes) to afford **2.34** as a white powder (1.2 g, 93% yield). Characterization data matched those previously reported.[77] **^{1}H NMR** (400 MHz, $CDCl_3$): 8.82 (s, 1H), 8.22 (dd, *J* = 8.6, 1.8 Hz, 1H), 8.03 (dd, *J* = 8.1, 0.7 Hz, 1H), 7.97 (d, *J* = 8.8 Hz, 1H), 7.94 (dd, *J* = 8.0, 0.6 Hz, 1H), 7.67-7.58 (m, 2H), 7.50-7.45 (m, 2H), 7.34-7.28 (m, 3H). **^{13}C NMR** (100 MHz, $CDCl_3$): 165.5, 151.2, 136.0, 132.7, 132.1, 129.7, 129.6, 128.8, 128.5, 128.0, 127.0, 126.9, 126.1, 125.6, 121.9.

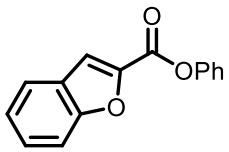

Benzofuran-2-carboxylic acid phenyl ester (2.51) was prepared via EDC coupling between phenol and benzofuran-2-carboxylic acid. A 25 mL round-bottomed flask was equipped with a stir bar, the carboxylic acid (3.0 mmol), phenol (282 mg, 3.00 mmol), EDC·HCl (575 mg, 3.00 mmol), and DMAP (37 mg, 0.20 mmol). The mixture was diluted with THF (15 mL) and stirred overnight at room temperature. After, the solution was quenched with a saturated aqueous solution of sodium bicarbonate (10 mL). The mixture was transferred into a separatory funnel, and the flask was further rinsed with ethyl acetate (20 mL). The organic phase was then washed with a 1 M aqueous solution of NaOH (10 mL), followed by a wash with brine (10 mL). The organic phase was then dried over Na_2SO_4, filtered, and concentrated *in vacuo*. The crude product was then purified via manual column chromatography (5% EtOAc in hexanes) to afford **2.51** as a white powder (0.44 g, 61% yield). Characterization data matched those previously reported.[79] **^{1}H NMR**

[79] Joshi, U. K.; Paradkar, M. V. *Indian Journal of Chemistry, Section B: Organic Chemistry Including Medicinal Chemistry* **1988**, *27*, 378–379.

(400 MHz, $CDCl_3$): 7.75 (td, *J* = 3.9, 0.8 Hz, 2H), 7.66 (dd, *J* = 8.4, 0.8 Hz, 1H), 7.54-7.49 (m, 1H), 7.48-7.44 (m, 2H), 7.39-7.35 (m, 1H), 7.33-7.26 (m, 3H). **^{13}C NMR** (100 MHz, $CDCl_3$): 158.0, 156.2, 150.4, 145.0, 129.7, 128.3, 127.1, 126.4, 124.2, 123.2, 121.7, 115.6, 112.7.

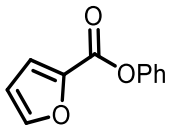

furan-2-carboxylic acid phenyl ester (2.55) was prepared following the same procedure as described above on a 2.0 mmol scale. Purification by column chromatography (gradient: 5 to 10% EtOAc in hexanes) afforded **2.55** as a white powder (0.25 g, 65% yield). Characterization data matched those previously reported.[80] **^{1}H NMR** (400 MHz, $CDCl_3$): 7.69 (dd, *J* = 1.8, 0.8 Hz, 1H), 7.46-7.41 (m, 2H), 7.40 (dd, *J* = 3.5, 0.8 Hz, 1H), 7.29 (tt, *J* = 7.4, 1.4 Hz, 1H), 7.24-7.21 (m, 2H), 6.61 (dd, *J* = 3.5, 1.8 Hz, 1H). **^{13}C NMR** (100 MHz, $CDCl_3$): 157.1, 150.4, 147.3, 144.2, 129.7, 126.2, 121.7, 119.5, 112.3.

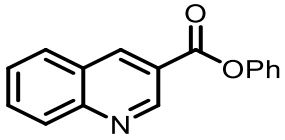

3-quinolinecarboxylic acid phenyl ester (2.57) was prepared following the same procedure as described above on a 3.0 mmol scale. Purification by column chromatography (30% Et_2O in hexanes) afforded **2.57** as a white powder (0.39 g, 53% yield). Characterization data matched those previously reported.[81] **^{1}H NMR** (400 MHz, $CDCl_3$): 9.61 (d, *J* = 2.2 Hz, 1H), 9.04 (d, *J* = 1.6 Hz, 1H), 8.23 (d, *J* = 8.0 Hz, 1H), 8.01 (d, *J* = 8.2 Hz, 1H), 7.92-7.88 (m, 1H), 7.70-7.66 (m, 1H), 7.51-7.46 (m, 2H), 7.35-7.28 (m, 3H). **^{13}C NMR** (100 MHz, $CDCl_3$): 164.2, 150.8, 150.3, 150.3, 139.7, 132.4, 129.8, 129.8, 129.4, 127.8, 127.0, 126.4, 122.6, 121.8.

[80] Shi, S.; Szostak, M. *Chem. Commun.* **2017**, *53*, 10584-10587.
[81] Ueda, T.; Konishi, H.; Manabe, K. *Org. Lett.* **2012**, *14*, 3100–3103.

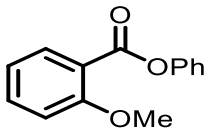

phenyl 2-methoxybenzoate (2.77) was prepared following the same procedure as described above on a 2.0 mmol scale. Purification by column chromatography (10% EtOAc in hexanes) afforded **2.77** as a white powder (0.27 g, 60% yield). Characterization data matched those previously reported.[81] **^{1}H NMR** (400 MHz, $CDCl_3$): 8.03 (dd, *J* = 7.9, 1.9 Hz, 1H), 7.58-7.54 (m, 1H), 7.45-7.40 (m, 2H), 7.29-7.23 (m, 3H), 7.08-7.04 (m, 2H), 3.96 (s, 3H). **^{13}C NMR** (100 MHz, $CDCl_3$): 164.5, 160.0, 151.2, 134.4, 132.3, 129.5, 125.8, 122.0, 120.4, 119.3, 112.4, 56.2.

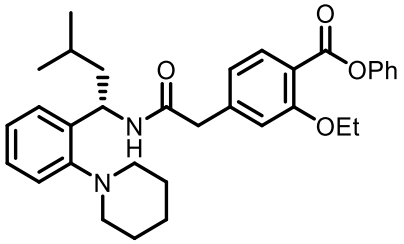

(S)-phenyl 4-(2-((1-(2-cyclohexylphenyl)-3-methylbutyl)amino)-2-oxoethyl)-2-ethoxybenzoate (2.100) was synthesized via EDC coupling between repaglinide and phenol. A 25 mL round-bottomed flask was equipped with a stir bar, repaglinide (1.06 g, 2.00 mmol), phenol (226 mg, 2.40 mmol, 1.20 equiv), EDC·HCl (460 mg, 2.40 mmol, 1.20 equiv), and DMAP (24 mg, 0.20 mmol, 10 mol%). The mixture was diluted with THF (10 mL) and stirred overnight at 50 ºC. After being cooled down, the solution was quenched with a saturated aqueous solution of sodium bicarbonate (10 mL). The mixture was transferred into a separatory funnel, and the flask was further rinsed with ethyl acetate (20 mL). The organic phase was then washed with a 1 M aqueous solution of NaOH (10 mL), followed by a wash with brine (10 mL). The organic phase was then dried over Na_2SO_4, filtered, and concentrated *in vacuo*. Purification by column chromatography (10% EtOAc in hexanes) afforded **2.100** as a white powder (0.81 g, 77% yield). **^{1}H NMR** (400

MHz, $CDCl_3$): 7.96 (d, *J* = 7.8 Hz, 1H), 7.45-7.40 (m, 2H), 7.28-7.26 (m, 1H), 7.24-7.20 (m, 4H), 7.12-7.06 (m, 2H), 6.92-6.90 (m, 2H), 6.75 (brs, NH), 5.39 (td, *J* = 8.6, 6.9 Hz, 1H), 4.11-4.02 (m, 2H), 3.58 (s, 2H), 2.95 (brs, 2H), 2.65 (brs, 2H), 1.73 (brs, 2H), 1.66-1.42 (m, 10H), 0.94 (dd, *J* = 6.6, 2.3 Hz, 6H). **^{13}C NMR** (100 MHz, $CDCl_3$): 168.7, 164.5, 159.7, 152.7, 151.2, 142.2, 138.8, 132.8, 129.5, 128.1, 127.9, 125.8, 125.3, 123.0, 122.0, 121.0, 118.3, 114.1, 64.8, 50.1, 46.9, 44.5, 26.9, 25.5, 24.3, 22.9, 22.7, 14.8. **IR**: ν (cm^{-1}) 3280, 3062, 2929, 2794, 1738, 1639, 1610, 1538, 1488, 1426, 1227, 1191, 1161, 1111, 1034, 918, 862, 797, 745, 690. **HRMS** (ESIQ-TOF): m/z calculated for $C_{33}H_{40}N_2O_4$ [M+H]+: 529.3066, found 529.3053. **mp**: 120–122 ºC.

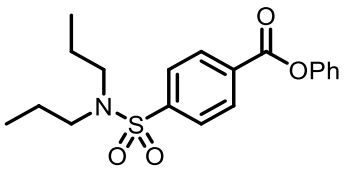

Phenyl 4-(N,N-dipropylsulfamoyl)benzoate (2.103) was prepared following the same procedure described above. The crude product was purified via manual column chromatography (30% Et_2O in hexanes) to afford **2.103** as a white powder (0.53 g, 70% yield). Note: On a larger scale (10 mmol), further recrystallization (Et_2O/pentane/toluene) was required after the column. **^{1}H NMR** (400 MHz, $CDCl_3$): 8.34 (d, *J* = 8.6 Hz, 2H), 7.96 (d, *J* = 8.6 Hz, 2H), 7.49-7.44 (m, 2H), 7.31 (t, *J* = 7.4 Hz, 1H), 7.25-7.22 (m, 2H), 3.16-3.12 (m, 4H), 1.58 (sxt, *J* = 7.5 Hz, 4H), 0.90 (t, *J* = 7.3 Hz, 6H). **^{13}C NMR** (100 MHz, $CDCl_3$): 164.0, 150.8, 145.0, 133.0, 130.9, 129.8, 127.3, 126.4, 121.6, 50.1, 22.1, 11.3. **IR**: ν (cm^{-1}) 2963, 2926, 2874, 1740, 1591, 1486, 1457, 1397, 1367, 1336, 1266, 1190, 1154, 1090, 1071, 1018, 990, 917, 855, 817, 799, 755, 732, 715, 687. **Accurate mass** (EI): m/z calculated for $C_{19}H_{23}NO_4S$: 361.1342, found 361.1075 (spectral accuracy = 98.2%). **mp**: 95–97 °C.

1.3.3. Coupling reactions: General procedures and characterization

General procedure for the synthesis of the B-alkyl-B-9BBN reagent

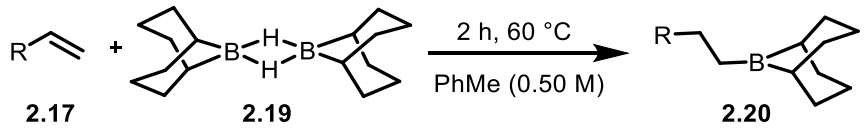

In a glovebox, a 1-dram screw-cap vial was charged with 9-BBN dimer (37 mg, 0.15 mmol), olefin (0.30 mmol), and toluene (0.60 mL). The vial was sealed with a Teflon lined screw cap and placed in a sand bath heated to 60 °C for 2 h. After cooling down, this solution was directly used in the coupling reactions.

General procedure A: Carbonyl-retentive couplings

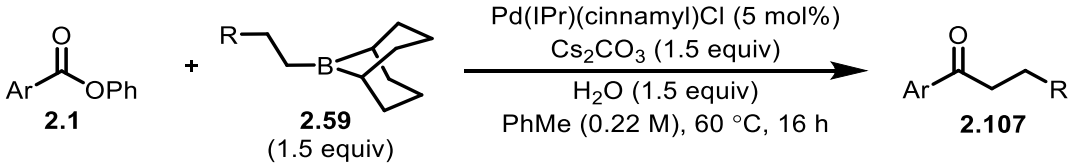

An 8 mL reaction vial was charged with a magnetic stir bar, cesium carbonate (98 mg, 0.30 mmol, 1.5 equiv), Pd(IPr)(cinnamyl)Cl (6.5 mg, 0.010 mmol, 5.0 mol %), and ester (0.20 mmol, 1.0 equiv). The vial was then shipped into a nitrogen-filled glovebox where toluene (0.30 mL), the B-alkyl-9-BBN reagent (0.30 mmol, 1.5 equiv), and water (5.4 μL, 0.30 mmol, 1.5 equiv) were added sequentially. The vial was sealed with a Teflon lined screw cap, taken out of the glovebox, and stirred at 60 °C for 16 h. After cooling, the solution was quenched with a saturated aqueous solution of ammonium chloride (3 mL) and extracted with ethyl acetate (3 x 5 mL). The crude product was concentrated in vacuo and purified by column chromatography.

General procedure B: Decarbonylative couplings

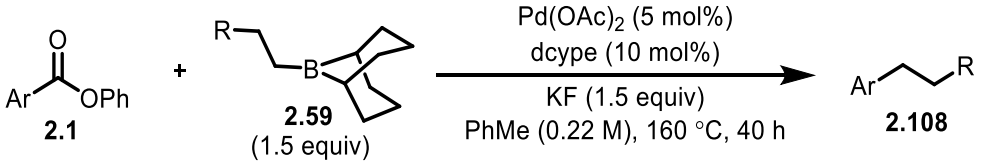

An 8 mL reaction vial was charged with a magnetic stir bar, potassium fluoride (17 mg, 0.30 mmol, 1.5 equiv), $Pd(OAc)_2$ (6.0 mg, 0.010 mmol, 5 mol %) or $Pd(COD)(CH_2TMS)_2$ (3.9 mg, 0.010 mmol, 5.0 mol %), dcype (8.4 mg, 0.020 mmol, 10 mol %), and the ester (0.20 mmol, 1.0 equiv). The vial was then shipped into a nitrogen-filled glovebox where toluene (0.30 mL), the B-alkyl-9-BBN reagent (0.30 mmol, 1.5 equiv) were added sequentially. The vial was sealed with a Teflon lined screw cap, taken out of the glovebox, and stirred at 160 °C for 40 h. After cooling, the solution was quenched with a saturated aqueous solution of ammonium chloride (3 mL) and extracted with ethyl acetate (3 x 5 mL). The crude product was concentrated in vacuo and purified by column chromatography.

Products obtained from carbonyl-retentive couplings

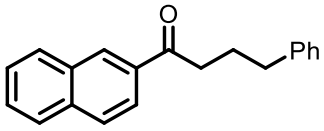

1-naphthalen-2-yl-4-phenylbutan-1-one (2.36) was prepared according to general procedure A. Purification by column chromatography (gradient: 30 to 50% DCM in hexanes) afforded **2.36** as a white powder (50 mg, 90% yield). **^{1}H NMR** (400 MHz, $CDCl_3$): 8.42 (s, 1H), 8.03 (dd, *J* = 8.6, 1.8 Hz, 1H), 7.95 (d, *J* = 8.0 Hz, 1H), 7.91-7.88 (m, 2H), 7.33 (t, *J* = 7.5 Hz, 2H), 7.27-7.22 (m, 3H), 3.13 (t, *J* = 7.3 Hz, 2H), 2.79 (t, *J* = 7.5 Hz, 2H), 2.17 (quin, *J* = 7.6 Hz, 2H). **^{13}C NMR** (100 MHz, $CDCl_3$): 200.2, 141.8, 135.7, 134.4, 132.7, 129.8, 129.7, 128.7, 128.6, 128.5, 128.5, 127.9, 126.8, 126.1, 124.0, 37.8, 35.4, 26.0. **IR**: ν (cm^{-1}) 3329, 2940,

1672, 1625, 1595, 1494, 1277, 1175, 980, 873, 828, 750, 696. **Accurate mass** (EI): m/z calculated for $C_{20}H_{18}O$: 274.1352, found 274.1302 (spectral accuracy = 98.9%). **mp**: 80–82 °C.

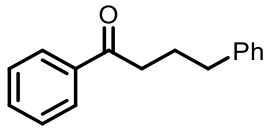

1,4-diphenylbutan-1-one (2.46) was prepared according to general procedure A. Purification by column chromatography (gradient: 0 to 5% EtOAc in hexanes) afforded **2.46** as a white powder (42 mg, 92% yield). Characterization data matched those previously reported.[82] **^{1}H NMR** (400 MHz, $CDCl_3$): 7.94 (m, 2H), 7.56 (tt, *J* = 7.5 Hz, 1.3 Hz, 1H), 7.47 (t, *J* = 7.6 Hz, 2H), 7.31 (t, *J* = 7.5 Hz, 2H), 7.24-7.20 (m, 3H), 3.00 (t, *J* = 7.3 Hz, 2H), 2.75 (t, *J* = 7.5 Hz, 2H), 2.11 (quin, *J* = 7.4 Hz, 2H). **^{13}C NMR** (100 MHz, $CDCl_3$): 200.2, 141.8, 137.1, 133.1, 128.7, 128.6, 128.5, 128.1, 126.1, 37.8, 35.3, 25.8.

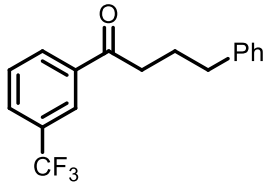

4-phenyl-1-[3-(trifluoromethyl)phenyl]butan-1-one (2.48) was prepared according to general procedure A. Purification by column chromatography (5% EtOAc in hexanes) afforded **2.48** as a colorless oil (38 mg, 64% yield). **^{1}H NMR** (400 MHz, $CDCl_3$): 8.18 (s, 1H), 8.10 (d, *J* = 7.8 Hz, 1H), 7.82 (d, *J* = 7.8 Hz, 1H), 7.60 (t, *J* = 7.8 Hz, 1H), 7.33-7.29 (m, 2H), 7.23-7.20 (m, 3H), 3.01 (t, *J* = 7.3 Hz, 2H), 2.75 (t, *J* = 7.4 Hz, 2H), 2.12 (quin, *J* = 7.4 Hz, 2H). **^{13}C NMR** (100 MHz, $CDCl_3$): 198.8, 141.5, 137.6, 131.4 (q, *J* = 32.5 Hz), 131.3, 129.5 (q, *J* = 3.6 Hz), 129.4, 128.6, 128.6, 126.2, 125.0 (q, *J* = 3.8 Hz), 123.8 (q, *J* = 270.8 Hz), 37.9, 35.2, 25.6. **IR**: ν (cm^{-1}) 3026, 2931, 1690, 1611, 1497, 1327, 1245, 1165, 1122, 1071, 909, 693.

[82] Roslin, S.; Odell, L. R. *Chem. Commun.* **2017**, *53*, 6895–6898.

Accurate mass (EI): m/z calculated for $C_{17}H_{15}F_3O$: 292.1070, found 292.1073 (spectral accuracy = 99.8%).

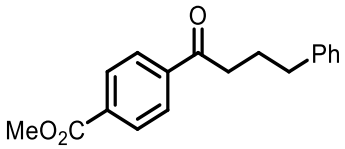

methyl 4-(4-phenylbutanoyl)benzoate (2.50) was prepared according to general procedure A. Purification by column chromatography (10% EtOAc in hexanes) afforded **2.50** as a white powder (39 mg, 68% yield). Characterization data matched those previously reported.[83] **^{1}H NMR** (400 MHz, $CDCl_3$): 8.11 (d, *J* = 8.6 Hz, 2H), 7.97 (d, *J* = 8.4 Hz, 2H), 7.31 (t, *J* = 7.5 Hz, 2H), 7.23-7.19 (m, 3H), 3.96 (s, 3H), 3.01 (t, *J* = 7.3 Hz, 2H), 2.74 (t, *J* =7.5 Hz, 2H), 2.11 (quin, *J* =7.4 Hz, 2H). **^{13}C NMR** (100 MHz, $CDCl_3$): 199.7, 166.4, 141.6, 140.3, 133.9, 129.9, 128.6, 128.6, 128.0, 126.2, 52.6, 38.1, 35.2, 25.6.

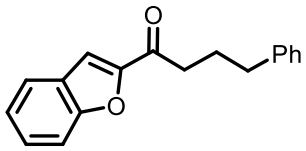

1-(1-benzofuran-2-yl)-4-phenylbutan-1-one (2.52) was prepared according to general procedure A. Purification by column chromatography (gradient 5 to 10% EtOAc in hexanes) afforded **2.52** as a white powder (47 mg, 89% yield). **^{1}H NMR** (400 MHz, $CDCl_3$): 7.71 (d, *J* = 7.8 Hz, 1H), 7.59 (d, *J* = 7.8 Hz, 1H), 7.51-7.46 (m, 2H), 7.34-7.30 (m, 3H), 7.25-7.21 (m, 3H), 2.99 (t, *J* = 7.3 Hz, 2H), 2.77 (t, *J* = 7.5 Hz, 2H), 2.15 (quin, *J* = 7.4 Hz, 2H). **^{13}C NMR** (100 MHz, $CDCl_3$): 191.3, 155.7, 152.7, 141.6, 128.6, 128.5, 128.3, 127.1, 126.1, 124.0, 123.3, 112.7, 112.5, 38.2, 35.2, 25.7. **IR**: ν (cm^{-1}) 3349, 3057, 3026, 1683, 1605, 1555, 1496,

[83] Crawley, M. L.; Phipps, K. M.; Goljer, L.; Mehlmann, J. F.; Lundquist, J. T.; Ullrich, J. W.; Yang, C.; Mahaney, P. E. *Org. Lett.* **2009**, *11*, 1183–1185.

1459, 1373, 1150, 1026, 1001, 939, 921, 835, 741, 696. **Accurate mass** (EI): m/z calculated for $C_{18}H_{16}O_2$: 264.1145, found 264.1114 (spectral accuracy = 97.2%). **mp**: 74–76 °C.

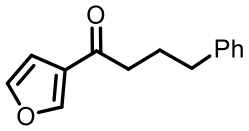

1-(furan-3-yl)-4-phenylbutan-1-one (2.54) was prepared according to general procedure A. Purification by column chromatography (10% EtOAc in hexanes) afforded **2.54** as a colorless oil (32 mg, 74% yield). **^{1}H NMR** (400 MHz, $CDCl_3$): 7.71 (d, *J* = 7.8 Hz, 1H), 7.59 (d, *J* = 7.8 Hz, 1H), 7.51-7.46 (m, 2H), 7.34-7.30 (m, 3H), 7.25-7.21 (m, 3H), 2.99 (t, *J* = 7.3 Hz, 2H), 2.77 (t, *J* = 7.5 Hz, 2H), 2.15 (quin, *J* = 7.4 Hz, 2H). **^{13}C NMR** (100 MHz, $CDCl_3$): 191.3, 155.7, 152.7, 141.6, 128.6, 128.5, 128.3, 127.1, 126.1, 124.0, 123.3, 112.7, 112.5, 38.2, 35.2, 25.7. **IR**: ν (cm^{-1}) 3060, 3025, 2924, 2855, 1719, 1671, 1508, 1497, 1453, 1153, 1079, 910, 873, 814, 744, 698. **Accurate mass** (EI): m/z calculated for $C_{14}H_{14}O_2$: 214.0988, found 214.0769 (spectral accuracy = 98.6%).

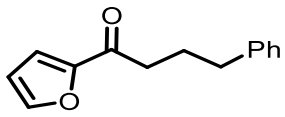

1-(furan-2-yl)-3-phenylpropan-1-one (2.56) was prepared according to general procedure A. Purification by column chromatography (gradient: 5 to 10% EtOAc in hexanes) afforded **2.56** as a white solid (42 mg, 98% yield). Characterization data matched those previously reported.[84] **^{1}H NMR** (400 MHz, $CDCl_3$): 7.57 (dd, *J* = 1.8, 0.8 Hz, 1H), 7.32-7.28 (m, 2H), 7.22-7.13 (m, 3H), 7.14 (dd, *J* = 3.6, 0.7 Hz, 1H), 6.52 (dd, *J* = 3.5, 1.8 Hz, 1H), 2.85 (t, *J* = 7.3 Hz, 2H), 2.72 (t, *J* = 7.5 Hz, 2H), 2.08 (quin, *J* = 7.4 Hz, 2H). **^{13}C NMR** (100 MHz, $CDCl_3$): 189.5, 152.9, 146.3, 141.7, 128.6, 128.5, 126.1, 117.0, 112.3, 37.8, 35.3, 25.8.

[84] Wang, C.-Y.; Ralph, G.; Derosa, J.; Biscoe, M. R. *Angew. Chem. Int. Ed.* **2017**, *56*, 856–860.

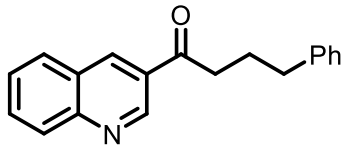

4-phenyl-1-quinolin-3-ylbutan-1-one (2.58) was prepared according to general procedure A. Purification by column chromatography (gradient: 20 to 40% Et_2O in hexanes), followed by trituration with pentane, afforded **2.58** as a white powder (40 mg, 73% yield). **^{1}H NMR** (400 MHz, $CDCl_3$): 9.41 (d, *J* = 2.2 Hz, 1H), 8.64 (d, *J* =2.0 Hz, 1H), 8.16 (d, *J* = 8.4 Hz, 1H), 7.93 (d, *J* = 8.2 Hz, 1H), 7.84 (ddd, *J* = 8.4, 7.0, 1.5 Hz, 1H), 7.63 (ddd, *J* = 8.1, 7.0, 1.0 Hz, 1H), 7.33-7.30 (m, 2H), 7.25-7.20 (m, 3H), 3.11 (t, *J* = 7.3 Hz, 2H), 2.78 (t, *J* = 7.4 Hz, 2H), 2.17 (quin, *J* = 7.3 Hz, 2H). **^{13}C NMR** (100 MHz, $CDCl_3$): 198.9, 149.9, 149.2, 141.5, 137.0, 132.0, 129.6, 129.4, 129.2, 128.7, 128.6, 127.6, 127.0, 126.2, 38.1, 35.2, 25.6. **IR**: ν (cm^{-1}) 3064, 3028, 2941, 2852, 1680, 1592, 1560, 1495, 1400, 1375, 1282, 1163, 1124, 953, 937, 789, 754, 741, 696. **Accurate mass** (EI): m/z calculated for $C_{19}H_{17}NO$: 275.1305, found 275.1293 (spectral accuracy = 94.4%). **mp**: 82–83 °C.

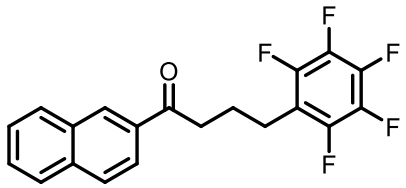

1-(naphthalen-2-yl)-4-(perfluorophenyl)butan-1-one (2.62) was prepared according to general procedure A. Purification by column chromatography (6% EtOAc in hexanes) afforded **2.62** as a white solid (43 mg, 59% yield). **^{1}H NMR** (400 MHz, $CDCl_3$): 8.45 (s, 1H), 8.02 (dd, *J* =8.6, 1.8 Hz, 1H), 7.98 (d, *J* =8.0 Hz, 1H), 7.92-7.88 (m, 2H), 7.64-7.55 (m, 2H), 3.18 (t, *J* =7.2 Hz, 2H), 2.87 (t, *J* =7.5 Hz, 2H), 2.12 (quin, *J* =7.4 Hz, 2H). **^{13}C NMR** (100 MHz, $CDCl_3$): 199.0, 145.2 (dm, *J* = 247 Hz), 139.8 (dm, *J* = 249 Hz), 137.6 (dm, *J* = 250 Hz), 135.8, 134.2,132.6, 129.7, 128.7, 128.6, 127.9, 127.0, 123.8, 114.8 (tm, *J* = 17.4 Hz), 37.6, 23.7, 21.9. **IR**: ν (cm^{-1}) 2900, 1741, 1674, 1519, 1495, 1375, 1278, 1177, 1119, 1057, 954, 852, 828, 747,

658. **Accurate mass** (EI): m/z calculated for $C_{20}H_{13}F_5O$: 364.0881, found 364.0761 (spectral accuracy = 97.6%). **mp**: 134–136 °C.

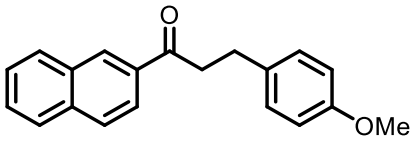

3-(4-methoxyphenyl)-1-(naphthalen-2-yl)propan-1-one (2.64) was prepared according to general procedure A. Purification by column chromatography (7% EtOAc in hexanes) afforded **2.64** as a colorless oil (47 mg, 81% yield). Characterization data matched those previously reported.[85] **^{1}H NMR** (400 MHz, $CDCl_3$): 8.47 (s, 1H), 8.05 (dd, *J* = 8.6, 1.8 Hz), 7.95 (d, *J* = 8.2 Hz, 1H), 7.91-7.87 (m, 2H), 7.63-7.54 (m, 2H), 7.23 (d, *J* = 8.8 Hz, 2H), 6.88 (d, *J* = 8.6 Hz, 2H), 3.81 (s, 3H), 3.44-3.40 (m, 2H), 3.11-3.07 (m, 2H). **^{13}C NMR** (100 MHz, $CDCl_3$): 199.4, 158.1, 135.7, 134.3, 133.5, 132.6, 129.8, 129.7, 129.5, 128.6, 128.5, 127.9, 126.9, 124.0, 114.1, 55.4, 40.9, 29.6.

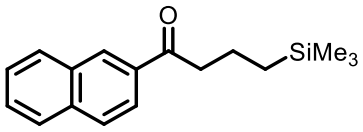

γ-(trimethylsilyl)butyro-2-naphthone (2.66) was prepared according to general procedure A. Purification by column chromatography (8% DCM in hexanes) afforded **2.66** as a white solid (33 mg, 71% yield). Characterization data matched those previously reported.[86] **^{1}H NMR** (400 MHz, $CDCl_3$): 8.48 (s, 1H), 8.05 (dd, *J* = 8.6, 1.8 Hz, 1H), 7.98 (d, J =8.0 Hz, 1H), 7.90 (t, *J* = 8.2 Hz, 2H), 7.63-7.54 (m, 2H), 3.14 (t, *J* = 7.3 Hz, 2H), 1.87-1.79 (m, 2H), 0.64 (m, 2H), 0.03 (s, 9H). **^{13}C NMR** (100 MHz, $CDCl_3$): 200.7, 135.6, 134.6, 132.7, 129.7, 129.7, 128.5, 128.5, 127.9, 126.8, 124.1, 42.5, 19.4, 16.9, -1.6.

[85] Downey, C. W.; Covington, S. E.; Obenschain, D. C.; Halliday, E.; Rague, J. T.; Confair, D. N. *Tet. Lett.* **2014**, *55*, 5213–5215.
[86] Lee, Y. J.; Ling, R.; Mariano, P. S.; Yoon, U. C.; Kim, D. U.; Oh, S. W. *J. Org. Chem.* **1996**, *61*, 3304–3314.

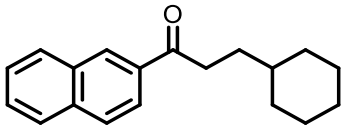

3-cyclohexyl-1-naphthalen-2-ylpropan-1-one (2.68) was prepared according to general procedure A. Purification by column chromatography (6% EtOAc in hexanes) afforded **2.68** as a white solid (39 mg, 73% yield). **^{1}H NMR** (400 MHz, $CDCl_3$): 8.48 (s, 1H), 8.05 (dd, *J* = 8.6, 1.8 Hz, 1H), 7.98 (d, *J* = 8.0 Hz, 1H), 7.91-7.86 (m, 2H), 7.63-7.54 (m, 2H), 3.12 (t, *J* = 7.5 Hz, 2H), 1.83-1.79 (m, 2H), 1.77-1.66 (m, 5H), 1.43-1.32 (m, 1H), 1.29-1.16 (m, 3H), 1.04-0.94 (m, 2H). **^{13}C NMR** (100 MHz, $CDCl_3$): 201.0, 135.6, 134.5, 132.7, 129.7, 129.7, 128.5, 128.4, 127.9, 126.8, 124.1, 37.6, 36.4, 33.4, 32.1, 26.7, 26.4. **IR**: ν (cm^{-1}): 3056, 2928, 2914, 2848, 1735, 1680, 1625, 1591, 1449, 1356, 1279, 1190, 1175, 1155, 1128, 1079, 1012, 817, 776, 765, 742, 690. **Accurate mass** (EI): m/z calculated for $C_{19}H_{22}O$: 266.1665, found 266.1516 (spectral accuracy = 85.8%). **mp**: 68–70 °C.

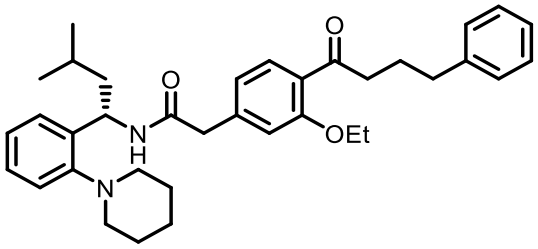

(S)-2-(3-ethoxy-4-(4-phenylbutanoyl)phenyl)-N-(3-methyl-1-(2-(piperidin-1-yl)phenyl)butyl)acetamide (2.101) was prepared according to general procedure A, with double catalyst loading. Purification by preparative TLC (20% dioxane in hexanes) afforded **2.101** as a yellow oil (50 mg, 45% yield). **^{1}H NMR** (400 MHz, $CDCl_3$): 7.65 (d, *J* = 7.6 Hz, 1H), 7.30-7.26 (m, 2H), 7.22-7.17 (m, 5H), 7.11-7.04 (m, 2H), 6.85-6.82 (m, 2H), 6.78 (br, NH), 5.42-5.36 (m, 1H), 4.05-3.91 (m, 2H), 2.16 (s, 2H), 3.01 (t, *J* = 7.6 Hz, 2H), 2.94 (br, 2H), 2.69 (t, *J* = 7.5 Hz, 2H), 2.62 (br, 2H), 2.02 (quin, *J* = 7.5 Hz, 2H), 1.71 (br, 2H),1.66-1.40 (m, 7H), 1.37 (t, *J* = 7.0 Hz, 3H), 0.93 (d, *J* = 6.5 Hz, 6H). **^{13}C NMR** (100 MHz, $CDCl_3$): 202.3, 168.9, 158.3, 152.6, 142.1, 141.2, 138.8, 130.9, 128.6, 128.4, 128.0, 127.8, 127.3, 125.9, 125.2,

122.9, 121.3, 113.0, 64.1, 50.0, 46.8, 44.3, 43.4, 35.5, 26.9, 26.1, 25.5, 24.2, 22.9, 22.6, 14.8. **IR**: ν (cm^{-1}) 3061, 3025, 2932, 2866, 2246, 1647, 1604, 1535, 1491, 1450, 1428, 1289, 1222, 1037, 990, 908, 860, 729, 699. **HRMS** (ESIQ-TOF): m/z calculated for $C_{36}H_{46}N_2O_3$ $[M+Na]^+$: 577.3406, found 577.3422.

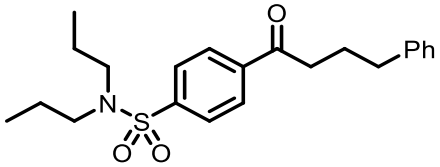

4-(4-phenylbutanoyl)-N,N-dipropylbenzenesulfonamide (2.104) was prepared according to the general procedure, on 2.8 mmol scale at 3.0 mol % [Pd] loading, in 5 mL of toluene, in a 50 mL Schlenk flask. Purification by column chromatography (gradient: 20 to 40% Et_2O in hexanes), followed by trituration in pentane, afforded **2.104** as a white solid (0.87 g, 80% yield). **^{1}H NMR** (400 MHz, $CDCl_3$): 8.01 (d, *J* = 8.4 Hz, 2H), 7.88 (d, *J* = 8.4 Hz, 2H), 7.32-7.29 (m, 2H), 7.23-7.20 (m, 3H), 3.12-3.09 (m, 4H), 3.00 (t, *J* = 7.3 Hz, 2H), 2.74 (t, *J* = 7.5 Hz, 2H), 2.11 (quin, *J* = 7.3 Hz, 2H), 1.60-1.51 (m, 4H), 0.88 (t, *J* = 7.3 Hz, 6H). **^{13}C NMR** (100 MHz, $CDCl_3$): 199.1, 144.2, 141.5, 139.7, 128.7, 128.6, 128.6, 127.4, 126.2, 50.1, 38.1, 35.1, 25.5, 22.1, 11.3. **IR**: ν (cm^{-1}) 2965, 2933, 2876, 2252, 1686, 1595, 1454, 1340, 1155, 1089, 989, 908, 869, 728, 699. **HRMS** (ESIQ-TOF): m/z calculated for $C_{22}H_{29}NO_3S$ $[M+Na]^+$: 410.1766, found 410.1751. **mp**: 59–61 °C.

<u>Products obtained from decarbonylative couplings</u>

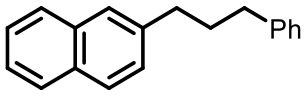

1-phenyl-3-(2-naphthyl)propane (2.70) was prepared according to general procedure using $Pd(OAc)_2$. Purification by column chromatography (gradient: 0 to 4% DCM in hexanes) afforded **2.70** as a colourless oil (39 mg, 78% yield). 81% yield was obtained following procedure with $Pd(COD)(CH_2TMS)_2$. Characterization data matched those

previously reported.[87] **^{1}H NMR** (400 MHz, $CDCl_3$): 7.87-7.81 (m, 3H), 7.67 (s, 1H), 7.52-7.45 (m, 2H), 7.40-7.33 (m, 3H), 7.27-7.23 (m, 3H), 2.87 (t, *J* = 7.4 Hz, 2H), 2.74 (t, *J* = 7.6 Hz, 2H), 2.11 (quin, *J* = 7.7 Hz, 2H). **^{13}C NMR** (100 MHz, $CDCl_3$): 142.4, 139.9, 133.8, 132.1, 128.6, 128.5, 128.0, 127.7, 127.5, 127.5, 126.6, 126.0, 125.9, 125.2, 35.7, 35.6, 33.0.

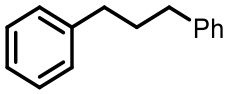

1,3-diphenylpropane (2.73) was prepared according to general procedure using Pd(COD)($CH_2TMS)_2$. Purification by column chromatography (hexanes) afforded **2.73** as a colourless oil (25 mg, 64% yield). Characterization data matched those previously reported.[88] **^{1}H NMR** (400 MHz, $CDCl_3$): 7.33 -7.28 (m, 4H), 7.22-7.18 (m, 6H), 2.68 (t, *J* = 7.6 Hz, 4H), 1.99 (quin, *J* = 7.8 Hz, 2H). **^{13}C NMR** (100 MHz, $CDCl_3$): 142.4, 128.6, 128.4, 125.9, 35.6, 33.1.

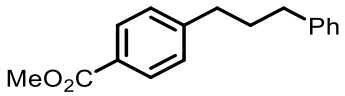

methyl 4-(3-phenylpropyl)benzoate (2.74) was prepared according to general procedure using $Pd(OAc)_2$. Purification by column chromatography (4% Et_2O in hexanes) afforded **2.74** as a colourless oil (33 mg, 65% yield). Characterization data matched those previously reported.[89] **^{1}H NMR** (400 MHz, $CDCl_3$): 7.98 (d, *J* = 8.2 Hz, 2H), 7.33-7.26 (m, 4H), 7.23-7.19 (m, 3H), 3.92 (s, 3H), 2.72 (t, *J* = 7.6 Hz, 2H), 2.67 (t, *J* = 7.6 Hz, 2H), 2.00 (quin, *J* = 7.8 Hz, 2H). **^{13}C NMR** (100 MHz, $CDCl_3$): 167.3, 148.0, 142.0, 129.8, 128.6, 128.5, 128.5, 127.9, 126.0, 52.1, 35.5, 35.5, 32.7.

[87] Liu, X.; Hsiao, C.-C.; Kalvet, I.; Leiendecker, M.; Guo, L.; Schoenebeck, F.; Rueping, M. *Angew. Chem. Int. Ed.* **2016**, *55*, 6093–6098.
[88] Li, H.; Breen, C. P.; Seo, H.; Jamison, T. F.; Fang, Y.-Q., Bio, M. M. *Org. Lett.* **2018**, *20*, 1338–1341.
[89] Tobisu, M.; Nakamura, R.; Kita, Y.; Chatani, N. *J. Am. Chem. Soc.* **2009**, *131*, 3174–3175.

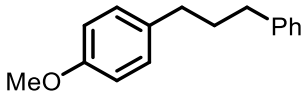

1-methoxy-4-(3-phenylpropyl)benzene (2.76) was prepared according to general procedure using $Pd(OAc)_2$. Purification by column chromatography (3% EtOAc in hexanes) afforded **2.76** as a colourless oil (36 mg, 80% yield). Characterization data matched those previously reported.[90] **^{1}H NMR** (400 MHz, $CDCl_3$): 7.32-7.28 (m, 2H), 7.21-7.18 (m, 3H), 7.12 (d, *J* = 8.8 Hz, 2H), 6.85 (d, *J* = 8.8 Hz, 2H), 3.81 (s, 3H), 2.66 (t, *J* = 7.8 Hz, 2H), 2.62 (t, *J* = 7.8 Hz, 2H), 1.95 (quin, *J* = 7.6 Hz, 2H). **^{13}C NMR** (100 MHz, $CDCl_3$): 157.8, 142.5, 134.5, 129.4, 128.6, 128.4, 125.8, 113.9, 55.4, 35.5, 34.6, 33.3.

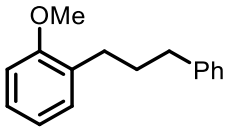

1-methoxy-2-(3-phenylprop-1-yl)benzene (2.78) was prepared according to general procedure using $Pd(OAc)_2$. Purification by column chromatography (3% EtOAc in hexanes) afforded **2.78** as a colourless oil (41 mg, 91% yield). Characterization data matched those previously reported.[91] **^{1}H NMR** (400 MHz, $CDCl_3$): 7.33-7.29 (m, 2H), 7.25-7.15 (m, 5H), 6.92 (td, *J* = 7.4, 1.1 Hz, 1H), 6.88 (d, *J* = 8.2 Hz, 1H), 3.85 (s, 3H), 2.73-2.69 (m, 4H), 1.97 (quin, *J* = 7.8 Hz, 2H). **^{13}C NMR** (100 MHz, $CDCl_3$): 157.6, 142.8, 130.9, 129.9, 128.6, 128.4, 127.1, 125.7, 120.5, 110.4, 55.4, 35.9, 31.5, 30.1.

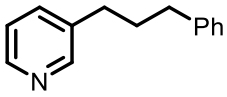

4-(3-phenylpropyl)-pyridine (2.79) was prepared according to the general procedure using $Pd(OAc)_2$. Purification by column chromatography (40% EtOAc in hexanes) afforded **2.79** as a colourless oil (24 mg, 61% yield). Characterization data matched those

[90] Komeyama, K.; Ohata, R.; Kiguchi, S.; Osaka, I. *Chem. Commun.* **2017**, *53*, 6401–6404.
[91] Czaplik, W. M.; Mayer, M.; Von Wangelin, A. J. *Angew. Chem. Int. Ed.* **2009**, *48*, 607–610.

previously reported.[92] **^{1}H NMR** (400 MHz, $CDCl_3$): 8.46-8.45 (m, 2H), 7.51 (d, *J* = 7.8 Hz, 1H), 7.32-7.99 (m, 2H), 7.24-7.18 (m, 4H), 2.69-2.64 (m, 4H), 1.98 (quin, *J* = 8.2 Hz, 2H). **^{13}C NMR** (100 MHz, $CDCl_3$): 150.0, 147.4, 141.8, 137.6, 136.0, 128.5, 128.5, 126.0, 123.4, 35.4, 32.7, 32.6.

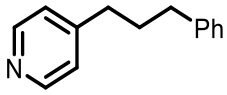

4-(3-phenylpropyl)pyridine (2.81) was prepared according to the general procedure using $Pd(OAc)_2$. Purification by column chromatography (40% EtOAc in hexanes) afforded **2.81** as a colourless oil (35 mg, 87% yield). Characterization data matched those previously reported.[93] **^{1}H NMR** (400 MHz, $CDCl_3$): 8.51-8.49 (m, 2H), 7.32-7.28 (m, 2H), 7.23-7.19 (m, 3H), 7.13-7.11 (m, 2H), 2.69-2.63 (m, 4H), 1.99 (quin, *J* = 7.5 Hz, 2H). **^{13}C NMR** (100 MHz, $CDCl_3$): 151.3, 149.8, 141.7, 128.6, 128.5, 126.1, 124.0, 35.4, 34.8, 31.9.

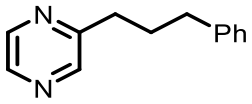

2-(3-phenylpropyl)pyrazine (2.83) was prepared according to the general procedure using $Pd(COD)(CH_2TMS)_2$. Purification by column chromatography (gradient: 15 to 30% EtOAc in hexanes) afforded **2.83** as an orange oil (21 mg, 52% yield). **^{1}H NMR** (400 MHz, $CDCl_3$): 8.50 (dd, *J* = 2.4, 1,5 Hz, 1H), 8.45 (d, *J* = 1.6 Hz, 1H), 8.40 (d, *J* = 2.5 Hz, 1H), 7.32-7.28 (m, 2H), 7.22-7.18 (m, 3H), 2.85 (t, *J* = 7.6 Hz, 2H), 2.71 (t, *J* = 7.6 Hz, 2H), 2.11 (quin, *J* = 7.5 Hz, 2H). **^{13}C NMR** (100 MHz, $CDCl_3$): 157.7, 144.8, 144.2, 142.3, 141/7, 128.6, 128.5, 126.1, 35.5, 35.0, 30.9. **IR**: ν (cm^{-1}) 3060, 3027, 2925, 2857, 1602, 1526, 1496, 1474, 1453, 1402, 1122, 1058, 1015, 909, 848, 731, 698. **Accurate mass** (EI): m/z calculated for $C_{13}H_{14}N_2$: 198.0919, found 198.1152 (spectral accuracy = 95.0%).

[92] Hansen, E. C.; Li, C.; Yang, S.; Pedro, D.; Weix, D. J. *J. Org. Chem.* **2017**, *82*, 7085-7092.
[93] Nakao, Y.; Yamada, Y.; Kashihara, N.; Hiyama, T. *J. Am. Chem. Soc.* **2010**, *132*, 13666–13668.

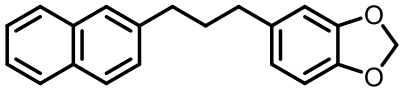

5-(3-(naphthalen-2-yl)propyl)benzo[d][1,3]dioxole (2.86) was prepared according to the general procedure using $Pd(OAc)_2$. Purification by column chromatography (gradient: 5 to 20% EtOAc in hexanes) afforded **2.86** as a light yellow oil (46 mg, 78% yield). Characterization data matched those previously reported.[94] **^{1}H NMR** (400 MHz, $CDCl_3$): 7.85-7.80 (m, 3H), 7.65 (s, 1H), 7.47 (quind, *J* = 7.2, 1.5 Hz, 2H), 7.36 (dd, *J* = 8.4, 1.8 Hz, 1H), 6.78 (d, *J* = 8.0 Hz, 1H), 6.74 (d, *J* = 1.6 Hz, 1H), 6.68 (dd, *J* = 7.8, 1.6 Hz, 1H), 5.95 (s, 2H), 2.83 (t, *J* = 7.6 Hz, 2H), 2.64 (t, *J* = 7.6 Hz, 2H), 2.04 (quin, *J* = 7.7 Hz, 2H). **^{13}C NMR** (100 MHz, $CDCl_3$): 147.7, 145.7, 139.9, 136.2, 133.8, 132.1, 128.0, 127.7, 127.5, 127.5, 126.6, 126.0, 125.2, 121.3, 109.0, 108.2, 100.9, 35.6, 35.3, 33.2.

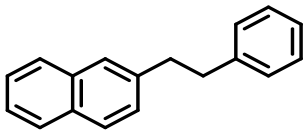

1-(2-naphthyl)-2-phenylethane (2.88) was prepared according to the general procedure using $Pd(COD)(CH_2TMS)_2$. Purification by column chromatography (8% DCM in hexanes) afforded **2.88** as a white solid (25 mg, 54% yield). Characterization data matched those previously reported.[87] **^{1}H NMR** (400 MHz, $CDCl_3$): 7.85-7.79 (m, 3H), 7.65 (s, 1H), 7.50-7.43 (m, 2H), 7.37 (dd, *J* = 8.4, 1.8 Hz, 1H), 7.34-7.30 (m, 2H), 7.25-7.21 (m, 3H), 3.14-3.10 (m, 2H), 3.07-3.02 (m, 2H). **^{13}C NMR** (100 MHz, $CDCl_3$): 141.9, 139.4, 133.8, 132.2, 128.6, 128.5, 128.0, 127.8, 127.6, 127.5, 126.6, 126.1, 126.0, 125.3, 38.2, 38.0.

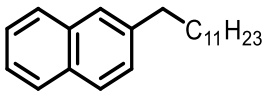

2-dodecyl-naphthalene (2.90) was prepared according to the general procedure using $Pd(OAc)_2$. Purification by column chromatography (gradient: 0 to 2% Et_2O in hexanes) afforded **2.90** as a colourless oil (37 mg, 63% yield). **^{1}H NMR** (400 MHz, $CDCl_3$): 7.84-7.78

(m, 3H), 7.64 (s, 1H), 7.49-7.41 (m, 2H), 7.36 (dd, *J* = 8.4, 1.8 Hz, 1H), 2.80 (t, *J* = 7.6 Hz, 2H), 1.77-1.70 (m, 2H), 1.42-1.30 (m, 19H), 0.92 (t, *J* = 6.7 Hz, 3H). **^{13}C NMR** (100 MHz, $CDCl_3$): 140.6, 133.8, 132.1, 127.9, 127.7, 127.6, 127.5, 126.4, 125.9, 125.1, 36.3, 32.1, 31.5, 29.8, 29.8, 29.8, 29.7, 29.5, 22.9, 14.3. Note: There are two peaks in the aliphatic region account for two carbons. **IR**: ν (cm^{-1}) 3051, 2921, 2851, 1601, 1508, 1458, 1269, 888, 851, 813, 743, 721, 698. **Accurate mass** (EI): m/z calculated for $C_{22}H_{32}$: 296.2499, found 296.2603 (spectral accuracy = 99.4%).

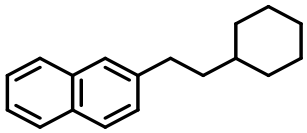

2-(2-cyclohexylethyl)naphthalene (2.91) was prepared according to the general procedure using $Pd(COD)(CH_2TMS)_2$. Purification by column chromatography (hexanes) afforded **2.91** as a colourless oil (23 mg, 48% yield). Characterization data matched those previously reported.[94] **^{1}H NMR** (400 MHz, $CDCl_3$): 7.83-7.77 (m, 3H), 7.63 (s, 1H), 7.49-7.41 (m, 2H), 7.36 (dd, *J* = 8.3, 1.5 Hz, 1H), 2.83-2.79 (m, 2H), 1.84-1.81 (m, 2H), 1.77-1.59 (m, 5H), 1.39-1.18 (m, 4H), 1.03-0.94 (m, 2H). **^{13}C NMR** (100 MHz, $CDCl_3$): 140.9, 133.8, 132.0, 127.9, 127.7, 127.6, 127.5, 126.3, 125.9, 125.1, 39.4, 37.5, 33.6, 33.5, 26.9, 26.5.

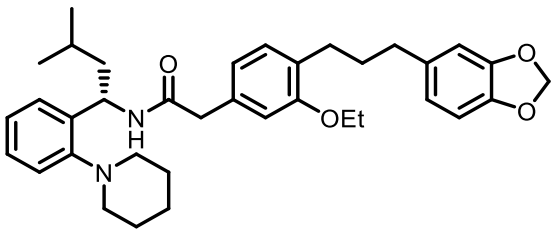

(S)-2-(4-(3-(benzo[d][1,3]dioxol-5-yl)propyl)-3-ethoxyphenyl)-N-(3-methyl-1-(2-(piperidin-1-yl)phenyl)butyl)acetamide (2.102) was prepared according to the general procedure using $Pd(OAc)_2$ on 0.10 mmol scale. Purification by preparative TLC (15%

[94] Guo, L.; Liu, X.; Baumann, C.; Rueping, M. *Angew. Chem. Int. Ed.* **2016**, *55*, 15415–15419.

acetone in hexanes) afforded **2.102** as a yellow oil (36 mg, 63% yield). **^{1}H NMR** (400 MHz, $CDCl_3$): 7.22-7.16 (m, 2H), 7.08-7.03 (m, 3H), 6.74 (d, *J* = 7.8 Hz, 2H), 6.70 (dd, *J* = 3.6, 1.5 Hz, 2H), 6.65 (dd, J =7.8, 1.8 Hz, 1H), 6.49 (br, NH), 5.92 (s, 2H), 5.43-5.37 (m, 1H), 3.97-3.89 (m, 2H), 3.53 (d, *J* = 3.1 Hz, 2H), 2.95 (br, 2H), 2.64-2.58 (m, 6H), 1.91-1.83 (m, 2H), 1.74-1.39 (m, 9H), 1.37 (t, *J* = 7.0 Hz, 3H), 0.91 (dd, *J* = 6.5, 5.1 Hz, 6H). **^{13}C NMR** (100 MHz, $CDCl_3$): 170.3, 157.3, 152.7, 147.6, 145.6, 139.1, 136.6, 134.1, 130.2, 129.9, 127.9, 127.6, 125.0, 122.7, 121.2, 121.1, 112.2, 109.0, 108.1, 100.8, 63.5, 49.6, 46.8, 44.3, 35.5, 31.6, 29.7, 26.8, 25.5, 24.3, 23.0, 22.7, 15.0. **IR**: ν (cm^{-1}) 3309, 3060, 2928, 2855, 2798, 2740, 1719, 1637, 1502, 1488, 1438, 1382, 1243, 1038, 858, 806, 763, 732. **HRMS** (ESIQ-TOF): m/z calculated for $C_{36}H_{46}N_2O_4$ $[M+Na]^+$: 593.3355, found 529.3354.

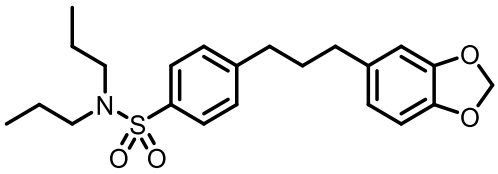

4-(3-(benzo[d][1,3]dioxol-5-yl)propyl)-N,N-dipropylbenzenesulfonamide (2.105) was prepared according to the general procedure using $Pd(OAc)_2$ on 3.0 mmol scale with 3 mol % [Pd] loading in 5 mL toluene in a 100 mL Schlenk flask. Purification by column chromatography (10% EtOAc in hexanes) afforded **2.105** as a colourless oil (0.83 g, 69%). **^{1}H NMR** (400 MHz, $CDCl_3$): 7.72 (d, *J* = 8.4 Hz, 2H), 7.29 (d, *J* = 8.2 Hz, 2H), 6.74 (d, *J* = 7.8 Hz, 1H), 6.67 (d, *J* = 1.6 Hz, 1H), 6.62 (dd, *J* = 7.8, 1.6 Hz, 1H), 5.93 (s, 2H), 3.09-3.06 (m, 4H), 2.69 (t, *J* = 7.8 Hz, 2H), 2.57 (t, *J* = 7.5 Hz, 2H), 1.93 (quin, *J* = 7.7 Hz, 2H), 1.56 (sxt, *J* = 7.5 Hz, 4H), 0.87 (t, *J* = 7.4 Hz, 6H). **^{13}C NMR** (100 MHz, $CDCl_3$): 147.7, 147.2, 145.8, 137.7, 135.7, 129.0, 127.3, 121.2, 108.9, 108.2, 100.9, 50.1, 35.2, 35.1, 32.9, 22.1, 11.3. **IR**: ν (cm^{-1}) 2965, 2932, 2875, 2255, 1597, 1503, 1488, 1441, 1334, 1243, 1185, 1152, 1091, 1039, 989, 909, 807, 728. **Accurate mass** (EI): m/z calculated for $C_{22}H_{29}NO_4S$: 403.1812, found 403.1618 (spectral accuracy = 96.8%).

Chapter 3. Nickel-Catalyzed Cross-Couplings of Methyl Esters

2.1. Background: Activation of methyl esters

In the last chapter, we highlighted the fact that esters are particularly interesting electrophilic coupling partners that can give rise to different coupling adducts. A good understanding of how we can control selectivity is key to exploit the potential of this transformation. We also provided the argument that esters are abundant and robust, and that these characteristics represent an important opportunity for late-stage functionalization and step-economy. However, phenyl esters are not naturally abundant and need to be synthesized from the corresponding carboxylic acids. Methyl and ethyl esters, on the other hand, are commercially available and widely abundant. As has been outlined in Chapter 1, the field of cross-couplings with carboxylic acid derivatives is slowly moving towards the activation of more robust substrates, and methyl/ethyl esters represent one of the most robust carboxylic acid derivatives (Figure 14).

Figure 14. Relative robustness of carboxylic acid derivatives coupling partners

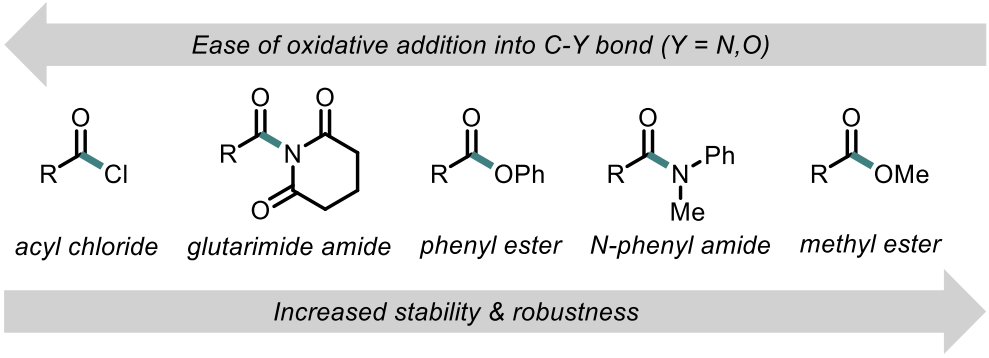

Saying that methyl/ethyl esters are readily available is an understatement; they are ubiquitous. For example, they are often associated with heterocycle synthesis;

condensation reactions with malonates result in the formation of ester-bearing heterocycles. Dienophiles containing methyl or ethyl esters are commonly used in Diels-Alder reactions because of their low energy LUMO, and the resulting cyclized products, therefore, contain esters. Methyl esters are regularly present in the synthesis of complex molecules such as natural products, wherein they remain intact throughout the early steps, and are often hydrolyzed and functionalized with stoichiometric activating agents later in the synthesis. Using these widely abundant and robust functionalities directly instead, via the means of catalysis, would be highly desirable. Cross-couplings using *phenyl* esters was a step forward in the field, but the coupling of unactivated methyl/ethyl esters would be of highest practicality. Because of their increased robustness, methyl esters are inherently harder substrates for low valent metals to oxidatively add into. For instance, the bond dissociation energy (BDE) of the C–O bond of methyl esters is ~20 kcal/mol higher than that of phenyl esters (Figure 15).[95]

Figure 15. BDE of methyl benzoate and phenyl benzoate

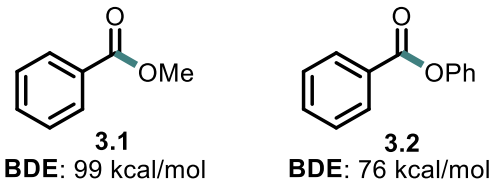

Because of these difficulties, cross-coupling reactions using methyl/ethyl esters as electrophiles have remained scarce. Garg's group disclosed the first cross-coupling reaction using methyl esters in 2016.[96] In this publication, the Ni-catalyzed cross-coupling of methyl esters with N-methyl anilines to make amides is reported (Scheme 56).

[95] Yue, H.; Zhu, C.; Rueping, M. *Org. Lett.* **2018**, *20*, 385−388.
[96] Hie, L.; Fine Nathel, N. F.; Hong, X.; Yang, Y.-F.; Houk, K. N.; Garg, N. K. *Angew. Chem. Int. Ed.* **2016**, *55*, 2810–2814.

Stoichiometric aluminium *tert*-butoxide was required to facilitate the oxidative addition into the strong C–O bond, and the ester scope was limited to methyl 1-naphthoates **3.3**.

Scheme 56. Garg's Ni-catalyzed amidation of methyl esters

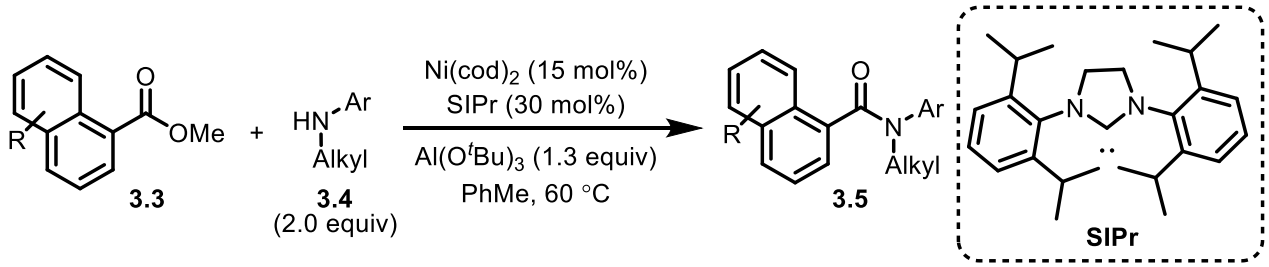

Hu et al. later disclosed, in 2017, the coupling of methyl esters with nitroarenes to form amides (Scheme 57).[97] In this reaction, stoichiometric zinc powder and TMSCl is used to reduce the nitroarene *in situ*. It is speculated that generation of a reactive Ni-nitrene intermediate can then facilitate insertion into the methyl ester. The ester scope was greatly improved over Garg's amidation; both aliphatic and (hetero)aromatic esters could be utilized.

Scheme 57. Hu's Ni-catalyzed amidation of methyl esters using nitroarenes

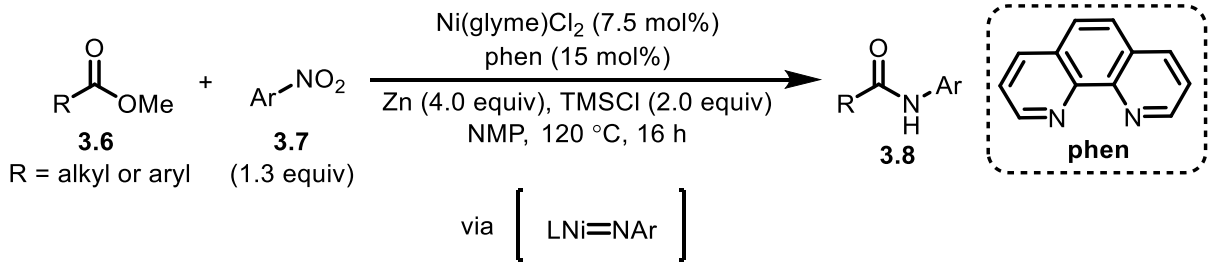

Very recently, Rueping et al. disclosed the Ni-catalyzed conversion of methyl esters into aryl stannanes (Scheme 58).[95] This represents the first decarbonylative cross-coupling of methyl esters.

[97] Cheung, C. W.; Ploeger, M. L.; Hu, X. *Nature Commun.* **2017**, *8*, 14878-14887

Scheme 58. Rueping's Ni-catalyzed coupling of methyl esters to form aryl stannanes

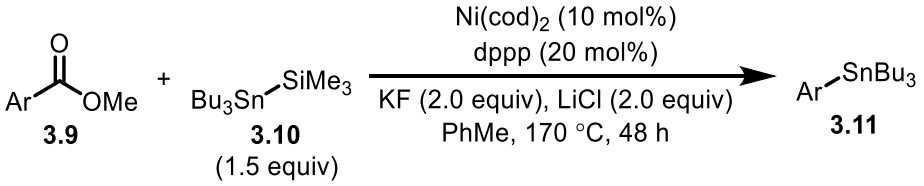

Even more recently, the Yamaguchi lab reported a Ni-catalyzed decarbonylative methylation of methyl esters (Scheme 59).[98] In this transformation, alkyl aluminium species **3.12** is thought to play the dual role of the nucleophile and the Lewis acid (to facilitate the oxidative addition of Ni(0) into the methyl ester C(acyl)–O bond).

Scheme 59. Yamaguchi's Ni-catalyzed methylation of methyl esters

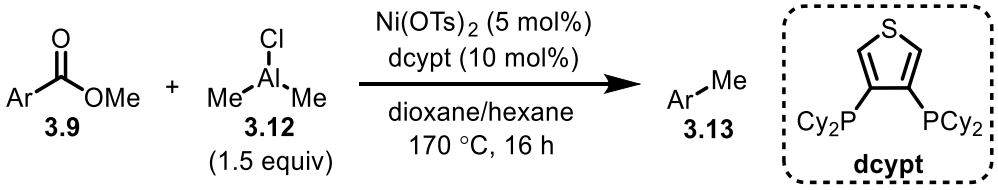

In summary, reports of cross-couplings with methyl esters have mostly remained limited to the use of stoichiometric Lewis acids (e.g. $Al(O^tBu)_3$ or $AlMeCl_2$) or the use of highly activated nucleophiles (e.g. nitrene). In this chapter, two additive-free Ni-catalyzed cross-coupling reactions of methyl esters will be reported.

2.2. Nickel-catalyzed amidation of methyl esters[99]

2.2.1. Amide bond formation from methyl esters

Despite the abundance of methyl esters, strategies to use them directly in amidation reactions are highly limited. One strategy to achieve amidation of such esters is to

[98] Okita, T.; Muto, K.; Yamaguchi, J. *Org. Lett.* **2018**, *20*, 3132–3135.

[99] The work described in Section 2.2 has been published in a peer-reviewed journal: Ben Halima, T.; Masson-Makdissi, J.; Newman, S. G. "Nickel-Catalyzed Amide Bond Formation from Methyl Esters," *Angew. Chem. Int. Ed.* **2018**, in press.

deprotonate the amine nucleophile **3.14** using harsh stoichiometric bases such as Grignard reagents,[100] $AlMe_3$,[101] or LHMDS (Scheme 60, Strategy A).[102] This strategy is undesirable if dealing with molecules having base-sensitive functional groups. Moreover, this method can lead to undesired epimerization of esters with α stereocenters.

Scheme 60. Strategies for the amidation of methyl esters

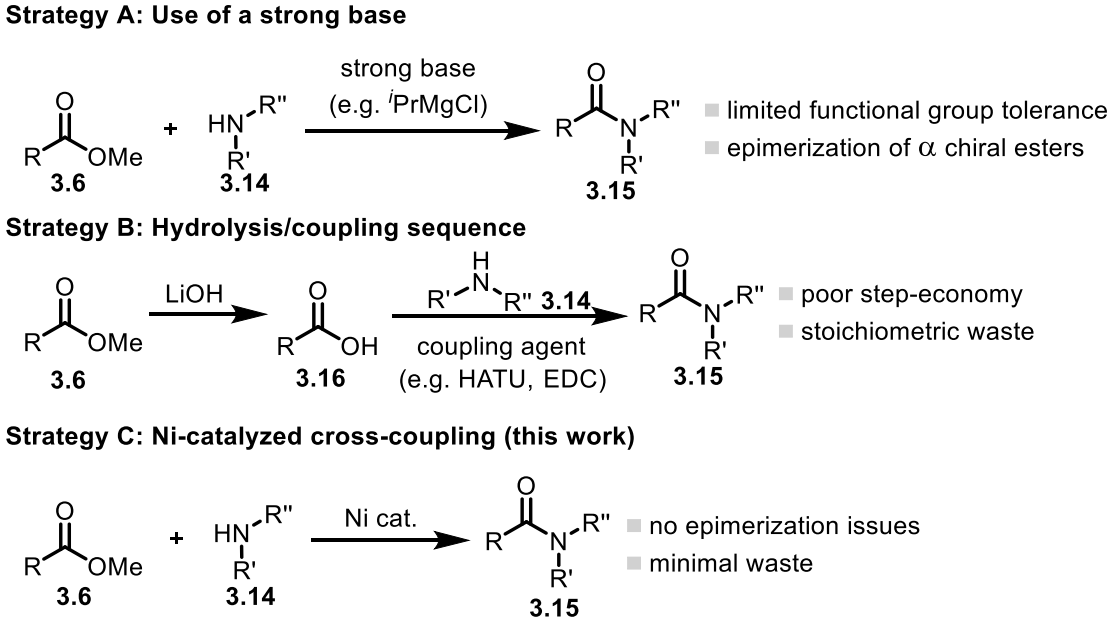

Another common route to achieve amidation of methyl esters is to hydrolyze them first (Scheme 60, Strategy B). The resulting carboxylic acids can then be converted to acyl chlorides (e.g. with thionyl chloride) and reacted with amines to form amides. The carboxylic acid can also be coupled to an amine using other stoichiometric activating agents such as EDC[103] or HATU.[104] It should be noted that catalytic alternatives to couple

[100] Muñoz, J. M.; Alcázar, J.; de la Hoz, A.; Díaz-Ortiz, Á; de Diego, S.-A. A. *Green Chem.* **2012**, *14*, 1335–1341.
[101] Basha, A.; Lipton, M.; Weinreb, M. S. M. *Tetrahedron Lett.* **1977**, *48*, 4171–4174.
[102] Vrijdag, J. L.; Delgado, F.; Alonso, N.; De Borggraeve, W. M.; Pérez-Macias, N.; Alcázar, J. *Chem. Commun.* **2014**, *50*, 15094–15097.
[103] Sheehan, J.; Cruickshank, P.; Boshart, G. *J. Org. Chem.* **1961**, *26*, 2525–2528.
[104] Carpino, L. A. *J. Am. Chem. Soc.*, **1993**, *115*, 4397–4398.

the hydrolyzed esters to amines using borate ester catalysts have also been developed.[105] Notwithstanding the importance of these organocatalyzed methods, a catalytic method that directly couples methyl esters to amines, obviating the need for a hydrolysis step, would be of high utility (Scheme 60, Strategy C).

2.2.2. Reaction discovery

The reaction disclosed herein was discovered by Ph. D. student Taoufik Ben Halima. I joined the project when the reaction conditions were already optimized, and the reaction scope had already been started. My contributions are highlighted herein.[106]

The optimized reaction conditions are illustrated in Scheme 61. The reaction works very efficiently with a simple Ni-IPr catalyst in the absence of any base or other additives. The only stoichiometric by-product generated is methanol.

Scheme 61. Additive-free Ni-catalyzed amidation of methyl esters

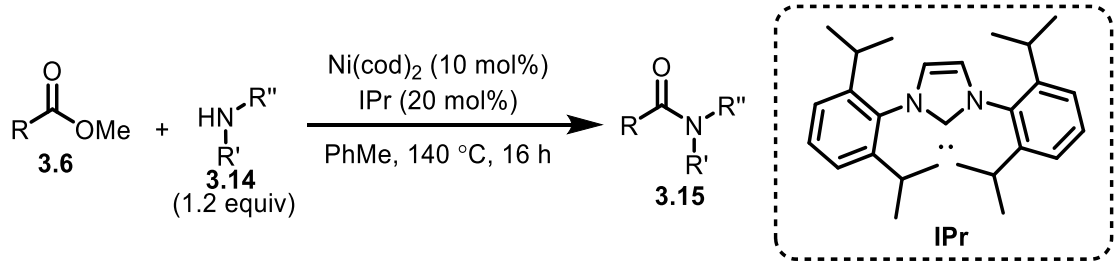

2.2.3. Ni-catalyzed amidation of methyl esters: Scope

In contrast to Garg's scope, which was limited to methyl 1-naphthoate derivatives, our scope could tolerate an extremely broad range of (hetero)aromatic and aliphatic esters. Some examples are provided in Table 13. The scope includes—but is not limited to—

[105] For some examples, see: (a) Noda, H.; Furutachi, M.; Asada, Y.; Shibasaki, M.; Kumagai, N. *Nature Chem.* **2017**, *9*, 571–577; (b) Mylavarapu, R. K.; GCM, K.; Kolla, N.; Veeramalla, R.; Koilkonda, P.; Bhattacharya, A.; Bandichhor, R. *Org. Process Res. Dev.* **2007**, *11*, 1065–1068; (c) Sabatini, M. T.; Boulton, L. T.; Sheppard, T. D. *Sci. Adv.* **2017**, *3*, e1701028.

[106] Some experiments performed by Taoufik Ben Halima have been included in this Chapter to complete the storyline. Roughly 50% of the results presented Tables 12 & 13 (taking into account starting material synthesis) were obtained by me. Results presented in Schemes 69 & 77 were obtained by Taoufik.

heteroaromatics such as pyrazine (entry 1), imidazole (entry 2), benzofuran (entry 3), and methyl-protected indole (entry 4). Aliphatic esters can also be coupled efficiently (entries 5-7). Notably, enantiopure esters with chiral α centers (entries 6 and 7) were converted to amides without any loss in enantiopurity. By contrast, if the respective esters **3.29** and **3.31** were to be coupled using a harsh base instead, epimerization would likely occur. This highlights the potential of our reaction in the context of amide bond formation of enantiopure materials.

Table 13. Ester scope of the Ni-catalyzed amidation reaction

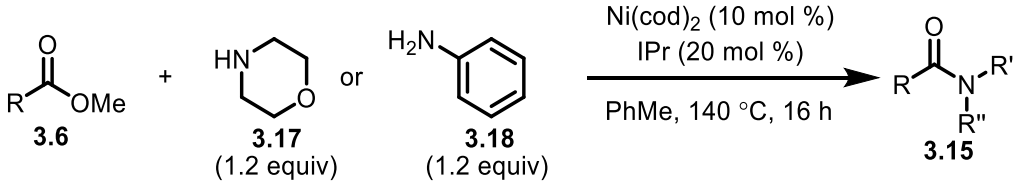

Entry	Ester starting material	Amide product	%Yield[a]
1	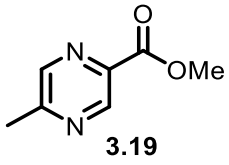 **3.19**	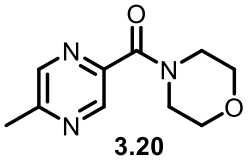 **3.20**	84
2	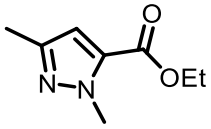 **3.21**	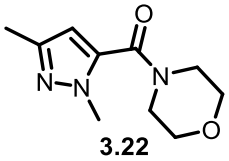 **3.22**	64
3	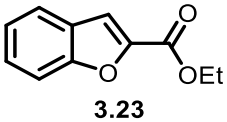 **3.23**	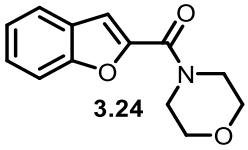 **3.24**	82
4	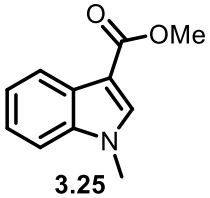 **3.25**	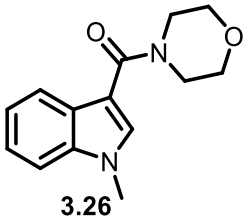 **3.26**	87

5	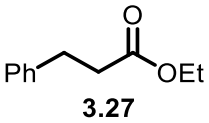 **3.27**	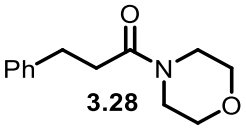 **3.28**	79
6	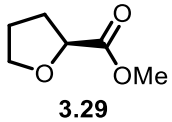 **3.29**	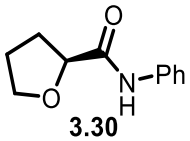 **3.30**	91
7	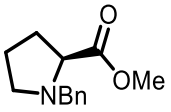 **3.31**	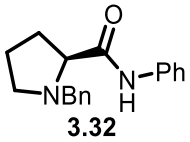 **3.32**	35

General conditions: Ester (0.20 mmol), aniline **3.17** or morpholine **3.18** (0.24 mmol), $Ni(cod)_2$ (5.5 mg, 10 mol%), IPr (16 mg, 20 mol%), PhMe (1.0 mL), at 140 °C for 16 h, under inert atmosphere. [a]Isolated yields.

Methyl benzoate was successfully coupled with several primary and secondary aliphatic amines as well as various aniline derivatives. Some examples are outlined in Table 14. Cyclic and acyclic secondary amines are efficient nucleophilic partners (entries 1 and 2). The tolerance of the acetal moiety in substrate **3.34** is particularly notable. Primary amines such as benzyl amine **3.38** and amines **3.40** and **3.42** also work very well (entries 3-5). Different aniline derivatives were coupled efficiently. Simple aniline **3.44** (entry 6), sterically-hindered aniline **3.46** (entry 7), and electron-poor aniline **3.48** (entry 8) provide excellent to moderate yields.

Table 14. Amine scope of the Ni-catalyzed amidation of methyl esters

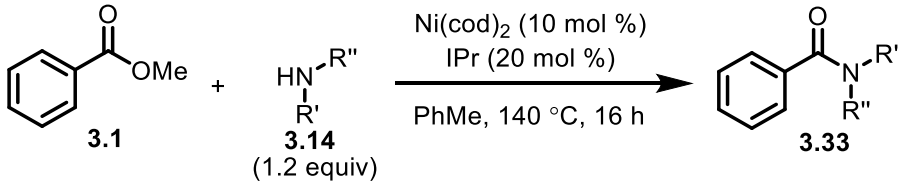

Entry	Amine starting material	Amide product	%Yield[a]
1	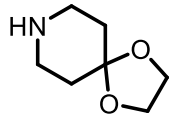 3.34	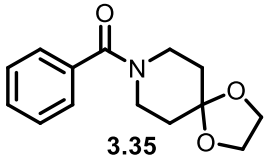 3.35	76[b]
2	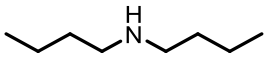 3.36	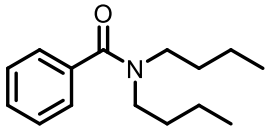 3.37	73
3	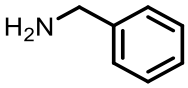 3.38	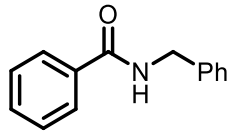 3.39	74
4	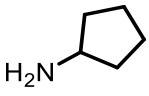 3.40	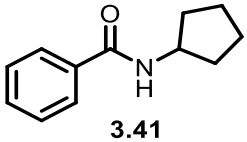 3.41	86
5	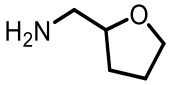 3.42	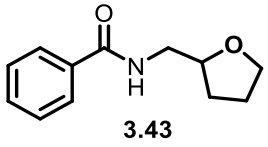 3.43	88
6	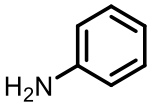 3.44	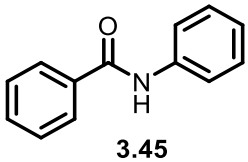 3.45	83
7	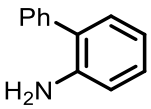 3.46	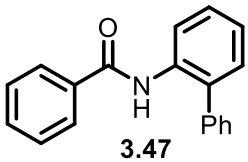 3.47	60

8	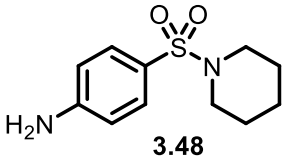 **3.48**	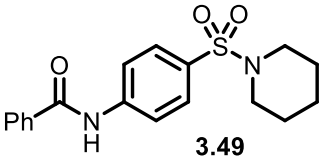 **3.49**	53

General conditions: Methyl benzoate **3.1** (25 μL, 0.20 mmol), amine (0.24 mmol), $Ni(cod)_2$ (5.5 mg, 10 mol%), IPr (16 mg, 20 mol%), PhMe (1.0 mL), at 140 °C for 16 h, under inert atmosphere. [a]Isolated yields. [b]Run in dioxane (1.0 mL) instead of toluene.

While a broad range of substrates could be tolerated in our coupling reaction, several limitations were encountered during the scope development. Some unsuccessful amines are shown in Scheme 62. Amines bearing nitrogen-containing heteroaromatics generally resulted in no product formation or very low yields (**3.50**-**3.55**). Moreover, secondary or primary amines bearing tertiary amines did not work at all (**3.56** and **3.57**). On the other hand, tertiary amines can be tolerated on the ester substrate, indicating that the bidentate nature of these amines might be responsible for their low efficiency. Also, slightly sterically congested secondary amines were incompatible (**3.58** and **3.59**). Steric congestion in the amine nucleophile could likely disfavour amine coordination for the ligand exchange step.

Scheme 62. Unsuccessful amines of the Ni-catalyzed amidation reaction[107]

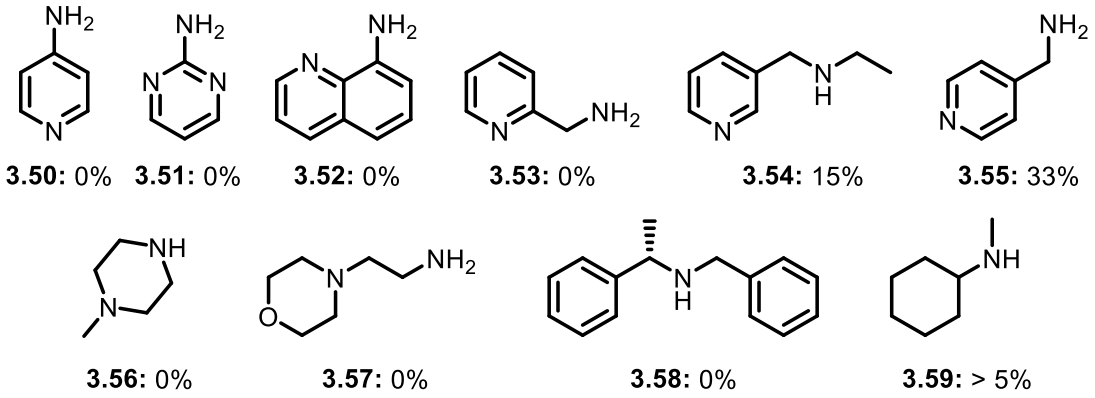

[107] All of these amines were tested with methyl benzoate as a model substrate.

A selection of unsuccessful esters is shown in Scheme 63. A methyl-protected indole can be coupled with morpholine in 87% yield (entry 4, Table 13). However, several indoles bearing different protecting groups did not provide any trace of product (**3.60**-**3.62**). For instance, when acetal-protected indole **3.60** was reacted with morpholine in the presence of the Ni-IPr catalyst, no desired product was obtained. Interestingly, complete deprotection of the indole substrate (-NAc to -NH) was observed instead. Partial deprotection of Boc-protected indole **3.61** was also observed with no formation of the amide product. Tosyl-protected indole **3.62** was also tried but proved unsuccessful. However, no deprotection occurred in this case. Other non-tolerated heteroaromatics on the ester substrate included thiazoles (**3.63**), thiophenes (**3.64**), and oxazoles (**3.65**). The starting material was recovered in these cases.

Scheme 63. Unsuccessful esters in the Ni-catalyzed amidation reaction[108]

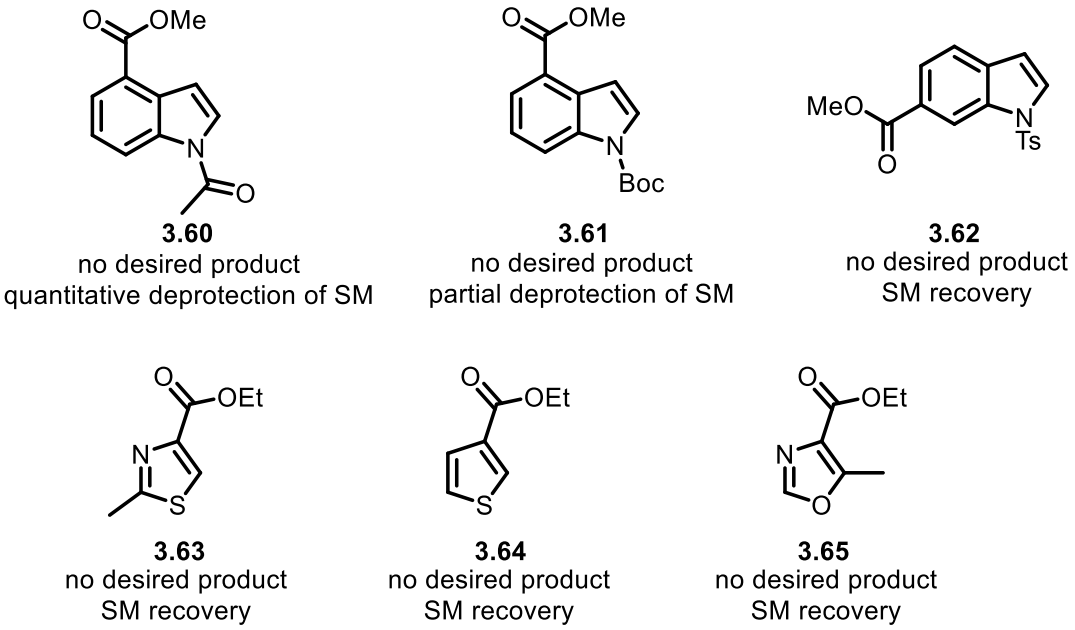

[108] All of the ester substrates were tried with morpholine.

2.2.4. Applications

To further demonstrate the practicality of the Ni-catalyzed amidation protocol, the synthesis of bioactive molecules and other special applications were carried out.

Step-economy in the synthesis of medicinal and agrochemical compounds

It is common routine in the synthesis of drugs or other bioactive molecules to hydrolyze esters and then couple them with an amine with the help of a stoichiometric activating agent to form amide linkages. This way of operating is not atom-economical nor step-economical. An efficient method to directly convert methyl or ethyl ester into amides in one step would be desirable. Our Ni-catalyzed amidation reaction has the potential of doing just that and to significantly minimize waste, by generating methanol or ethanol as the only stoichiometric by-product. Some attempts at utilizing our amidation protocol for the synthesis of bioactive molecules are described below.

Fluxapyroxad

Fluxapyroxad is a fungicide that is sold by BASF (Scheme 64). Ethyl ester **3.68** is easily obtained via a condensation reaction between **3.66** and methyl hydrazine **3.67**. In the patented procedure,[109] hydrolysis of ethyl ester **3.68** is then carried out in the same pot to afford carboxylic acid **3.69**. The carboxylic acid is then reacted with thionyl chloride to afford the corresponding acyl chloride **3.70**. The final step is the amidation between acyl chloride **3.70** and amine **3.71**.[110]

While all the yields for these steps are excellent, the process is not atom-economical. We thus attempted to apply our Ni-catalyzed amidation reaction to afford fluxapyroxad

[109] Wolf, B. U. S. Patent. 9,990. January 28, 2010.
[110] Reichert, W.; Koradin, C.; Smidt, S. P.; Maywald, V.; Wolf, B.; Rack, M.; Zierke, T.; Keil, M. U. S. Patent. 54,183. March 3, 2011.

directly from ethyl ester **3.68**. Unfortunately, not a trace of fluxapyroxad was obtained using our method (starting material recovery).

Scheme 64. Alternative route for the BASF fungicide, fluxapyroxad

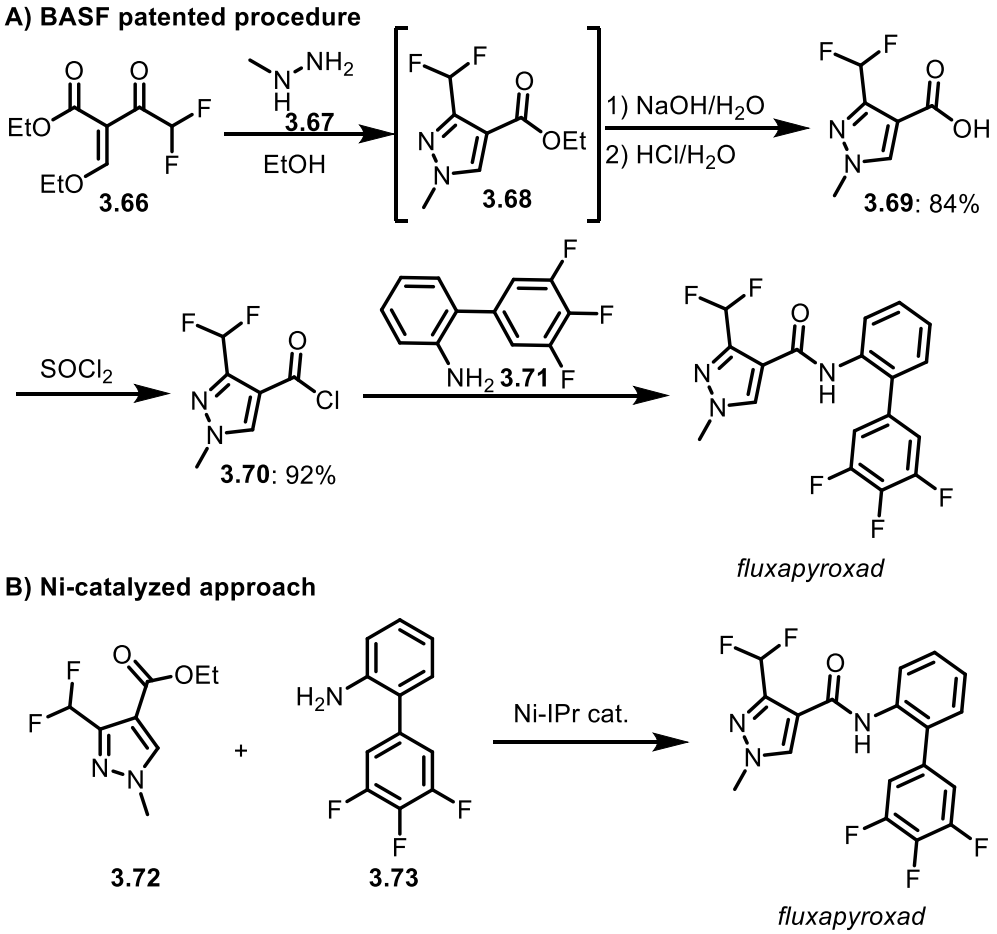

AS-136A

AS-136A is an anti-viral drug candidate for the treatment of measles.[111] Ethyl ester **3.76** can be obtained in one-step via a silver-mediated cycloaddition (Scheme 65A).[112] The nitrogen atom at position 1 of the pyrazole ring is then protected with methyl iodide, followed by hydrolysis to afford carboxylic acid **3.77**. The carboxylic acid is later

[111] Sun, A.; Chandrakumar, N.; Yoon, J.-J.; Plemperb, R. K.; Snydera, J. P. *Bioorg. Med. Chem. Lett.* **2007**, *17*, 5199–5203.

[112] Li, F.; Nie, J.; Sun, L.; Zheng, Y.; Ma, J.-A. *Angew. Chem. Int. Ed.* **2013**, *52*, 6255 –6258.

converted into an acyl chloride, followed by amidation with amine **3.48**. Again, there is an opportunity to avoid the hydrolysis/acyl chloride synthesis steps. Methyl-protected pyrazole ester **3.78** could, in theory, be coupled with amine **3.48** via Ni catalysis to afford **AS-136A** more directly (Scheme 65B).

Scheme 65. Synthesis of AS-136A

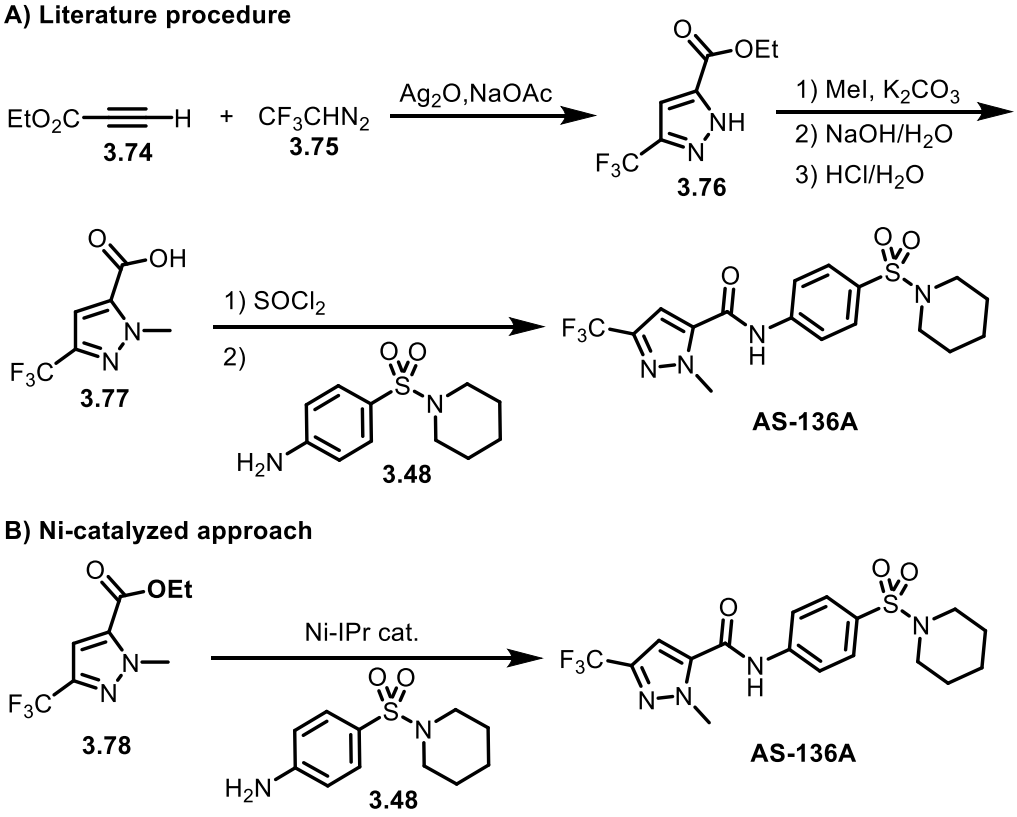

Towards this goal, we initially tested the coupling of readily available ester **3.79** and amine **3.48** (Scheme 66). Unfortunately, the desired product **3.80** could not be afforded in more than 20% NMR yield (ester starting material was recovered). The addition of bases or an increase in catalyst loading failed to improve the yield any further.

Scheme 66. Model reaction for the synthesis of AS-136A

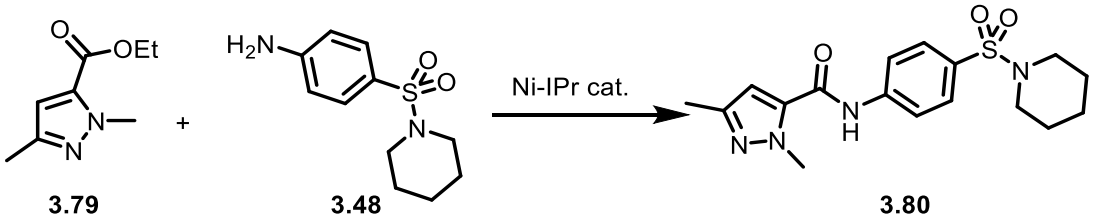

EMPA

EMPA is a selective antagonist for the OX_2 receptor, which is involved in sleep regulation.[113] Again, the multi-step synthesis used to synthesize this drug relies on a hydrolysis/coupling sequence (Scheme 67).[114] By contrast, our coupling reaction could potentially afford the drug directly from methyl ester **3.83**.

[113] Malherbe, P.; Borroni, E.; Gobbi, L.; Knust, H.; Nettekoven, M.; Pinard, E.; Roche, O.; Rogers-Evans, M.; Wettstein, J. G.; Moreau, J.-L. *Br. J. Pharmacol.* **2009**, *156*, 1326–1341.

[114] Wang, C.; Moseley, C. K.; Carlin, S. M.; Wilson, C. M.; Neelamegam, R.; Hooker, J. M. *Bioorg. Med. Chem. Lett.* **2013**, *23*, 3389–3392.

Scheme 67. Synthesis of EMPA

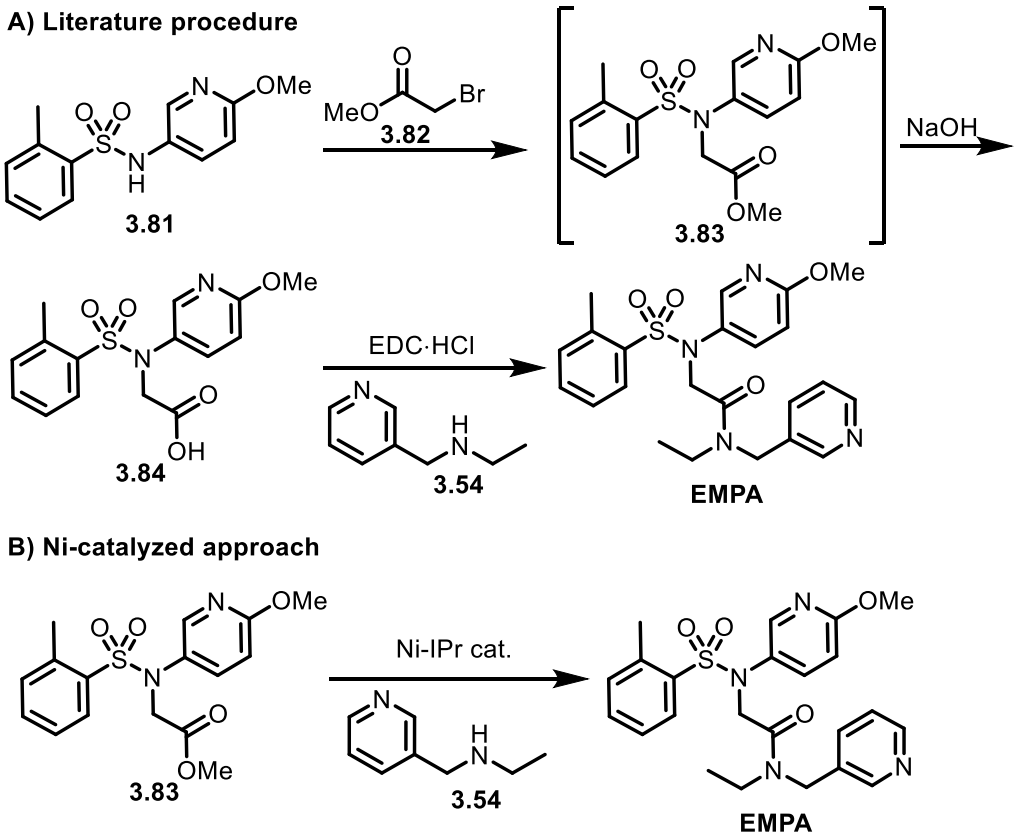

When methyl ester **3.83** and amine **3.54** were reacted in the presence of the Ni-IPr catalyst, no trace of EMPA was obtained. The starting material **3.83** was found to be almost entirely decomposed at the end of the reaction, but the decomposition by-products could not be clearly characterized. The reaction of methyl ester **3.83** with simple aniline did not afford any of the corresponding amide product either, and decomposition of the starting material was again observed.

Coumarin derivatives

Coumarin carboxamide derivatives have recently been shown as efficient inhibitors of monoamine oxidase B, which make them potential therapeutics for neurodegenerative

diseases such as Alzheimer and Parkinson.[115] Coumarin carboxamide **3.90** is synthesized via hydrolysis/EDC coupling of ethyl ester **3.87**, which is easily synthesized via a condensation reaction between diethyl malonate **3.86** and the corresponding salicylaldehyde derivative **3.85** (Scheme 68A).[116] Alternatively, the Ni-catalyzed protocol could couple ethyl ester **3.87** directly with aniline derivative **3.89**, skipping the hydrolysis step and avoiding the unnecessary waste associated with EDC couplings (Scheme 68B).

Scheme 68. Synthesis of coumarin derivatives

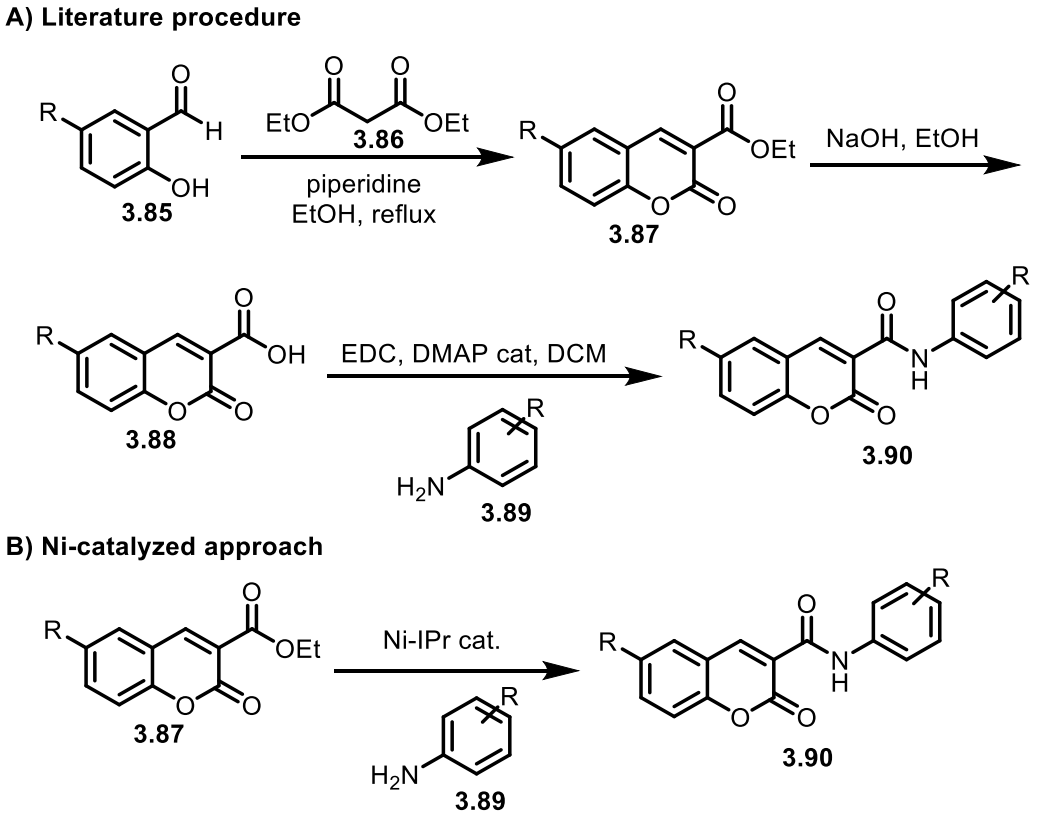

Amidation of coumarin ethyl esters was moderately successful using the Ni-catalyzed approach. The reaction was initially tested between ethyl ester **3.91** and aniline on 0.10

[115] Chimenti, F.; Secci, D.; Bolasco, A.; Chimenti, P.; Bizzarri, B.; Granese, A.; Carradori, S.; Yáñez, M.; Orallo, F.; Ortuso, F.; Alcaro, S. *J. Med. Chem.* **2009**, *52*, 1935–1942.

[116] Fonseca, A.; Reis, J.; Silva, T.; Matos, M. J.; Bagetta, D.; Ortuso, F.; Alcaro, S.; Uriarte, E.; Borges, F. *J. Med. Chem.* **2017**, *60*, 7206−7212.

mmol scale, which afforded the amide **3.93** in 65% yield (Table 15, entry 1). Running the reaction on 0.20 mmol scale reduced the yield to 48% (Table 15, entry 2), but running the reaction more concentrated solved the problem and afforded amide **3.93** in 60% yield (Table 15, entry 3). Similarly, coumarin carboxamide derivative **3.94** could also be obtained in 50% yield (Table 15, entry 4).

Table 15. Synthesis of coumarin carboxamides via Ni catalysis

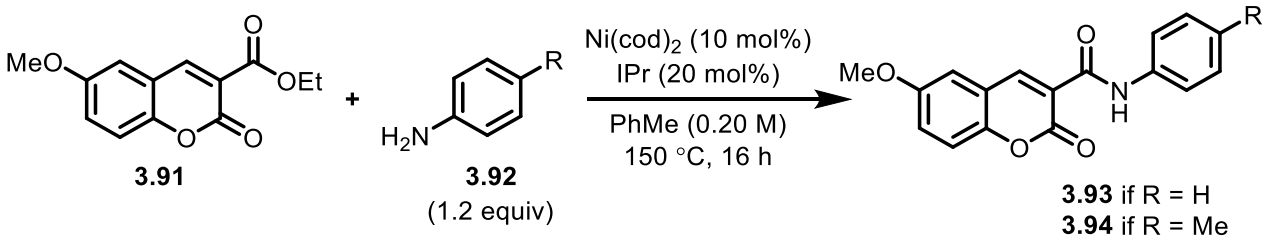

Entry	R =	Scale (mmol)	%Yield[a]
1	H	0.10	65
2	H	0.20	48
3[b]	H	0.20	60
4[b]	Me	0.20	50

[a]Crude yields calculated by ^{1}H NMR using 1,3,5-trimethoxybenzene as an internal standard. [b]Run at 0.40 M.

Orthogonal reactivity

Methyl para-fluorobenzoate **3.95** was a suitable substrate under our coupling conditions, providing product **3.98**. However, in the absence of the catalyst, with a base and in a polar solvent, this substrate undergoes S_NAr reactivity instead of amidation. This orthogonal reactivity is quite interesting and highlights the power of Ni catalysis to enable new types of disconnections that cannot be achieved easily using more traditional methods.

Scheme 69. Reaction with methyl para-fluorobenzoate: S_NAr vs amidation

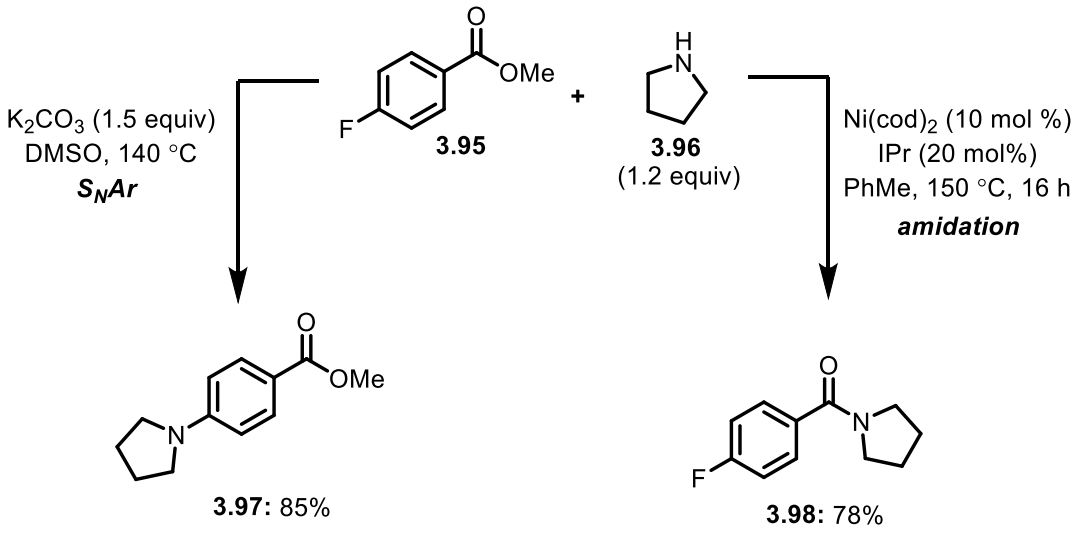

From the same train of thoughts, we pondered whether the Ni-IPr catalyst could selectively react with a methyl ester in the presence of an epoxide. It is known that epoxides can be opened by amines in the presence of water or of an appropriate Lewis acid.[117] By contrast, the use of a Ni catalyst could potentially enable selective amidation as opposed to opening the epoxide. To test our hypothesis, epoxidized methyl oleate was reacted with morpholine in the presence of the Ni-IPr catalyst. The reaction was unsuccessful, providing no trace of the desired product **3.100**, but interesting by-products were obtained. The epoxide functionality had been fully consumed and converted to a ketone.

[117] (a) Pujala, B.; Chakraborti, A. K. *J. Org. Chem.* **2007**, *72*, 3713-3722; (b) Azizi, N.; Saidi, M. R. *Org. Lett.* **2005**, *7*, 3649-3651.

Scheme 70. Attempted amidation of epoxidized methyl oleate

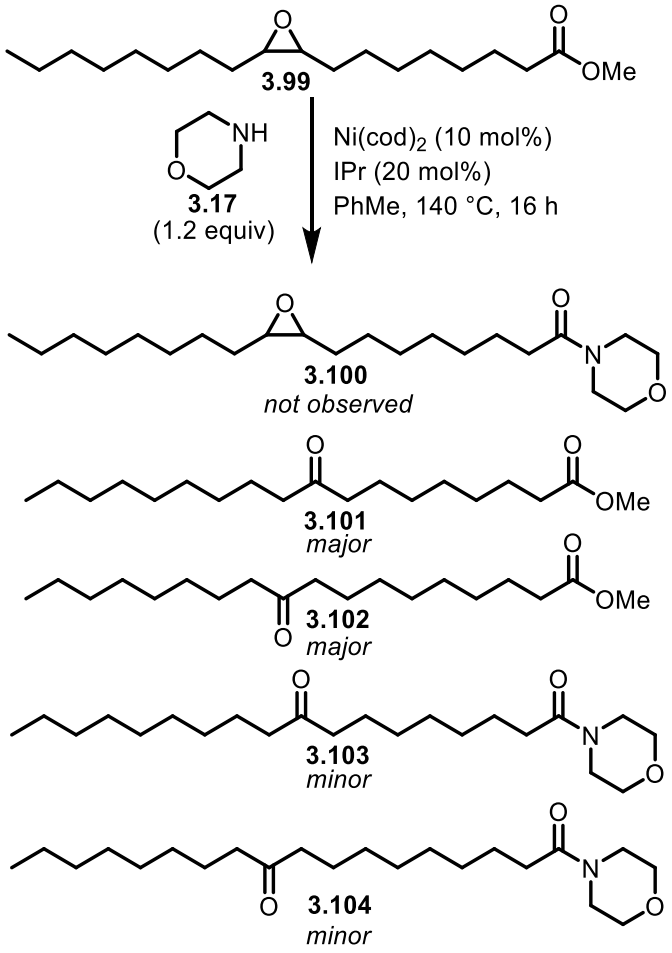

A plausible mechanism for the conversion of the epoxide into a ketone could involve oxidative addition of Ni into the epoxide C–O bond, followed by β-hydride elimination, and reductive elimination, affording an enol product which can then tautomerize to the ketone. This type of transformation (epoxide to ketone) has been disclosed previously by the Kunz lab who used a rhodium-NHC-pincer complex to do so.[118] They note that this type of reactivity is complementary to the Meinwald rearrangement of epoxides, which involves opening of an epoxide with a Lewis acid catalyst, forming a carbocation, followed by alkyl or hydride shift to afford a ketone or aldehyde. Interestingly, with

[118] Jürgens, E.; Wucher, B.; Rominger, F.; Törnroos, K. W.; Kunz, D. *Chem. Commun.* **2015**, *51*, 1897-1900.

terminal epoxides **3.105**, the aldehyde product **3.106** is favoured, but with the transition metal-catalyzed approach, the methyl ketone **3.107** is obtained selectively (Scheme 71). The selectivity in the Meinwald rearrangement can be rationalized by the formation of the most stable intermediate carbocation **Int3.1**, whereas, with a Ni or Rh catalyst, oxidative addition into the less hindered C–O bond is favoured (**Int3.2**).

Scheme 71. Lewis acid- vs transition metal-catalyzed opening of epoxides

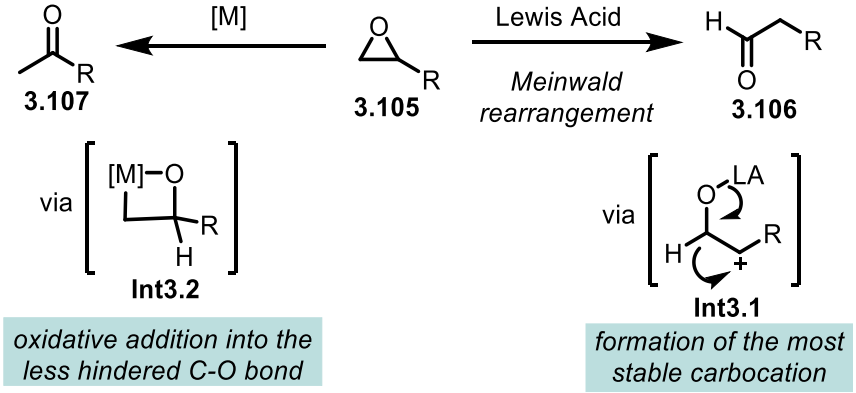

Alternative disconnections: Lidocaine derivatives

Lidocaine is a commonly used local anesthetic (Figure 16).[119] However, in certain patients, especially those suffering from asthma, lidocaine can have serious adverse effects. A lidocaine derivative with limited side-effects would thus be valuable. For instance, a recent study suggests that analog **JM25-1** could be a promising alternative to lidocaine.[120]

Figure 16. Chemical structures of lidocaine and JM25-1

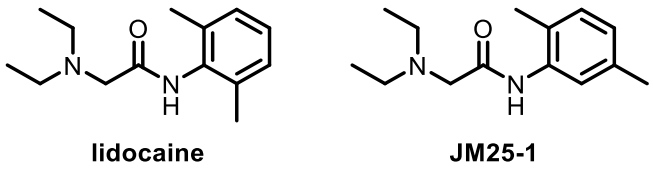

[119] Ej Golzari, S.; Soleimanpour, H.; Mahmoodpoor, A.; Safari, S.; Ala, A. *Anesth Pain Med.* **2014**, *4*: 15444.
[120] Serra, M. F.; Neves, J. S.; Couto, G. C.; Cotias, A. C.; Pão, C. R. *Anesthesiology* **2016**, *124*, 109–120.

Lidocaine derivatives are usually synthesized in two steps (Scheme 72, Method A). Chloroacetyl chloride **3.108** is first reacted with the aniline derivative **3.89** to form amide **3.109**. Then, amide **3.109** is reacted with diethyl amine to afford the lidocaine derivative **3.110**. An alternative disconnection approach could involve the reaction of methyl chloroacetate **3.111** with diethyl amine (Scheme 72, Method B). Methyl ester **3.112** could then be a common precursor used for the synthesis of all lidocaine derivatives by reacting it with the appropriate aniline derivative **3.89** in the presence of the Ni-IPr catalyst.

Scheme 72. Classical vs cross-coupling approach to the synthesis of lidocaine derivatives

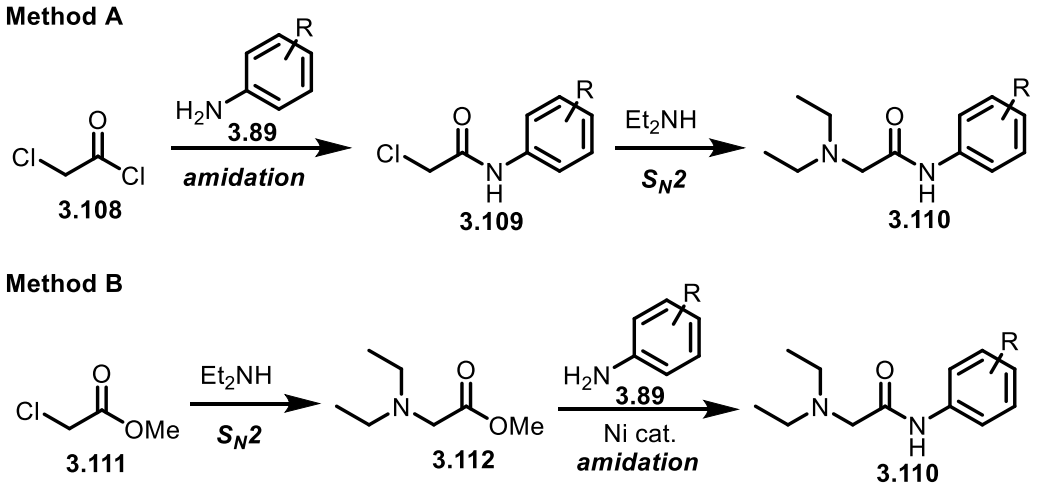

Toward the goal of enabling Method B, the synthesis of lidocaine was first attempted in the presence of the Ni-IPr catalyst (Scheme 73). Unfortunately, no trace of lidocaine was observed. An increase in temperature or in catalyst loading and addition of bases all proved ineffective.

Scheme 73. Attempted synthesis of lidocaine

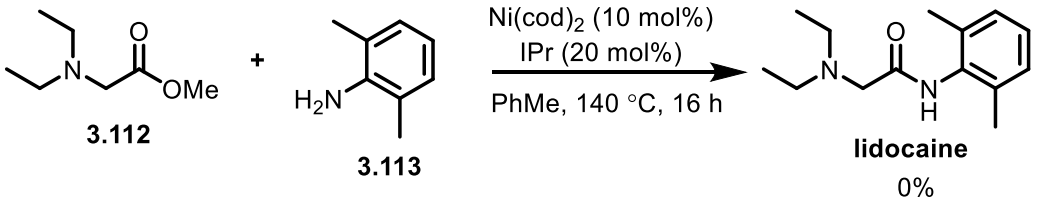

We hypothesized that the hindered nature of aniline derivative **3.113** might be one of the reasons why the above transformation failed. When methyl ester **3.112** was reacted with simple aniline **3.18** instead, a satisfactory yield of 68% was initially obtained. Running the reaction for longer improved the yield to nearly 80% (Scheme 74).[121]

Scheme 74. Synthesis of unhindered lidocaine derivative

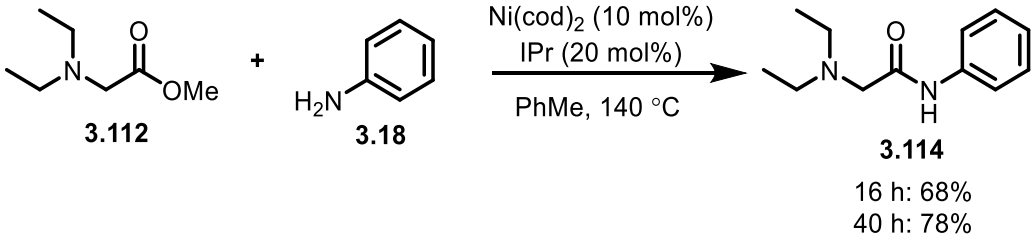

When scaling up the reaction for scope (from 0.10 mmol to 0.20 mmol), the initial isolated yield of **3.114** was only 49%. Fortunately, increasing the reaction concentration fixed the issue, affording lidocaine derivative 3.114 in 77% isolated yield (Scheme 75). The synthesis of other derivatives was also carried out. For example, lidocaine derivative **3.115** could be obtained in a similar yield of 78%. A slightly more electron-poor aniline derivative could also be successfully coupled with methyl ester **3.112**, affording **3.116** in 59% yield. Hindered aniline derivative with a methyl group in the ortho position could also be used but required increased catalyst loading to provide moderate yields (**JM25-1** and **JM23-1**).

[121] ^{1}H NMR yields determined with 1,3,5-trimethoxybenzene as an internal standard.

Scheme 75. Scope of the lidocaine derivatives

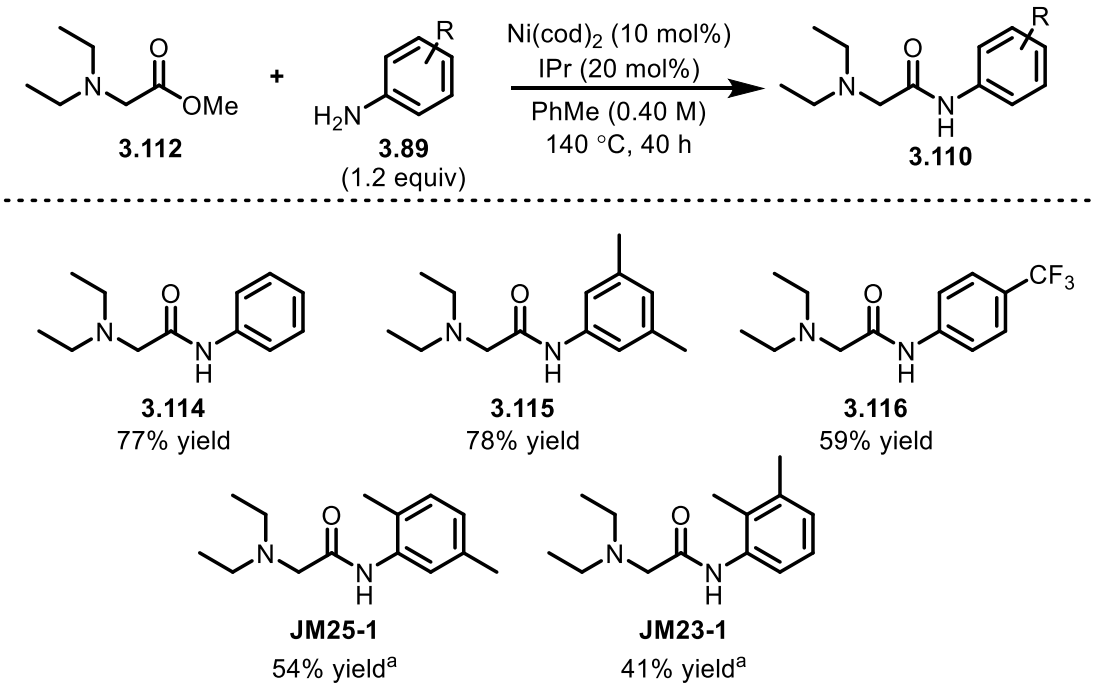

[a]20 mol% $Ni(cod)_2$ and 40 mol% IPr was used.

The incompatibility of highly hindered anilines is a significant limitation of our protocol. Clearly, the catalytic system could benefit from further optimization. Nonetheless, our protocol represents a good proof-of-concept: Ni catalysis can enable alternative disconnections, which has the potential to simplify synthesis of pharmaceutically relevant molecules.

2.2.5. Reversibility of the reaction

While our coupling reaction works well with methyl and ethyl esters, esters with heavier alcohol leaving groups such as propyl, butyl, or hexyl alcohols give lower yields. We wanted to probe whether our catalyst could selectively react with methyl esters in the presence of other heavier esters. To do so, a competition experiment was carried out (Scheme 76). No selectivity was observed between the two esters, and more interestingly, the exchange between the two alcohol chains occurred. The lack of selectivity for which

amide forms (1:1 ratio observed by GC/MS) indicates that oxidative addition into the C(acyl)–O bond of propyl or butyl esters is feasible and cannot justify the inefficiency of the latter coupling partners. It is likely that the volatility of the alcohol leaving group is the determining factor. The fact that alcohol exchange was observed between the two starting materials indeed suggests that the alcohol by-product can act as a nucleophile and compete for amidation. However, in the case of methyl ester starting materials, evaporation of the methanol by-product can likely drive the amidation reaction forward.

Scheme 76. Competition experiment between methyl and propyl esters

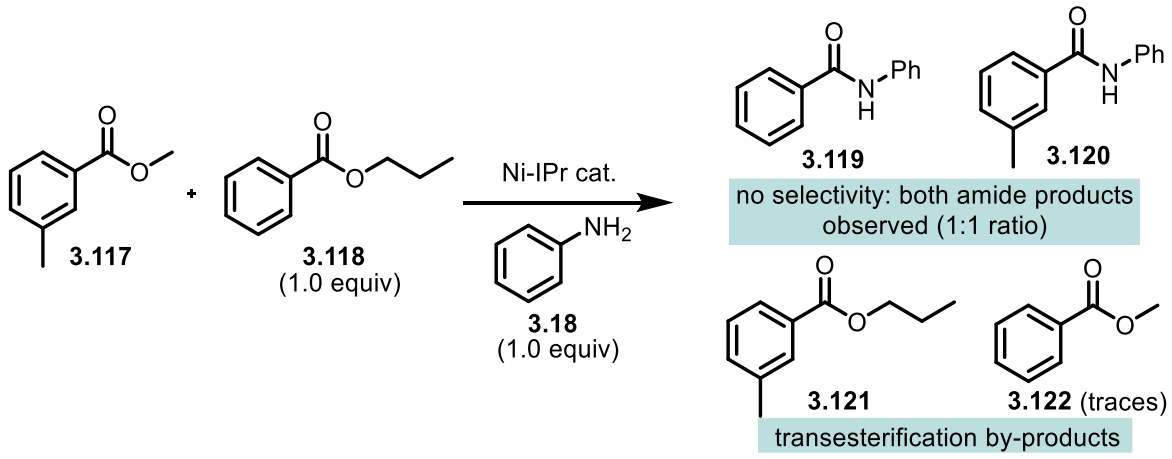

Additional experiments were run to confirm the reversibility of the reaction. The reaction between hexyl benzoate **3.123** and aniline **3.18** gives a low yield of 25% (Scheme 77A). The reverse reaction, that is the reaction between benzanilide **3.124** and hexanol **3.215**, affords hexyl benzoate **3.123** in 54% yield (Scheme 77B).

Scheme 77. Equilibrium experiments for the amidation of hexyl benzoate

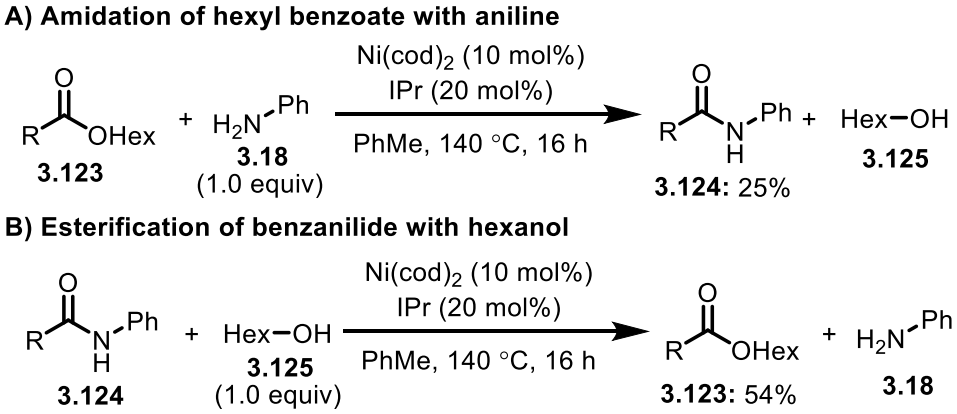

These experiments suggest that the reaction is indeed reversible and that the reverse reaction, esterification, is more facile.

2.3. Nickel-catalyzed transesterification of methyl esters

2.3.1. Transesterification: Background[122]

The competition experiment described above suggested that a protocol for a Ni-catalyzed transesterification of methyl esters would be viable. But would it be useful? It is known that transesterification of esters can occur without transition metal catalysis. Transesterification is an equilibrium reaction (Scheme 78) and requires a driving force to favour the formation of the desired product. It can be catalyzed by a Bronsted or Lewis acid or it can be mediated by a strong base.

Scheme 78. Transesterification

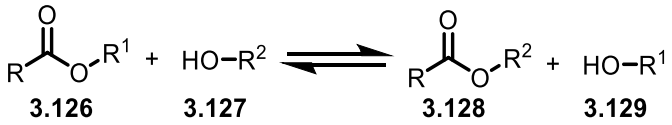

[122] Otera, J.; Nishikido, J. (2010) *Esterification. Methods, Reactions, and Applications (2nd Ed)* Weinheim: Wiley.

Methods relying on acid catalysis require large excess of the alcohol (Scheme 78), which is undesirable if the alcohol's accessibility is limited. Bronsted acid-catalyzed transesterification require anhydrous conditions to prevent undesired hydrolysis. For instance, HCl usually cannot be used directly, but it can be generated in situ instead (e.g. from TMSCl + the alcohol).[123] Lewis acids can also be used to catalyze the reaction. For example, $Ti(OR)_4$ is a common Lewis acid used for transesterification, although fairly high loadings are usually required (20-60 mol%).[124]

Scheme 79. Acid-catalyzed transesterification

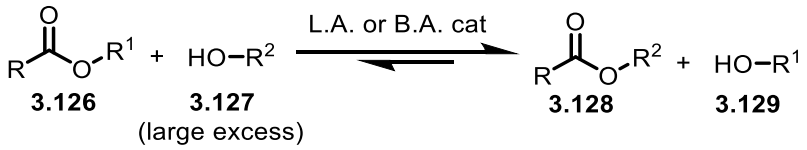

Strong bases can also mediate transesterification. In theory, the reaction can be catalyzed with a base, but in practice, one equivalent of base is used to avoid very long reaction times. In contrast to acid-catalyzed processes, base-mediated transesterification does not require a large excess of alcohol. Methyl esters usually react readily with roughly 1 equivalent of the alcohol if it is secondary or tertiary or a slight excess if primary (~3 equiv). nBuLi or sodium hydride are common bases used to deprotonate the alcohol before reacting it with the ester substrate. This transesterification strategy is not compatible with enantiopure esters with α chiral centers or with base-sensitive functionalities.

[123] Eras, J.; Llovera, M.; Ferran, X.; Canela, R. *Synth. Commun.* **1999**, *29*, 1129–1133.
[124] Seebach, D.; Hungerbuhler, E.; Naef, R.; Schnurrenberger, P.; Weidmann, B.; Züger, M. *Synthesis* **1982**, 138–141.

Scheme 80. Base-mediated transesterification

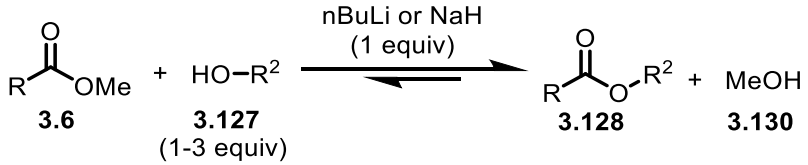

A Ni-catalyzed transesterification of methyl ester could overcome some of the limitations encountered in the base or acid-mediated protocols: incompatibilities with acid- or base-sensitive functional groups, the requirement of a large excess of the alcohol component (for acid-catalyzed method), or epimerization of α chiral centers (for base-mediated method). Moreover, the development of such a protocol would strongly benefit the field of cross-couplings with esters. Cross-couplings of methyl esters are very desirable yet difficult to accomplish. This report would represent one of the rare additive-free cross-coupling with methyl esters.

2.3.2. Initial optimization

Initial optimization aimed at enabling a Ni-catalyzed transesterification of methyl esters was carried by Honours student Émile Pinault-Masson. It was found that dcype was an effective ligand for this transformation (Table 16, entry 1), while other less electron-rich bidentate phosphines proved inefficient (entries 2-5).

Table 16. Initial optimization data for the Ni-catalyzed transesterification

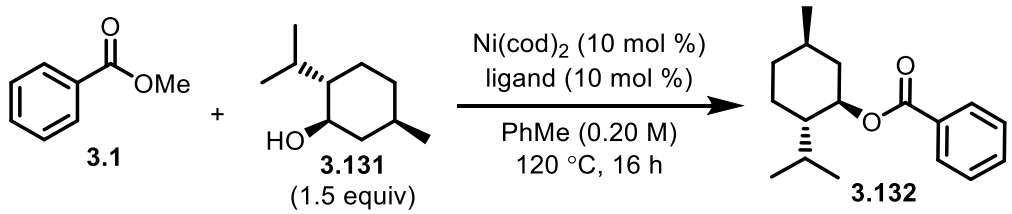

Entry	Ligand	%Yield of 3.132
1	dcype	65
2	BINAP	0
3	dppp	0
4	dppe	0
5	dppf	Traces

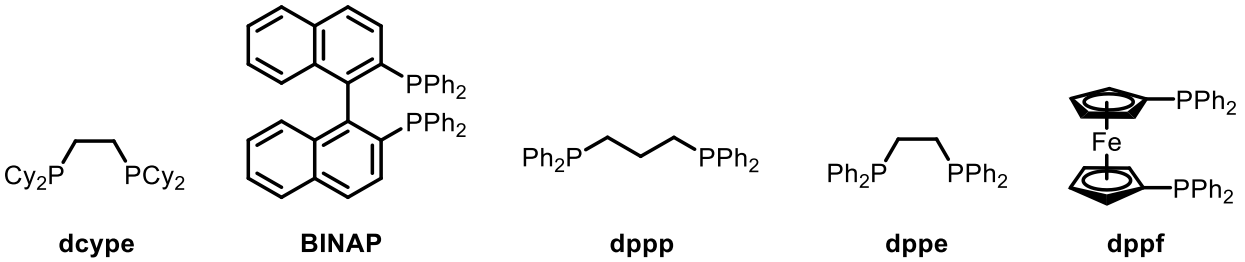

Upon increasing the reaction concentration, and decreasing the catalyst loading, high yields of the desired ester product could be obtained (Scheme 81). The reaction conditions outlined in Scheme 81 were initially used for the reaction scope. Unfortunately, lower yields than expected were obtained.

Scheme 81. Optimized reaction conditions developed by Émile

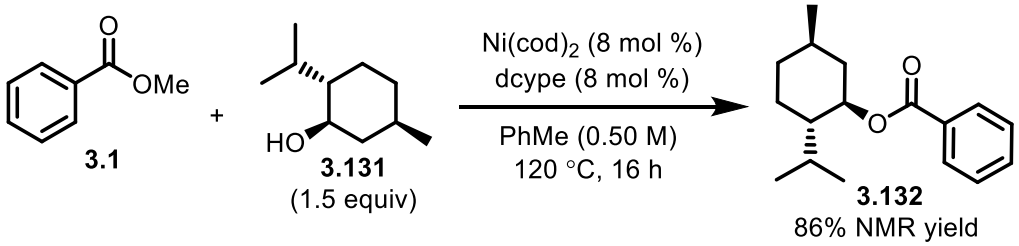

2.3.3. Re-optimization using high-throughput experimentation

Optimizing a catalytic reaction using a single model substrate is somewhat limiting. Usually, the optimized reaction conditions will be excellent for the model substrate and closely related starting materials. However, scope limitations are common, and challenging substrates can often require targeted re-optimization. To avoid these issues, the ideal would be to carry out the initial optimization with several model substrates that are, together, representative of the desired reaction scope. However, this would be very time-consuming if the optimization was to be performed on the bench. On the other hand, it can be carried out very efficiently using the high-throughput screening (HTPS) facility.

Thus, to find a general catalyst system that works efficiently for a wide variety of ester substrates, we carried out a second optimization using the HTPS facility. Six different esters were selected, and each of them was tested with sixteen different ligands.[125] In addition to methyl benzoate **3.1**, heteroaromatic ester **3.135**, ortho-substituted ester **3.136,** benzylic ester **3.137,** secondary aliphatic ester **3.138**, and primary aliphatic ester **3.139** were screened**.** For quick analysis, the 96-well plate was run on the GC/MS, and, for each ester, the highest integration of product over integration of internal standard was normalized to 100% "relative performance". This normalization is fine to evaluate the efficiency of a ligand compared to the other ligands for a given ester. However, it should be noted that it does not allow us to compare reaction efficiency between different esters (i.e. the yield associated with 100% relative performance for ester **3.1** is not the same yield as the one associated with 100% relative performance for ester **3.135**). Since our goal was to identify the optimal ligand for each class of substrates, this normalization was sufficient to give us this information.

[125] Ligand selection was done with the help of Dr. Yanlong Zheng, who is working on the Gen. 2.0 amidation project. The NHC ligands that were not commercially available were all synthesized by Yanlong.

Figure 17. HTPS optimization of Ni-catalyzed transesterification

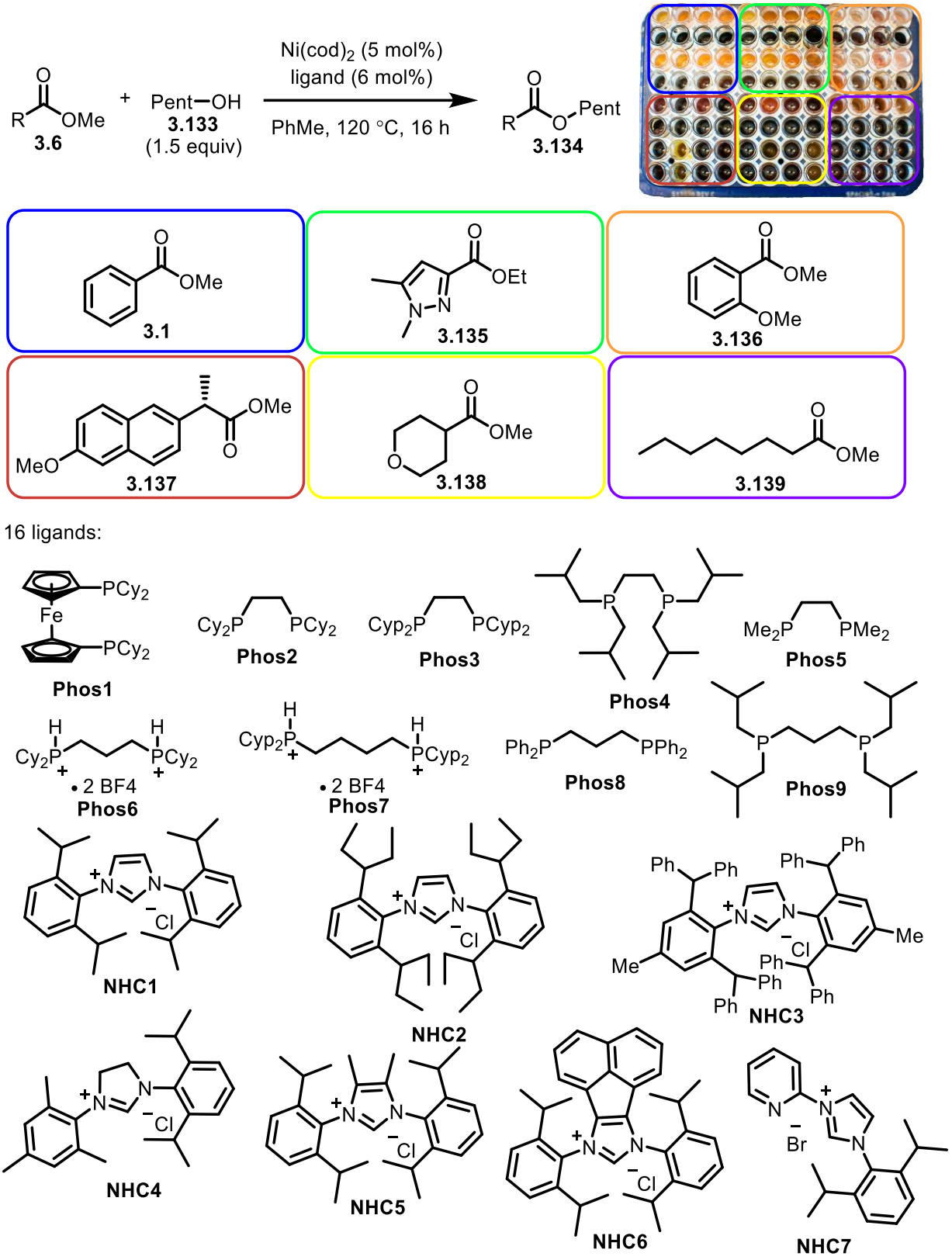

Methyl benzoate (**3.1**): The results for the transesterification reaction between methyl benzoate **3.1** and pentanol **3.133** are illustrated in Figure 18. Interestingly, most ligands were found to be similarly efficient for this transformation. Notably, all the NHC ligands provided high relative performances. Most bidentate ligands were efficient as well, except dcypf (**Phos1**), dmpe (**Phos5**), dppp (**Phos8**), and **Phos9**.

Figure 18. HTPS results for methyl benzoate

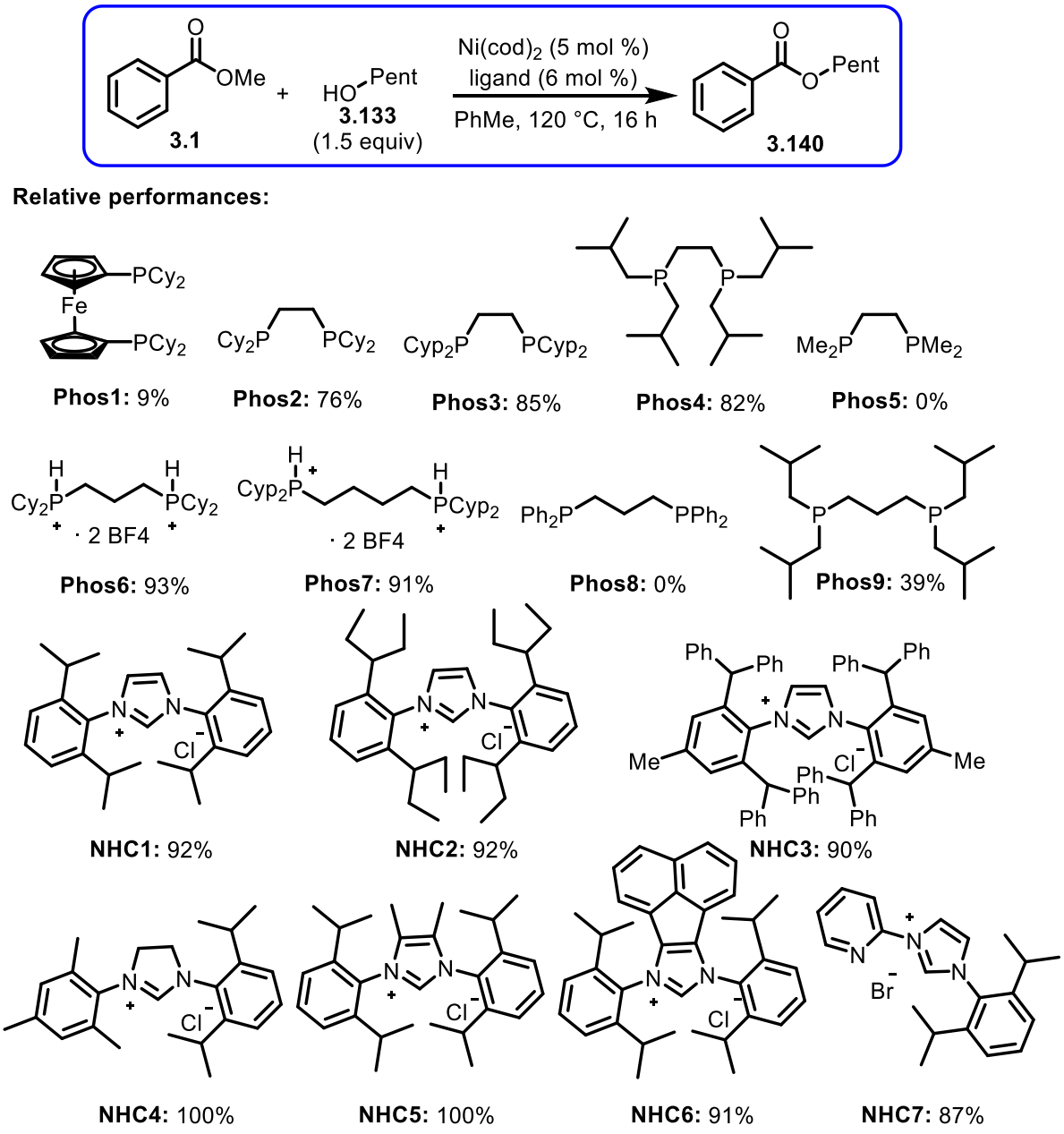

Ethyl 1,5-dimethyl-1H-pyrazole-3-carboxylate (**3.135**): For this ester, all the NHC ligands gave moderate to excellent relative performances (Figure 19). Again, dcypf (**Phos1**), dmpe (**Phos5**), dppp (**Phos8**), and **Phos9** were found to be inefficient. Dcype (**Phos2**) was not a great ligand for this transformation but still gave some conversion (40% relative performance). The other bidentate phosphine ligands (**Phos3**, **Phos4**, **Phos6**, **Phos7**) all worked efficiently. The best ligand was **NHC7**.

Figure 19. HTPS results for heteroaromatic ester 3.135

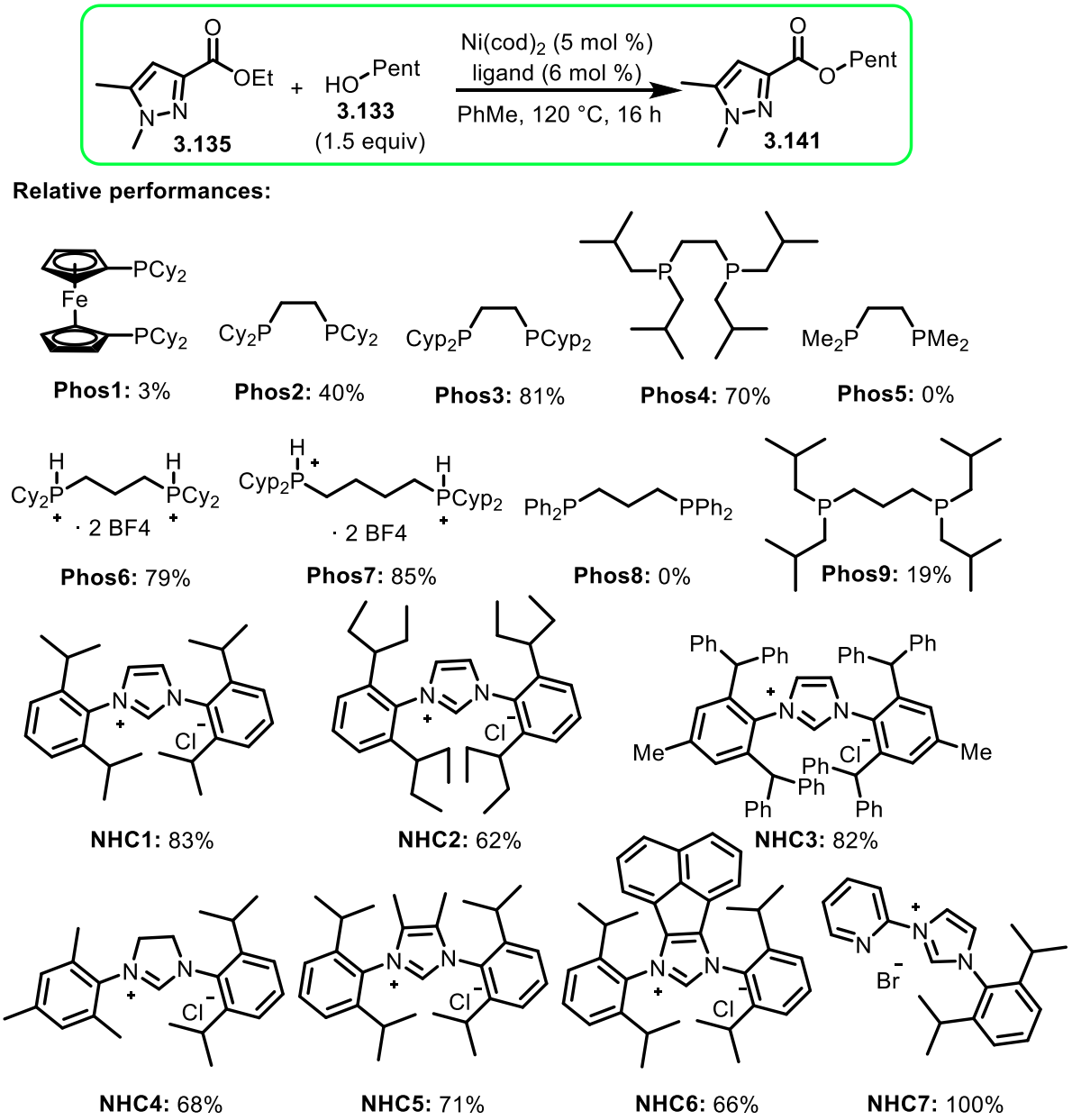

Methyl *o*-methoxybenzoate (**3.142**): For this electron-rich and hindered aromatic ester, many ligands gave low to moderate relative performances (Figure 20). Most bidentate phosphines were inefficient for this transformation, except **Phos6** and **Phos7**. By contrast, NHC ligands were more efficient in general. **NHC7** was again the most effective ligand, with **Phos7** and **NHC5** coming in close seconds.

Figure 20. HTPS results for methyl o-methoxybenzoate

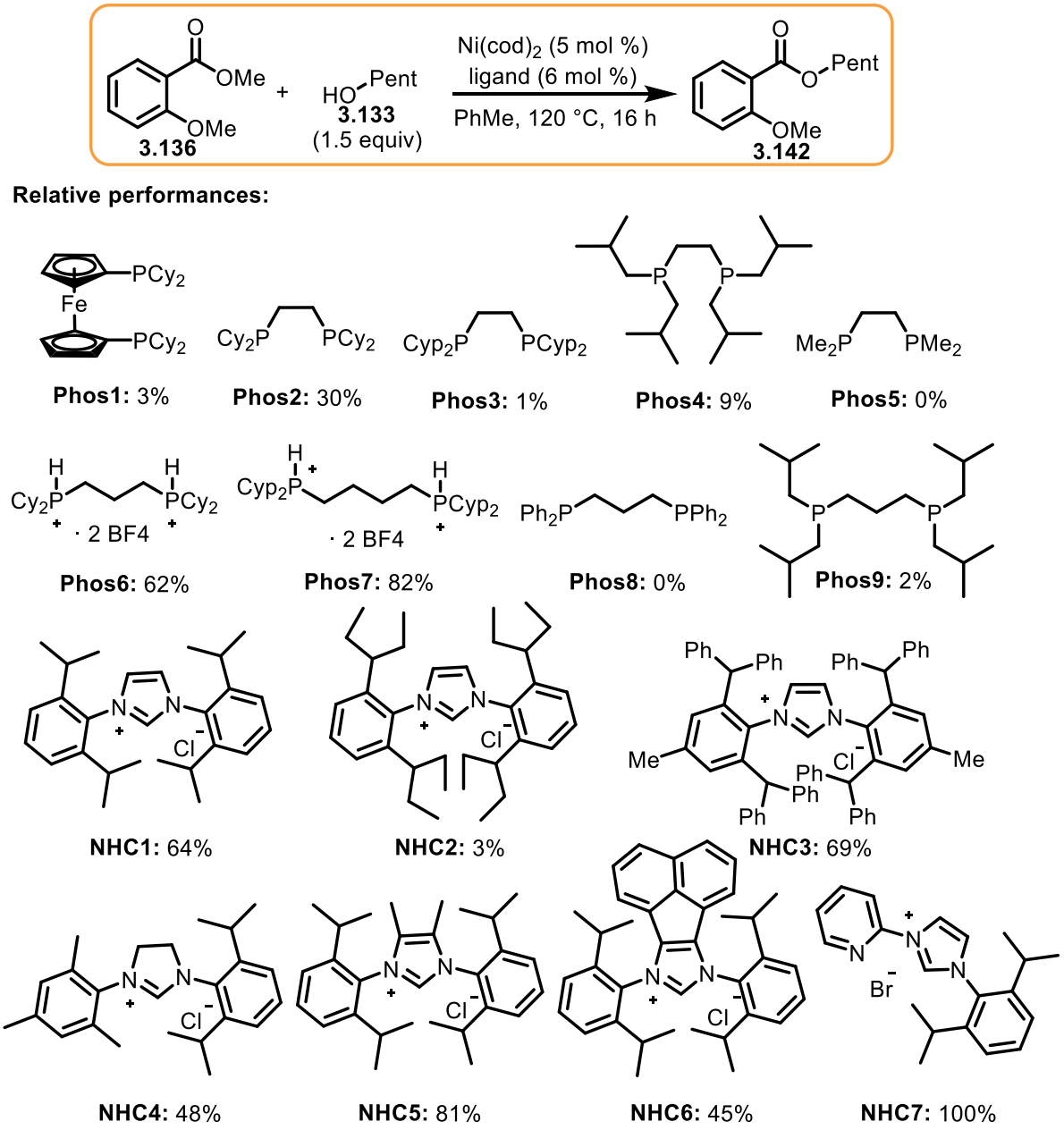

Naproxen methyl ester (**3.143**): The results of this drug derivative are outlined in Figure 21. Among the bidentate phosphine ligands, dcype (**Phos2**), **Phos3**, **Phos6** and **Phos7** were moderately effective. The best ligand was **NHC5**, and the second most efficient ligand was **NHC7**.

Figure 21. HTPS results for the naproxen methyl ester

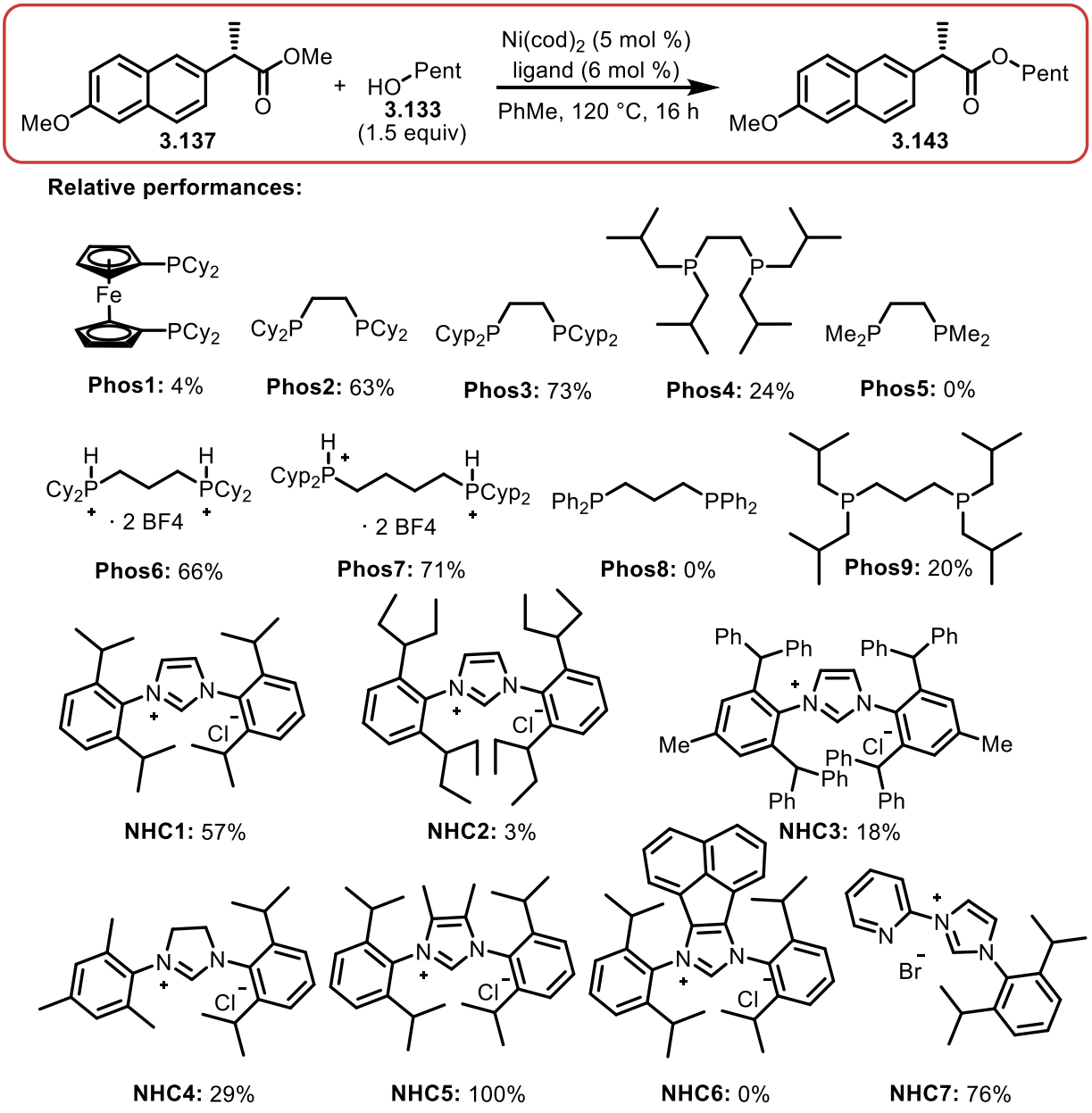

Methyl tetrahydro-2H-pyran-4-carboxylate (**3.138**): The results for this ester are shown in Figure 22. More significant differences in relative performances were observed for this secondary aliphatic ester. Surprisingly, most NHC ligands were inefficient for this esterification, except **NHC7**, which gave a relative performance of 62%. Three bidentate phosphines were found to be the most efficient: dcype (**Phos2**), **Phos3** and **Phos7**.

Figure 22. HTPS results for secondary aliphatic ester 3.138

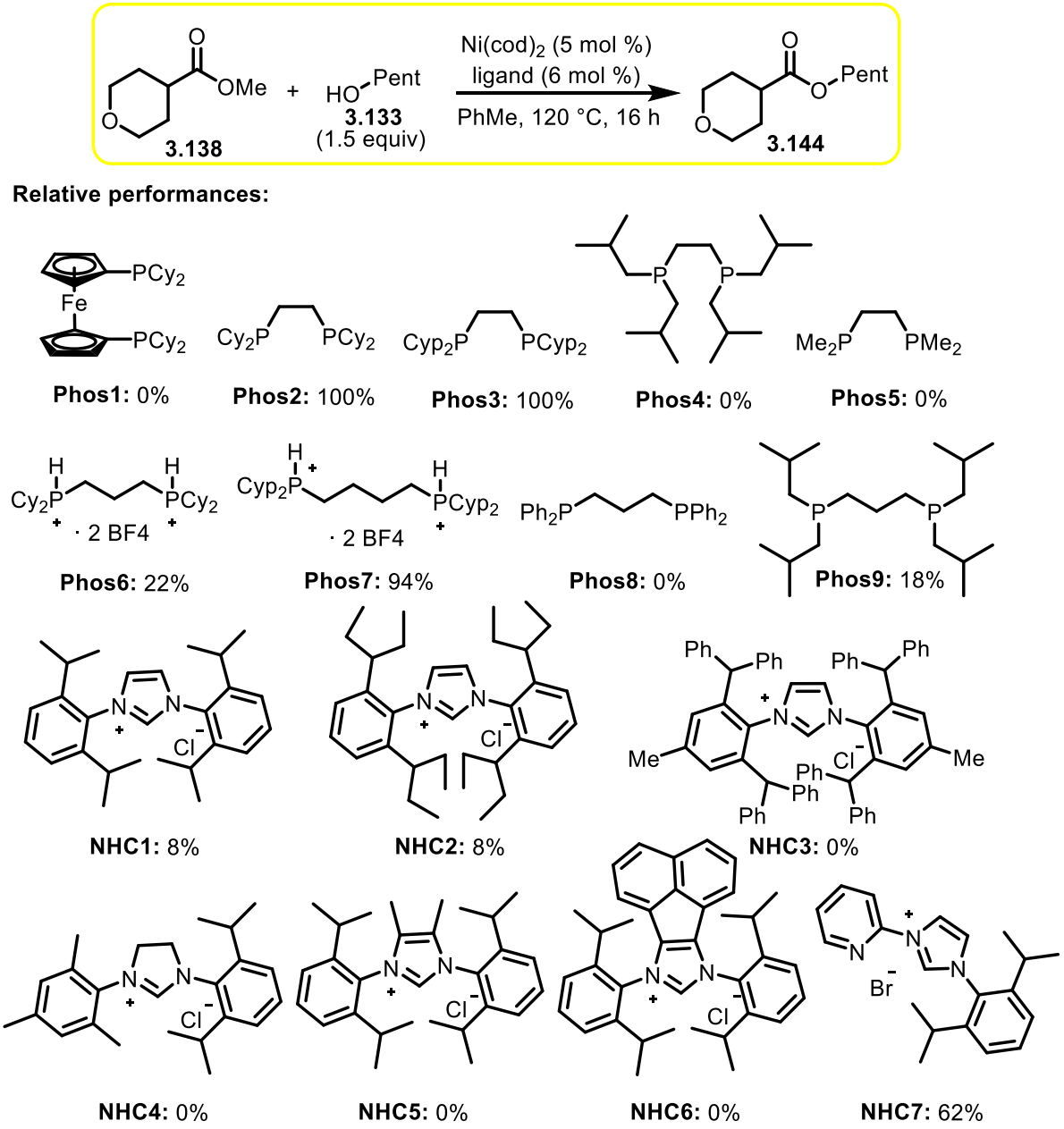

Methyl octanoate (**3.145**): Finally, the results for methyl octanoate are presented in Figure 23. The best ligand, in this case, was **Phos6**. Then, **Phos7**, **NHC1**, **NHC3**, **NHC4,** and **NHC7** all gave ~70% relative performances.

Figure 23. HTPS results for methyl octanoate

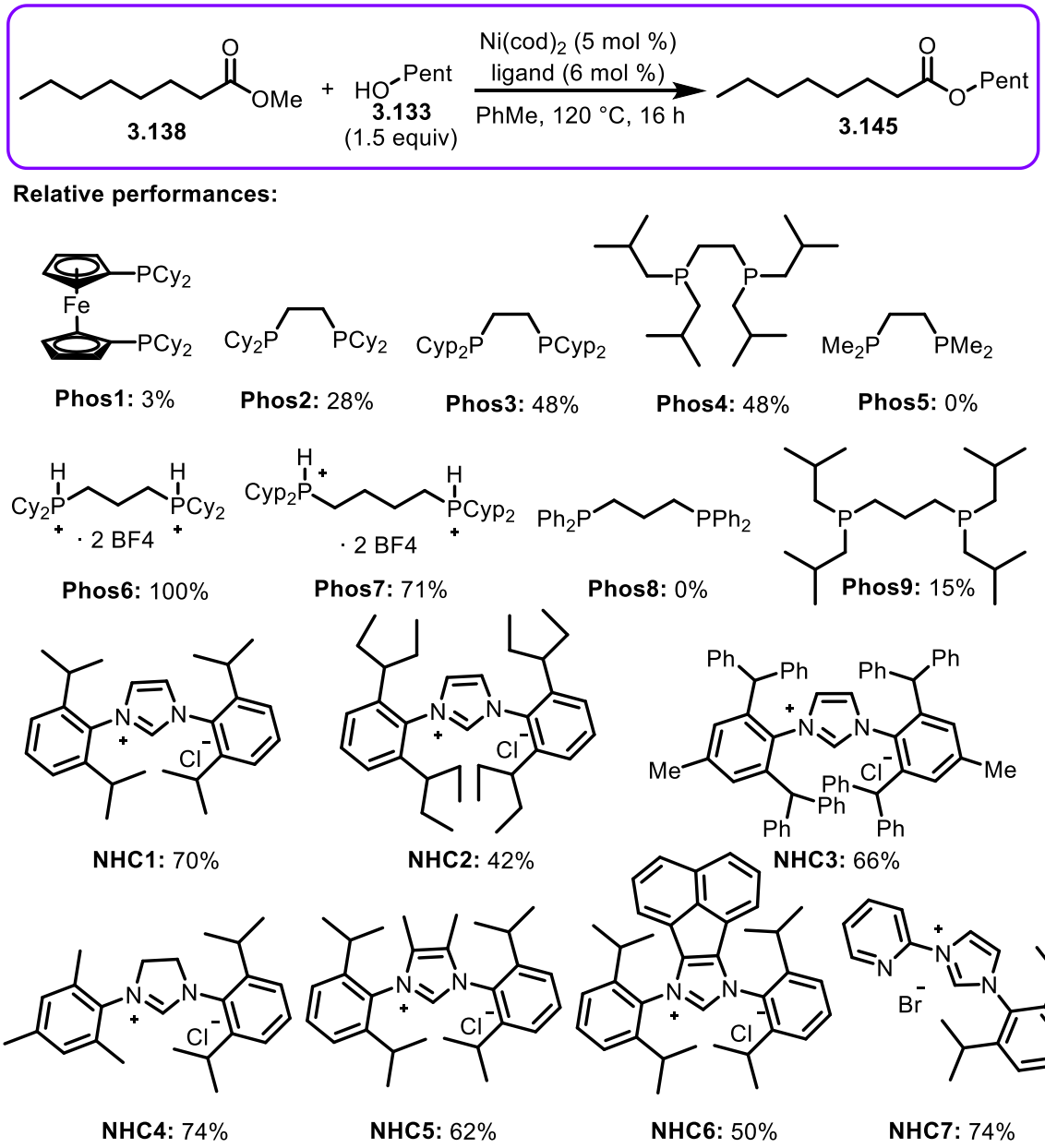

Summary of HTPS results: As expected, the best ligand varies depending on which substrate is used. Nonetheless, two ligands consistently gave high performances across the different esters. **Phos7** and **NHC7** provided the highest average relative performances (Table 17). Moreover, average relative performances for aliphatic esters vs. aromatic esters were calculated. **Phos7** was found to be the optimal ligand for aliphatic esters, while **NHC7** was the best ligand for aromatic esters. The highest relative performances are highlighted in Table 17.

Table 17. Average relative performances of the sixteen different ligands

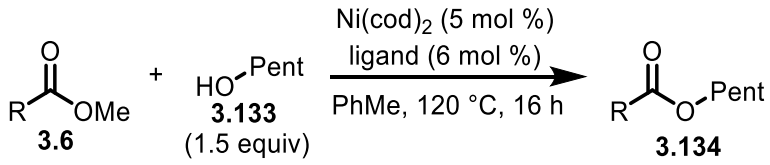

Ligand[a]	Average %relative performance	Average %relative performance for aliphatic esters	Average %relative performance for aromatic esters
Phos1	4	2	5
Phos2	56	64	49
Phos3	65	74	56
Phos4	39	24	54
Phos5	0	0	0
Phos6	70	63	78
Phos7	82	79	86
Phos8	0	0	0
Phos9	19	17	20
NHC1	62	45	80
NHC2	35	18	52

NHC3	54	28	80
NHC4	53	34	72
NHC5	69	54	84
NHC6	42	17	67
NHC7	83	71	96

[a]Chemical structures of the ligands can be found in Figure 23.

Thus, both **NHC7** and **Phos7** were elected for the scope, and the reaction was further optimized on the bench (Table 18).

Table 18. Optimization of the Ni-catalyzed transesterification of methyl esters

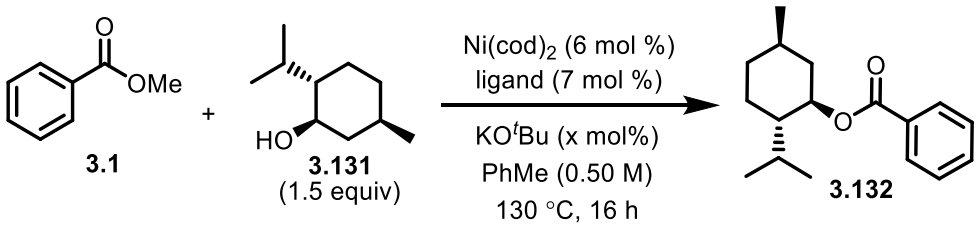

Entry	Ligand	x	Modification	%Yield of 3.132[a]
1	Phos7	14	none	95
2	NHC7	7	none	91
3	Phos7	14	1.0 M	50
4	Phos7[b]	10	4 mol% [Ni]	64
5	Phos7	14	120 °C	78
6	Phos7	14	110 °C	75
7	Phos7	14	1.0 equiv **3.131**	64
8	Phos7	14	30 min	96

General conditions: Methyl benzoate **3.1** (25.2 μL, 0.20 mmol), menthol **3.131** (46.9 mg, 0.30 mmol), $Ni(cod)_2$ (3.3 mg, 6 mol%), ligand (7 mol%), KOtBu (x mol%), PhMe (0.40 mL), at 130 °C for 16 h, under inert atmosphere. [a]Yields of **3.132** were calculated by ^1H NMR with 1,3,5-trimethoxybenzene as the internal standard. [b]5 mol% of Phos7 was used.

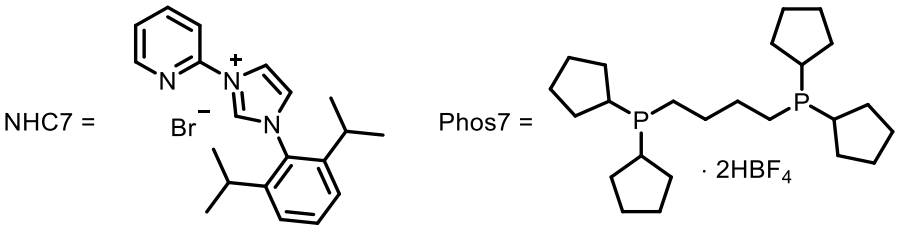

Near quantitative yields of ester **3.132** could be obtained with only 6 mol% catalyst loading of $Ni(cod)_2$ (entries 1 and 2). 0.50 M was found to be a good concentration; doubling the reaction concentration leads to a reduced yield of **3.132** (entry 3). Lowering the catalyst loading to 4 mol% decreases the yield by 30% (entry 4). Lowering the temperature by 10 °C leads to a rough 15% decrease in yield (entry 5). Interestingly, there is not a significant difference in yield when the reaction is run at 110 °C as opposed to 120 °C (entries 5-6). It was confirmed that a slight excess of alcohol is indeed required since using 1.0 equivalent of menthol **3.131** provides product **3.132** in only 64% yield (entry 7). Lastly, we wanted to test whether it was necessary to run the reaction overnight. We found that the reaction between methyl benzoate **3.1** and menthol **3.131** was completed after only 30 min (entry 8). The reaction time was further studied with more challenging substrates, with both **NHC7** and **Phos7**, and it was concluded that 2 hours was enough to reach maximum completion.

2.3.4. Reaction scope

A preliminary scope is presented in Table 19. Each scope example was tried with both **Phos7** and **NHC7**. Crude yields were calculated by ^1H NMR using mesitylene as an internal standard, and the reaction giving the highest yield was then subjected to flash column chromatography.

Table 19. Preliminary reaction scope of the Ni-catalyzed transesterification of methyl esters

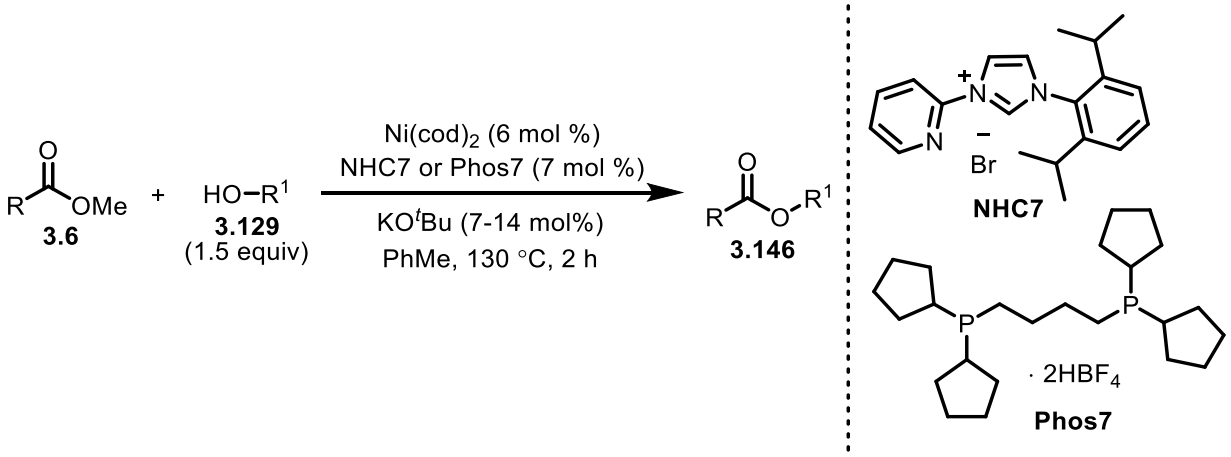

Entry	Ester starting material	Ester product	%Yield[a]
1	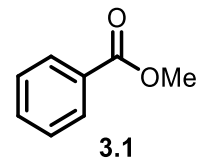 3.1	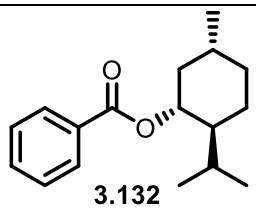 3.132	**NHC7**: 91% **Phos7**: 96% (79%)
2	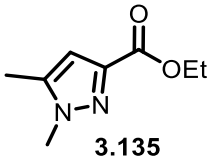 3.135	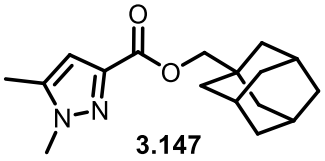 3.147	**NHC7**: 86% (70%) **Phos7**: 43%
3	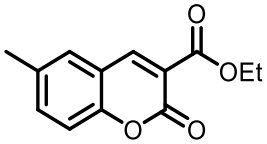 3.148	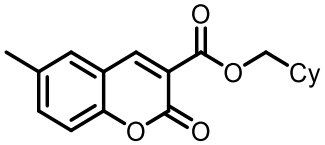 3.149	**NHC7**: 75% **Phos7**: 91% (87%)
4	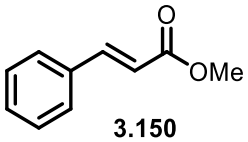 3.150	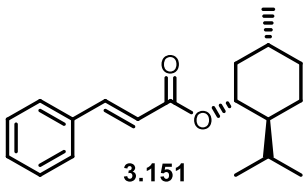 3.151	**NHC7**: 44% **Phos7**: 100%

General conditions: Ester (0.20 mmol), alcohol (0.30 mmol), $Ni(cod)_2$ (3.3 mg, 6.0 mol%), ligand (7.0 mol%), KOtBu (7.0 mol% for **NHC7**, 14 mol% for **Phos7**), PhMe (0.40 mL), at 130 °C for 2 h, under inert atmosphere. [a]Yields were calculated by ^1H NMR with mesitylene as the internal standard. Isolated yields in parentheses.

The reaction between methyl benzoate **3.1** and menthol **1.131** afforded ester **3.132** in excellent yield (entry 1). The pyrazole ethyl ester **3.135** could be reacted with bulky primary alcohol without any issue (entry 2). Coumarin ester **3.148**, which gave low to moderate yields in the amidation reaction, could be coupled in high yield with cyclohexane methanol (entry 3). Notably, transesterification of methyl cinnamate **3.150** with menthol occurred selectively without any Michael addition side-reactions (entry 4). In this case, **NHC7** was less effective; this was associated with starting material recovery and some reduction of the conjugated double bond.

2.3.5. Applications

The fundamental aspect of the Ni-catalyzed transesterification project is important. This new reaction greatly contributes to the field of catalytic activation of methyl esters as it represents one of the rare examples where methyl esters are used as coupling partners in the absence of any Lewis acid additives. To highlight practical use, we designed some application reactions.

The first idea was to use alcohols that contain alkenes or alkynes to enable a cascade reaction (Scheme 82). In theory, Ni intermediate **Int3.3,** obtained after oxidative addition and ligand exchange with the alcohol, could interact with the intramolecular alkene or alkyne, followed by an insertion of the latter into the Ni–O bond to afford intermediate **Int3.4**. This intermediate could then reductively eliminate to give ketone adduct **3.153** or decarbonylate first to afford decarbonylated adduct **3.154**. This reaction would achieve molecular complexity from simple starting materials with high atom-economy (methanol as the sole stoichiometric by-product).

Scheme 82. Ni-catalyzed esterification/intramolecular Heck cascade

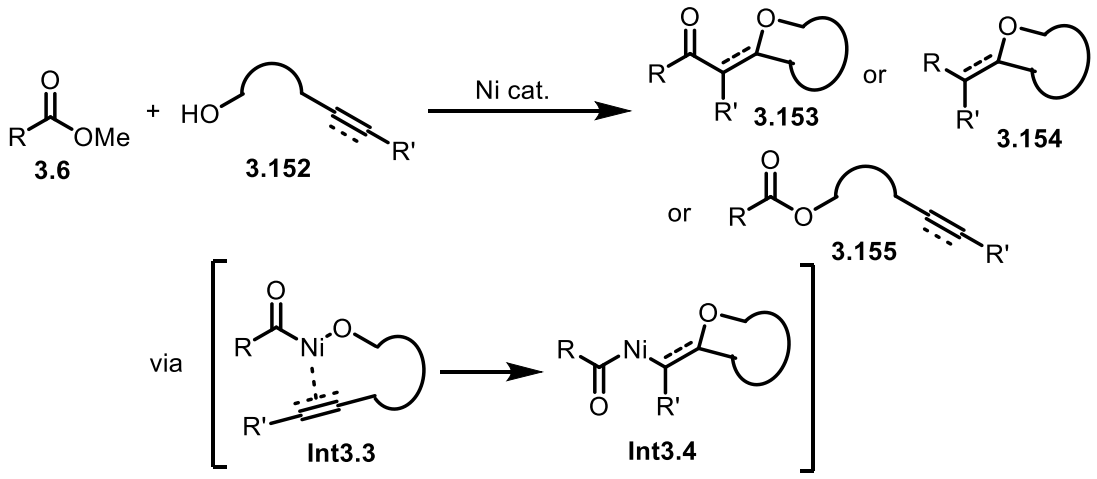

Towards enabling this cascade reaction, the reaction illustrated in Scheme 83 was initially attempted. Unfortunately, reacting ester **3.156** in the presence of the Ni catalyst resulted in high starting material recovery and no evidence of product by GC/MS. Plausibly, the alkyne in ester **3.156** cannot properly aligned for insertion.

Scheme 83. Ni-catalyzed esterification/alkyne insertion cascade

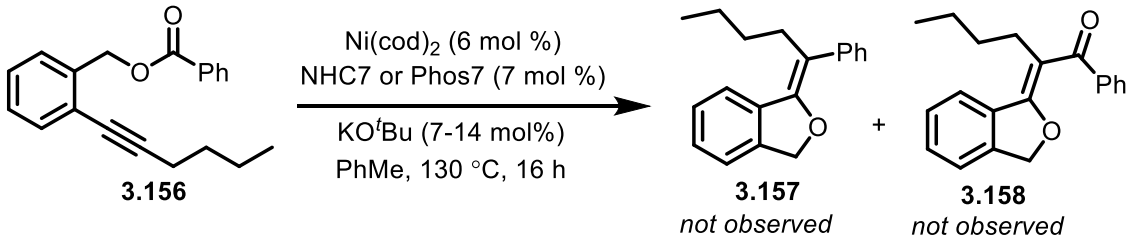

Other applications to try in the future

Although the first attempt at enabling a cascade reaction involving an intramolecular Heck coupling was unsuccessful (Scheme 83), other substrates should still be tried. Another substrate is proposed in Scheme 84. Alcohol **3.159** could be easily accessed by reduction of the corresponding carboxylic acid which is commercially available (CAS: 16386-93-9). The gem-dimethyl might facilitate the cyclization step.

Scheme 84. Cascade reaction to try

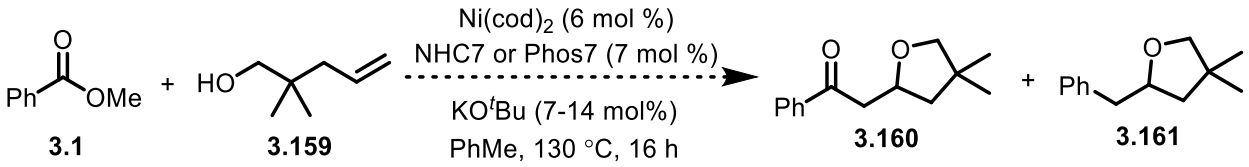

It would also be interesting to see if our protocol could be extended to thioesterification. A test reaction that could be run is shown in Scheme 85.

Scheme 85. Ni-catalyzed thioesterification of methyl benzoate

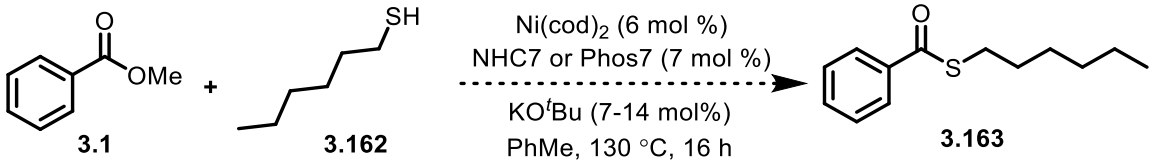

A useful application where our Ni-catalyzed approach could outcompete base- or acid-catalyzed processes is *macrolactonization*. Acid-catalyzed approaches that rely on the use of excess alcohol are non-viable here because the reaction is intramolecular, meaning the ratio of ester to alcohol is inherently equimolar. Traditionally, in the synthesis of complex macrolactones, a methyl ester is there early on in the synthesis and later hydrolyzed before the macrolactonization step. Stoichiometric agents like Yamaguchi's reagent **3.165** (2,4,6-trichlorobenzoyl chloride) are then usually employed to carry out the macrolactonization.[126] Two examples of such hydrolysis/coupling sequence in the formation of macrolactone natural products are provided in Scheme 86.[127]

[126] Inanaga, J.; Hirata, K.; Saeki, H.; Katsuki, T.; Yamaguchi, M. *Bull. Chem. Soc. Jpn.* **1979**, *52*, 1989–1993.
[127] (a) Evans, D. A.; Connell, B. T. *J. Am. Chem. Soc.* **2003**, *125*, 10899–10905; (b) Palimkar, S. S.; Uenishi, J. *Org. Lett.* **2010**, *12*, 4160–4163.

Scheme 86. Macrolactonization in natural product synthesis

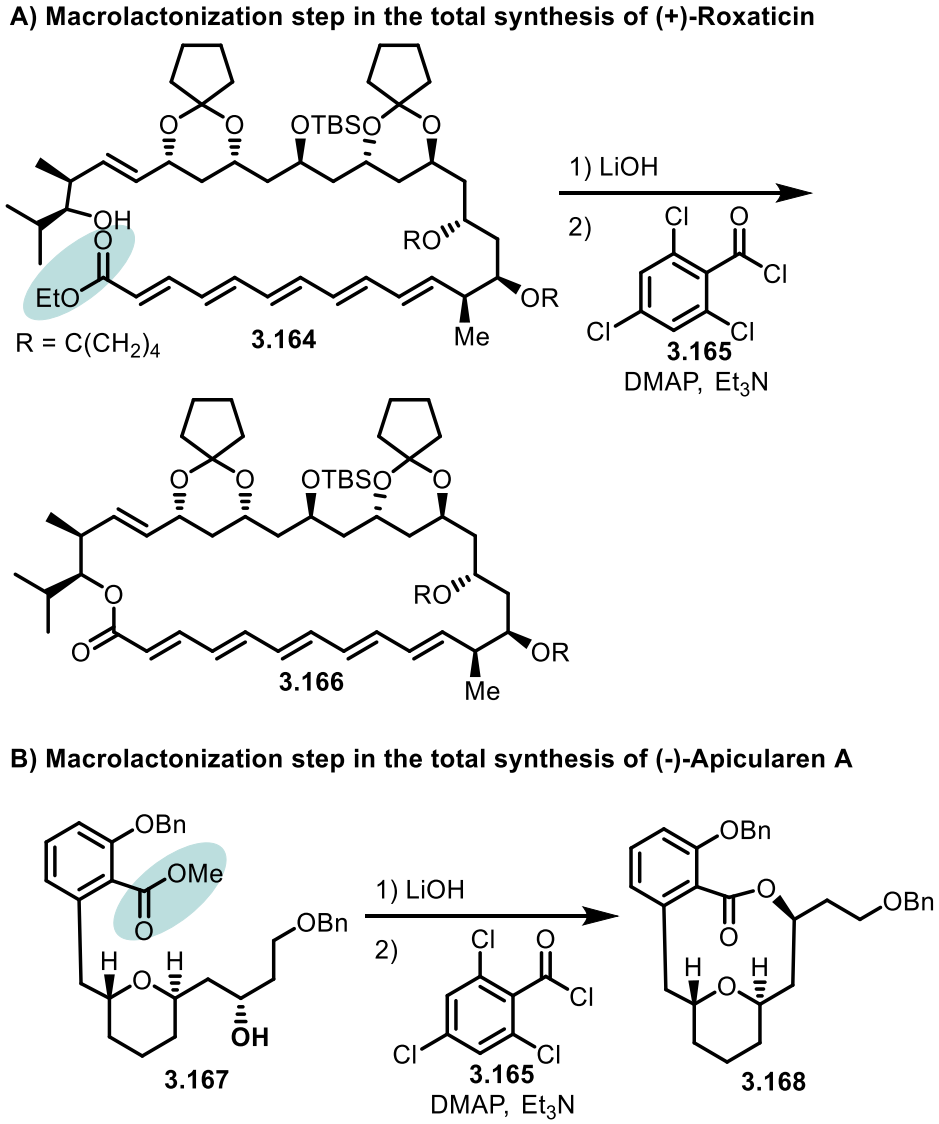

A recent report showed a catalytic macrolactonization approach starting from the carboxylic acid.[128] To the best of our knowledge, no catalytic approach to carry out the macrocyclization directly from the methyl or ethyl ester exists. Our Ni-catalyzed transesterification could potentially fulfill this gap. However, difficulties are expected

[128] Léséleuc, M.; Collins, S. K. *ACS Catal.* **2015**, *5*, 1462−1467.

since these macrolactonization reactions are often run highly dilute to avoid intermolecular reactions.

2.4. Discussion and future work

Ni-catalyzed amidation of methyl esters

We have developed the first additive-free Ni-catalyzed amidation of methyl esters. Our method generates methanol as the only stoichiometric waste, which greatly contrasts traditional amidation of methyl esters involving hydrolysis followed by coupling with sthoichiometric activating agents. Since no base is required in our protocol, α-chiral esters can be converted to amides without any loss of stereochemical integrity. A broad range of aliphatic and (hetero)aromatic esters can be coupled to aliphatic amines and anilines. This strongly contrasts Garg's report which required stoichiometric aluminum *tert*-butoxide and was limited to the coupling of methyl 1-naphthoates and *N*-alkyl aniline derivatives (Scheme 87).[129]

Scheme 87. Our Ni-catalyzed amidation vs Garg's

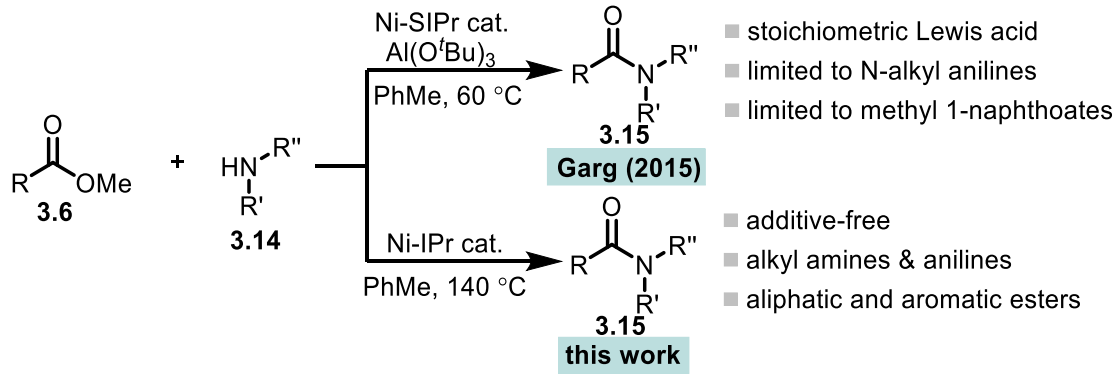

[129] Hie, L.; Fine Nathel, N. F.; Hong, X.; Yang, Y.-F.; Houk, K. N.; Garg, N. K. *Angew. Chem. Int. Ed.* **2016**, *55*, 2810–2814.

A 2015 publication from the Garg lab, wherein the Ni-catalyzed esterification of *N*-methyl benzanilides is reported, helps to put our reaction into context (Figure 24).[130] They performed extensive DFT calculations in collaboration with the Houk lab. Since the conversion of esters to amides is the microscopic reverse of amide→ester, a lot of useful information can be extracted from these mechanistic studies. The oxidative addition of Ni-SIPr into amide **3.169** requires 26.0 kcal/mol of energy, and ligand exchange is facile and reversible. The reductive elimination has an activation barrier of only 7.5 kcal/mol and is thermodynamically downhill by 22.5 kcal/mol.

Figure 24. DFT calculations from Garg and Houk

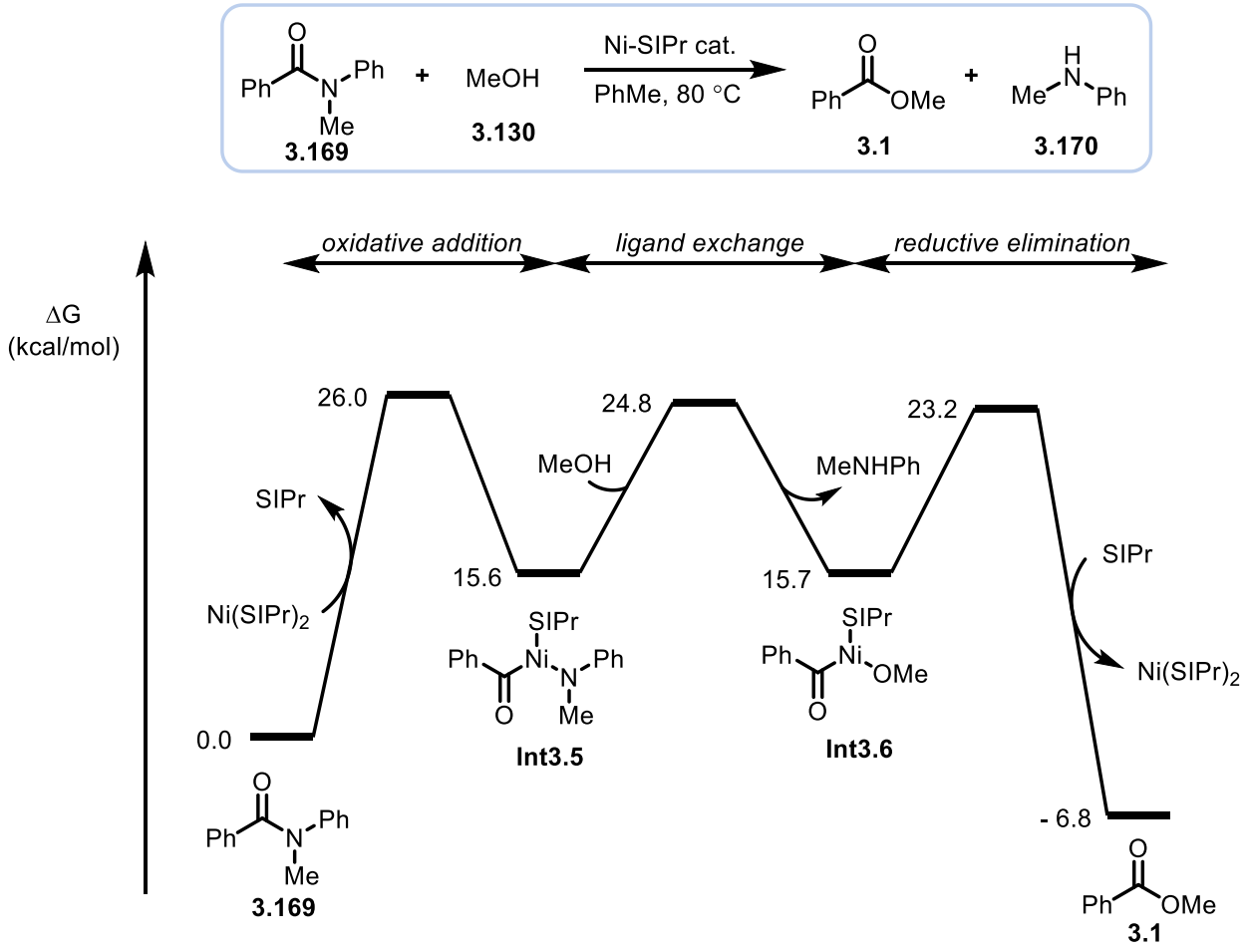

[130] Hie, L.; Fine Nathel, N. F.; Shah, T. K.; Baker, E. L.; Hong, X.; Yang, Y.-F.; Liu, P.; Houk, K. N.; Garg, N. K. *Nature* **2015**, *524*, 79–83.

In our case, oxidative addition into methyl benzoate (microscopic reverse of their reductive elimination step), which requires 30.0 kcal/mol, is a reasonable step at 140 °C. Experiments carried out in our group confirmed the reversibility of this reaction (see Section 2.2.5) and suggested that evaporation of the methanol is essential to drive the reaction towards amide bond formation, a reaction that is otherwise thermodynamically unfavoured with amine nucleophiles such as morpholine and anilines.[131]

Although our scope was extremely broad relative to what had been previously disclosed, there were some significant limitations. For instance, sterically hindered amines didn't work well. The ligand exchange step with hindered amines likely has a higher energy barrier and is probably thermodynamically unfavoured due to a steric clash between the amine and the bulky NHC ligand. Diamines bearing tertiary amines were incompatible as well.

Moreover, couplings of functionally rich pharmaceutical agents were often unsuccessful. Screening of more catalysts for these challenging substrates would be required. A high-throughput screen, similar to the one carried out for the transesterification reaction (see Section 2.3.3), could be an efficient way of doing so. Further improvements needed to render our amidation protocol more generally useful include: lowering catalyst loadings, finding efficient set-up for methanol removal, switching from $Ni(cod)_2$ to bench-stable Ni(II) pre-catalysts and moving away from NHC ligands as they are generally undesired on larger scales.

Ni-catalyzed transesterification of methyl esters

We also developed a protocol for a Ni-catalyzed transesterification of methyl esters. Our reaction does not require any base, acid, or other additives. A highly efficient catalyst

[131] The Garg and Houk lab calculated that the conversion of methyl benzoate 3.1 into 4-benzoylmorpholine is thermodynamically unfavoured by 1.1 kcal/mol and the conversion of methyl benzoate 3.1 into benzanilide 3.124 is thermodynamically unfavoured by 4.3 kcal/mol.

system was identified via high-throughput screening experimentation. Again, this reaction represents one of the rare cross-couplings using unactivated alkyl esters as the electrophilic partners. Although only a preliminary scope has been obtained so far, there is good evidence that the transesterification reaction will have fewer scope limitations than the amidation protocol described above. This is not surprising since the transesterification reaction is expected to be relatively thermoneutral, whereas the amidation of methyl esters with anilines or morpholine is thermodynamically unfavoured. For instance, coumarin ester **3.148** achieved ~30% higher yield in the transesterification reaction, and methyl cinnamate **3.150**, which was an incompatible substrate in the amidation reaction, provided near quantitative yield in the transesterification reaction.

Figure 25 offers some suggestions of alcohols that could be tried next in our coupling reaction. Couplings with poly-alcohols such as **D-(+)-glucose** and **3.171** could be attempted. It would be interesting to see if the primary alcohol could react selectively over the other secondary ones and if the aliphatic alcohol could react preferentially in the presence of phenol in substrate **3.171**. Alcohol **3.172** bearing a tertiary amine or alcohol **3.173** bearing an acid-sensitive moiety could be tried as well. It would also be valuable to see to what extent our reaction can favour product formation in very thermodynamically unfavoured processes. For instance, the reaction between methyl benzoate **3.1** and alcohol **3.174** is expected to be very thermodynamically uphill.

Figure 25. Alcohols to try

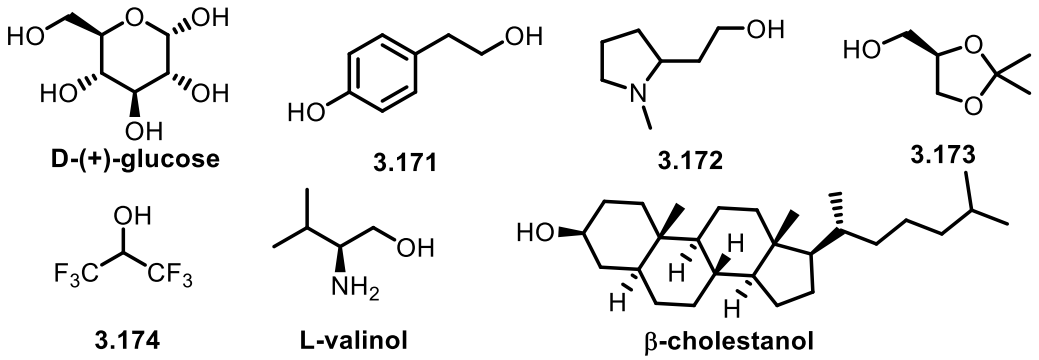

Additionally, L-valinol, which contains both an amine and an alcohol could be tried; the resulting selectivity would give valuable insights. Lastly, β-cholestanol would be an interesting secondary alcohol to try as well.

Figure 26 illustrates esters that should be tried next for the reaction scope. Heteroaromatic esters **3.19** and **3.23** should be tried. More importantly, heteroaromatic compounds that failed in the amidation (**3.64**, **3.65**, **3.175**) should be attempted to push the boundaries of our transesterification protocol. Enantiopure esters with chiral α centers should be tested, including ester **3.29**, naproxen methyl ester **3.137** and amino acid derivatives **3.31** and **3.176**. In these cases, deprotonated version of ligands NHC7 and Phos7 should be used to avoid epimerization with the catalytic potassium *tert*-butoxide.

Figure 26. Esters to try

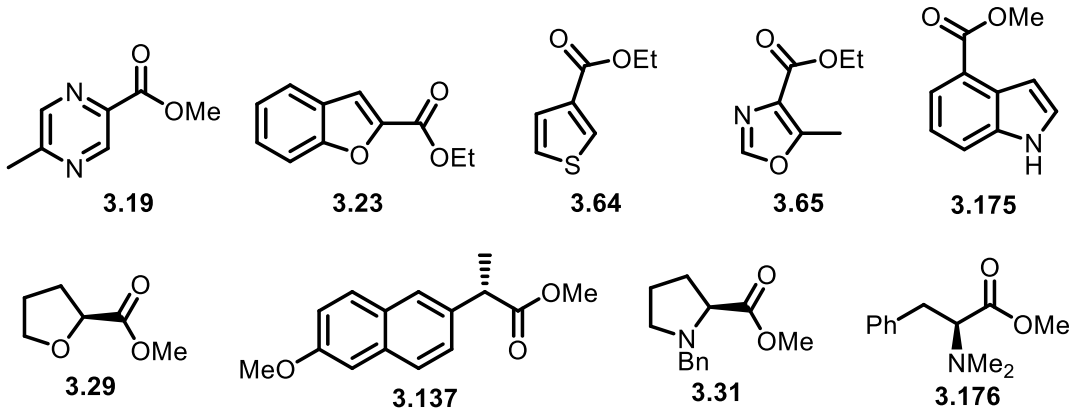

To conclude, the first additive free Ni-catalyzed coupling of methyl esters with alcohols and amines have been disclosed. The activation of methyl esters in cross-coupling reactions has been a long-standing goal in the field due to their ubiquity and robustness. Our Ni-catalyzed coupling reaction of methyl esters represent one of the rare reports using methyl esters as coupling partners in the absence of any stoichiometric additives. Therefore, our efforts contribute strongly to the field of cross-coupling with esters from a fundamental perspective. Moreover, the disclosed reactions are of high atom-economy since they utilize widely available starting materials to produce value-added amide and ester products, producing methanol or ethanol as the only stoichiometric waste product. Future endeavours will aim at reducing catalyst loading, increasing reaction mildness, and broaden the reaction scope to render our catalytic reactions more synthetically practical.

2.5. Experimental

2.5.1. General considerations

General experimental details: Unless otherwise indicated, reactions were conducted under an atmosphere of argon in 8 mL screw-capped vials that were oven dried (120 °C). Column chromatography was performed manually using Silicycle F60 40−63 μm silica gel. Analytical thin layer chromatography (TLC) was conducted with aluminum-backed EMD Millipore Silica Gel 60 F254 pre-coated plates. Visualization of developed plates was performed under UV light (254 nm) and using $KMnO_4$.

General instrumentation: ^{1}H NMR and ^{13}C NMR were recorded on a Bruker AVANCE 400 MHz spectrometer. ^{1}H NMR spectra were internally referenced to the residual solvent signal (e.g., $CDCl_3$ = 7.27 ppm). ^{13}C NMR spectra were internally referenced to the residual solvent signal (e.g., $CDCl_3$ = 77.16 ppm). Data for ^{1}H NMR are reported as follows: chemical shift (δ ppm), multiplicity (s = singlet, d = doublet, t = triplet, q = quartet,

quin = quintet, m = multiplet), coupling constant (Hz), integration. NMR yields for optimization studies were obtained by ^{1}H NMR analysis of the crude reaction mixture using 1,3,5-trimethoxybenzene as an internal standard. IR spectra were obtained using a Nicolet 6700 FT-IR spectrometer with a diamond ATR crystal (ThermoScientific) and are reported in terms of frequency of absorption (cm−1). Melting point ranges were determined on a Canlab GallenKamp Melting Point Apparatus. GC yields for optimization studies were obtained via a 5-point calibration curve using FID analysis on an Agilent Technologies 7890B GC with 30 m × 0.25 mm HP-5 column. Accurate mass data (EI) was obtained from an Agilent 5977A GC/MSD using MassWorks 4.0 from CERNO Bioscience. HRMS data was obtained from a Micromass Q-TOF 2 quadrupole – time-of-flight mass spectrometer with ESI source. The determination of enantiomeric excess was performed by chiral phase HPLC analysis using an Agilent 1200 Series instrument and Diacel ChiralPak columns. Optical rotations were measured with an Anton Paar MCP 500 Polarimeter.

Materials: Organic solvents were purified by rigorous degassing with nitrogen before passing through a PureSolv solvent purification system, and low water content was confirmed by Karl Fischer titration (< 25 ppm for all solvents). Unless otherwise noted, reagents were used as received. $Pd(OAc)_2$ was purchased from Strem Chemicals. $[Pd(cinnamyl)Cl]_2$, dcype, Cs_2CO_3, KF were purchased from Sigma-Aldrich. The following starting materials were synthesized using literature procedures: ester **3.25**,[132]

[132] Manning, D. D.; Cioffi, C. L. 5-HT3 Receptor Modulators, Methods of Making, and Use Thereof. US Patent US2009/298809 (2009).

amine **3.48**,[133] ester **3.60**,[134] ester **3.61**,[135] ester **3.62**,[136] amine **3.73**,[137] **3.83**,[138] ester **3.91**,[139] and ester **3.148.**[139]

Figure 27. Starting materials synthesized according to literature procedures

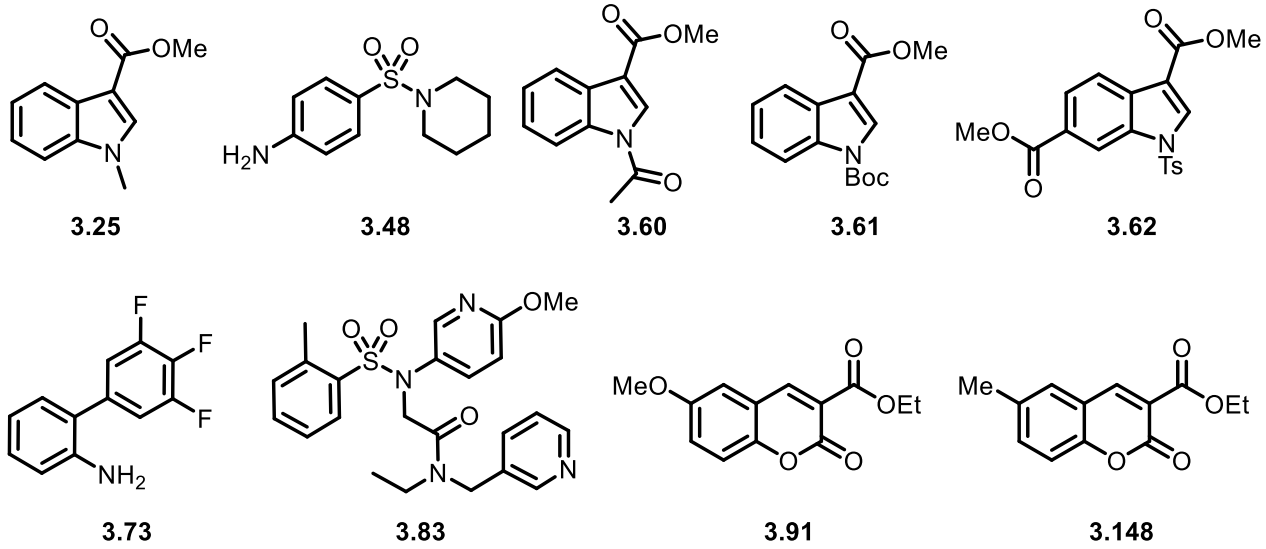

[133] Patel, P. R.; Ramalingan, C.; Park, Y.-T. *Bio. Med. Chem. Lett.* **2007**, *17*, 6610–6614.
[134] Potavathri, S.; Dumas, A. S.; Dwight, T. A.; Naumiec, G. R.; Hammann, J. M.; DeBoef, B. *Tetrahedron Lett.* **2008**, *49*, 4050–4053.
[135] Fauq, A. H.; Hong, F.; Cusack, B.; Tyler, B. M.; Ping-Pang, Y.; Richelson, E. *Tetrahedron Asymmetry* **1998**, *9*, 4127–4134.
[136] Liu, W.; Lim, H. J.; Rajanbabu, T. V. *J. Am. Chem. Soc.* **2012**, *134*, 5496–5499.
[137] Maleckis, A.; Kampf, J. W.; Sanford, M. S. *J. Am. Chem. Soc.* **2013**, *135*, 6618–6625.
[138] Wang, C.; Moseley, C. K.; Carlin, S. M.; Wilson, C. M.; Neelamegam, R.; Hooker, J. M. *Bioorg. Med. Chem. Lett.* **2013**, *23*, 3389–3392.
[139] Fonseca, A.; Reis, J.; Silva, T.; Matos, M. J.; Bagetta, D.; Ortuso, F.; Alcaro, S.; Uriarte, E.; Borges, F. *J. Med. Chem.* **2017**, *60*, 7206−7212.

2.5.2. Synthesis of starting materials

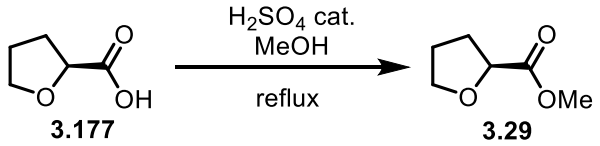

(S)-methyl tetrahydrofuran-2-carboxylate (3.29) was synthesized from a procedure adapted from the patent literature.[140] A 10 mL round-bottomed flask was equipped with a stir bar and condenser. (S)-Tetrahydro-2-furoic acid **3.177** (388 μL, 4.00 mmol) was added and diluted in methanol (2.0 mL). Sulfuric acid (18 μL, 0.22 mmol) was then added, and the reaction mixture was refluxed at 75-80 °C overnight. After being cooled down, the mixture was diluted with water (2 mL). The mixture was extracted with dichloromethane (10 mL) and washed with a saturated aqueous solution of $NaHCO_3$ (2 x 10 mL), and brine (10 mL). The organic phase was dried over Na_2SO_4, filtered, and the solvent was removed *in vacuo*. The product was then purified by column chromatography (10% ether in pentane) to afford **3.29** as a colourless liquid (0.35 g, 66% yield, 97.5:2.5 e.r.). Characterization data matched those previously reported.[141] **^{1}H NMR** (400 MHz, $CDCl_3$): 4.47 (dd, *J* = 8.3, 5.4 Hz, 1H), 4.04-3.99 (m, 1H), 3.94-3.89 (m, 1H), 3.75 (s, 3H), 2.29-2.20 (m, 1H), 2.07-1.86 (m, 3H).**^{13}C NMR** (100 MHz, $CDCl_3$): 173.9, 76.8, 69.5, 52.2, 30.3, 25.4. **HPLC**: CHIRALCEL AD-H, 1.5% ^{i}PrOH in hexanes, 0.80 mL/min, 230 nm, t_{R1}(minor) = 17.4 min, t_{R2}(major) = 16.5 min.

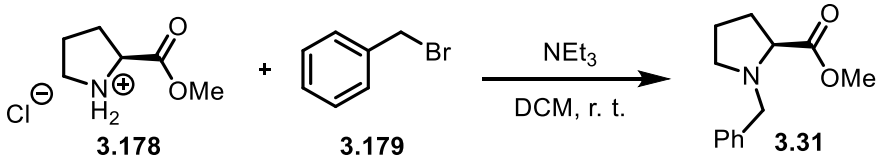

N-Benzyl-(S)-proline methyl ester (3.31) was synthesized from L-proline methyl ester hydrochloride and benzyl bromide. A 50 mL round-bottomed flask was first charged with a stir bar and L-proline methyl ester hydrochloride (331 mg, 2.00 mmol).

[140] Masada, S., Terao, Y.; Murata, T. Indole derivative. Patent WO2011/083804 (2011).
[141] Sebeka, M.; Holzb, J.; Börner, A.; Jähnisch, K. *Synlett* **2009**, *3*, 461–465.

Dichloromethane (6 mL) was then added, followed by benzyl bromide (0.29 mL, 2.4 mmol). Triethylamine (0.61 mL, 4.4 mmol) was added dropwise. The reaction was stirred at room temperature overnight. The solution was then diluted with DCM (10 mL) and washed with a saturated aqueous solution of sodium carbonate (2 x 10 mL) and brine (10 mL). The organic phase was dried over Na_2SO_4 and filtered. The solvent was evaporated *in vacuo*, and the crude product was purified by column chromatography (gradient 10 → 20% EtOAc in hexanes). **3.31** was obtained as a light-yellow oil (0.31 g, 70%). Characterization data matched those previously reported.[142] **^{1}H NMR** (400 MHz, $CDCl_3$): 7.35-723 (m, 5H), 3.89 (d, *J* = 12.7 MHz, 1H), 3.65 (s, 3H), 3.58 (d, *J* = 12.7 Hz, 1H), 3.26 (dd, *J* = 8.9, 6.4 Hz, 1H), 3.07 (m, 1H), 2.40 (q, *J* = 8.8 Hz, 1H), 2.19-2.08 (m, 1H), 2.01-1.85 (m, 2H), 1.82-1.74 (m, 1H). **^{13}C NMR** (100 MHz, $CDCl_3$): 174.7, 138.4, 129.4, 128.3, 127.2, 65.5, 58.9, 53.4, 51.8, 29.5, 23.1.

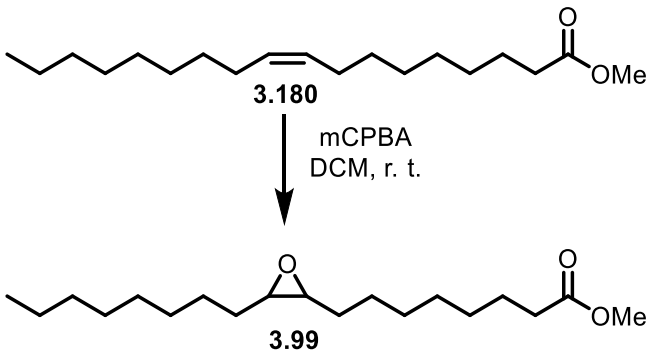

Epoxidized methyl oleate (3.99) was synthesized with mCPBA. A 25 mL round-bottomed flask was charged with mCPBA (0.52 g, 3.0 mmol) and dichloromethane (6 mL) was then added). The reaction was stirred at room temperature, followed by dropwise addition of methyl oleate **3.180** (1.0 mL, 3.0 mmol). The reaction was stirred overnight. The reaction was then extracted with dichloromethane (20 mL), washed with a saturated aqueous solution of $NaHCO_3$ (2 x 20 mL) and then with brine (20 mL). The organic phase was then dried over Mg_2SO_4 and filtered. The crude mixture was concentrated *in vacuo*

[142] Sparr, C.; Tanzer, E.-M.; Bachmann, J.; Gilmour, R. *Synthesis* **2010**, *8*, 1394–1397.

and purified via flash column chromatography (eluent: 5% EtOAc in hexanes). The fractions were monitored by TLC, with an iodine stain for visualization. Epoxidized methyl oleate **3.99** was obtained as a colourless oil (0.32 g, 34% yield). Characterization data matched those previously reported.[143] **^{1}H NMR** (400 MHz, $CDCl_3$): 3.67 (s, 3H), 2.91 (br, 2H), 2.31 (t, *J* = 7.5 Hz, 2H), 1.67-1.60 (m, 2H), 1.53-1.27 (m, 24H), 0.91-0.87 (m, 3H). **^{13}C NMR** (100 MHz, $CDCl_3$): 174.4, 57.4, 57.3, 51.6, 34.2, 32.0, 29.7 (x2), 29.5, 29.4, 29.3, 29.2, 28.0, 27.9, 26.8, 26.7, 25.1, 22.8, 14.3.

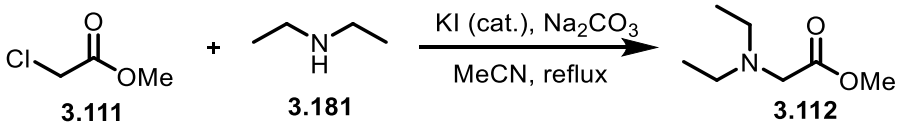

3.111 **3.181** **3.112**

N,N-Diethylglycine methyl ester (3.112) was synthesized according to a procedure adapted from the literature.[144] A 300 mL round-bottomed flask was charged with a stir bar, potassium iodide (581 mg, 3.50 mmol), and sodium bicarbonate (3.24 g, 30.6 mmol). Acetonitrile (200 mL) was then added, followed by addition of diethylamine (3.5 mL, 34 mmol). The reaction mixture was stirred at room temperature, and methyl chloroacetate (2.6 mL, 30 mmol) was added dropwise. The reaction was refluxed at 85–90°C for 4 h. After being cooled down, the crude mixture was filtered, and the solvent was evaporated *in vacuo*. Ether (80 mL) was added, resulting in the formation of a precipitate. The mixture was filtered, and the solvent was again evaporated *in vacuo*. The crude residue was purified by column chromatography (gradient of 30% → 50% EtOAc in hexanes), yielding **3.112** as an orange oil (1.30 g, 30% yield). Characterization data matched those previously reported.[145] **^{1}H NMR** (400 MHz, $CDCl_3$): 3.71 (s, 3H), 3.32 (s, 2H), 2.64 (q, 4H), 1.06 (t, 6H). **^{13}C NMR** (100 MHz, $CDCl_3$): 172.2, 54.4, 51.7, 47.9, 12.2.

[143] Deruer, E. ; Duguet, N. ; Lemaire, M. *ChemSusChem* **2015**, *8*, 2481–2486.
[144] Schulze, R.; Beckhaus, H.-D.; Rüchardt, C. *J. prakt. Chem* **1990**, *332*, 325–330.
[145] Singer, S. S. *J. Org. Chem.* **1982**, *47*, 3839–3844.

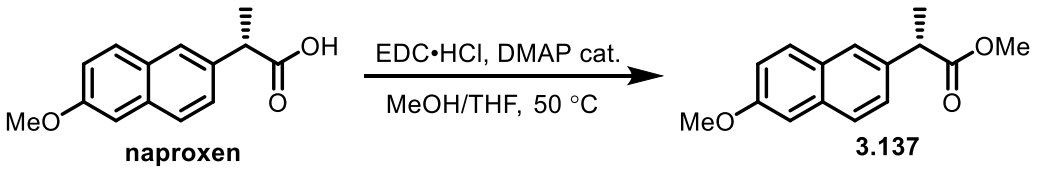

(S)-naproxen methyl ester (3.137) was synthesized via EDC coupling of naproxen with methanol. A 25 mL round-bottomed flask was equipped with a magnetic stir bar, naproxen (0.69 g, 3.0 mmol), DMAP (37 mg, 10 mol%) and EDC·HCl (0.69 g, 3.6 mmol). THF (15 mL) was added, followed by addition of methanol (1.2 mL, 30 mmol). The reaction mixture was stirred at 50 °C overnight. The mixture was then extracted with EtOAc (20 mL) and washed with a saturated aqueous solution of $NaHCO_3$ (2 x 20 mL) and with brine (20 mL). The organic phase was then dried over Na_2SO_4 and filtered. The crude mixture was concentrated *in vacuo* and subjected to flash column chromatography (eluent: 10% acetone in hexanes). Ester **3.137** was obtained as a white solid (0.56 g, 76% yield). Characterization data matched those previously reported.[146] **^{1}H NMR** (400 MHz, $CDCl_3$): 7.71 (d, *J* = 8.5 Hz, 2H), 7.67 (d, *J* = 1.9 Hz, 1H), 7,41 (dd, *J* = 8.4, 1.8 Hz, 1H), 7.17-7.12 (m, 2H), 3.92 (s, 3H), 3.87 (q, *J* = 7.2 Hz, 1H), 3.68 (s, 3H), 1.59 (d, *J* = 7.2 Hz, 3H). **^{13}C NMR** (100 MHz, $CDCl_3$): 175.3, 158.0, 135.8, 133.9, 129.4, 129.1, 127.3, 126.3, 126.1, 119.1, 105.7, 55.4, 52.2, 45.5, 18.7.

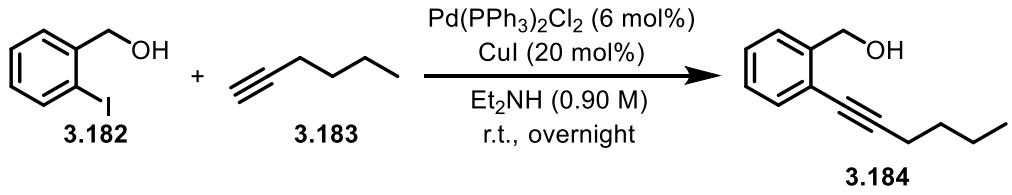

(2-(hex-1-yn-1-yl)phenyl)methanol (3.184) was synthesized via a Sonogashira coupling. A 25 mL round-bottomed flask was equipped with a magnetic stir bar, 2-iodobenzyl alcohol **3.182** (0.85 g, 3.6 mmol), $Pd(PPh_3)_2Cl_2$ (0.15 g, 6.0 mol%) and copper iodide (0.14 g, 20 mol%). The flask was degassed with an argon balloon. Degassed diethylamine (4 mL) was then added, followed by dropwise addition of the alkyne **3.183** (0.84 mL, 7.3

[146] Audubert, C.; Marin, O. J. G.; Lebel, H. *Angew.Chem. Int.Ed.* **2017**, *56*, 6294 –6297.

mmol). The reaction was stirred at room temperature overnight. After, the reaction mixture was concentrated *in vacuo*, extracted with ethyl acetate (30 mL) and washed with water (20 mL) and brine (20 mL). The organic phase was then dried over sodium sulphate, filtered, and concentrated *in vacuo*. The crude product was subjected to manual column chromatography (eluent: 6 to 10% acetone in hexanes), which afforded **3.184** as an orange liquid (0.63 g, 92% yield). Characterization data matched those previously reported.[147] **^{1}H NMR** (400 MHz, $CDCl_3$): 7.39 (d, *J* = 8.2 Hz, 2H), 7.28 (d, *J* = 8.4 Hz, 2H), 4.68 (s, 2H), 2.42 (t, J = 7.1 Hz, 2H), 1.69 (br s, 1H), 1.64-1.56 (m, 2H), 1.53-1.44 (m, 2H), 0.96 (t, *J* = 7.3 Hz, 3H). **^{13}C NMR** (100 MHz, $CDCl_3$): 140.2, 131.9, 126.7, 123.6, 90.7, 80.5, 65.2, 31.0, 22.2, 19.3, 13.8.

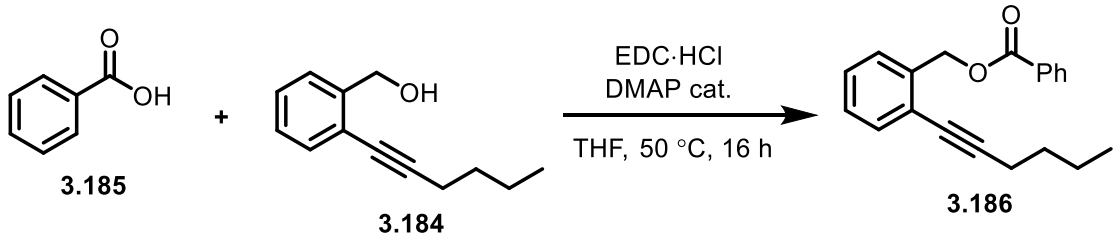

2-(hex-1-yn-1-yl)benzyl benzoate (3.186) was prepared via EDC coupling between alcohol **3.184** and benzoic acid **3.185**. A 25 mL round-bottomed flask was equipped with a stir bar, benzoic acid (0.25 g, 2.0 mmol), alcohol **3.184** (0.42 g, 2.2 mmol), EDC·HCl (0.46 g, 2.4 mmol), and DMAP (24 mg, 0.20 mmol). The mixture was diluted with THF (15 mL) and stirred overnight at room temperature. After, the solution was quenched with a saturated aqueous solution of sodium bicarbonate (10 mL). The mixture was transferred into a separatory funnel, and the flask was further rinsed with ethyl acetate (20 mL). The organic phase was then washed with a 1M aqueous solution of NaOH (10 mL), followed by a wash with brine (10 mL). The organic phase was then dried over Na_2SO_4, filtered, and concentrated *in vacuo*. The crude product was then purified via manual column chromatography (2% acetone in hexanes) to afford **3.186** as a yellow liquid (0.42 g, 72%

[147] Albano, G.; Morelli, M.; Aronica, L. A. *Eur. J. Org. Chem.* **2017**, 3473–3480.

yield). **^{1}H NMR** (400 MHz, $CDCl_3$): 8.10-8.07 (m, 2H), 7.60-7.55 (m, 1H), 7.47-7.41 (m, 4H), 7.38-7.36 (m, 2H), 5.35 (s, 2H), 2.42 (t, *J* = 7.1 Hz, 2H), 1.64-1.56 (m, 2H), 1.53-1.44 (m, 2H), 0.96 (t, *J* = 7.3 Hz, 3H). **^{13}C NMR** (100 MHz, $CDCl_3$): 166.5, 135.4, 133.2, 131.9, 130.2, 129.9, 128.5, 128.1, 124.2, 91.1, 80.3, 66.5, 31.0, 22.2, 19.3, 13.8. **IR (neat)**: 2956, 2930, 2863, 2227, 1718, 1601, 1509, 1451, 1314, 1265, 1176, 1096, 1070, 1027, 823, 708 cm^{-1}. **Accurate mass (MS)**: m/z calculated for $C_{20}H_{20}O_2$: 292.1458, found 292.1474 (spectral accuracy = 99.6%).

2.5.3. General procedure and characterization for Ni-catalyzed amidation

Representative procedure for the Ni-catalyzed amidation of methyl esters

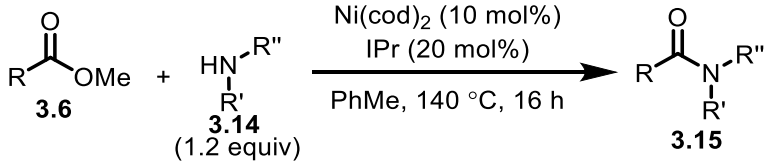

In a glovebox, an oven dried screw-capped vial was charged with a magnetic stir bar, Ni(cod)2 (5.5 mg, 10 mol%), and IPr (16 mg, 20 mol%). Thoroughly degassed toluene (1.0 mL, 0.20 M) obtained from a solvent purification system was then added. The reaction mixture was shaken vigorously, then ester (0.20 mmol) and amine (0.24 mmol, 1.2 equiv) were subsequently added. The vial was sealed with a Teflon-lined screw cap and shipped outside of the glovebox. The reaction was stirred vigorously (700 rpm) in a silicone oil bath at 140 °C for 16 h. After cooling to room temperature, the reaction mixture was quenched with a saturated aqueous solution of ammonium chloride, diluted with ethyl acetate, and filtered through a plug of silica gel (10 mL of EtOAc eluent). The crude mixture was then concentrated in vacuo and subjected to column chromatography. When separation of the amide product from the excess amine starting material was challenging, the mixture was dissolved in EtOAc and washed with 1 M HCl (aq).

Characterization of amide products

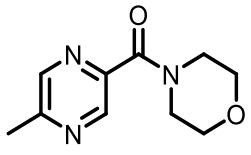

(5-methylpyrazin-2-yl)(morpholino)methanone (3.20) was prepared according to the general procedure. Purification by column chromatography (gradient of 100% EtOAc → 20% MeOH in EtOAc) afforded **3.20** as a yellow oil (35 mg, 84%). **^{1}H NMR** ($CDCl_3$, 400 MHz): δ 8.86 (d, *J* = 1.4 Hz, 1H), 8.39 (d, *J* = 1.0 Hz, 1H), 3.80 (s, 4H), 3.69 (s, 4H), 2.61 (s, 3H). **^{13}C NMR** ($CDCl_3$, 100 MHz): δ 165.5, 155.3, 145.9, 145.0, 142.2, 67.1, 66.9, 47.8, 43.0, 21.8. **IR (neat)**: 2964, 2921, 2855, 1626, 1575, 1489, 1432, 1380, 1363, 1321, 1299, 1277, 1263, 1246, 1163, 1111, 1068, 1037, 1020, 937, 9078, 848, 827, 783, 729, 690 cm^{-1}. **Accurate mass (MS)**: m/z calculated for $C_{10}H_{13}N_3O_2$: 207.1002, found 207.1008 (spectral accuracy = 99.5%).

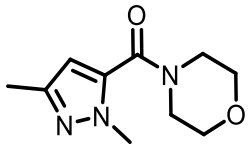

4-(2,5-dimethyl-2H-pyrazole-3-carbonyl)-morpholine (3.22) was prepared according to the general procedure starting from the corresponding ethyl ester. Purification by column chromatography (gradient of 100% EtOAc → 20% MeOH in EtOAc) afforded **3.22** as a brown solid (27 mg, 64%). **^{1}H NMR** ($CDCl_3$, 400 MHz): δ 6.07 (s, 1H), 3.90 (s, 3H), 3.70 (br s, 8H), 2.26 (s, 3H). **^{13}C NMR** ($CDCl_3$, 100 MHz): δ 161.4, 147.1, 135.4, 106.3, 67.0, 48.0, 42.7, 37.9, 13.4. **IR (neat)**: 3113, 2959, 2925, 2863, 1623, 1541, 1466, 1439, 1358, 1302, 1274, 1246, 1167, 1113, 1065, 1008, 936, 890, 841, 823, 779, 751, 677, 661 cm^{-1}. **Accurate mass (MS)**: m/z calculated for $C_{10}H_{15}N_3O_2$: 209.1159, found 209.1093 (spectral accuracy = 99.6%). **m.p.**: 68–70 °C.

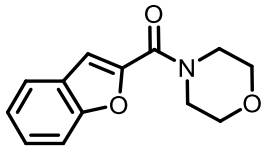

benzofuran-2-yl(morpholino)methanone (3.24) was prepared according to the general procedure from the corresponding ethyl ester. Purification by column chromatography (gradient of 10% → 40% EtOAc in hexanes) afforded **3.24** as a red solid (38 mg, 82%). Characterization data matched those previously reported.[148] **^{1}H NMR** ($CDCl_3$, 400 MHz): δ 7.66 (d, *J* = 7.8 Hz, 1H), 7.52 (d, *J* = 8.2 Hz, 1H), 7.41 (t, *J* = 7.3, 1.2 Hz, 1H), 7.35 (s, 1H), 7.30 (t, *J* = 7.3 Hz, 1H), 3.98-3.82 (m, 4H), 3.79-3.78 (m, 4H). **^{13}C NMR** ($CDCl_3$, 100 MHz): δ 159.9, 154.7, 148.9, 127.0, 126.7, 123.8, 122.4, 112.6, 112.0, 67.1, 47.2, 43.6.

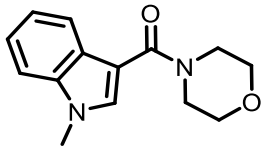

(1-methyl-1H-indol-4-yl)(morpholino)methanone (3.26) was prepared according to the general procedure. Purification by column chromatography (gradient of 50% → 100% EtOAc in hexanes) afforded 3.**26** as a white solid (43 mg, 87%). **^{1}H NMR** ($CDCl_3$, 400 MHz): δ 7.37 (d, *J* = 8.2 Hz, 1H), 7.25 (t, *J* = 7.6 Hz, 1H), 7.15 (dd, *J* = 7.3, 0.8 Hz, 1H), 7.12 (d, *J* = 3.1 Hz, 1H), 6.49 (dd, *J* = 3.0, 0.7 Hz, 1H), 3.95-3.27 (m, 8H), 3.81 (s, 3H). **^{13}C NMR** ($CDCl_3$, 100 MHz): δ 170.3, 136.9, 130.1, 127.7, 125.7, 121.4, 118.4, 110.7, 100.0, 67.3, 48.0, 42.8, 33.1. **IR (neat)**: 3105, 2921, 2854, 1617, 1575, 1512, 1498, 1432, 1366, 1339, 1304, 1291, 1276, 1262, 1209, 1195, 1154, 1112, 1084, 1074, 1031, 966, 925, 891, 879, 849, 825, 804, 751, 737, 711, 685 cm^{-1}. **Accurate mass (MS)**: m/z calculated for $C_{14}H_{16}N_2O_2$: 244.1179, found 244.1206 (spectral accuracy = 99.0%). **m. p.**: 152-154 °C.

[148] Baba, H.; Moriyama, K.; Togo, H. *Synlett* **2012**, *23*, 1175–1180.

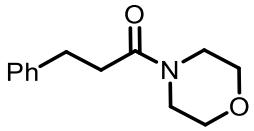

4-(3-phenyl-propionyl)-morpholine (3.28) was prepared according to the general procedure from the corresponding ethyl ester. Purification by column chromatography (gradient of 10% → 80% EtOAc in hexanes) afforded **3.28** as a colourless oil (35 mg, 79%). Characterization data matched those previously reported.[149] **^{1}H NMR** ($CDCl_3$, 400 MHz): δ 7.32-7.28 (m, 2H), 7.23-7.20 (m, 3H), 3.63 (br s, 4H), 3.51 (t, *J* = 4.9 Hz, 2H), 3.36 (t, *J* = 5.1 Hz, 2H), 2.99 (t, *J* = 8.2 Hz, 2H), 2.62 (t, *J* = 7.6 Hz, 2H). **^{13}C NMR** ($CDCl_3$, 100 MHz): δ 171.0, 141.2, 128.7, 128.6, 126.4, 67.0, 66.6, 46.1, 42.1, 34.9, 31.6.

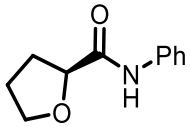

(S)-N-phenyloxolane-2-carboxamide (3.30) was prepared according to the general procedure starting from (S)-methyl tetrahydrofuran-2-carboxylate (**3.30**) (97.5:2.5 e.r.). Purification by column chromatography (gradient of 5% → 30% EtOAc in hexanes) afforded **3.30** as a light yellow oil (35 mg, 91%, 97:3 e.r.). Characterization data matched those previously reported.[150] **^{1}H NMR** ($CDCl_3$, 400 MHz): δ 8.47 (br s, 1H), 7.59 (d, *J* = 8.4 Hz, 2H), 7.34 (t, *J* = 7.9 Hz, 2H), 7.13 (t, *J* = 7.5 Hz, 1H), 4.48 (dd, *J* = 8.4, 5.9 Hz, 1H), 4.08-3.94 (m, 2H), 2.42-2.33 (m, 1H), 2.24-2.16 (m, 1H), 2.03-1.88 (m, 2H). **^{13}C NMR** ($CDCl_3$, 100 MHz): δ 171.4, 137.4, 129.2, 124.5, 119.7, 78.8, 69.8, 30.3, 25.7. **HPLC**: CHIRALCEL AD-H, gradient 2% to 5% ^{i}PrOH in hexanes, 1.0 mL/min, 230 nm, t_{R1}(minor) = 32.5 min, t_{R2}(major) = 38.4 min. $[\alpha]_D^{22}$ = +7.41 (c = 0.00054 g/mL, MeCN).

[149] Davidsona, R. W. M.; Fuchter, M. J. *Chem. Commun.* **2016**, *52*, 11638–11641.

[150] Zhang, L.; Wang, W.; Wang, A.; Cui, Y.; Yang, X.; Huang, Y.; Liu, X.; Liu, W.; Son, J.-Y.; Oji, H.; Zhang, T. *Green Chem.* **2013**, *15*, 2680–2684.

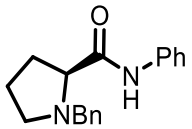

(S)-1-benzyl-N-phenylpyrrolidine-2-carboxamide (3.32) was prepared according to the general procedure. Purification by column chromatography (gradient of 10% → 30% EtOAc in hexanes) afforded **3.32** as a white solid (20 mg, 35%, >99:1 e.r.). Characterization data matched those previously reported.[151] **^{1}H NMR** ($CDCl_3$, 400 MHz): δ 9.47 (br s, 1H), 7.56 (d, *J* = 8.5 Hz, 2H), 7.39-7.26 (m, 7H), 7.11 (t, *J* = 7.5 Hz, 1H), 3.96 (d, *J* = 13.1 Hz, 1H), 3.61 (d, *J* = 12.9 Hz, 1H), 3.36 (dd, *J* = 10.2, 4.7 Hz, 1H), 3.15 (ddd, *J* = 9.2, 6.8, 2.3 Hz, 1H), 2.48 (td, *J* = 9.8, 6.5, 1H), 2.37-2.27 (m, 1H), 2.08-2.00 (m, 1H), 1.88-1.74 (m, 2H). **^{13}C NMR** ($CDCl_3$, 100 MHz): δ 172.9, 138.5, 137.9, 129.1, 128.8, 128.8, 127.6, 124.1, 119.4, 68.1, 60.2, 54.2, 30.9, 24.5. **HPLC**: CHIRALCEL AD-H, gradient 7% ^{i}PrOH in hexanes, 1.0 mL/min, 254 nm, t_{R1}(minor) = 7.9 min, t_{R2}(major) = 9.9 min. $[\alpha]_D^{22}$ = -147 (c = 0.00036 g/mL, MeCN).

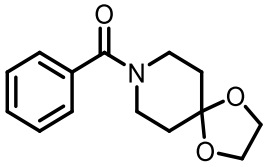

(1,4-dioxa-8-azaspiro[4.5]dec-8-yl)phenylmethanone (3.35) was prepared according to the general procedure with dioxane as the solvent instead of toluene. Purification by column chromatography (gradient of 20% → 60% EtOAc in hexanes) afforded **3.35** as a brown oil (38 mg, 76%). Characterization data matched those previously reported.[152] **^{1}H NMR** ($CDCl_3$, 400 MHz): δ 7.42-7.39 (m, 5H), 3.99 (br s, 4H), 3.86 (br s, 2H), 3.49 (br s, 2H), 1.81-1.64 (m, 4H). **^{13}C NMR** ($CDCl_3$, 100 MHz): δ 170.5, 136.2, 129.7, 128.6, 126.9, 107.1, 64.6, 45.8, 40.4, 35.9, 34.9.

[151] Yang, H.; Xi, C.; Miao, Z.; Chen, R. *Eur. J. Org. Chem.* **2011**, 3353–3360.
[152] Narasimhulu Naidu, B.; Sorenson, M. E. HIV Integrase Inhibitors. US Patent US2007/281917, 2007.

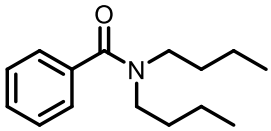

N,N-dibutylbenzamide (3.37) was prepared according to the general procedure. Purification by column chromatography (gradient of 20% → 30% EtOAc in hexanes) afforded **3.37** as a yellow oil (47 mg, 73%). Characterization data matched those previously reported.[153] **^{1}H NMR** ($CDCl_3$, 400 MHz): δ 7.39-7.33 (m, 5H), 3,49 (br, 2H), 3.19 (br, 2H), 1.76-0.78 (m, 14H); **^{13}C NMR** ($CDCl_3$, 100 MHz): δ 171.76, 137.53, 129.11, 128.45, 126.58, 48.87, 44.58, 30.94, 29.83, 20.44, 19.88, 14.07, 13.74.

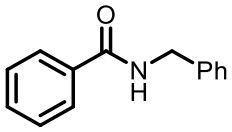

N-benzylbenzamide (3.39) was prepared according to the general procedure. Purification by column chromatography (gradient of 10% → 40% EtOAc in hexanes) afforded **3.39** as a white solid (31 mg, 74%). Characterization data matched those previously reported.[154] **^{1}H NMR** ($CDCl_3$, 400 MHz): δ 7.80 (d, *J* = 7.1 Hz, 2H), 7.51 (t, *J* = 7.4 Hz, 1H), 7.43 (t, *J* = 7.0 Hz, 2H), 7.37-7.28 (m, 5H), 6.53 (br s, 1H), 4.65 (d, *J* = 5.7 Hz, 2H). **^{13}C NMR** ($CDCl_3$, 100 MHz): δ 167.5, 138.3, 134.5, 131.8, 128.9, 128.7, 128.0, 127.7, 127.1, 44.3.

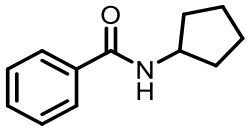

N-cyclopentylbenzamide (3.41) was prepared according to the general procedure. Purification by column chromatography (gradient of 30% → 40% EtOAc in hexanes)

[153] Mane, R. S.; Bhanage, B. M. *J. Org. Chem.* **2016**, *81*, 1223–1228.
[154] Kosal, A. D.; Wilson, E. E.; Ashfeld, B. L. *Angew. Chem. Int. Ed.* **2012**, *51*, 12036–12040.

afforded **3.41** as a white solid (33 mg, 86%). Characterization data matched those previously reported.[155] **^{1}H NMR** ($CDCl_3$, 400 MHz): δ 7.72 (d, *J* = 7.1 Hz, 2H), 7.45 (t, *J* = 7.5 Hz, 1H), 7.38 (t, *J* = 7.3 Hz, 2H), 6.13 (br s, 1H), 4.37 (sxt, *J* = 7.0 Hz, 1H), 2.09-2.01 (m, 2H), 1.74-1.57 (m, 4H), 1.51-1.43 (m, 2H). **^{13}C NMR** ($CDCl_3$, 100 MHz): δ 167.3, 135.1, 131.3, 128.6, 126.9, 51.8, 33.3, 23.9.

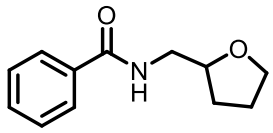

N-((tetrahydrofuran-2-yl)methyl)benzamide (3.43) was prepared according to the general procedure. Purification by column chromatography (gradient of 60% → 80% EtOAc in hexanes) afforded **3.43** as a brown oil (36 mg, 88%). Characterization data matched those previously reported.[156] **^{1}H NMR** ($CDCl_3$, 400 MHz): δ 7.78 (d, *J* = 7.4 Hz, 2H), 7.48 (t, *J* = 7.1 Hz, 1H), 7.41 (m, 2H), 6.61 (s, 1H), 4.07 (qd, *J* = 7.2, 3.2 Hz, 1H), 3.88 (m, 1H), 3.77 (m, 2H), 3.34 (ddd, *J* = 13.7, 7.4, 4.9 Hz, 1H), 2.02 (m, 1H), 1.91 (m, 2H), 1.61 (m, 1H). **^{13}C NMR** ($CDCl_3$, 100 MHz): δ 167.6, 134.6, 131.5, 128.6, 127.1, 77.9, 68.2, 43.7, 28.8, 26.0.

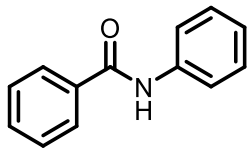

N-phenylbenzamide (3.45) was prepared according to the general procedure. Purification by column chromatography (gradient of 10% → 40% EtOAc in hexanes) afforded **3.45** as a white solid (methyl benzoate: 33 mg, 83%; ethyl benzoate: 32 mg, 81%). Characterization data matched those previously reported.[157] **^{1}H NMR** ($CDCl_3$, 400 MHz):

[155] Tran, B. L.; Li, B.; Driess, M.; Hartwig, J. F. *J. Am. Chem. Soc.* **2014**, *136*, 2555–2563.
[156] Lenstra, D. C.; Nguyen, D. C.; Mecinović, J. *Tetrahedron* **2015**, *71*, 5547–5553.
[157] Rao, Y., Li, X.; Danishefsky, S. J. *J. Am. Chem. Soc.* **2009**, *131*, 12924–12926.

δ 7.96 (br s, 1H), 7.88-7.86 (m, 2H), 7.66 (d, *J* = 7.6 Hz, 2H), 7.55 (t, *J* = 7.6 Hz, 1H), 7.47 (t, *J* = 7.8 Hz, 2H), 7.37 (t, *J* = 7.3 Hz, 2H), 7.16 (t, *J* = 8.0 Hz, 1H); **^{13}C NMR** ($CDCl_3$, 100 MHz): δ 165.9, 138.1, 135.1, 132.0, 129.2, 128.9, 127.2, 124.7, 120.4.

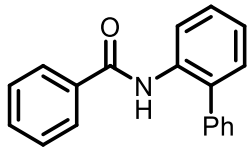

N-([1,1'-biphenyl]-2-yl)benzamide (3.47) was prepared according to the general procedure. Purification by column chromatography (gradient of 10% → 40% EtOAc in hexanes) afforded **3.47** as a white solid (33 mg, 60%). Characterization data matched those previously reported.[158] **^{1}H NMR** ($CDCl_3$, 400 MHz): δ = 8.55 (d, *J* = 8.0 Hz, 1H), 8.01 (br s, 1H), 7.63–7.60 (m, 2H), 7.53–7.51 (m, 2H), 7.50–7.44 (m, 5H), 7.42–7.38 (m, 2H), 7.33–7.31 (m, 1H), 7.26–7.21 (m, 1H). **^{13}C NMR** ($CDCl_3$, 100 MHz): δ 165.35, 138.37, 135.2, 135.1, 132.7, 132.0, 130.3, 129.8, 129.7, 129.5, 129.1, 128.9, 128.5, 127.1, 124.71, 121.5, 115.7.

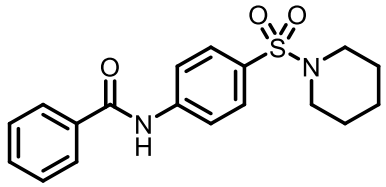

1-(N-benzoyl-sulfanilyl)-piperidine (3.49) was prepared according to the general procedure. Purification by column chromatography (gradient of 40% → 50% EtOAc in hexanes) afforded **3.49** as a white solid (36 mg, 53%). **^{1}H NMR** ($CDCl_3$, 400 MHz): δ 8.11 (br s, 1H), 7.90 (d, *J* = 7.0 Hz, 2H), 7.84 (d, *J* = 8.8 Hz, 2H), 7.75 (d, *J* = 8.8 Hz, 2H), 7.60 (t, *J* = 7.3 Hz, 1H), 7.53 (t, *J* = 7.8 Hz, 2H), 2.99 (t, *J* = 5.3 Hz, 4H), 1.68-1.62 (m, 4H), 1.46-1.40 (m, 2H). **^{13}C NMR** ($CDCl_3$, 100 MHz): δ 166.1, 142.0, 134.4, 132.6, 131.6, 129.1, 127.3, 119.9,

[158] Hie, L. et al. Nature **2015**, *524*, 79–83.

47.1, 25.3, 23.6. **IR (neat)**: 3404, 2921, 2845, 1687, 1584, 1520, 1498, 1467, 1446, 1397, 1357, 1329, 1309, 1279, 1247, 1210, 1148, 1099, 1051, 1028, 998, 927, 893, 855, 834, 817, 798, 735, 706 cm^{-1}. **HRMS** (ESI-Q-TOF): m/z calculated for $C_{18}H_{20}N_2O_3SNa$ $[M+Na]^+$: 367.1092, found 367.1086. **m.p.**: 190-192 °C.

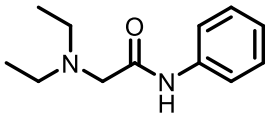

2-diethylamino-N-phenylacetamide (3.114) was prepared according to a modified general procedure at 145 °C for 40 h at 0.40 M. Purification by column chromatography (gradient of 40% → 100% EtOAc in hexanes) afforded **3.114** as a yellow oil (32 mg, 77%). Characterization data matched those previously reported.[159] **^{1}H NMR** ($CDCl_3$, 400 MHz): δ 9.43 (br s, 1H), 7.59 (dd, *J* = 8.5 Hz, 1.1 Hz, 2H), 7.34 (t, *J* = 8.4 Hz, 2H), 7.11 (t, *J* = 7.5 Hz, 1H), 3.16 (s, 2H), 2.66 (q, *J* = 7.1 Hz, 4H), 1.10 (t, *J* = 7.5 Hz, 6H). **^{13}C NMR** ($CDCl_3$, 100 MHz): δ 170.2, 137.8, 129.1, 124.2, 119.4, 58.2, 49.0, 12.6.

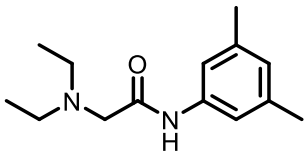

2-(diethylamino)-N-(3,5-dimethyl-phenyl)acetamide (3.115) was prepared according to a modified general procedure at 145 °C for 40 h at 0.40 M. Purification by column chromatography (gradient of 50% EtOAC in hexanes → 10% MeOH in EtOAc) afforded **3.115** as an orange oil (37 mg, 78%). **^{1}H NMR** ($CDCl_3$, 400 MHz): δ 9.31 (br s, 1H), 7.22 (s, 2H), 6.76 (s, 1H), 3.14 (s, 2H), 2.65 (q, *J* = 7.3 Hz, 4H), 2.32 (s, 6H), 1.10 (t, *J* = 7.2 Hz, 6H). **^{13}C NMR** ($CDCl_3$, 100 MHz): δ 170.1, 138.8, 137.7, 125.9, 117.1, 58.3, 49.0, 21.5, 12.6. **IR**

[159] Yoshimitsu, T.; Matsuda, K.; Nagaoka, H.; Tsukamoto, K.; Tanaka, T. *Org Lett.* **2007**, *9*, 5115–5118.

(neat): 3291, 2968, 2923, 2827, 1686, 1611, 1530, 1450, 1421, 1376, 1323, 1296, 1270, 1204, 1162, 1118, 1089, 1068, 1038, 978, 908, 888, 838, 786, 739, 688 cm^{-1}. **Accurate mass (MS)**: m/z calculated for $C_{14}H_{22}N_2O$: 234.1727, found 234.1740 (spectral accuracy = 99.0%).

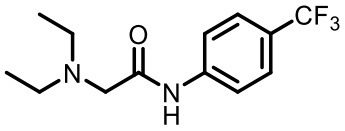

2-(diethylamino)-N-(4-trifluoromethyl-phenyl)acetamide (3.116) was prepared according to a modified general procedure at 145 °C for 40 h at 0.40 M. Purification by column chromatography (gradient 70% → 100% EtOAc in hexanes) afforded **3.116** as an orange solid (33 mg, 59%). **^{1}H NMR** ($CDCl_3$, 400 MHz): δ 9.62 (br s, 1H), 7.71 (d, *J* = 8.4 Hz, 2H), 7.56 (d, *J* = 8.4 Hz, 2H), 3.14 (s, 2H), 2.64 (q, *J* = 7.1 Hz, 4H), 1.07 (t, *J* = 7.2 Hz, 6H). **^{13}C NMR** ($CDCl_3$, 100 MHz): δ 170.7, 140.8, 126.4 (q, *J* = 3.7 Hz), 125.9 (q, *J* = 32 Hz), 124.3 (q, *J* = 270 Hz), 119.0, 58.2, 49.1, 12.6. **IR (neat)**: 3264, 2964, 2930, 2870, 2824, 1683, 1614, 1592, 1524, 1503, 1409, 1370, 1318, 1261, 1206, 1185, 1159, 1125, 1113, 1083, 1066, 1017, 996, 978, 865, 837, 785, 747, 732, 695 cm^{-1}. **HRMS** (ESI-Q-TOF): m/z calculated for $C_{13}H_{18}F_3N_2O$ $[M+H]^+$: 275.1371, found 275.1377. **m.p.**: 44-46 °C.

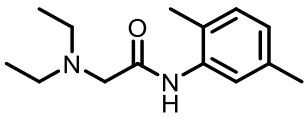

2-(diethylamino)-N-(2,5-dimethyl-phenyl)acetamide (JM25-1) was prepared according to a modified general procedure at 145 °C for 40 h at 0.40 M with 20 mol% catalyst loading. Purification by column chromatography (70% EtOAC in hexanes) afforded **JM25-1** as an orange oil (26 mg, 54%). **^{1}H NMR** ($CDCl_3$, 400 MHz): δ 9.47 (br s, 1H), 8.01 (s, 1H), 7.06 (d, *J* = 7.6 Hz, 1H), 6.86 (d, *J* = 8.6 Hz, 1H), 3.19 (s, 2H), 2.67 (q, *J* = 7.1 Hz, 4H), 2.34 (s, 3H), 1.11 (t, *J* = 7.2 Hz, 6H). **^{13}C NMR** ($CDCl_3$, 100 MHz): δ 170.0, 136.8, 135.9, 130.2, 125.0, 124.0, 121.5, 58.6, 48.9, 21.4, 17.4, 12.8. **IR (neat)**: 3300, 2968, 2925, 2871, 2826, 1691,

1581, 1528, 1483, 1450, 1421, 1377, 1347, 1288, 1260, 1204, 1161, 1122, 1089, 1067, 1039, 1003, 980, 888, 803, 731, 680 cm^{-1}. **HRMS** (ESI-Q-TOF): m/z calculated for $C_{14}H_{23}N_2O$ $[M+H]^+$: 235.1810, found 235.2026.

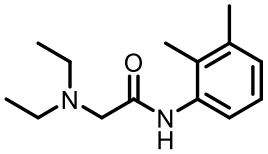

2-(diethylamino)-N-(2,3-dimethyl-phenyl)acetamide (JM23-1) was prepared according to a modified general procedure at 145 °C for 40 h at 0.40 M with 20 mol% catalyst loading. Purification by column chromatography (70% EtOAC in hexanes) afforded **JM25-1** as an orange oil (19 mg, 41%). **^{1}H NMR** ($CDCl_3$, 400 MHz): δ 9.49 (br, 1H), 7.88 (d, *J* = 8.0 Hz, 1H), 7.13 (t, *J* = 7.7 Hz, 1H), 6.98 (d, *J* = 7.4 Hz, 1H), 3.20 (s, 2H), 2.68 (q, *J* = 7.1 Hz, 4H), 2.32 (s, 3H), 2.19 (s, 3H), 1.12 (t, *J* = 7.2 Hz, 6H). **^{13}C NMR** ($CDCl_3$, 100 MHz): δ 170.1, 137.2, 135.9, 126.8, 126.4, 126.2, 119.8, 58.5, 48.9, 20.8, 13.5, 12.7.

2.5.4. General procedure and characterization of the Ni-catalyzed transesterification

Representative procedure for the Ni-catalyzed transesterification of methyl esters

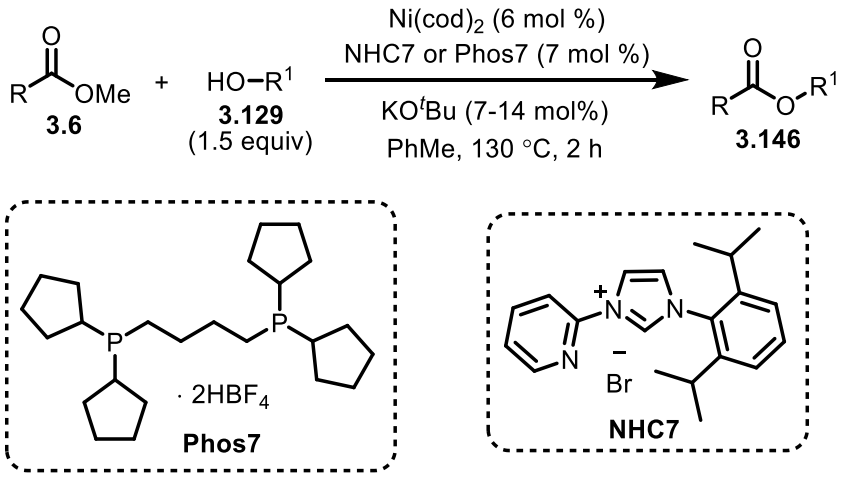

In a glovebox, an oven dried screw-capped vial was charged with a magnetic stir bar, Ni(cod)2 (3.3 mg, 6.0 mol%), **NHC7** (5.4 mg, 7.0 mol%) or **Phos7** (8.0 mg, 7.0 mol%), and potassium *tert*-butoxide (7.0 mol% if using **NHC7**, 14 mol% if using **Phos7**). Thoroughly degassed toluene (0.40 mL, 0.50 M) obtained from a solvent purification system was then added. Then, ester (0.20 mmol) and alcohol (0.30 mmol) were subsequently added. The vial was sealed with a Teflon-lined screw cap and shipped outside of the glovebox. The reaction was stirred vigorously (700 rpm) in a silicone oil bath at 130 °C for 2 h. After cooling to room temperature, the reaction mixture was quenched with a saturated aqueous solution of ammonium chloride, diluted with ethyl acetate, and filtered through a plug of silica gel (10 mL of EtOAc eluent). The crude mixture was then concentrated *in vacuo* and analyzed by ^{1}H NMR, followed by purification via column chromatography.

Characterization of ester products

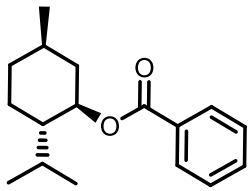

L-menthyl benzoate (3.132) was prepared according to the general procedure. Purification by column chromatography (gradient of 10% → 40% EtOAc in hexanes) afforded **3.132** as a colourless oil (41 mg, 79%). Characterization data matched those previously reported.[160] **^{1}H NMR** ($CDCl_3$, 400 MHz): δ 8.07-8.05 (m, 2H), 7.58-7.54 (m, 1H), 7.47-7.43 (m, 2H), 4.95 (td, *J* = 10.9 Hz, 1H), 2.17-2.12 (m, 1H), 2.01-1.94 (m, 1H), 1.77-1.71 (m, 2H), 1.20-1.07 (m, 2H), 0.93 (dd, *J* = 6.9, 4.3 Hz, 7H), 0.81 (d, *J* = 7.1 Hz, 3H). **^{13}C NMR** ($CDCl_3$, 100 MHz): δ 166.2, 132.8, 131.0, 129.7, 128.4, 75.0, 47.4, 41.1, 34.5, 31.6, 26.6, 23.8, 21.2, 20.9, 16.7.

[160] Liu, Z.; Ma, Q.; Liu, Y.; Wang, Q. *Org. Lett.* **2014**, *16*, 236–239.

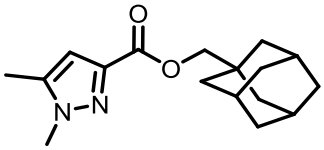

Adamantan-1-ylmethyl 1,5-dimethyl-1H-pyrazole-3-carboxylate (3.147) was prepared according to the general procedure. Purification by column chromatography (gradient of 4% → 10% EtOAc in hexanes) afforded **3.147** as a white solid (40 mg, 70%). **^{1}H NMR** ($CDCl_3$, 400 MHz): δ 6.62 (s, 1H), 4.11 (s, 3H), 3.86 (s, 2H), 2.27 (s, 3H), 2.00 (br s, 3H), 1.79-1.60 (m, 12H). **^{13}C NMR** ($CDCl_3$, 100 MHz): δ 160.2, 147.0, 133.2, 110.4, 74.4, 39.5, 39.2, 37.9, 33.5, 28.1, 13.4. **IR (neat)**: 2897, 2845, 1720, 1535, 1450, 1364, 1344, 1249, 1159, 1090, 1048, 1011, 988, 942, 917, 812, 755 cm^{-1}. **Accurate mass (MS)**: m/z calculated for $C_{18}H_{20}O_4$: 300.1356, found 300.1092 (spectral accuracy = 97.8%). **m.p**.: 98.2-98.8 °C.

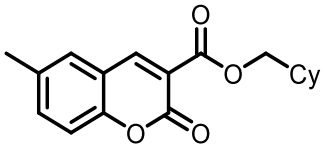

Cyclohexylmethyl 6-methyl-2-oxo-2H-chromene-3-carboxylate (3.149) was prepared according to the general procedure. Purification by column chromatography (gradient of 10% → 20% EtOAc in hexanes) afforded **3.149** as a white solid (52 mg, 87%). **^{1}H NMR** ($CDCl_3$, 400 MHz): δ 8.43 (s, 1H), 7.43 (d, *J* = 8.4 Hz, 1H), 7.39 (s, 1H), 7.23 (d, *J* = 8.6 Hz, 1H), 4.14 (d, *J* = 6.3 Hz, 2H), 2.41 (s, 3H), 2.41 (s, 3H), 1.83-1.67 (m, 5H), 1.32-1.14 (m, 4H), 1.09-1.00 (m, 2H). **^{13}C NMR** ($CDCl_3$, 100 MHz): δ 163.4, 157.0, 153.4, 148.5, 135.5, 134.7, 129.2, 118.4, 117.7, 116.6, 71.0, 37.2, 29.7, 26.4, 25.7, 20.8. **IR (neat)**: 3063, 2919, 2850, 1736, 1625, 1572, 1489, 1450, 1301, 1251, 1222, 1146, 1014, 976, 885, 831, 796, 686 cm^{-1}. **Accurate mass (MS)**: m/z calculated for $C_{17}H_{24}N_2O_2$: 288.1832, found 288.1636 (spectral accuracy = 97.6%). **m.p**.: 115.3-116.9 °C.

Appendix A: NMR Spectra for Chapter 2

Phenyl 2-naphthoate (**2.34**) $CDCl_3$, 400 MHz:

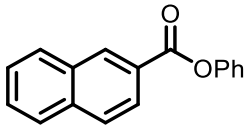

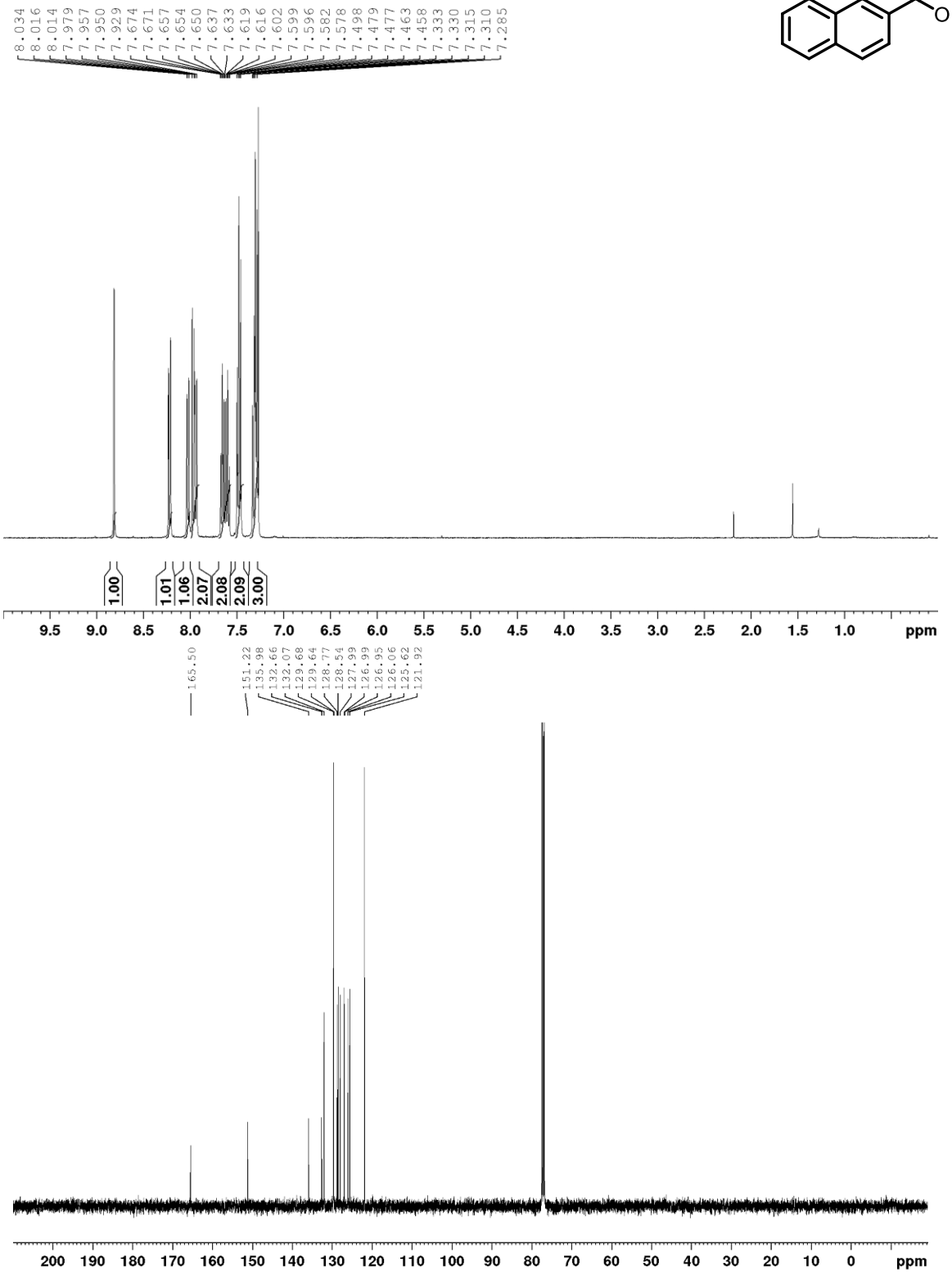

Benzofuran-2-carboxylic acid phenyl ester (**2.51**) $CDCl_3$, 400 MHz:

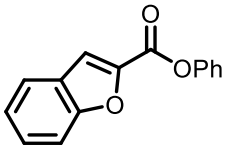

furan-2-carboxylic acid phenyl ester (**2.55**) $CDCl_3$, 400 MHz:

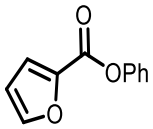

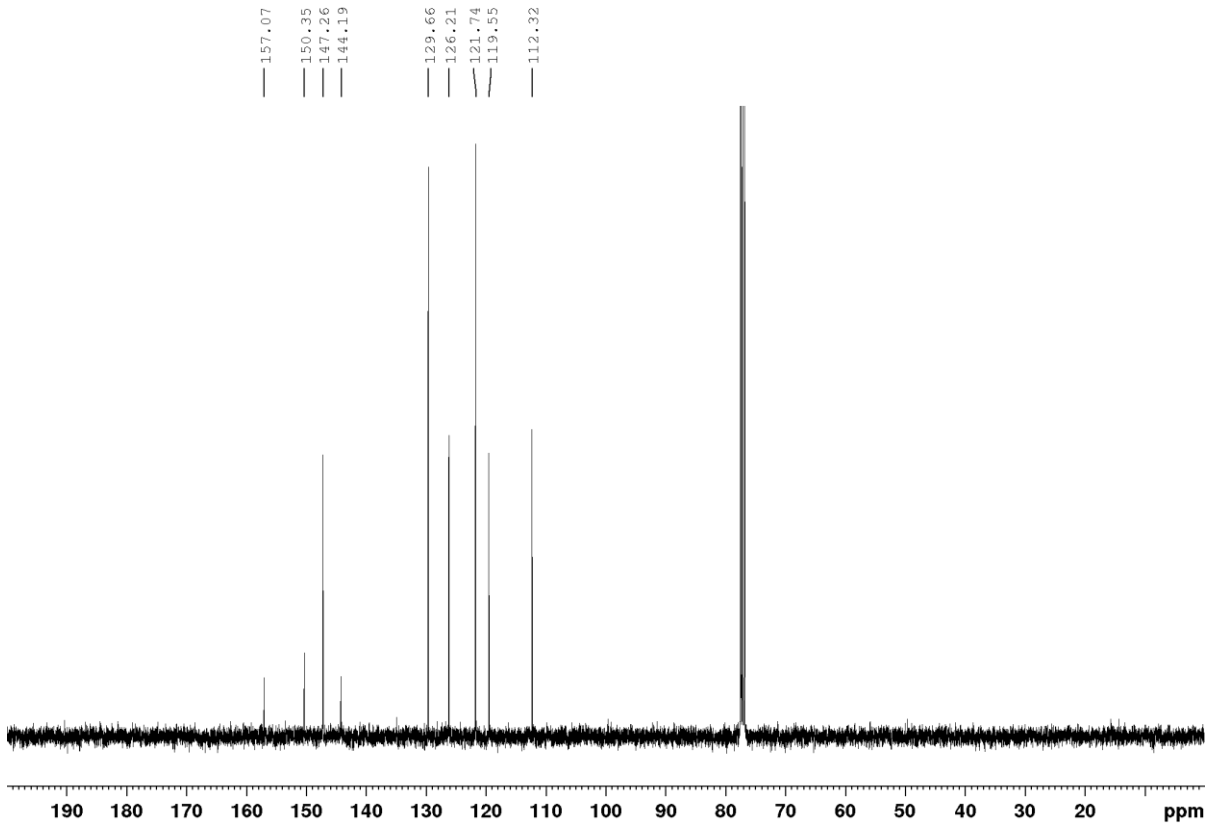

3-quinolinecarboxylic acid phenyl ester (**2.57**) $CDCl_3$, 400 MHz:

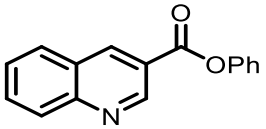

phenyl 2-methoxybenzoate (**2.77**) $CDCl_3$, 400 MHz:

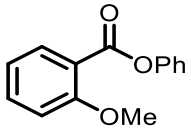

(S)-phenyl 4-(2-((1-(2-cyclohexylphenyl)-3-methylbutyl)amino)-2-oxoethyl)-2-ethoxybenzoate (**2.100**) $CDCl_3$, 400 MHz:

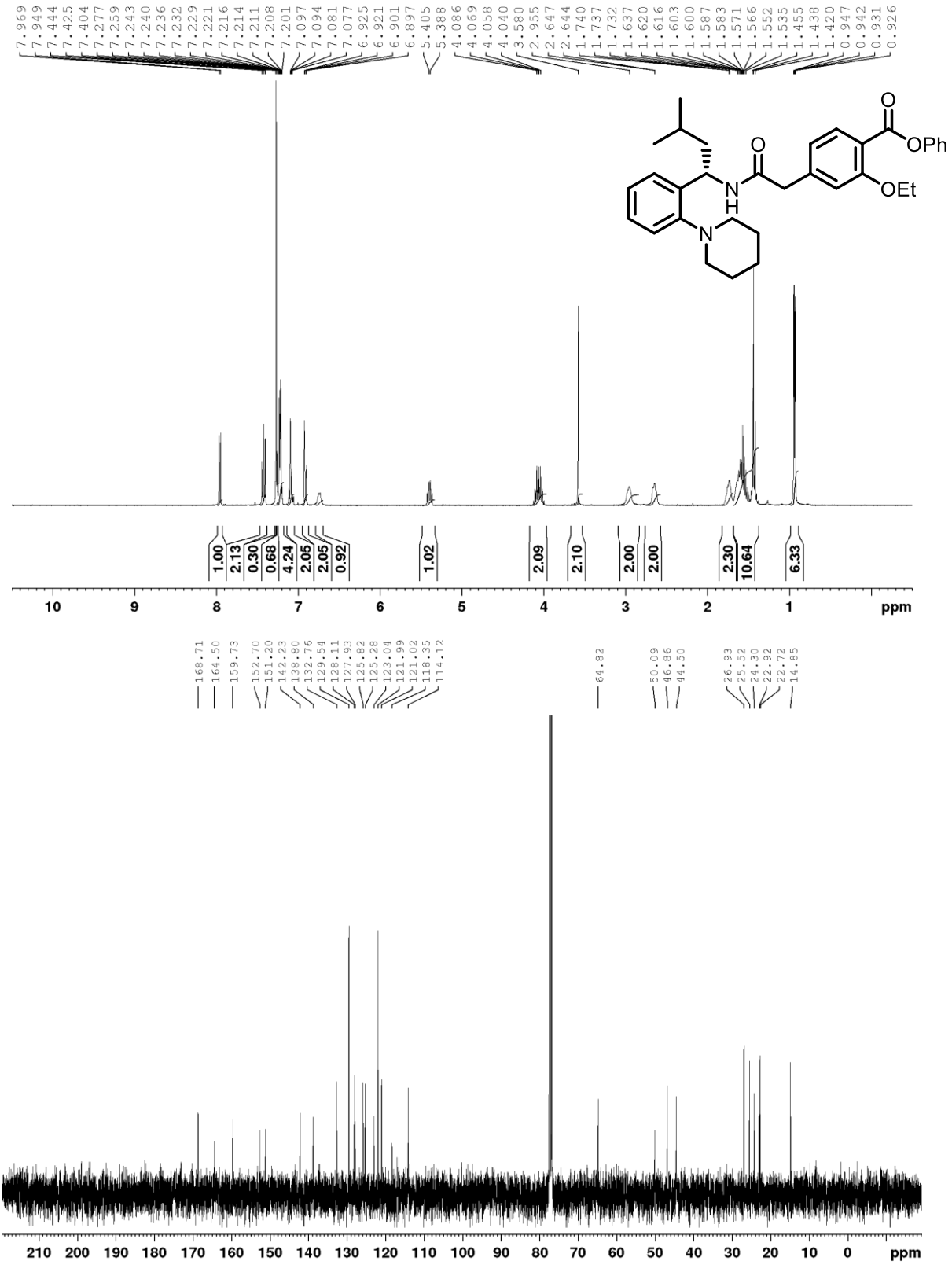

Phenyl 4-(N,N-dipropylsulfamoyl)benzoate (**2.103**) $CDCl_3$, 400 MHz:

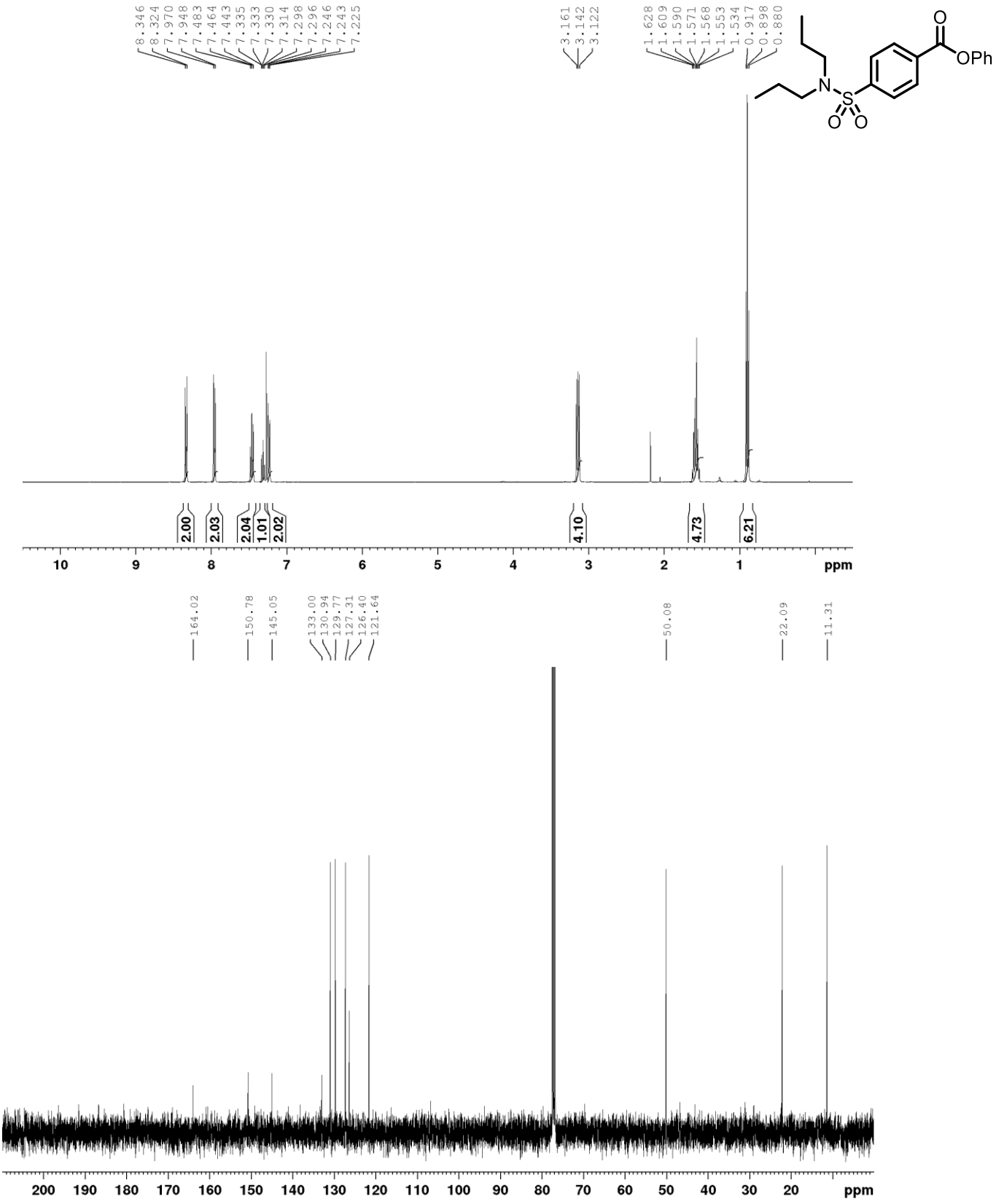

1-naphthalen-2-yl-4-phenylbutan-1-one (**2.36**) $CDCl_3$, 400 MHz:

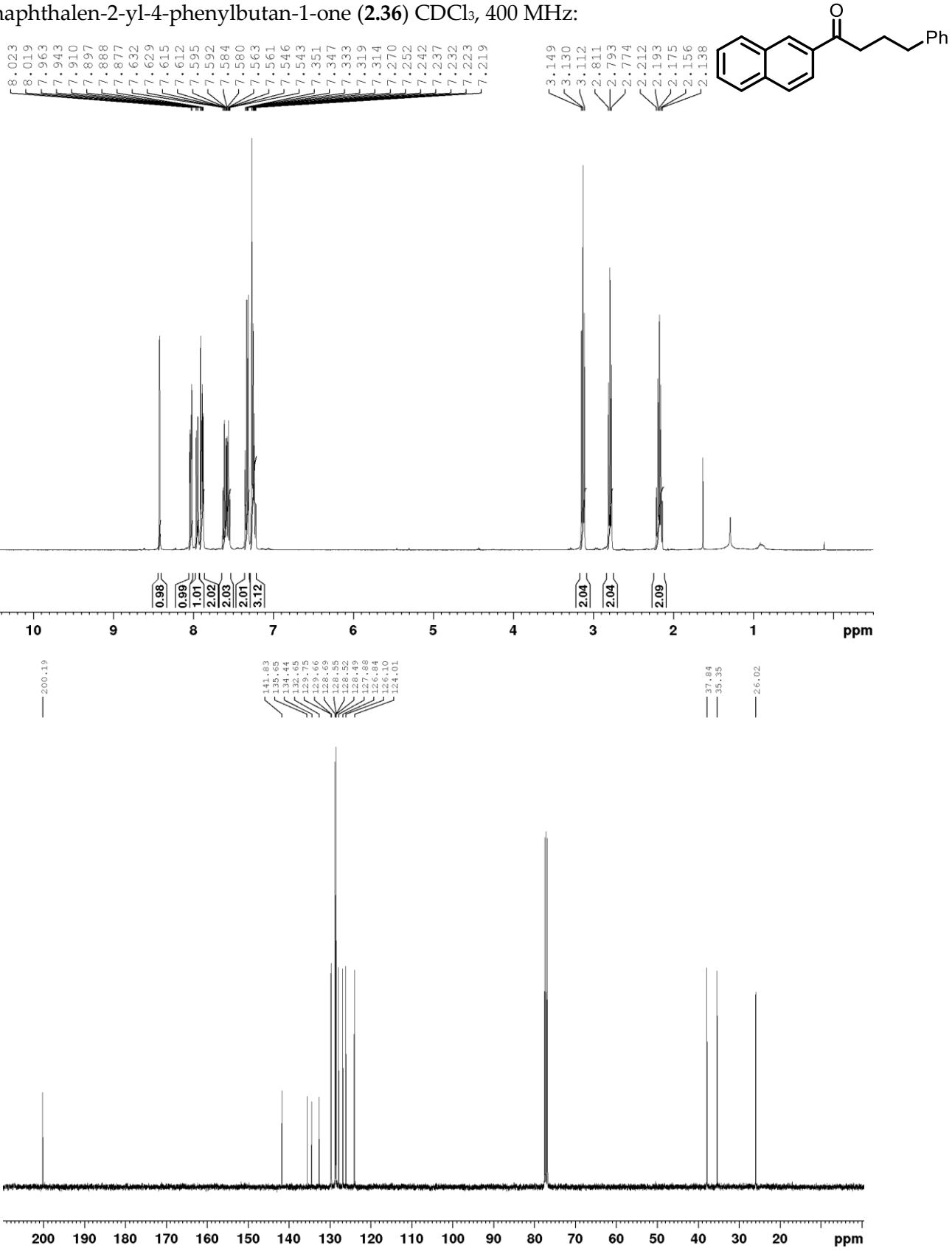

1,4-diphenylbutan-1-one (**2.46**) $CDCl_3$, 400 MHz:

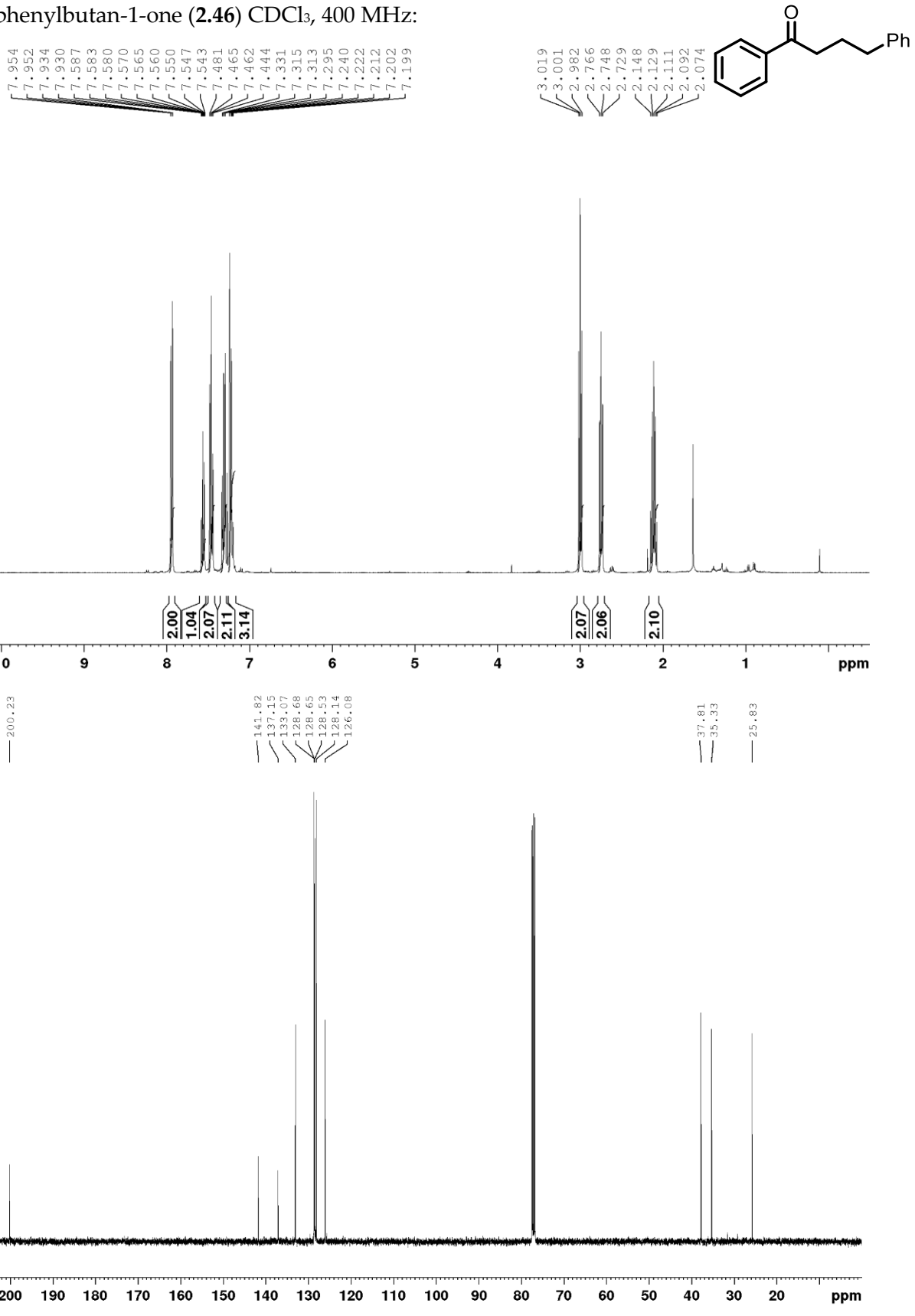

4-phenyl-1-[3-(trifluoromethyl)phenyl]butan-1-one (**2.48**) $CDCl_3$, 400 MHz:

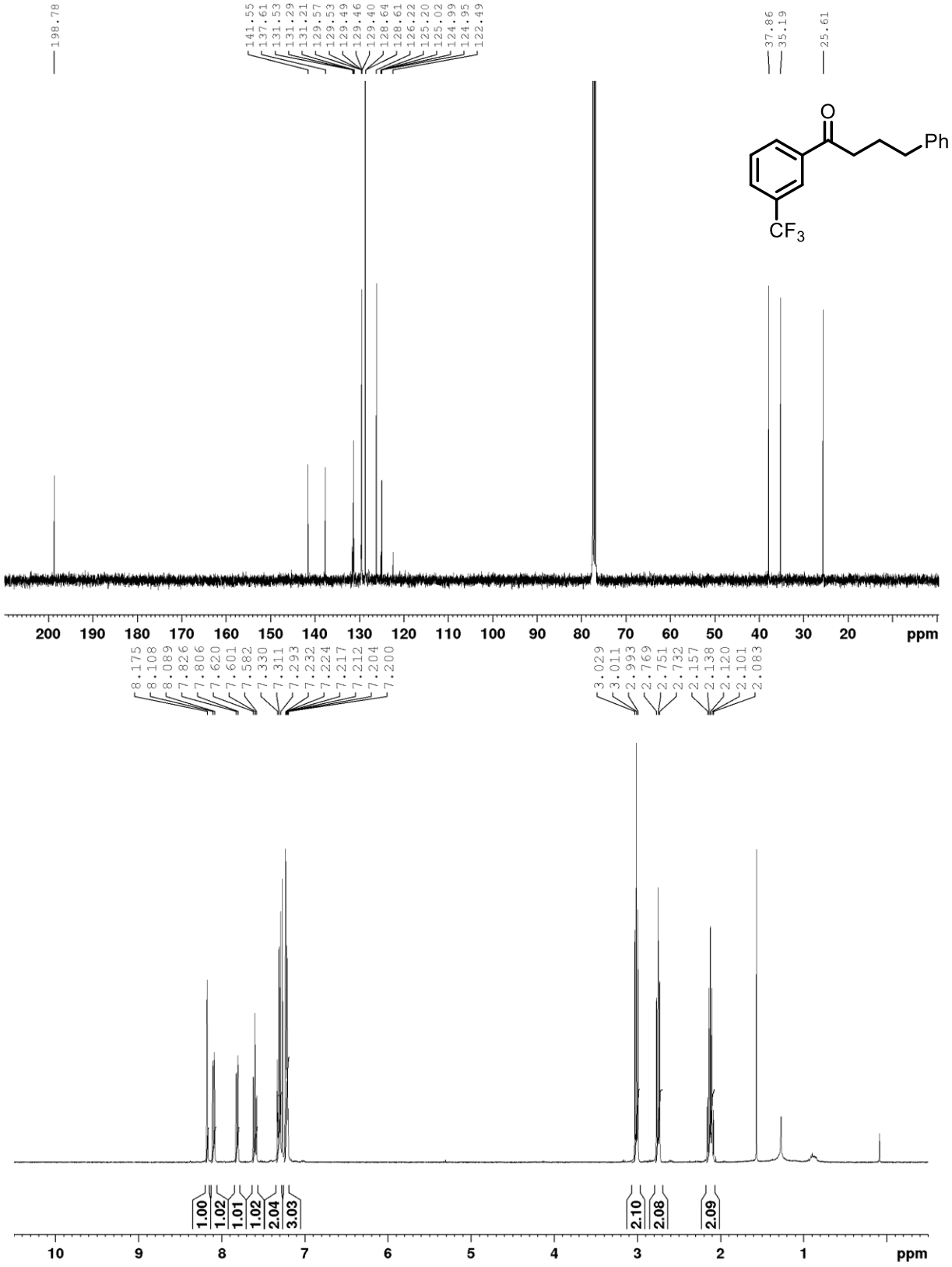

methyl 4-(4-phenylbutanoyl)benzoate (**2.50**) $CDCl_3$, 400 MHz:

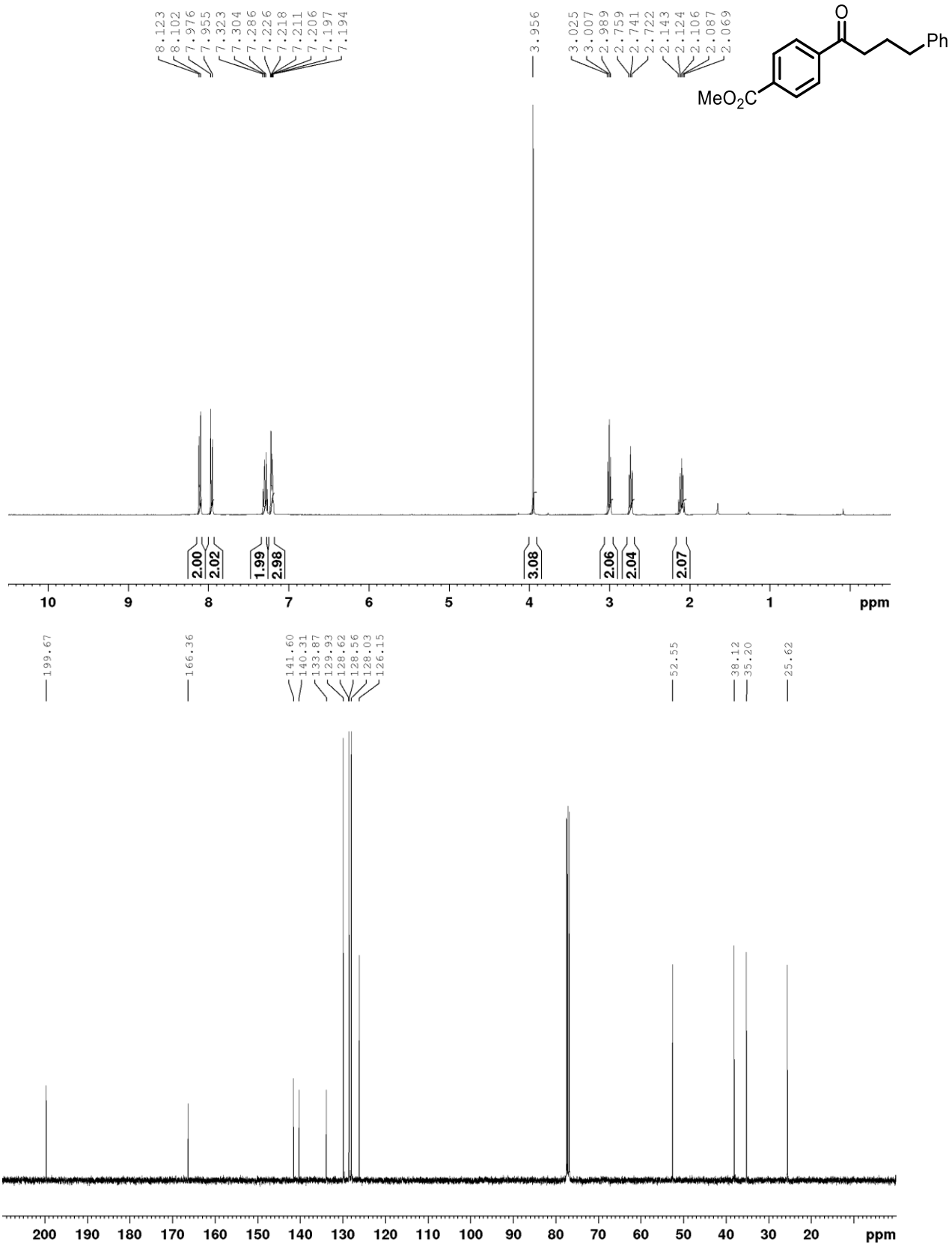

1-(1-benzofuran-2-yl)-4-phenylbutan-1-one (**2.52**) $CDCl_3$, 400 MHz:

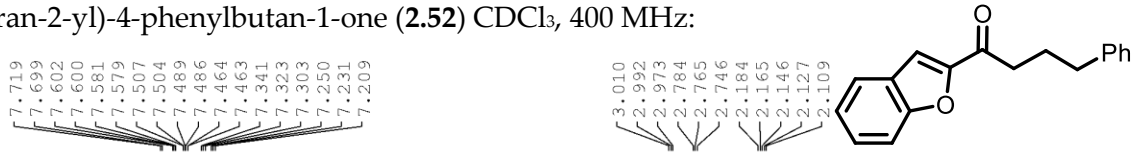

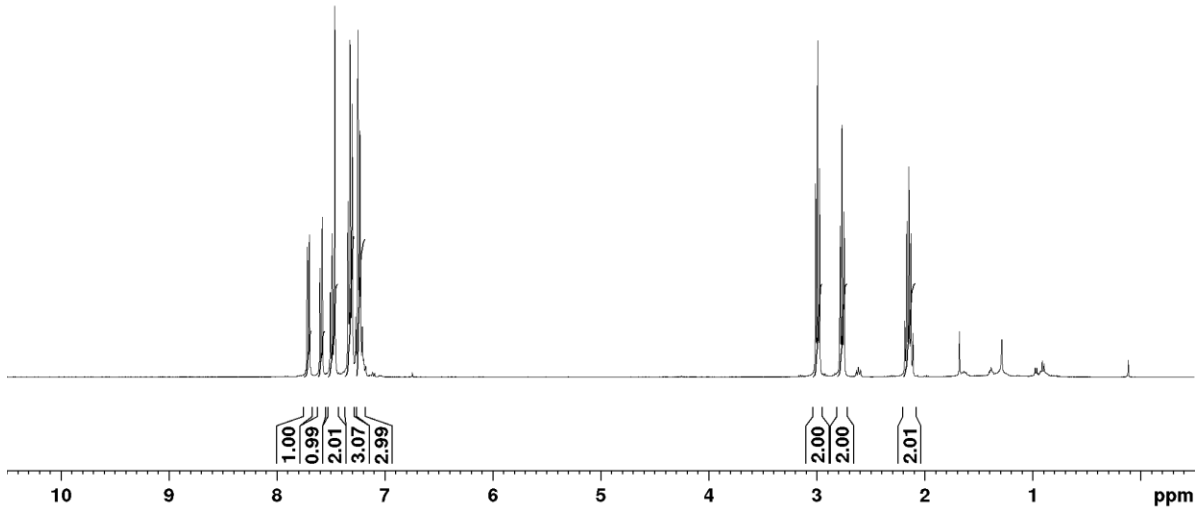

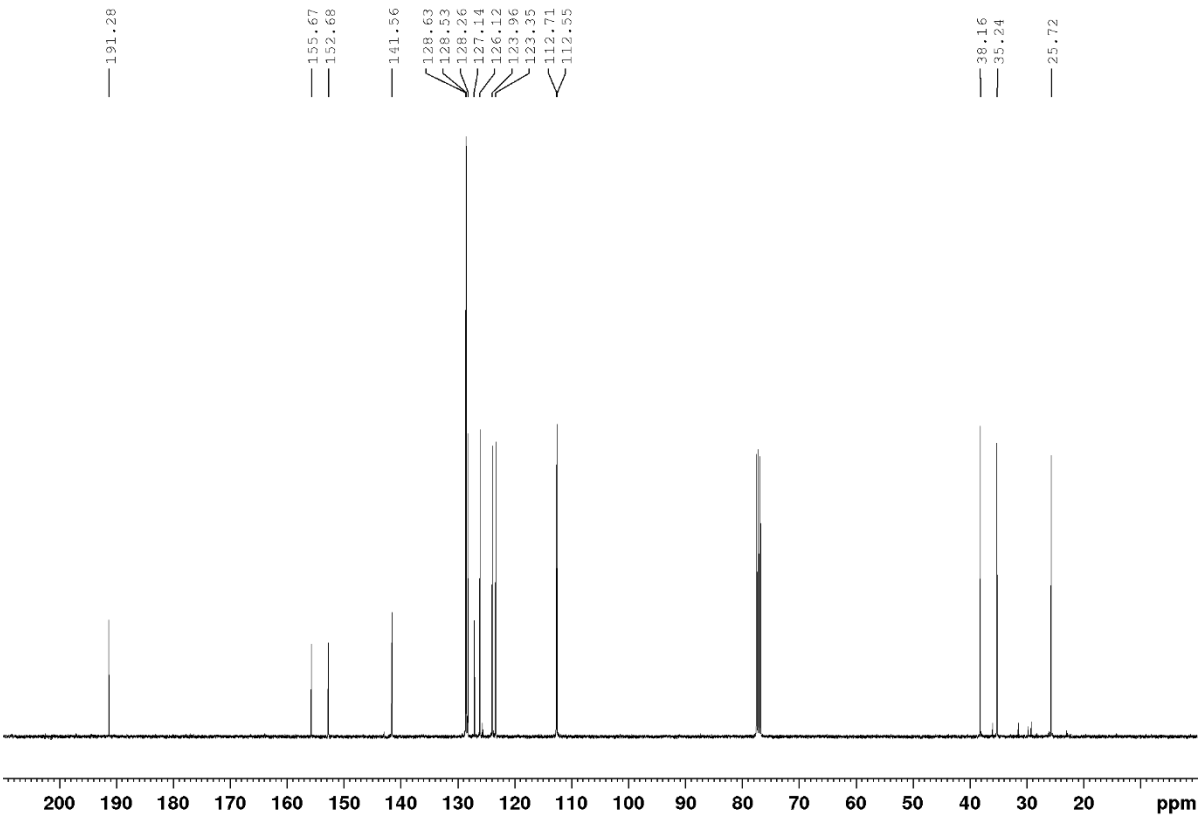

1-(furan-3-yl)-4-phenylbutan-1-one (**2.54**) $CDCl_3$, 400 MHz:

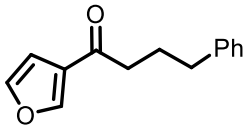

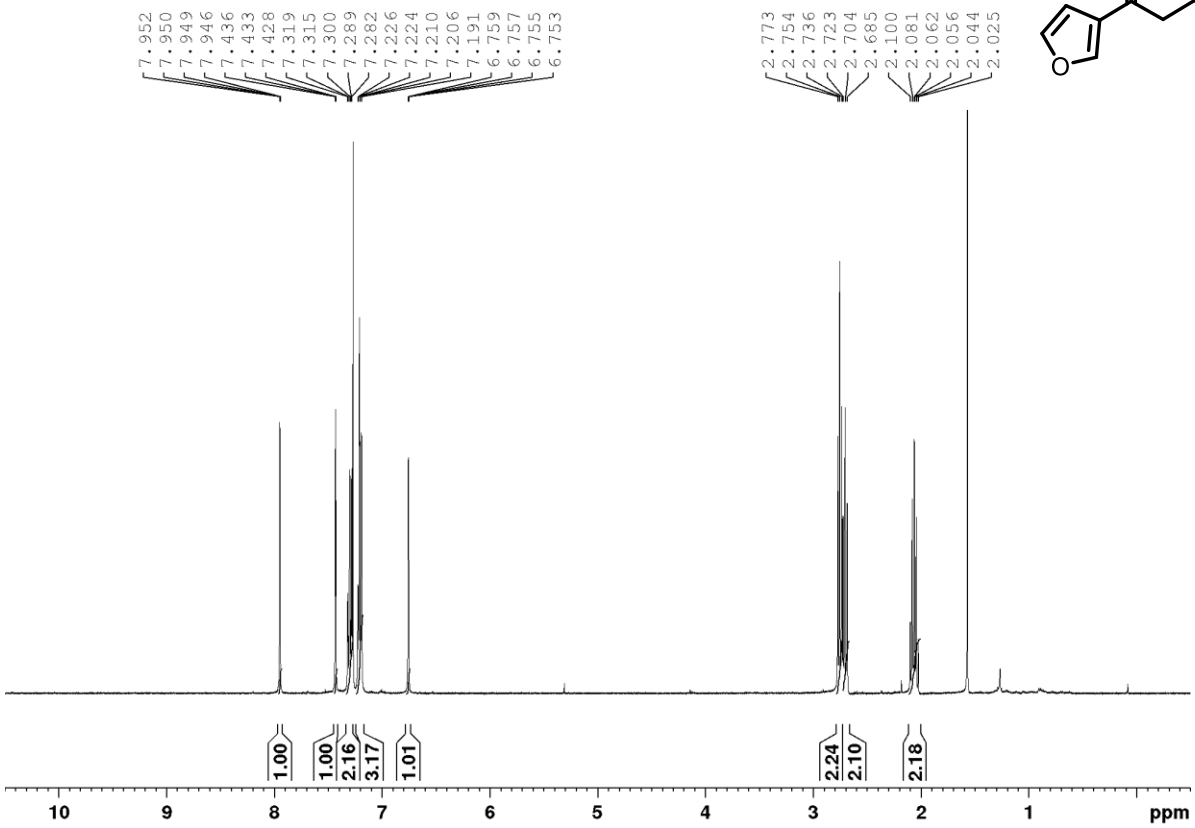

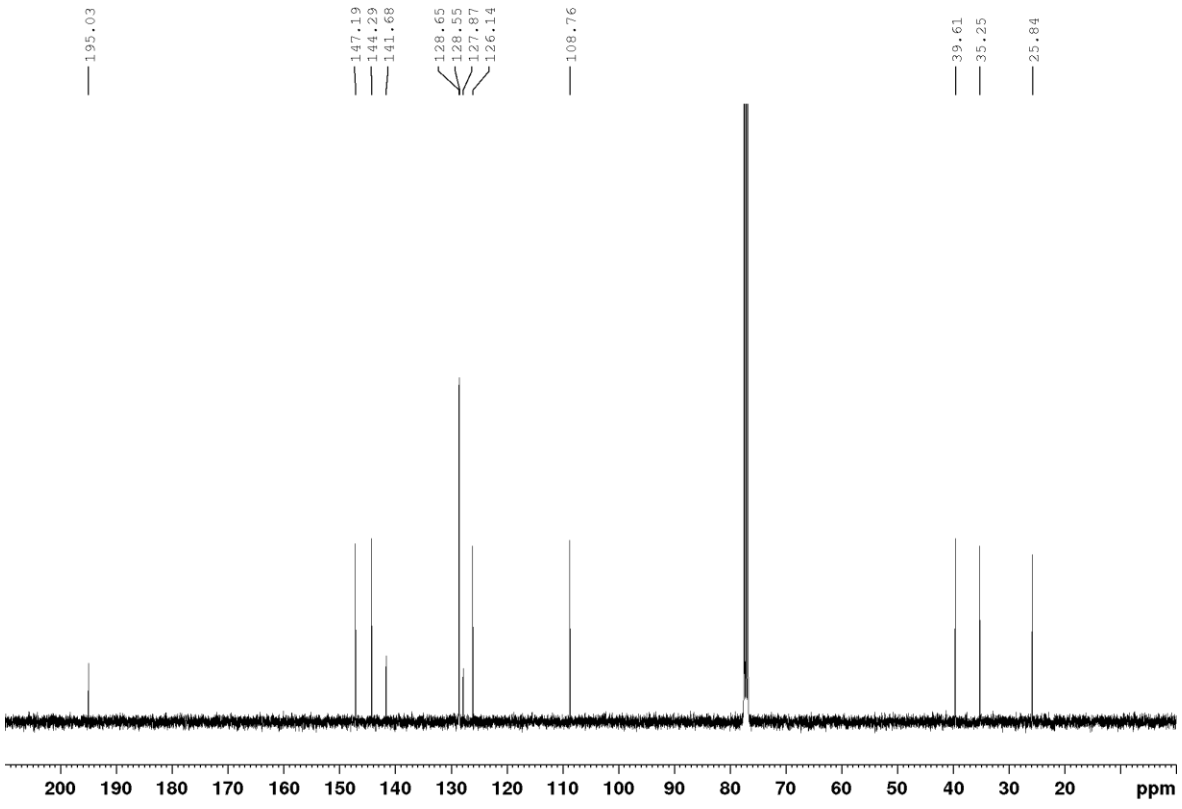

1-(furan-2-yl)-3-phenylpropan-1-one (**2.56**) $CDCl_3$, 400 MHz:

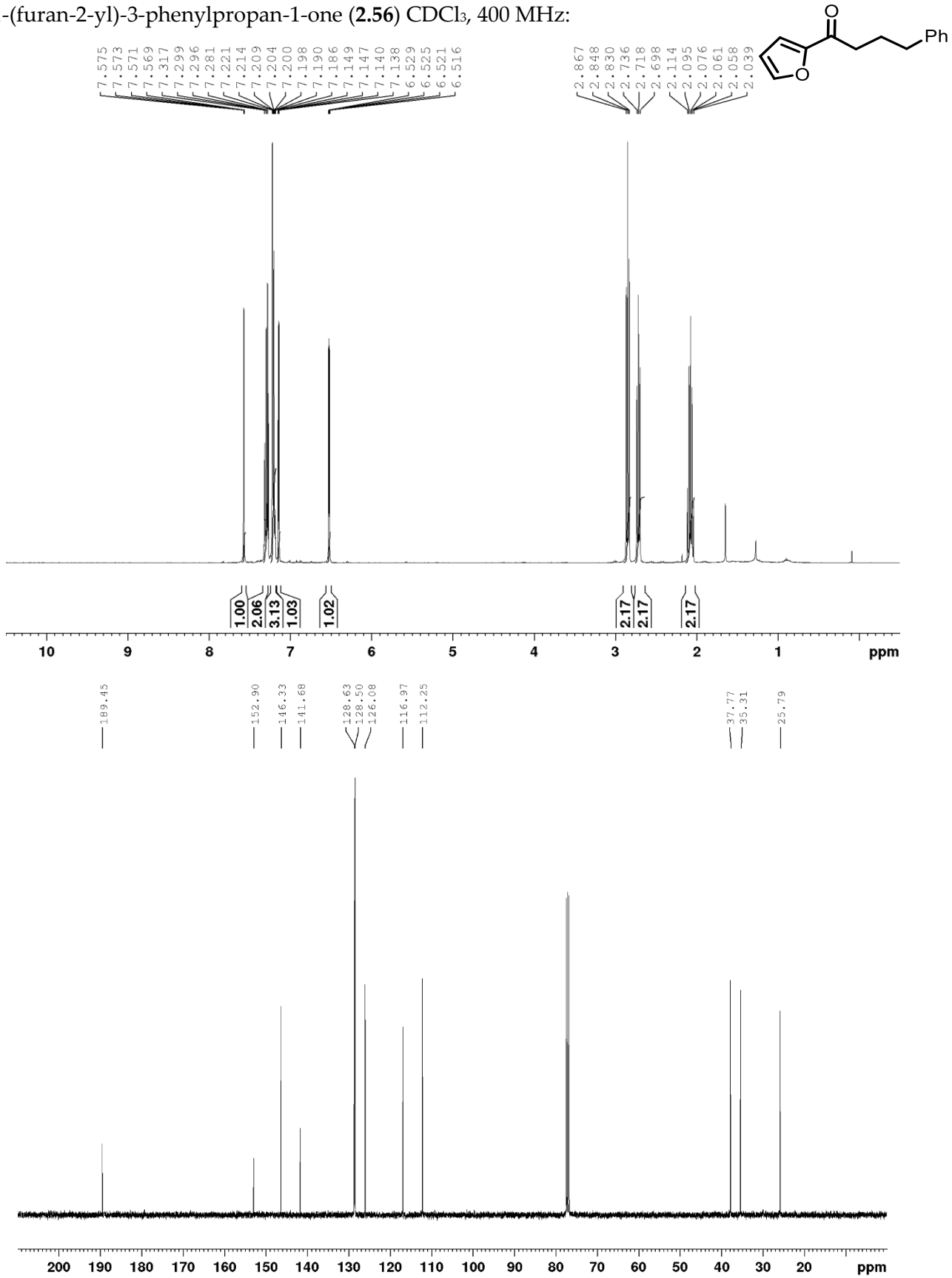

4-phenyl-1-quinolin-3-ylbutan-1-one (**2.58**) $CDCl_3$, 400 MHz:

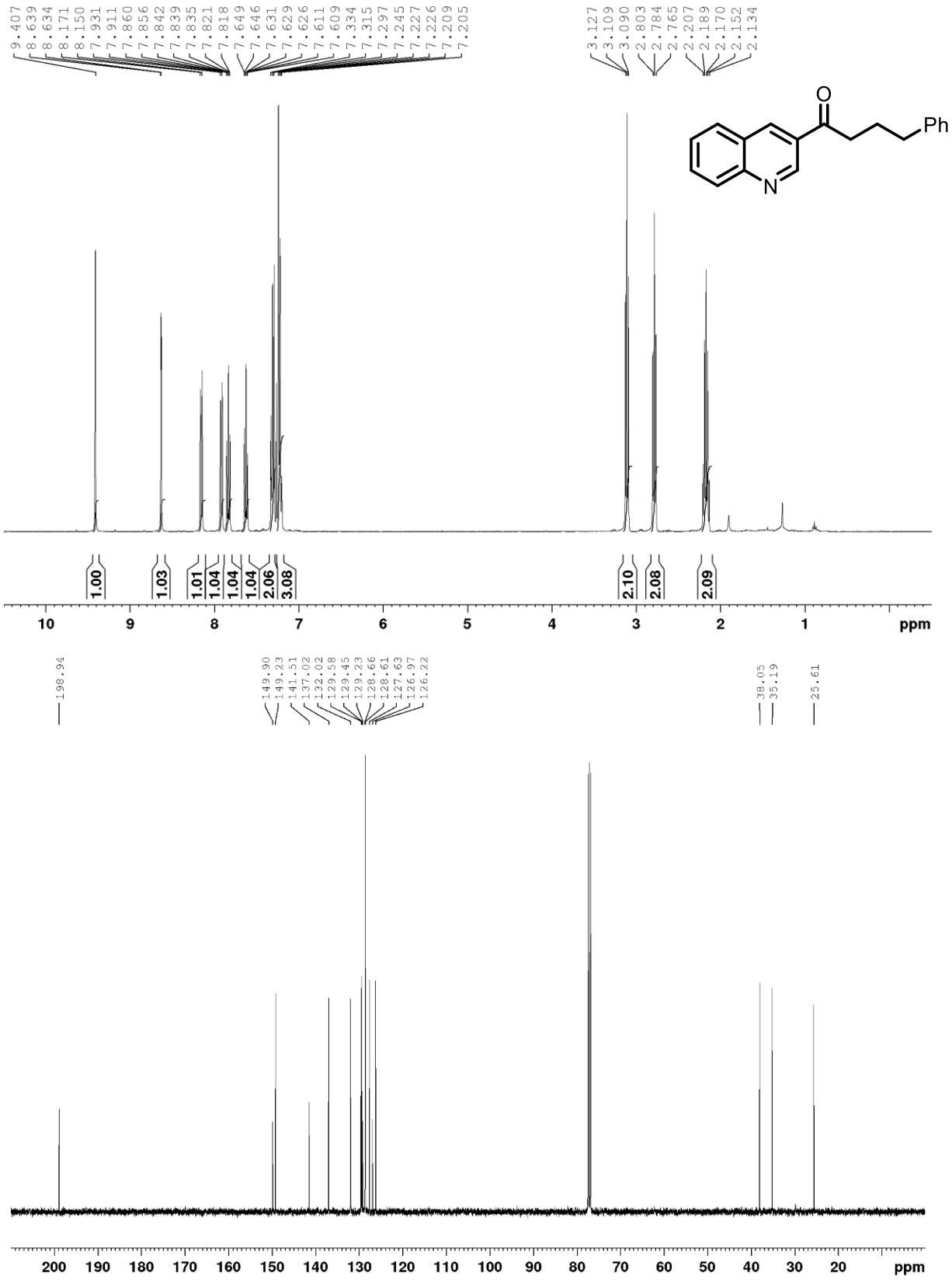

1-(naphthalen-2-yl)-4-(perfluorophenyl)butan-1-one (**2.62**) $CDCl_3$, 400 MHz:

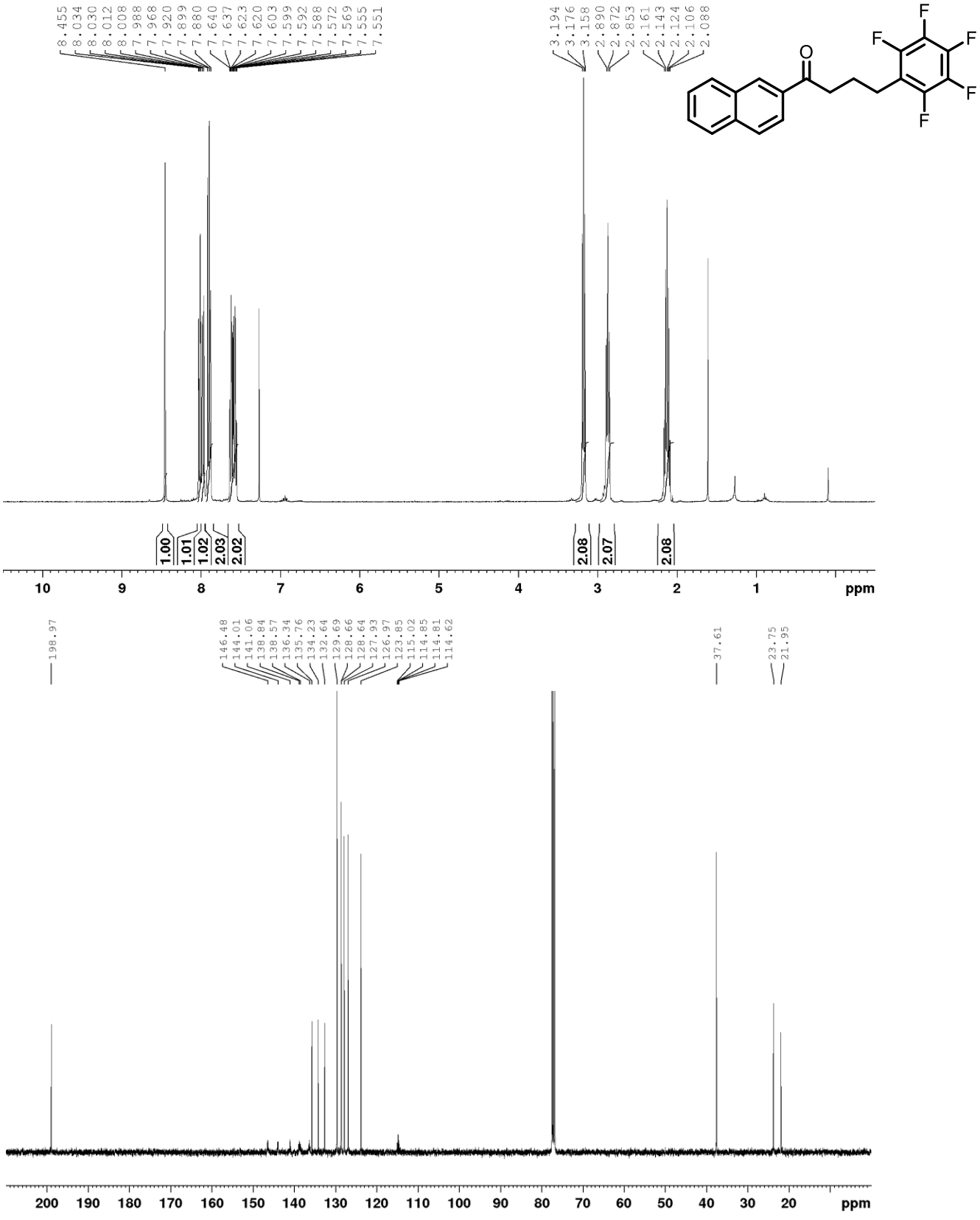

3-(4-methoxyphenyl)-1-(naphthalen-2-yl)propan-1-one (**2.64**) $CDCl_3$, 400 MHz:

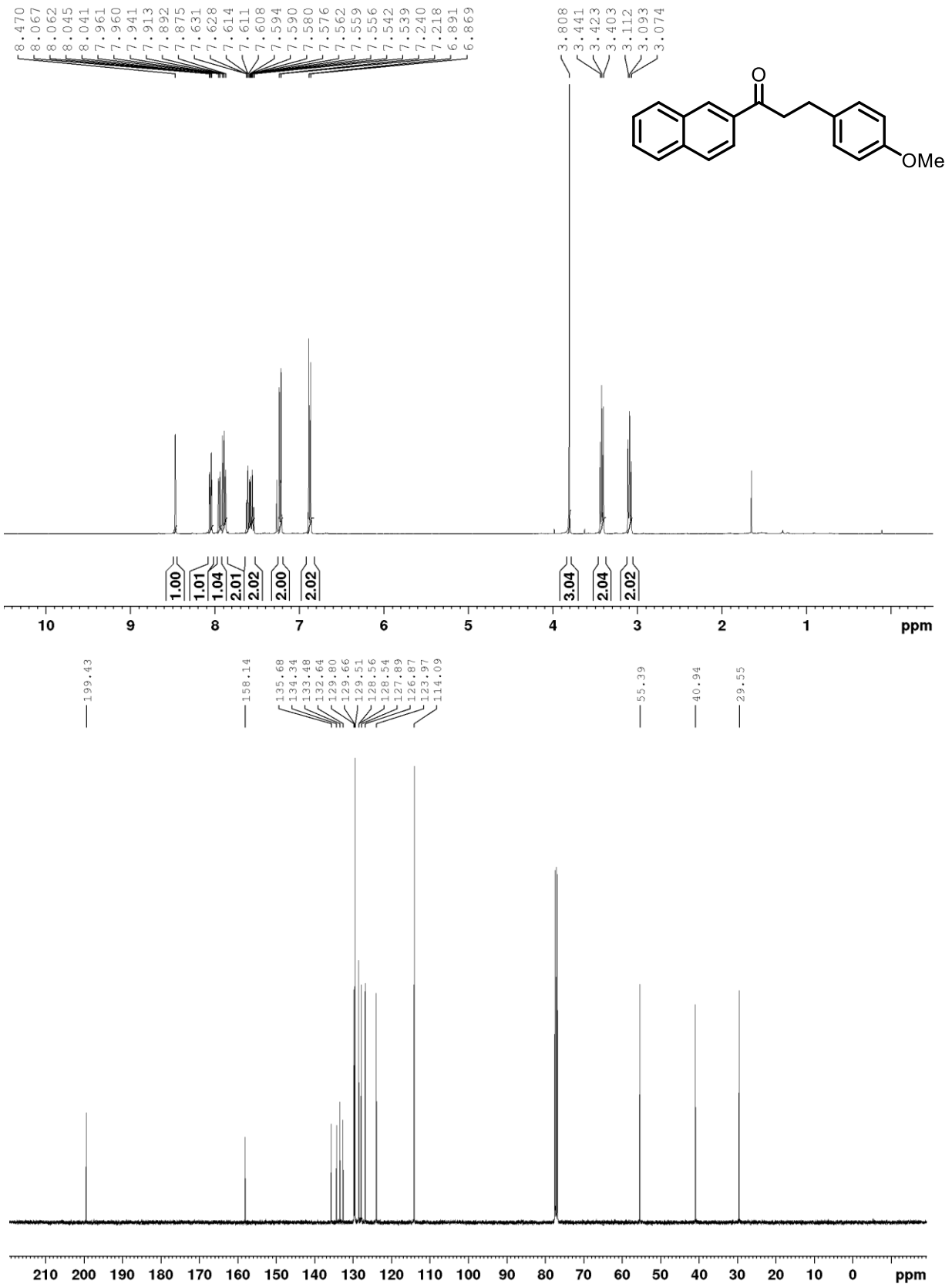

γ-(trimethylsilyl)butyro-2-naphthone (**2.66**) $CDCl_3$, 400 MHz:

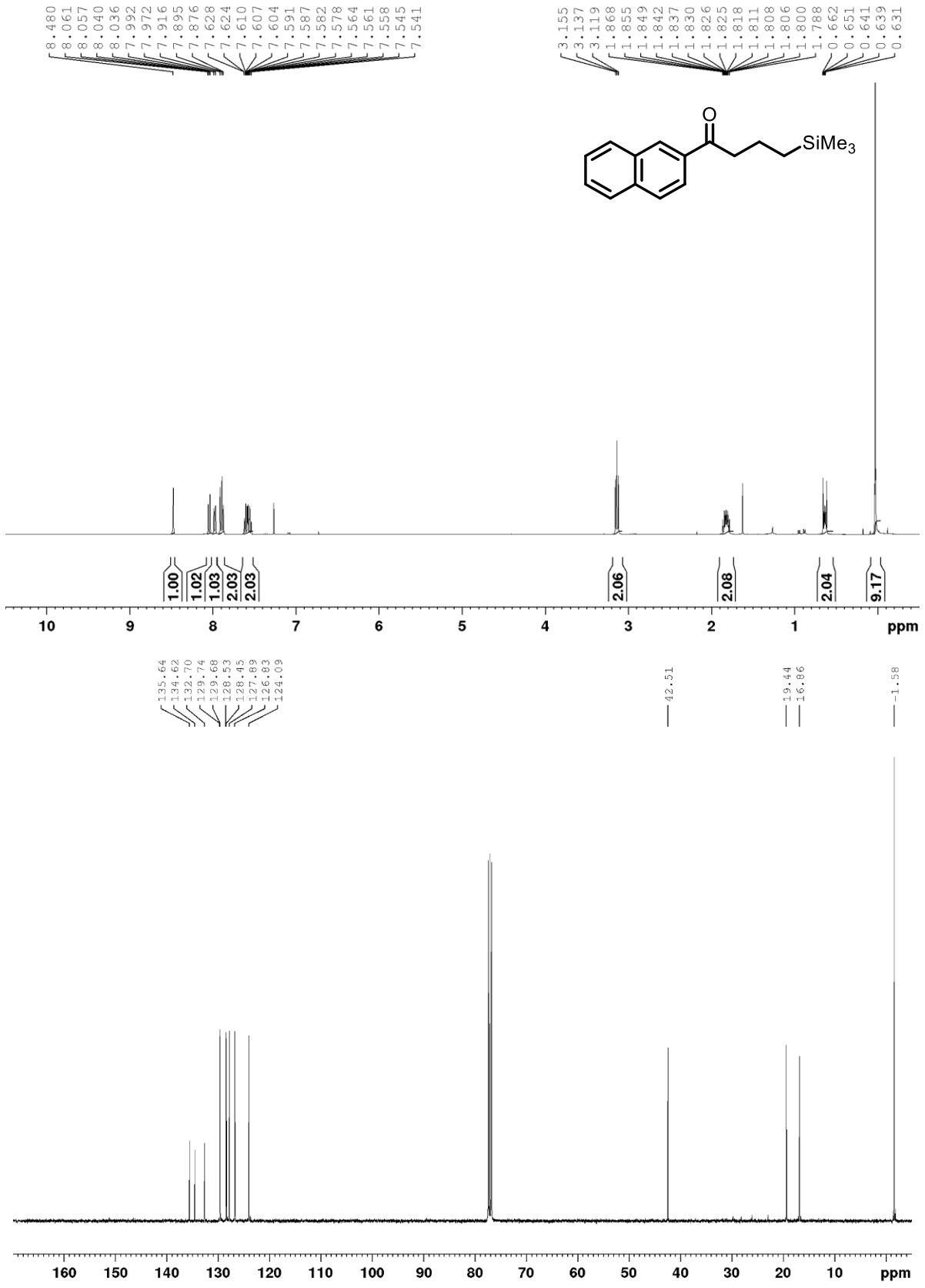

3-cyclohexyl-1-naphthalen-2-ylpropan-1-one (**2.68**) $CDCl_3$, 400 MHz:

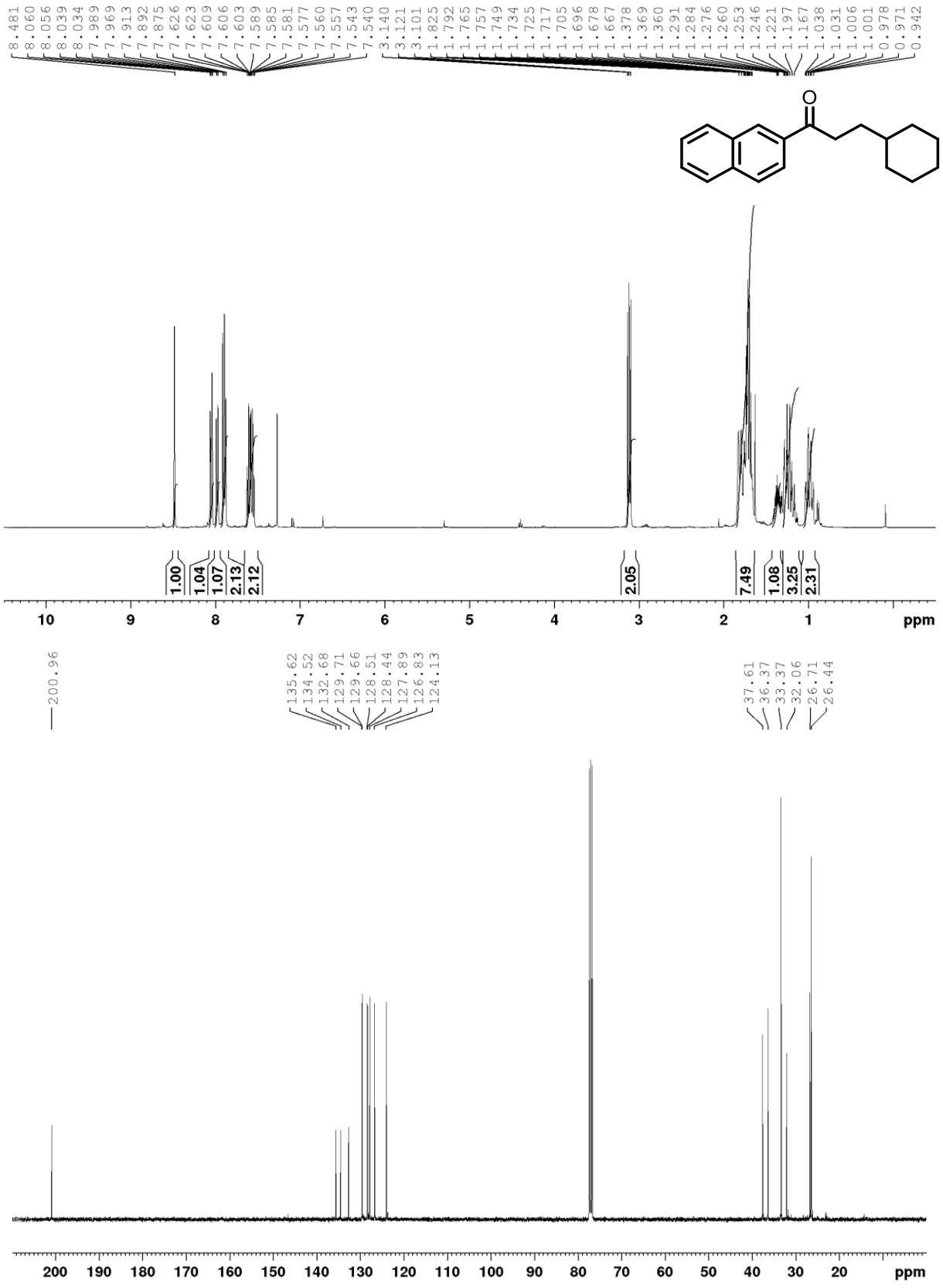

(S)-2-(3-ethoxy-4-(4-phenylbutanoyl)phenyl)-N-(3-methyl-1-(2-(piperidin-1-yl)phenyl)butyl)acetamide (**2.101**) $CDCl_3$, 400 MHz:

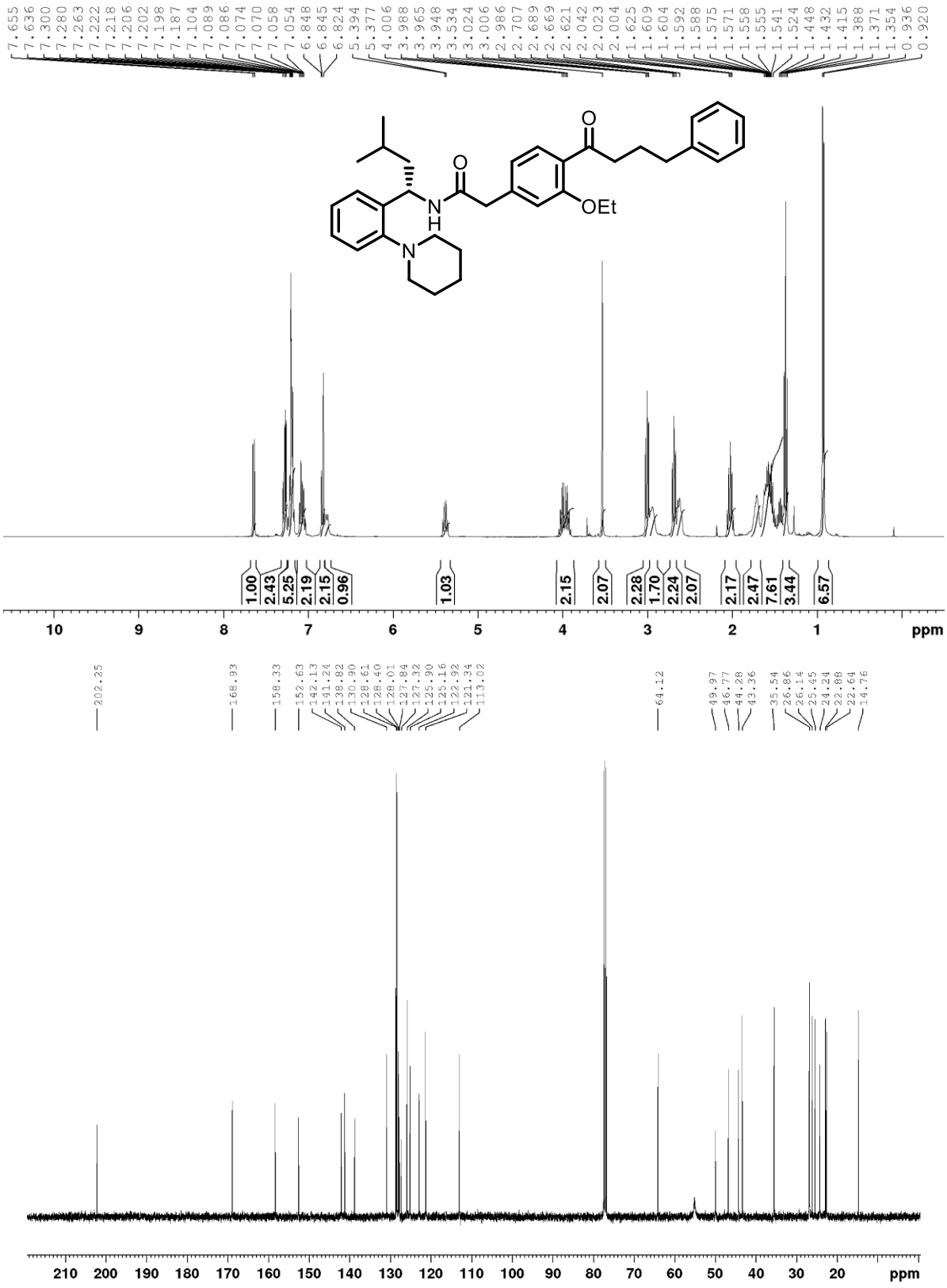

4-(4-phenylbutanoyl)-N,N-dipropylbenzenesulfonamide (**2.104**) $CDCl_3$, 400 MHz:

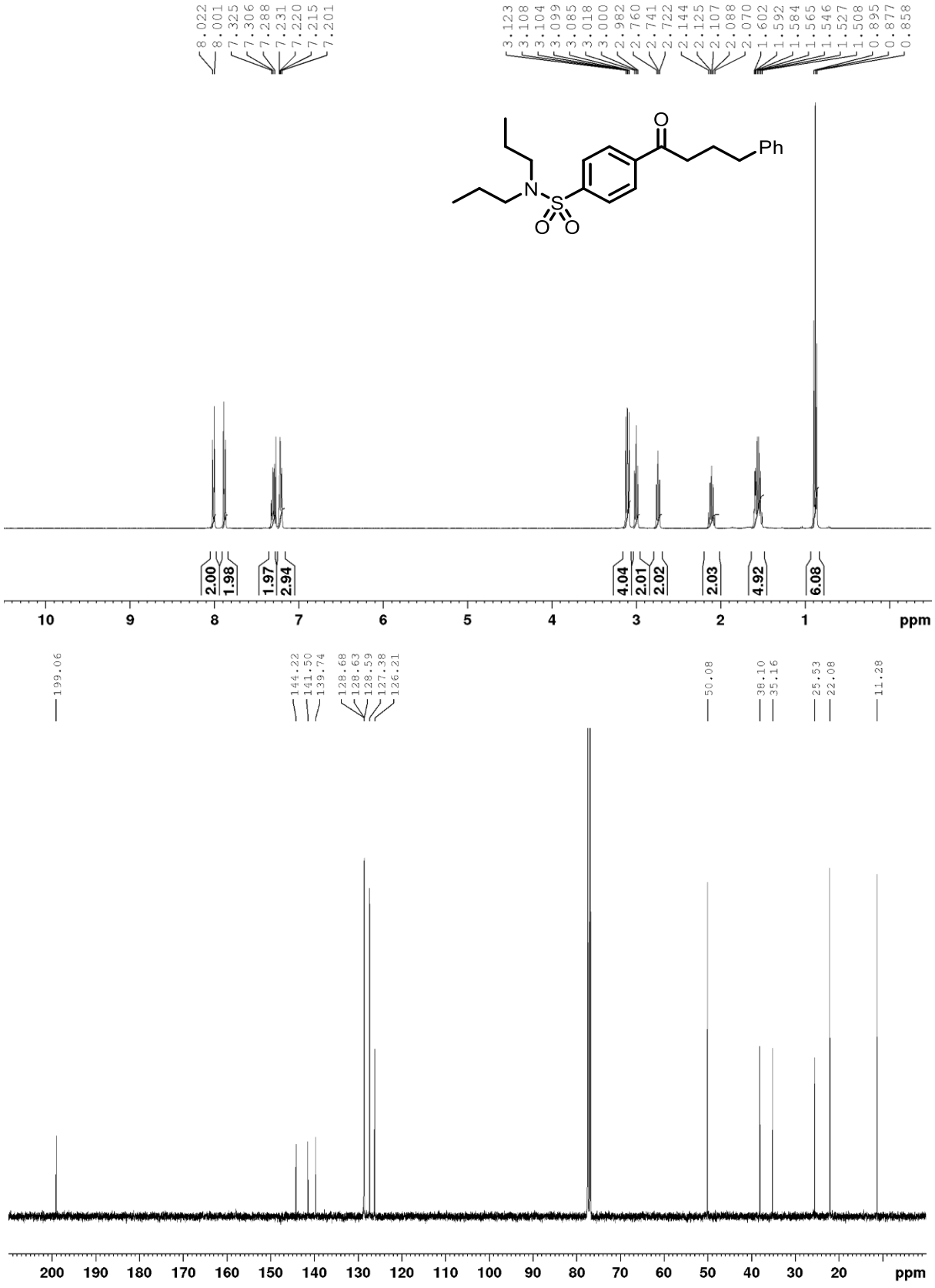

1-phenyl-3-(2-naphthyl)propane (**2.70**) $CDCl_3$, 400 MHz:

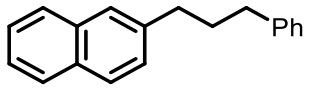

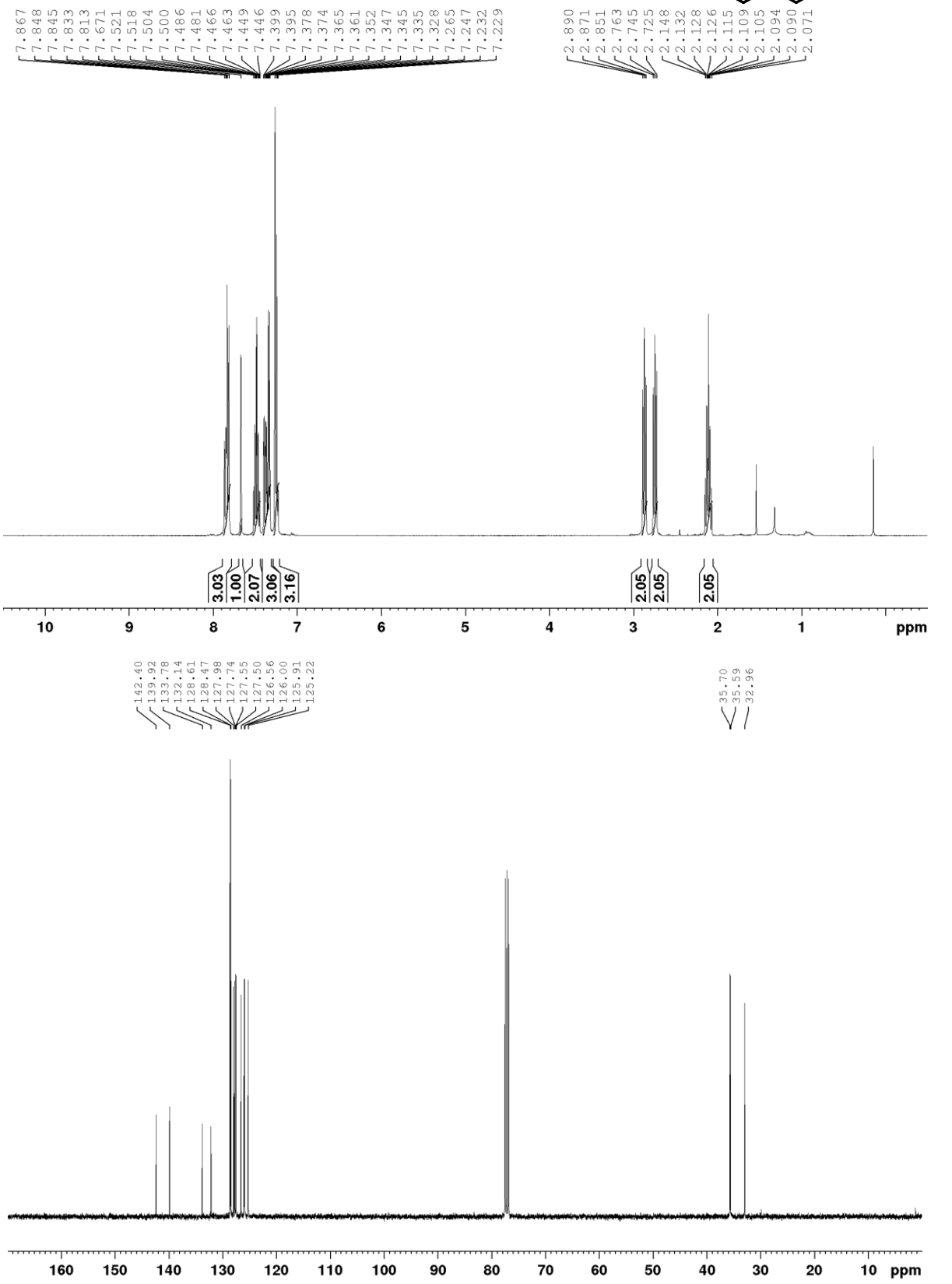

1,3-diphenylpropane (**2.73**) $CDCl_3$, 400 MHz:

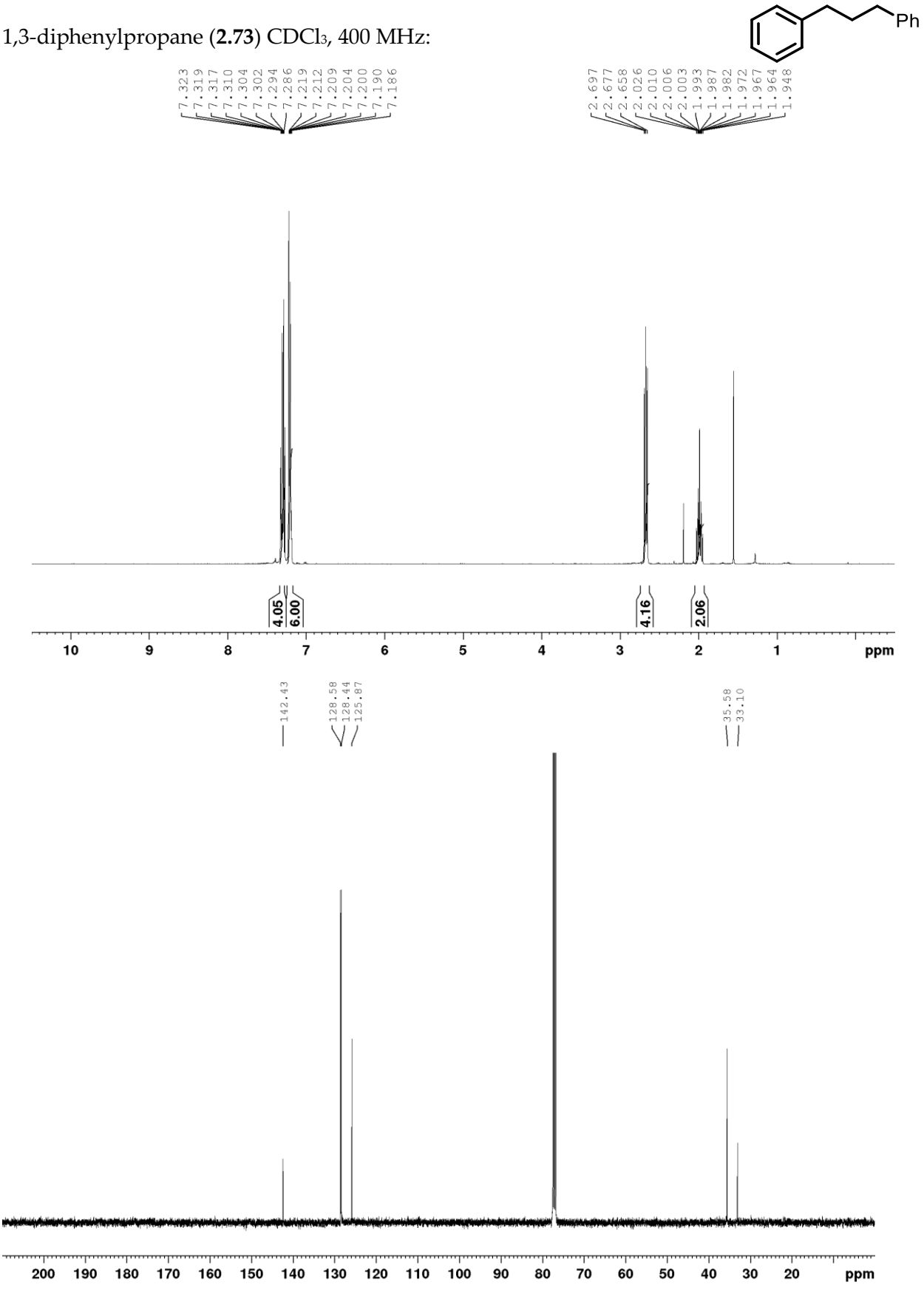

methyl 4-(3-phenylpropyl)benzoate (**2.74**) $CDCl_3$, 400 MHz:

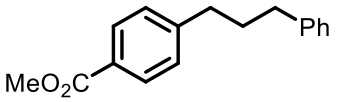

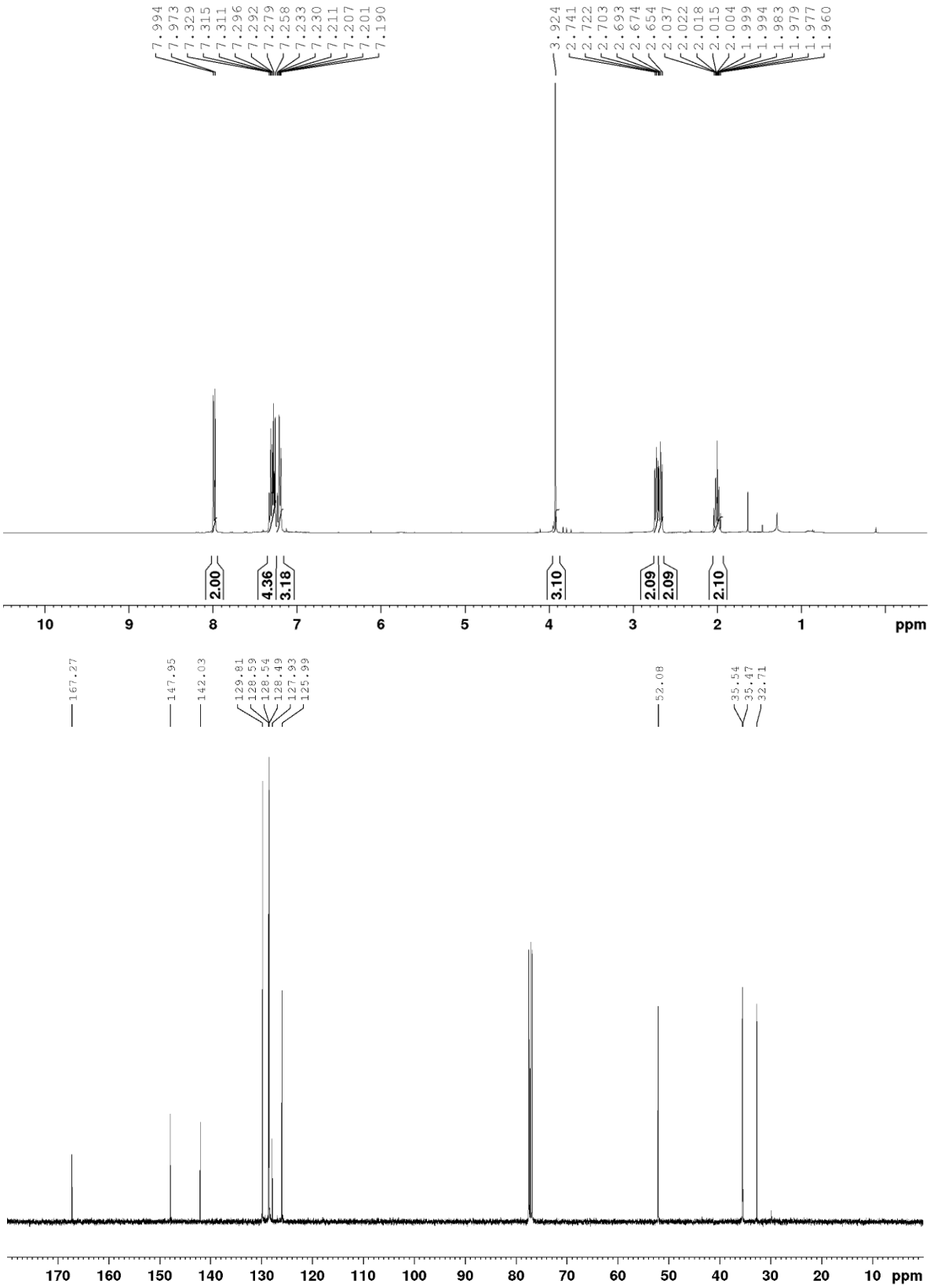

1-methoxy-4-(3-phenylpropyl)benzene (**2.76**) $CDCl_3$, 400 MHz:

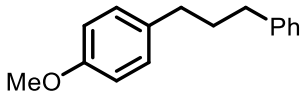

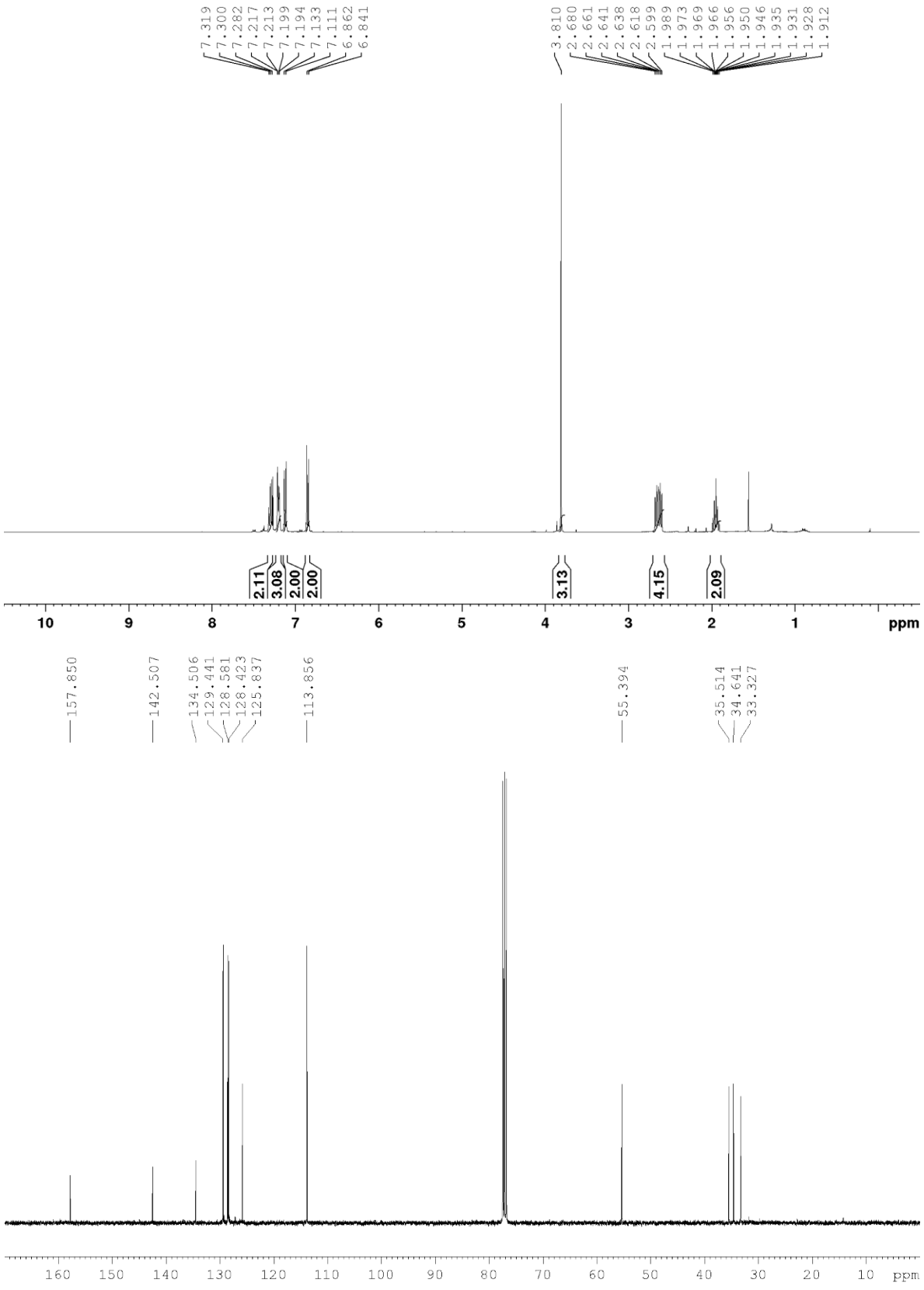

1-methoxy-2-(3-phenylprop-1-yl)benzene (**2.78**) $CDCl_3$, 400 MHz:

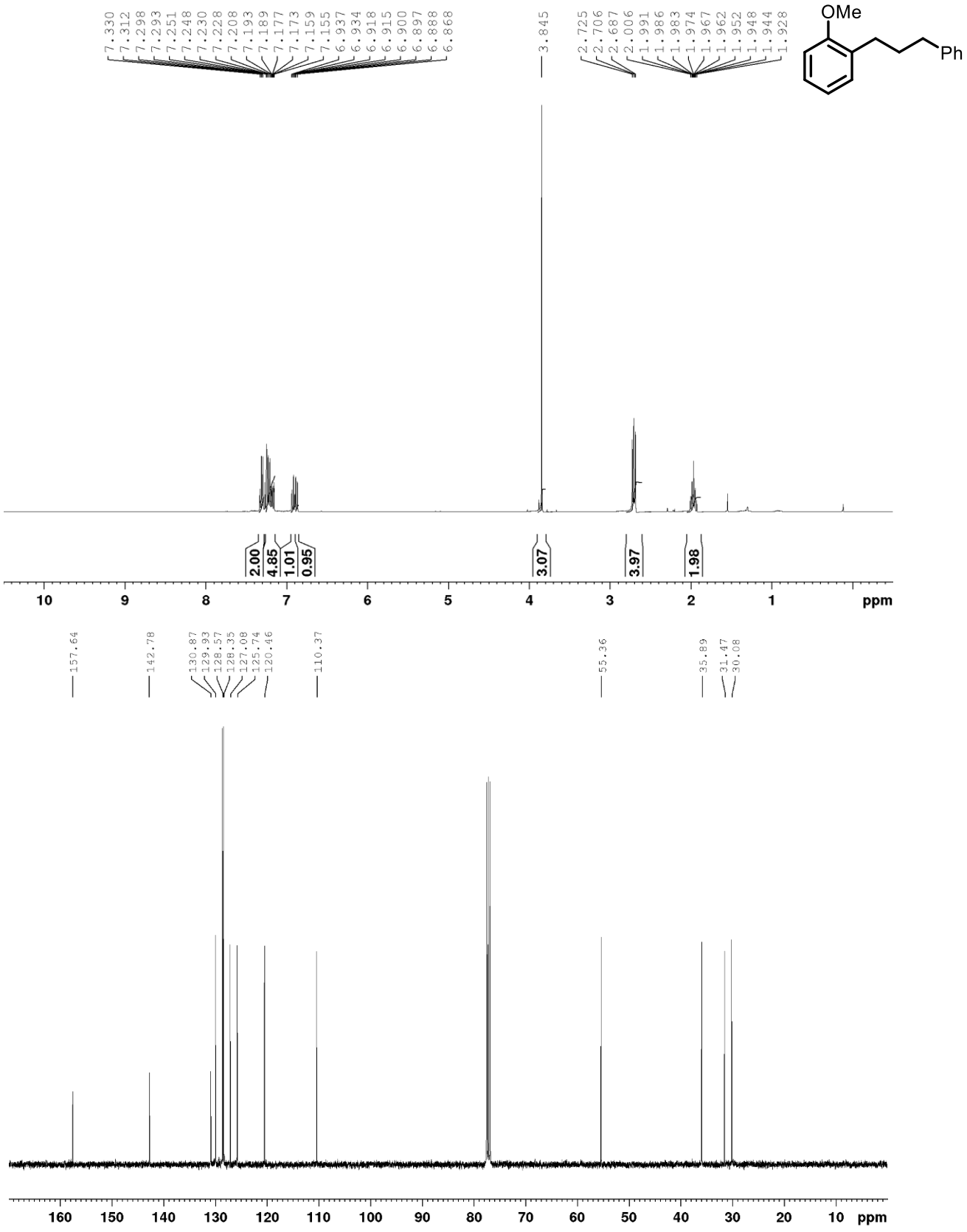

4-(3-phenylpropyl)-pyridine (**2.79**) $CDCl_3$, 400 MHz:

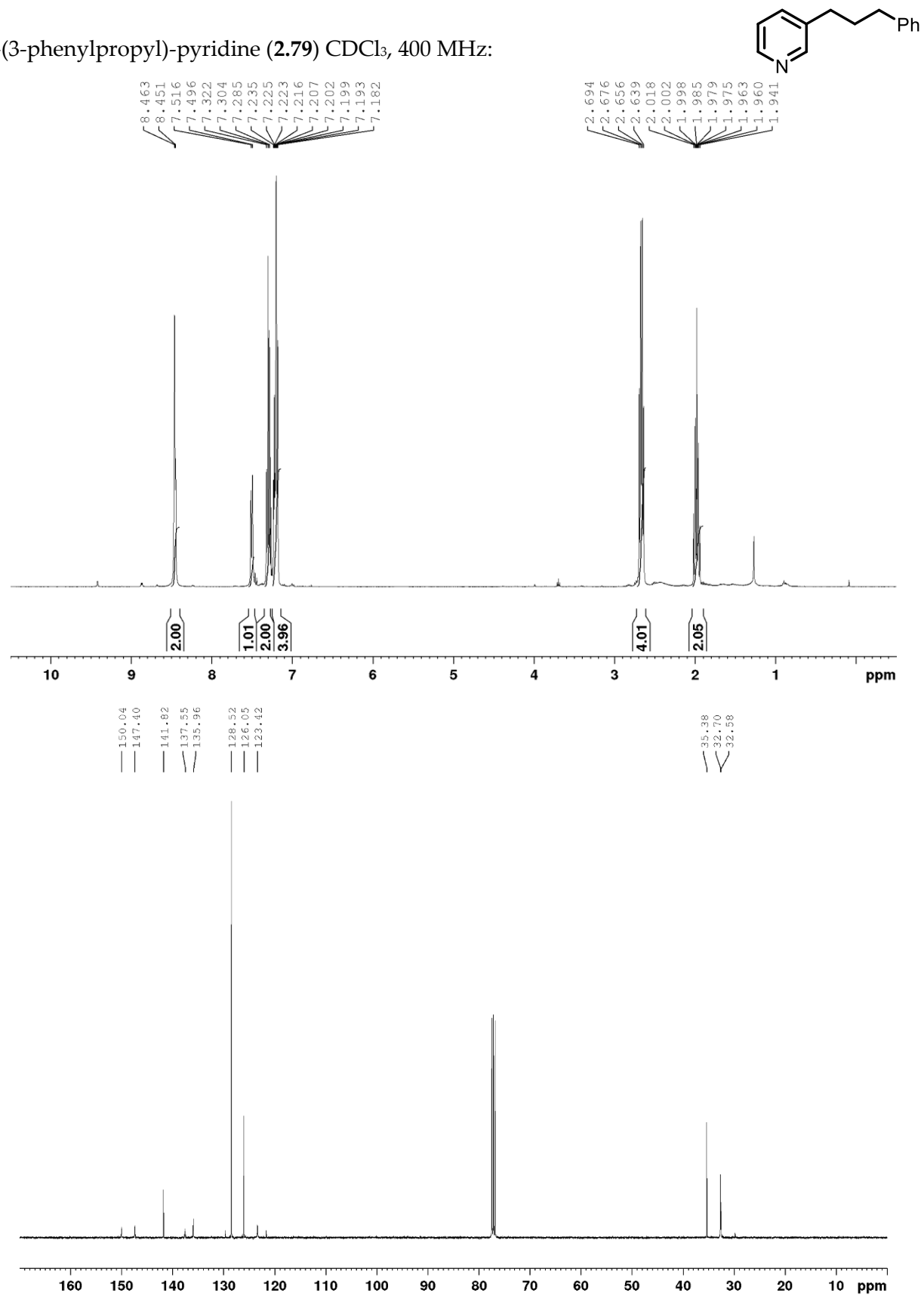

4-(3-phenylpropyl)pyridine (**2.81**) $CDCl_3$, 400 MHz:

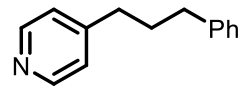

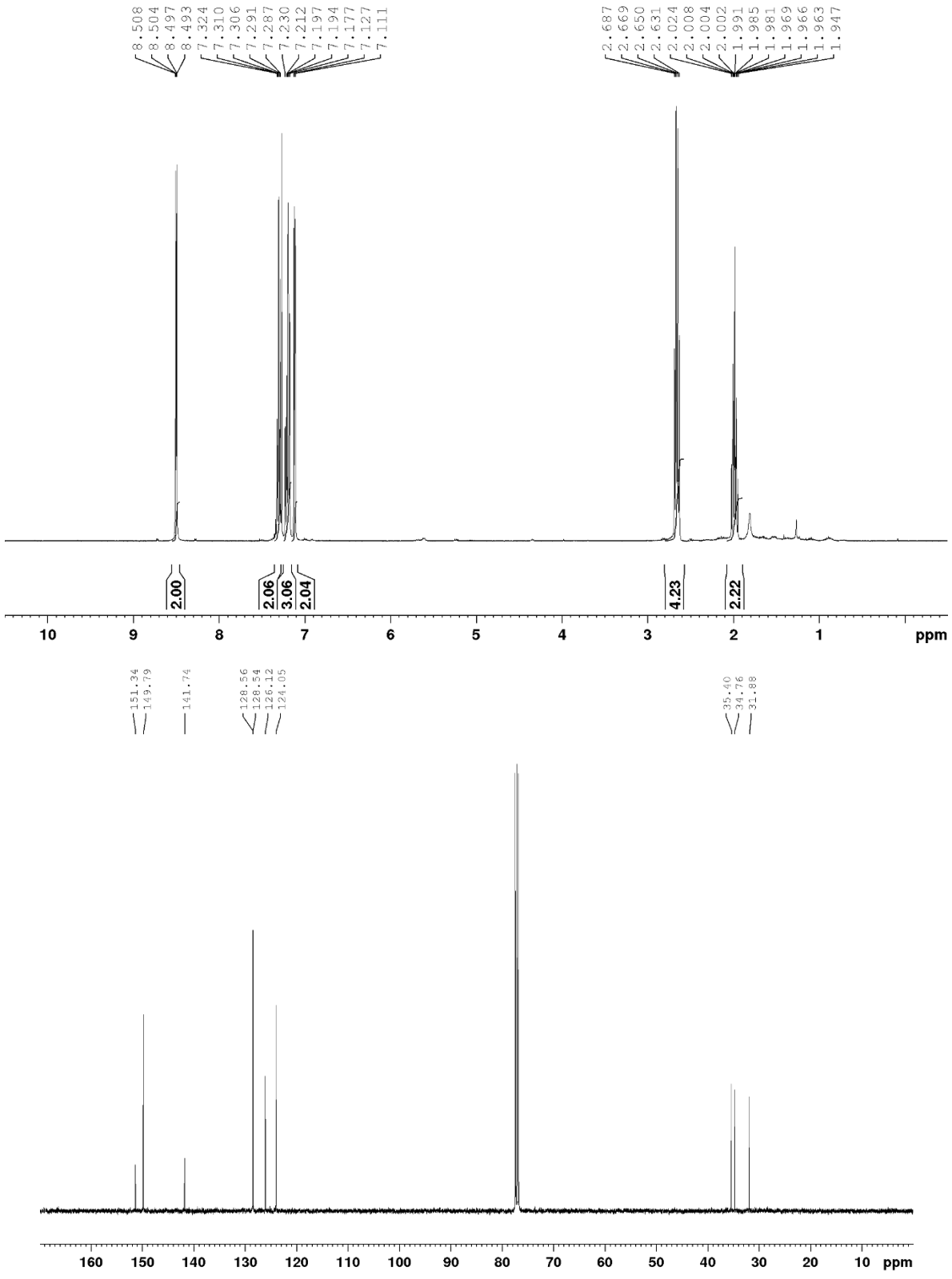

2-(3-phenylpropyl)pyrazine (**2.83**) $CDCl_3$, 400 MHz:

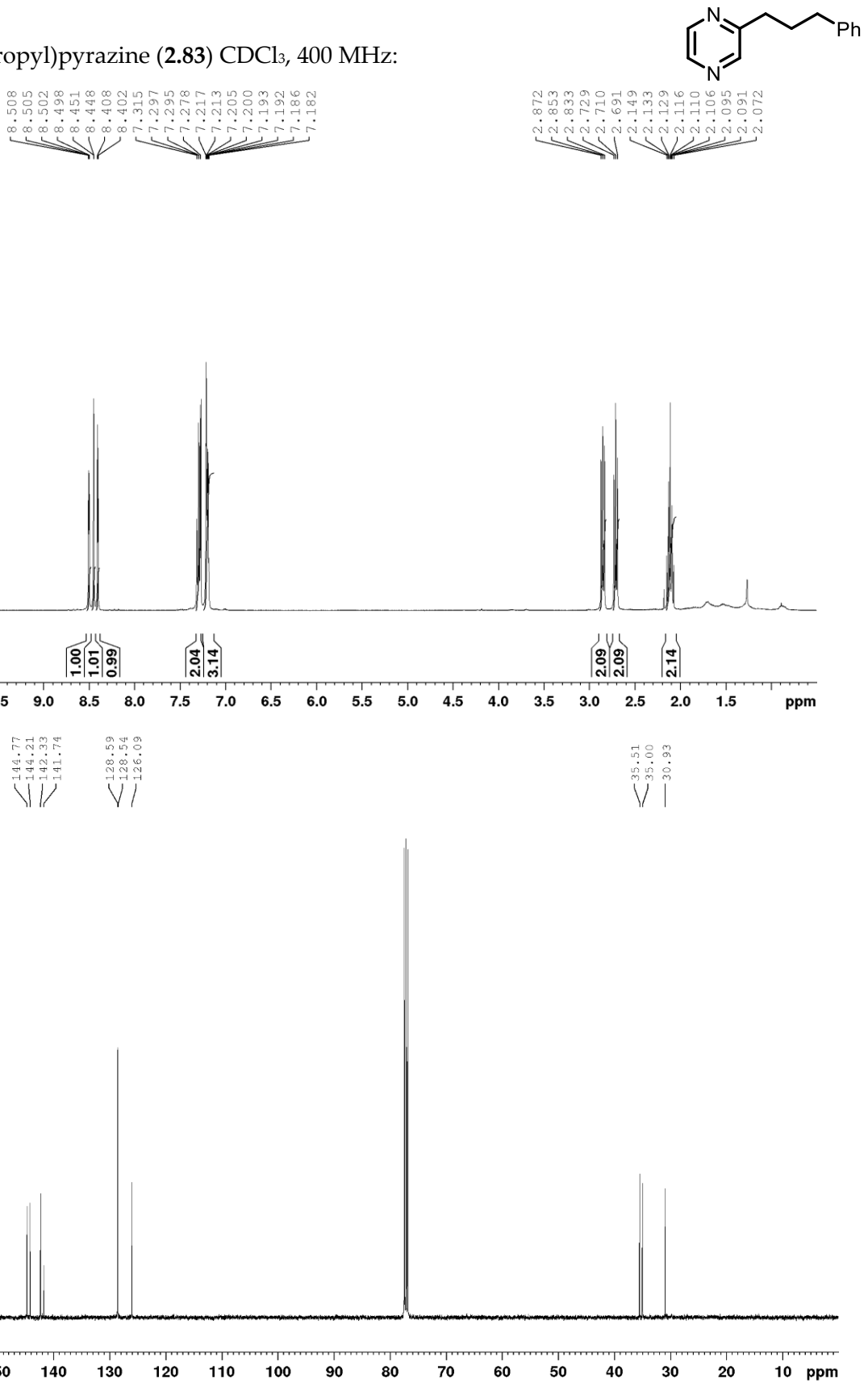

2-(2-cyclohexylethyl)naphthalene (**2.86**) $CDCl_3$, 400 MHz:

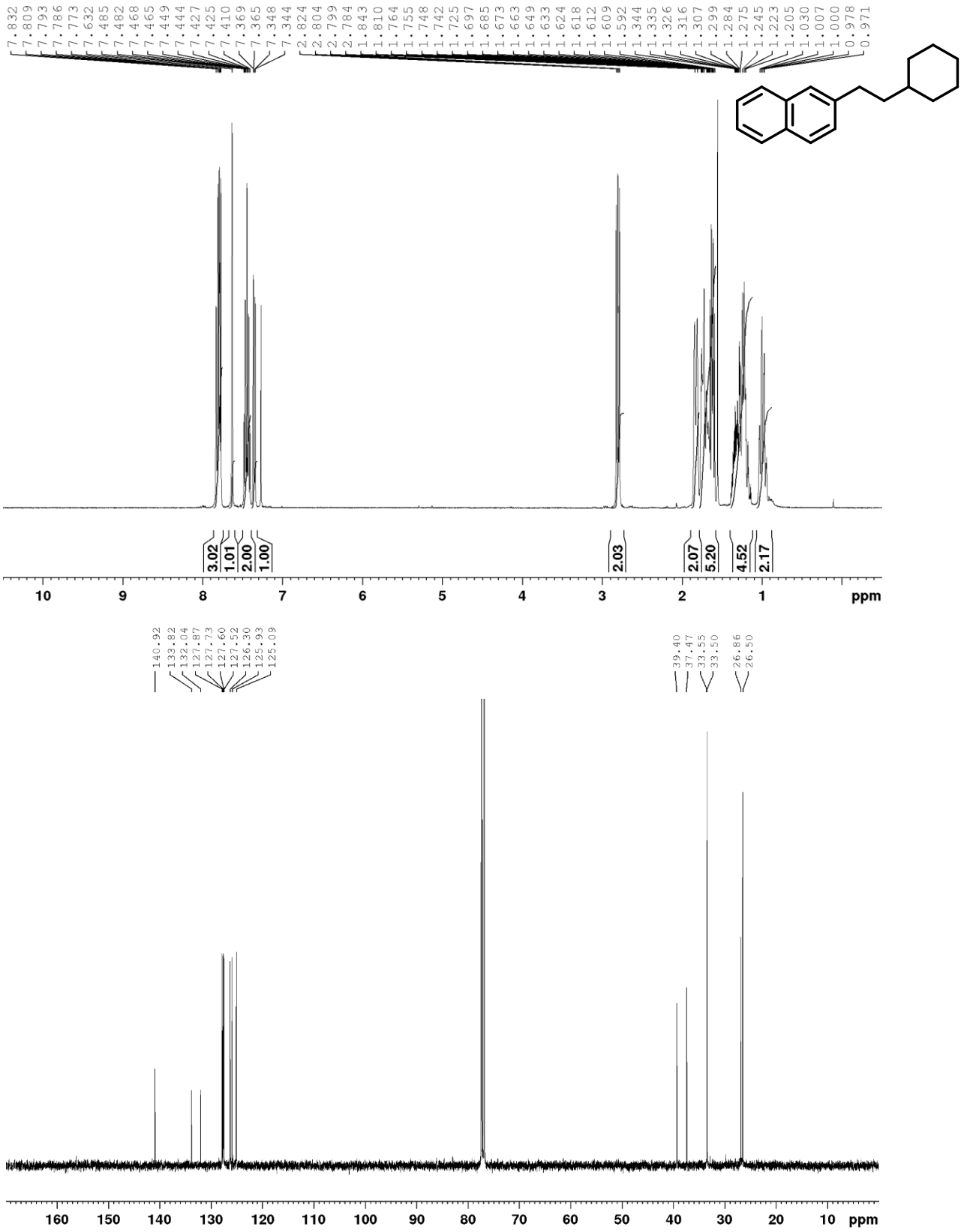

5-(3-(naphthalen-2-yl)propyl)benzo[d][1,3]dioxole (**2.88**) $CDCl_3$, 400 MHz:

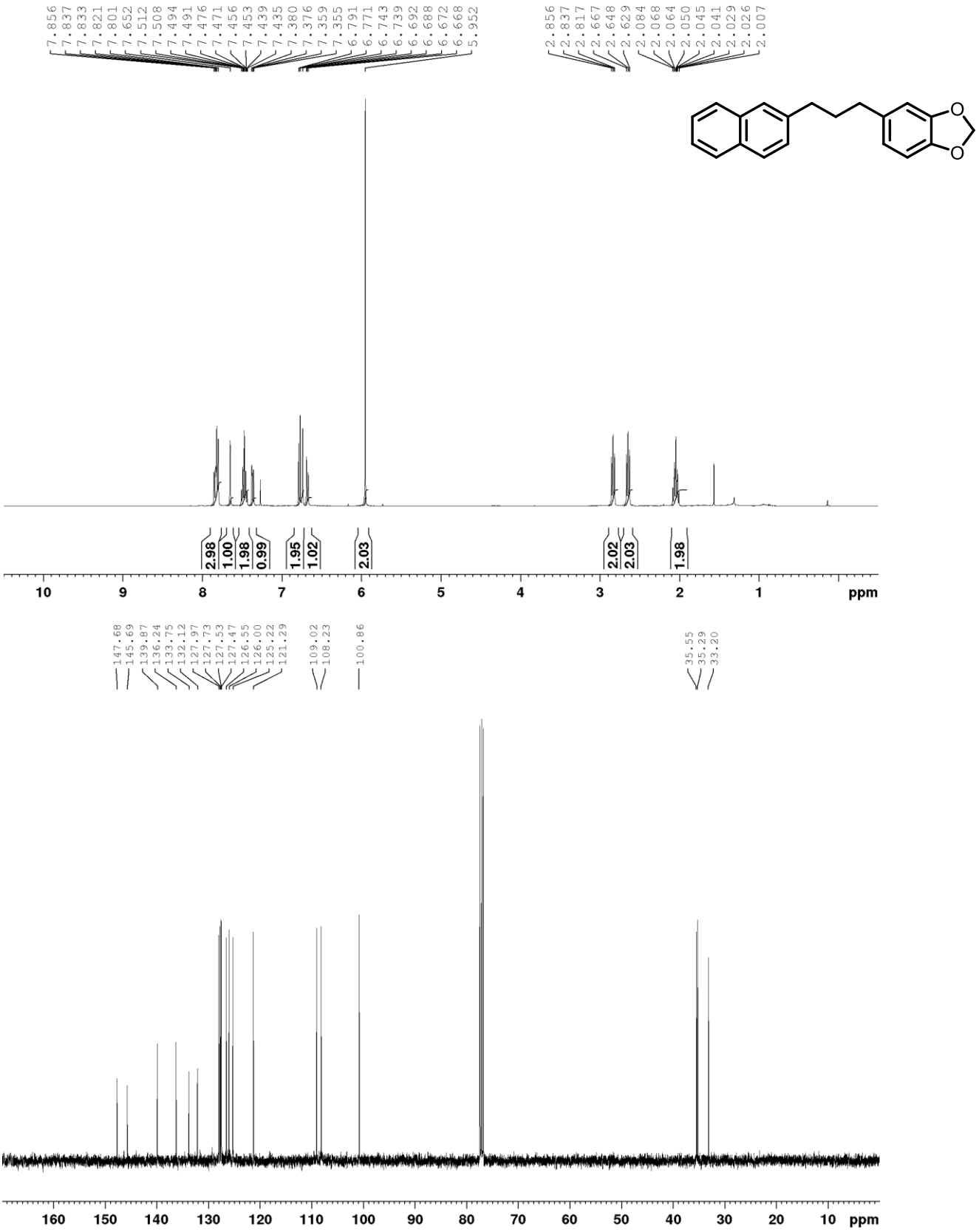

2-dodecyl-naphthalene (**2.90**) $CDCl_3$, 400 MHz:

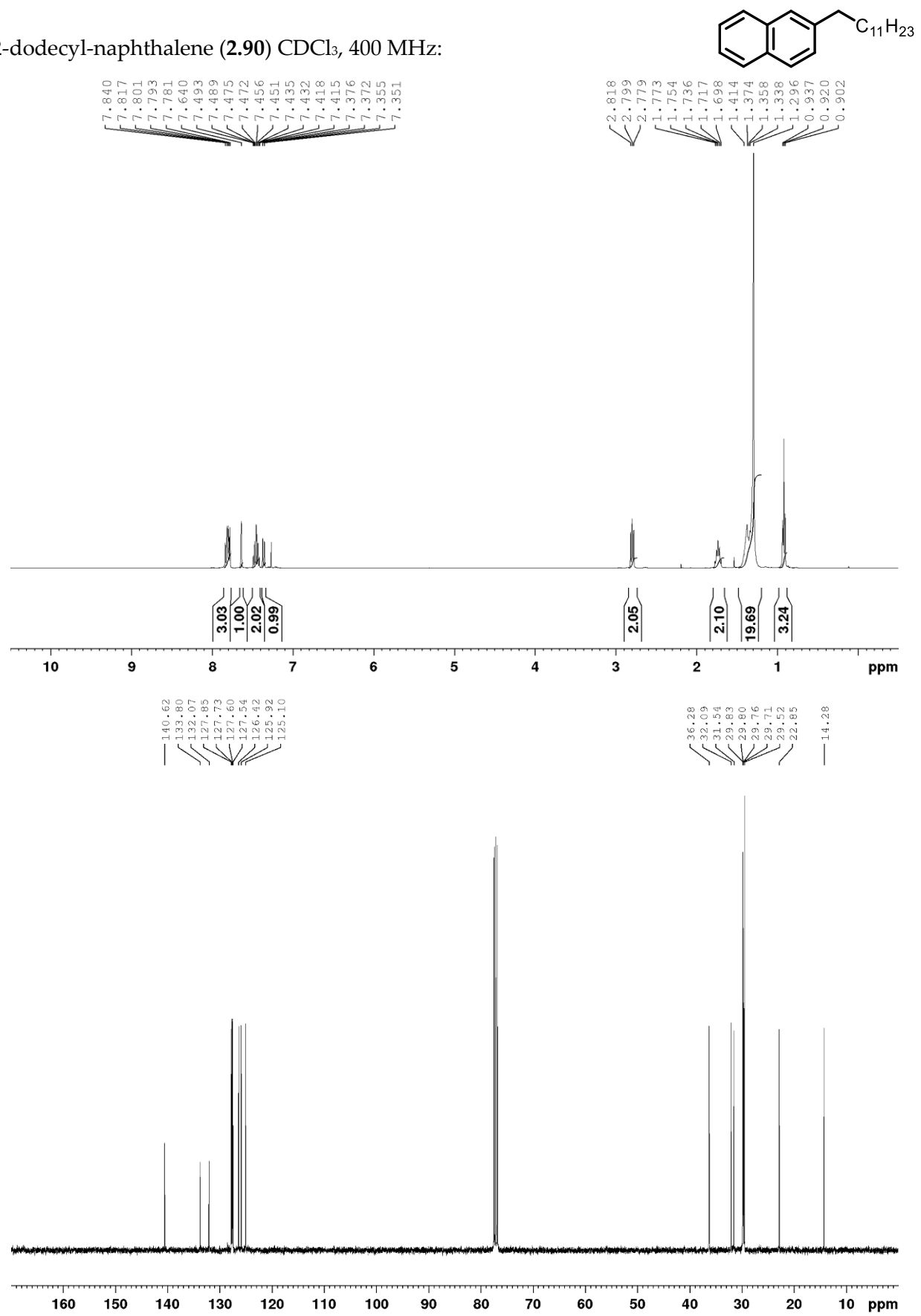

1-(2-naphthyl)-2-phenylethane (**2.91**) $CDCl_3$, 400 MHz:

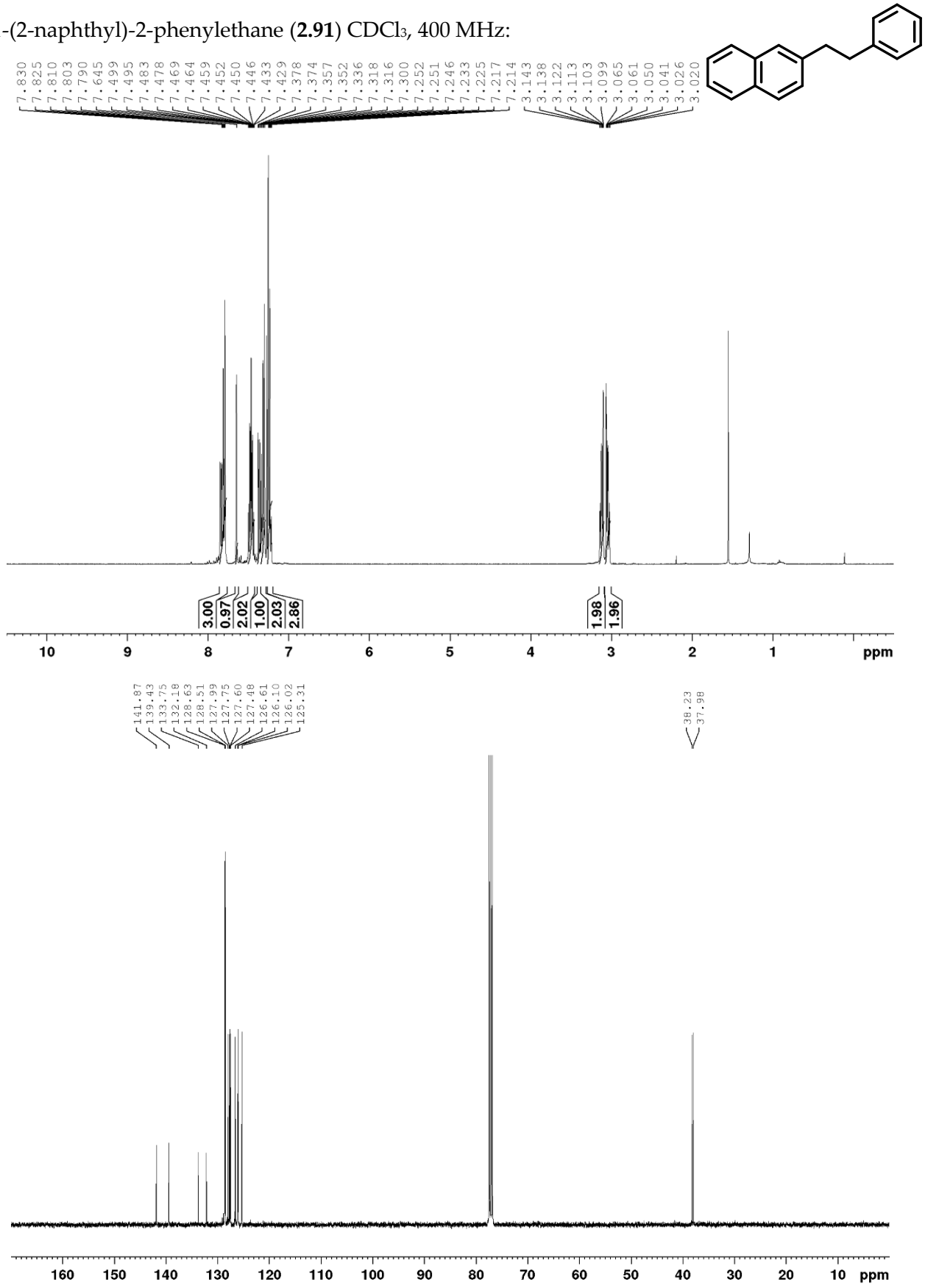

(S)-2-(4-(3-(benzo[d][1,3]dioxol-5-yl)propyl)-3-ethoxyphenyl)-N-(3-methyl-1-(2-(piperidin-1-yl)phenyl)butyl)acetamide (**2.102**) $CDCl_3$, 400 MHz:

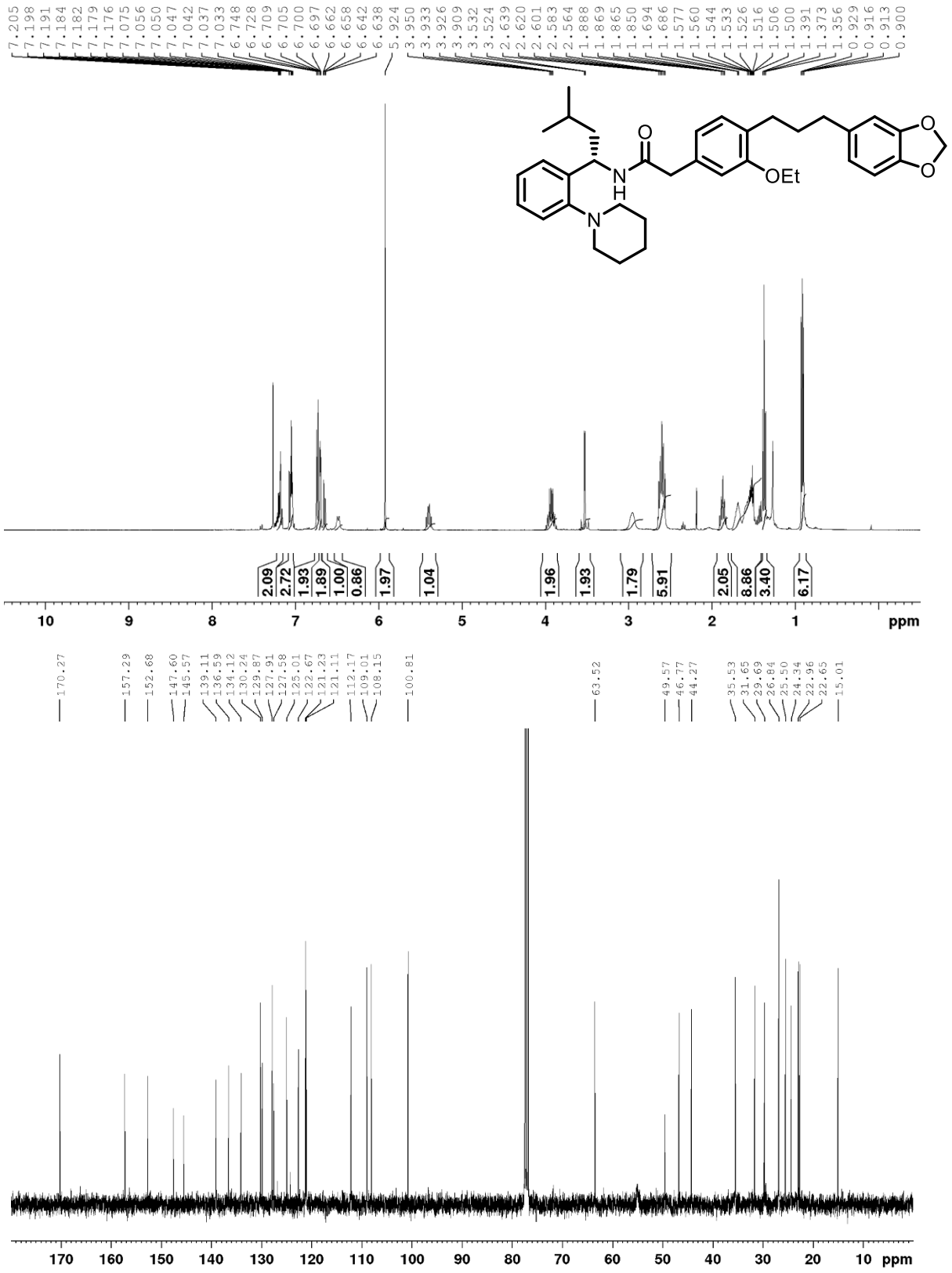

4-(3-(benzo[d][1,3]dioxol-5-yl)propyl)-N,N-dipropylbenzenesulfonamide (**2.105**) $CDCl_3$, 400 MHz:

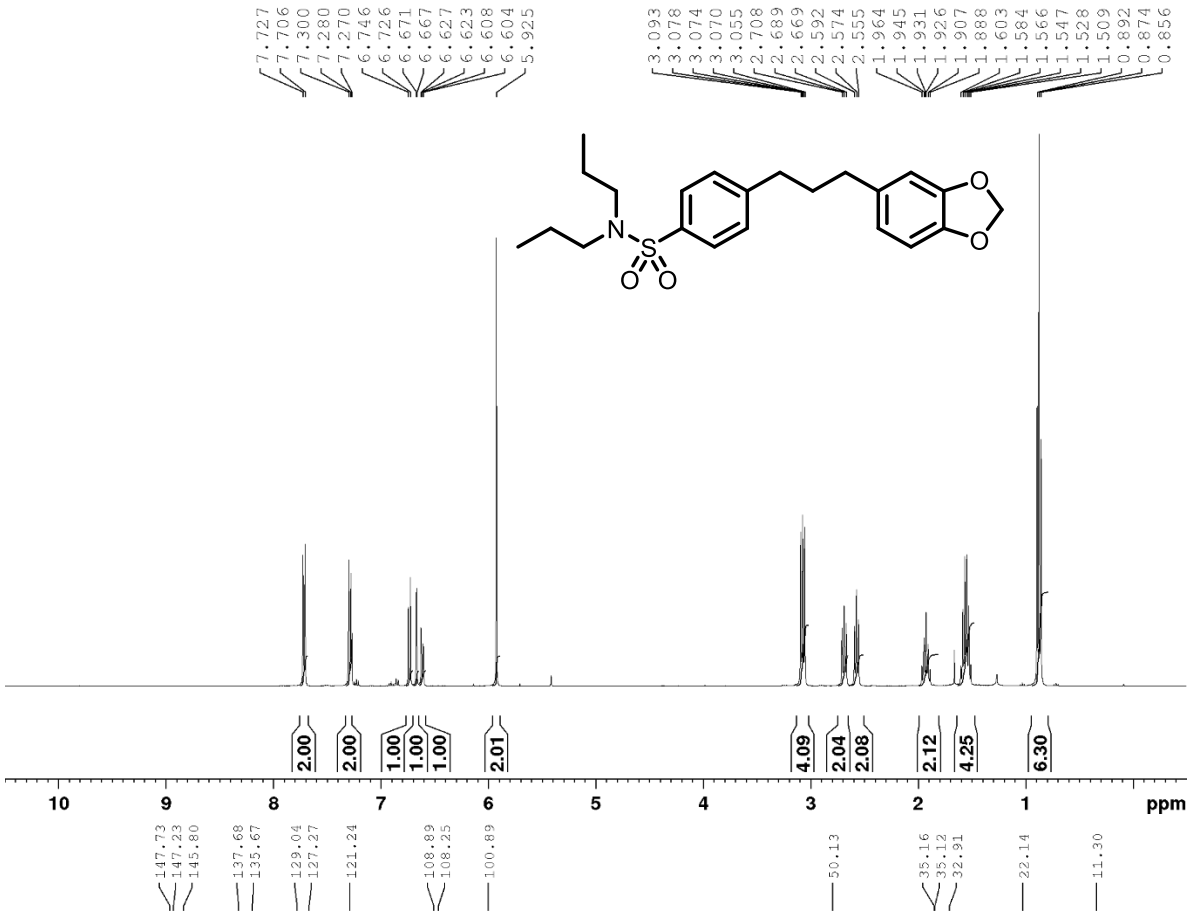

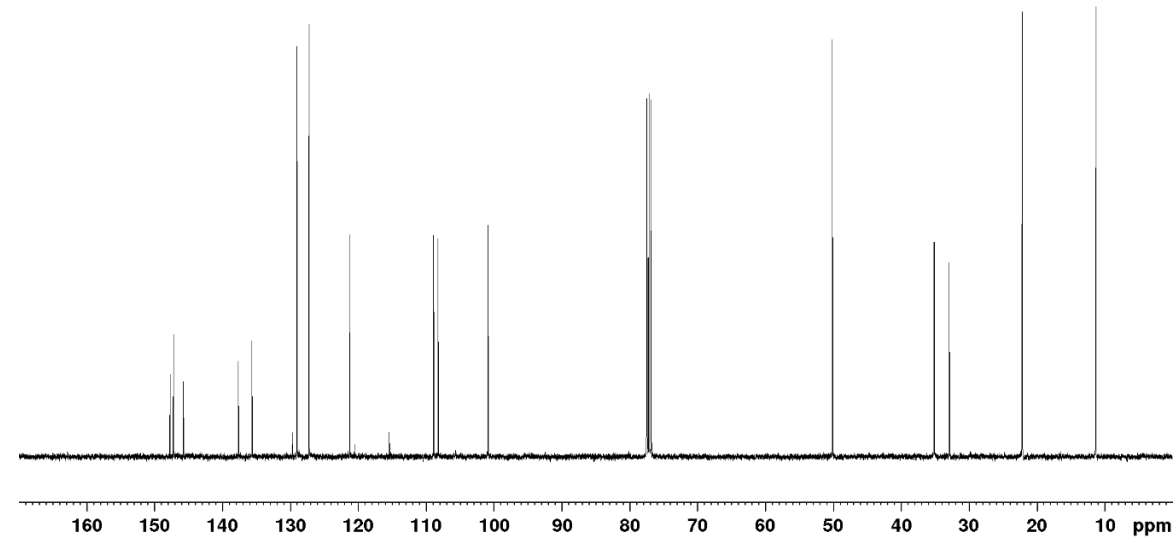

Appendix B: NMR Spectra for Chapter 3

(S)-methyl tetrahydrofuran-2-carboxylate (**3.29**). $CDCl_3$, 400 MHz:

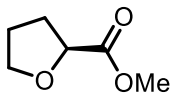

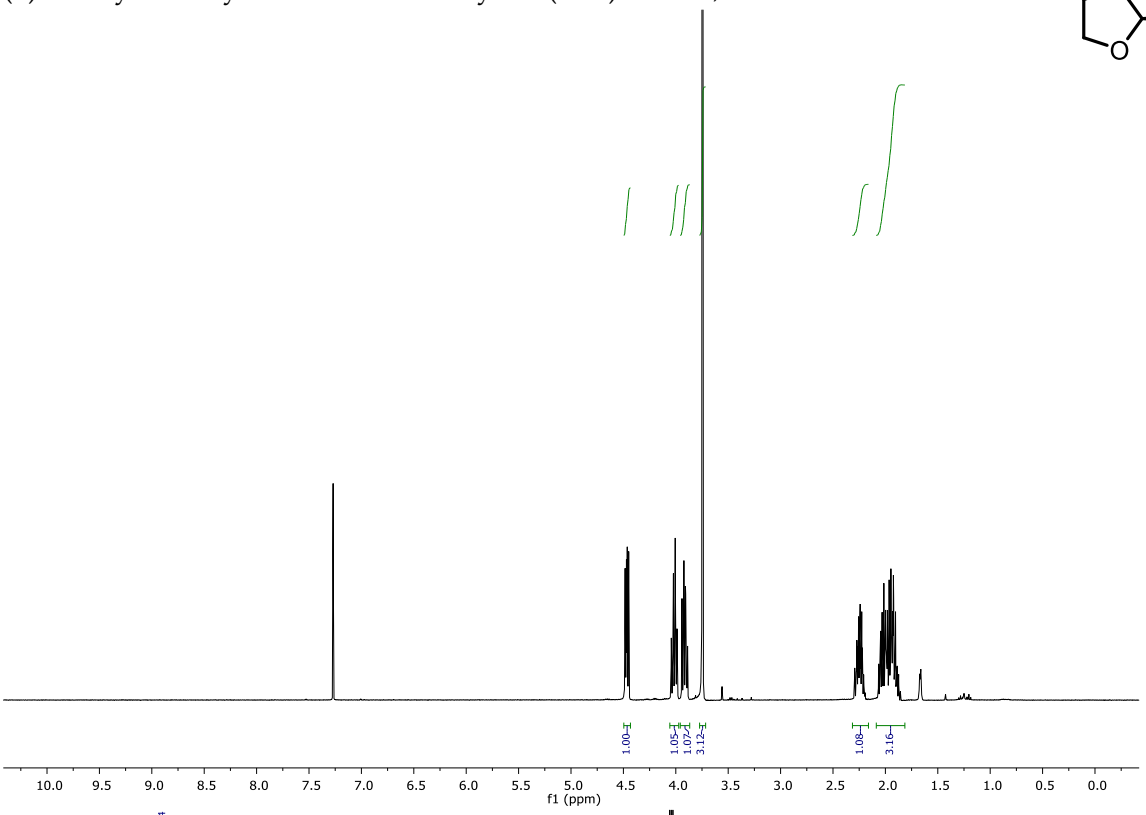

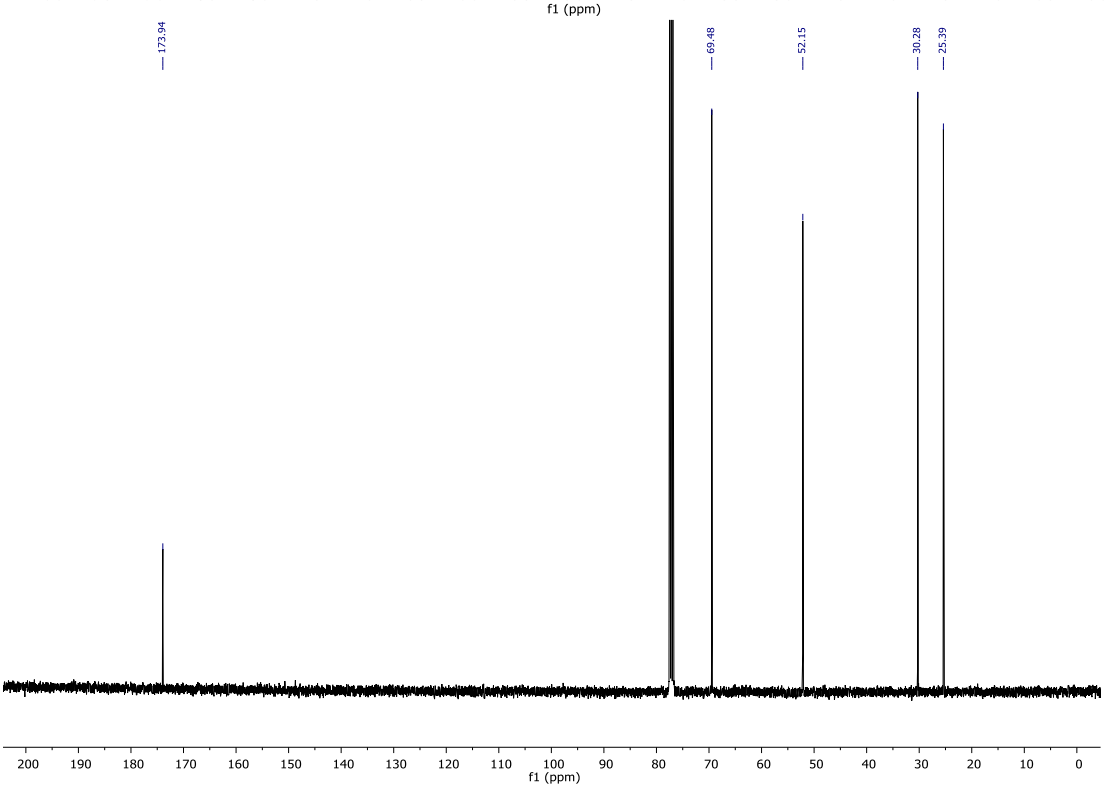

N-Benzyl-(S)-proline methyl ester (**3.31**). $CDCl_3$, 400 MHz:

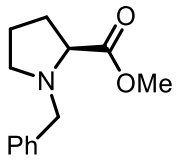

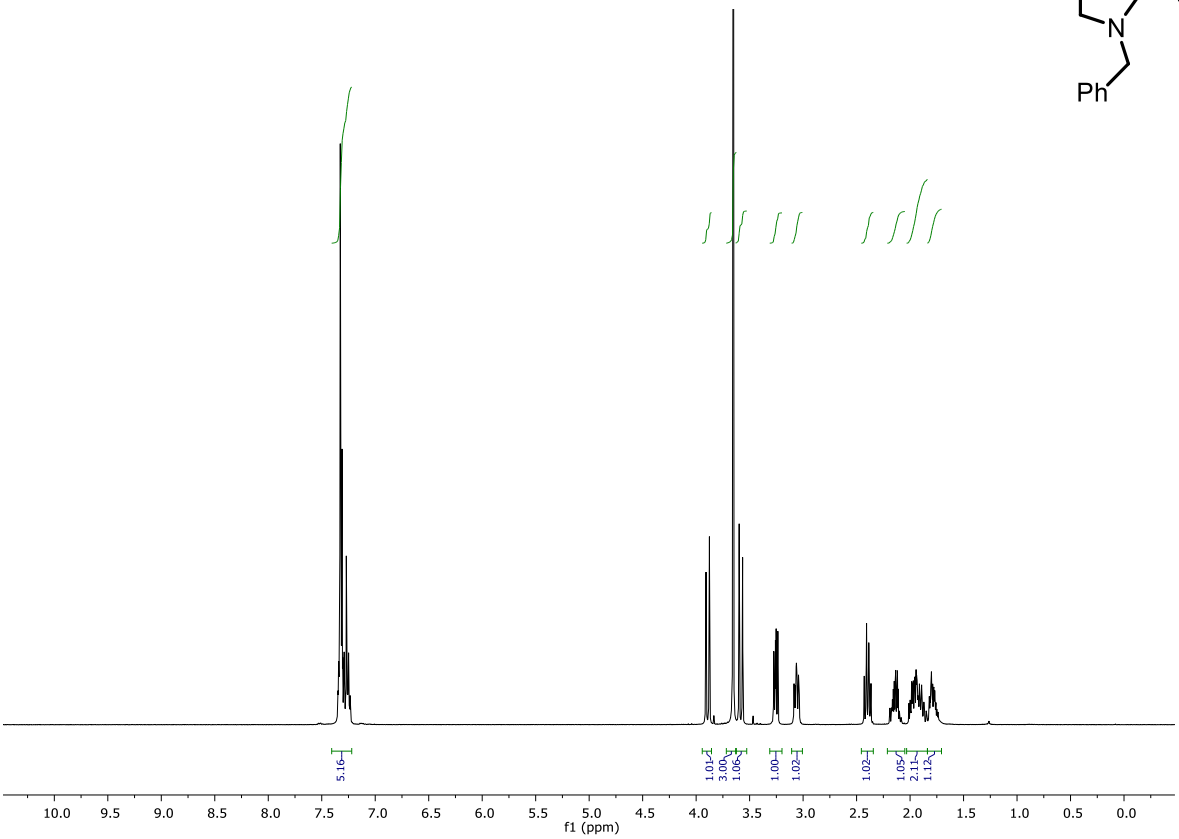

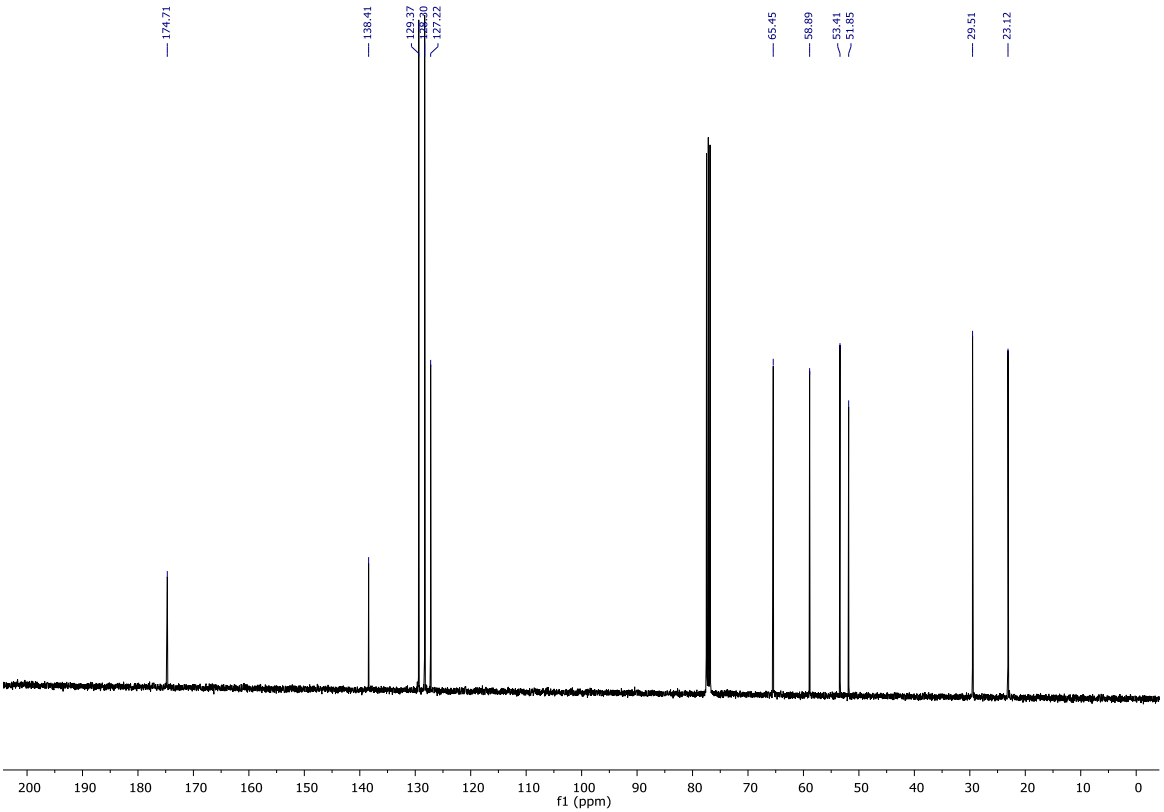

Epoxidized methyl oleate (**3.99**). $CDCl_3$, 400 MHz:

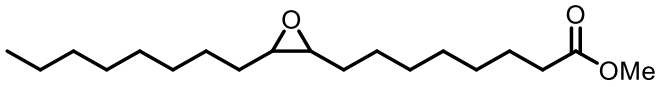

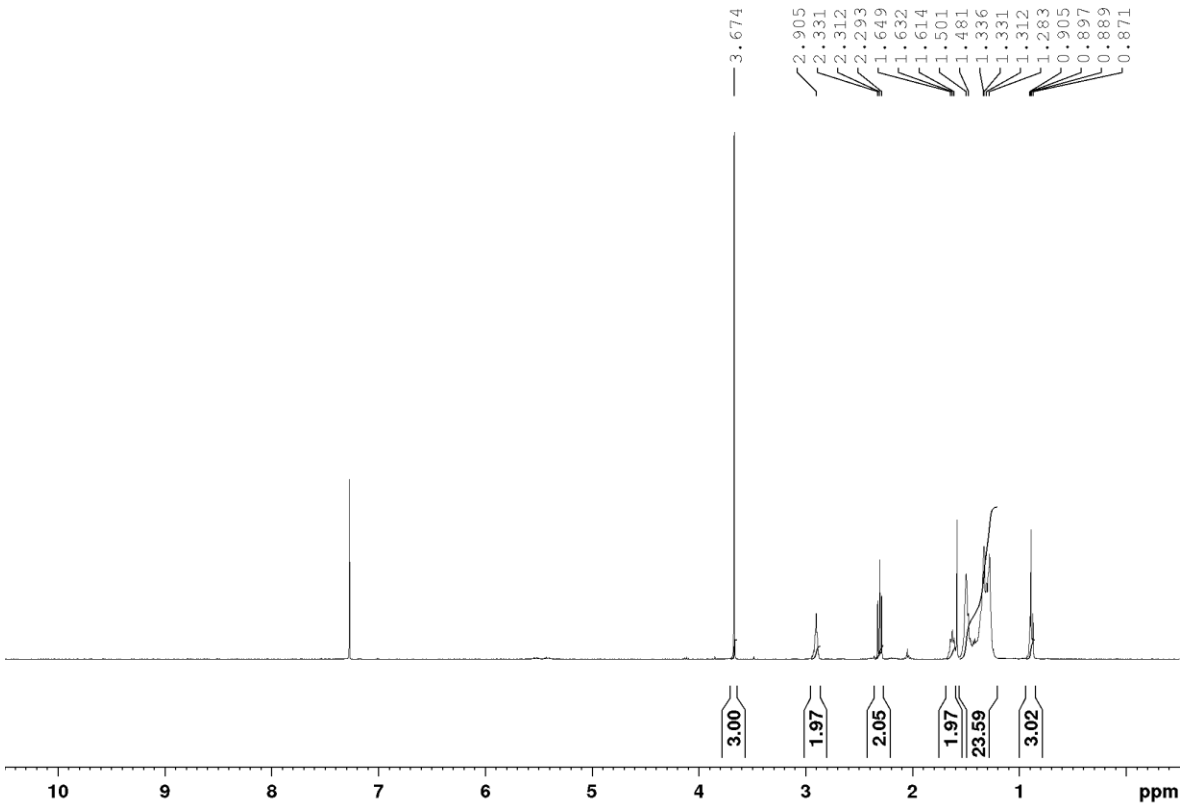

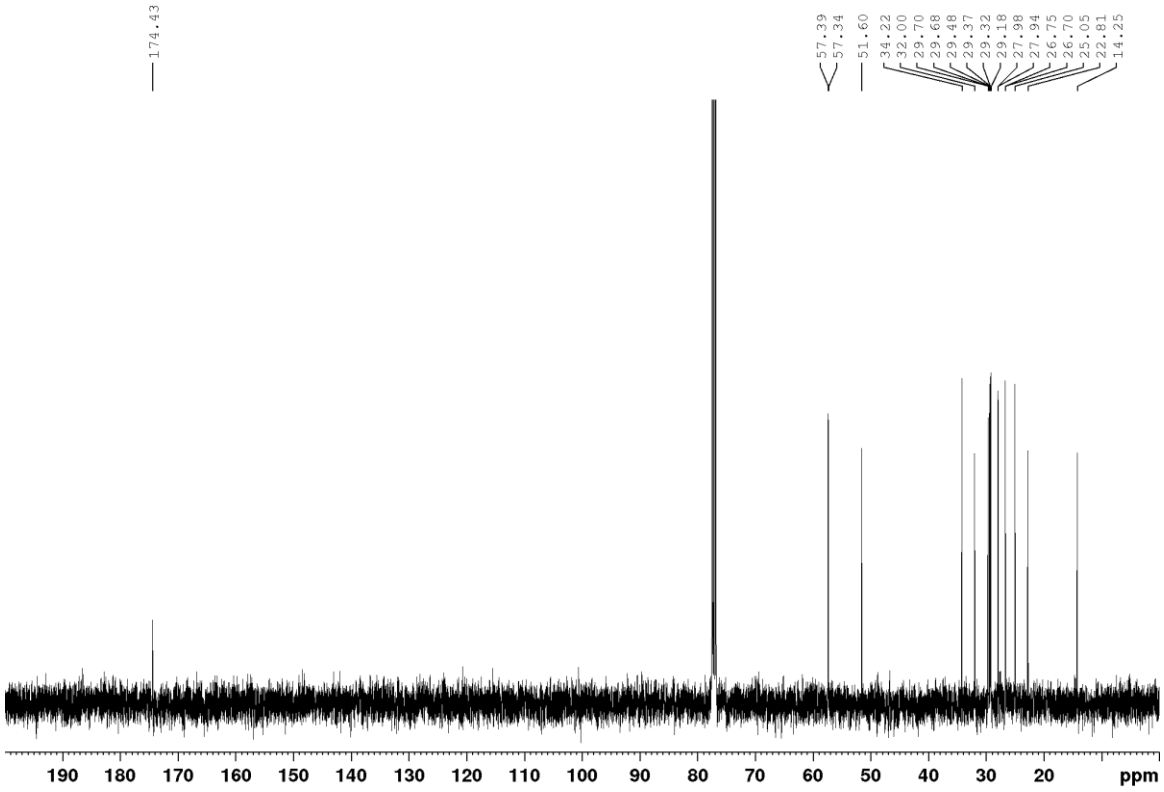

N,N-Diethylglycine methyl ester (**3.112**). $CDCl_3$, 400 MHz:

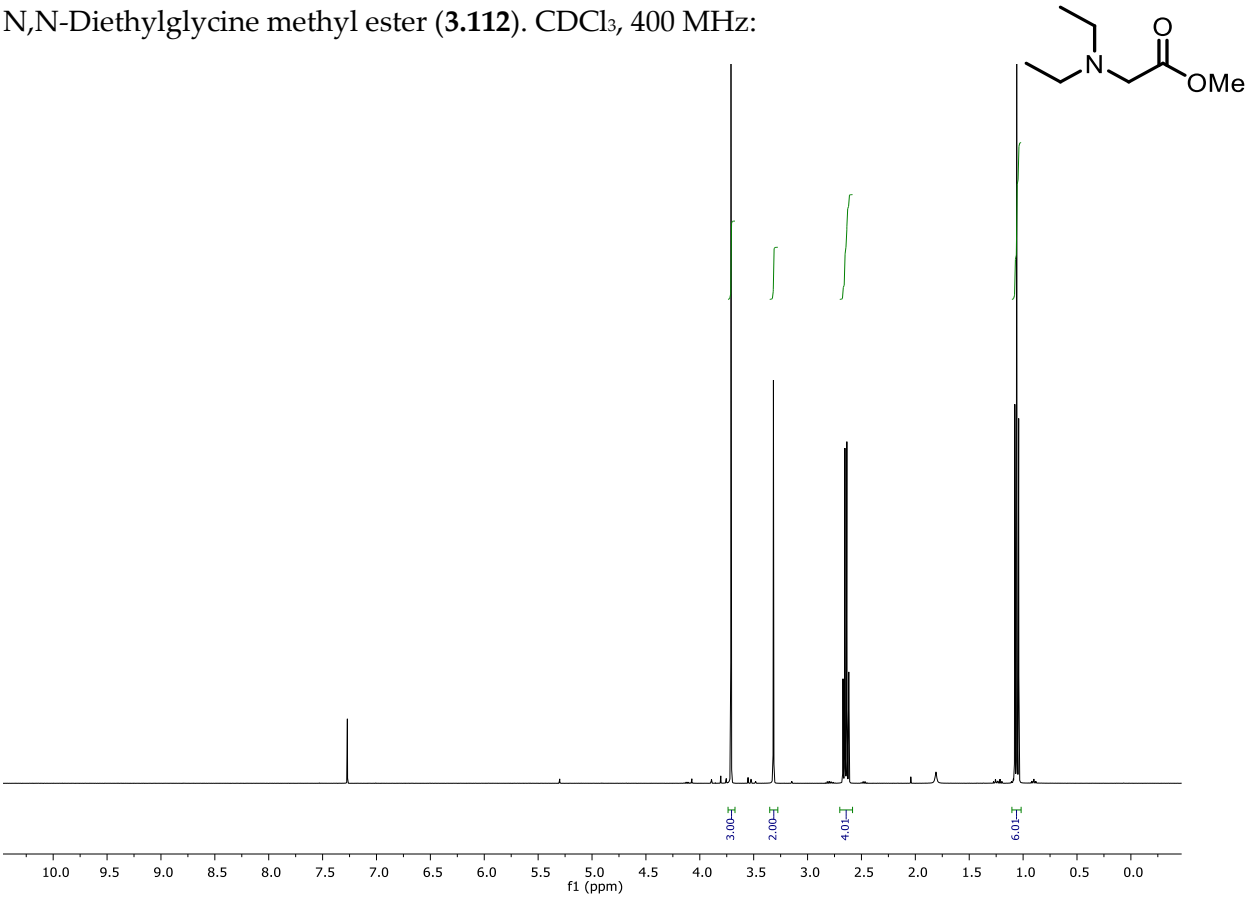

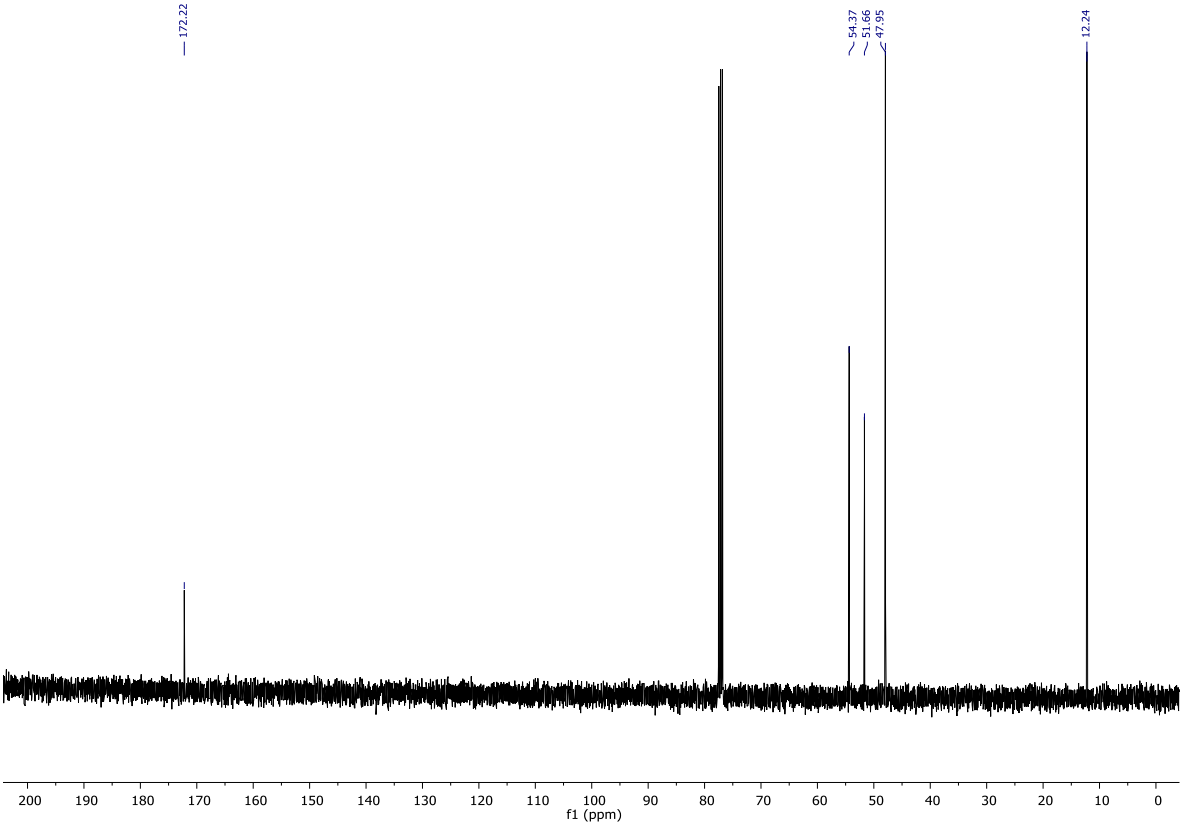

(S)-naproxen methyl ester (**3.137**). $CDCl_3$, 400 MHz:

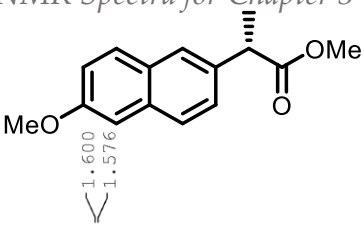

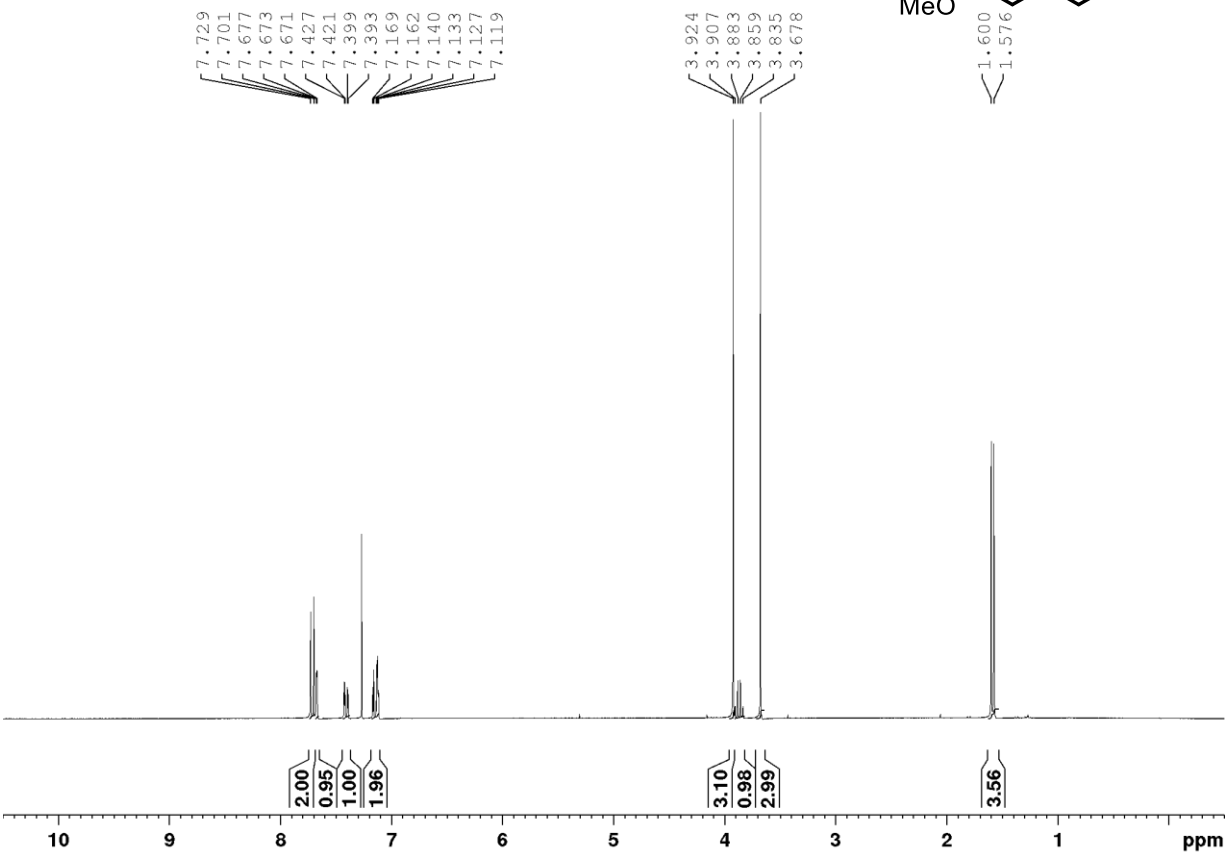

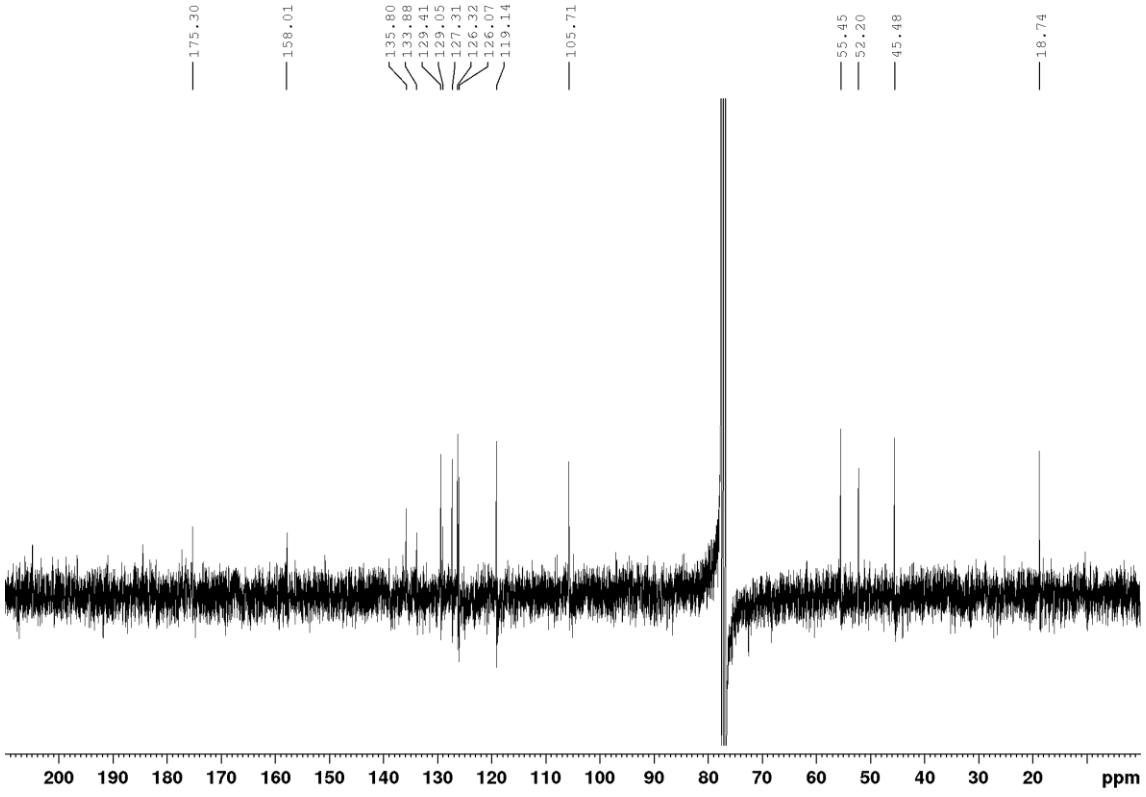

2-(hex-1-yn-1-yl)benzyl benzoate (**3.186**). $CDCl_3$, 400 MHz:

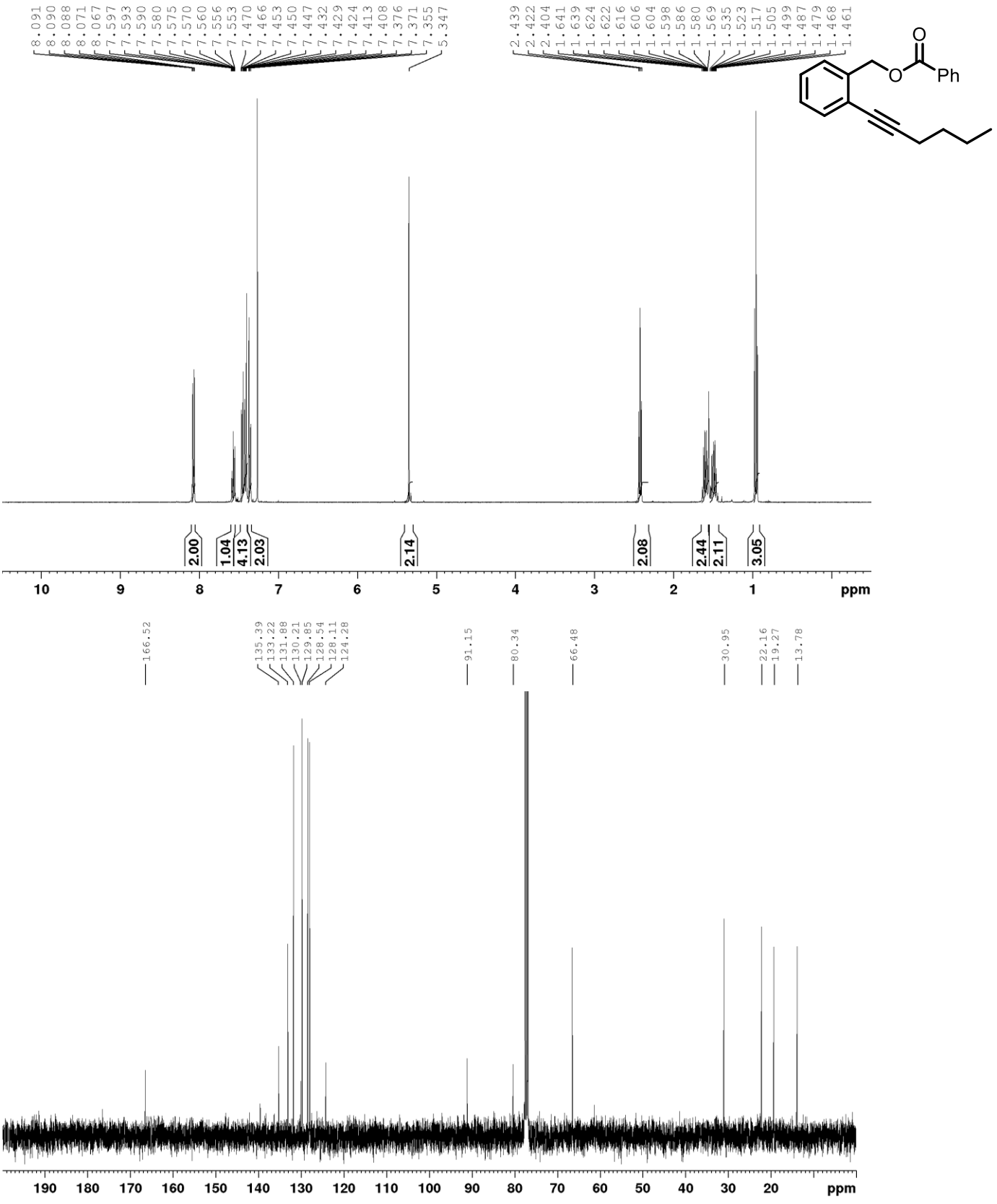

(5-methylpyrazin-2-yl)(morpholino)methanone (**3.20**). $CDCl_3$, 400 MHz:

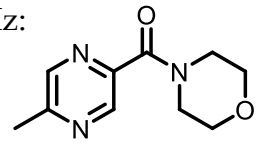

4-(2,5-dimethyl-2H-pyrazole-3-carbonyl)-morpholine (**3.22**). $CDCl_3$, 400 MHz:

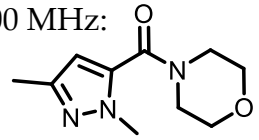

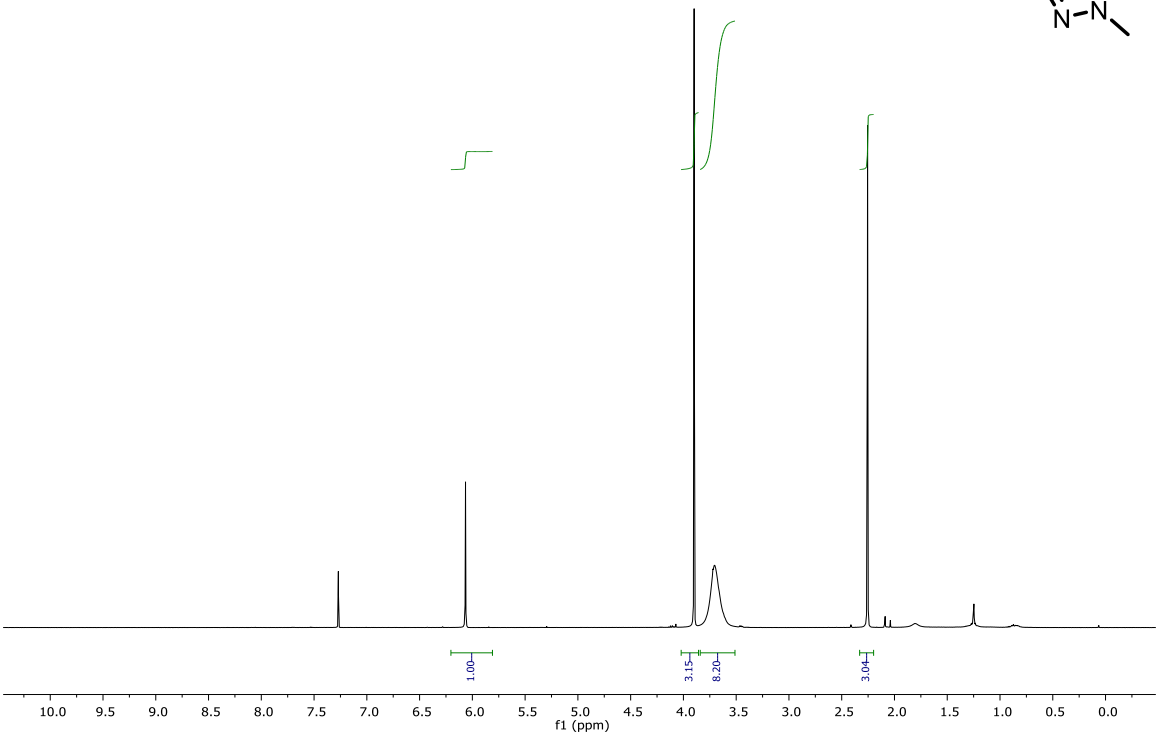

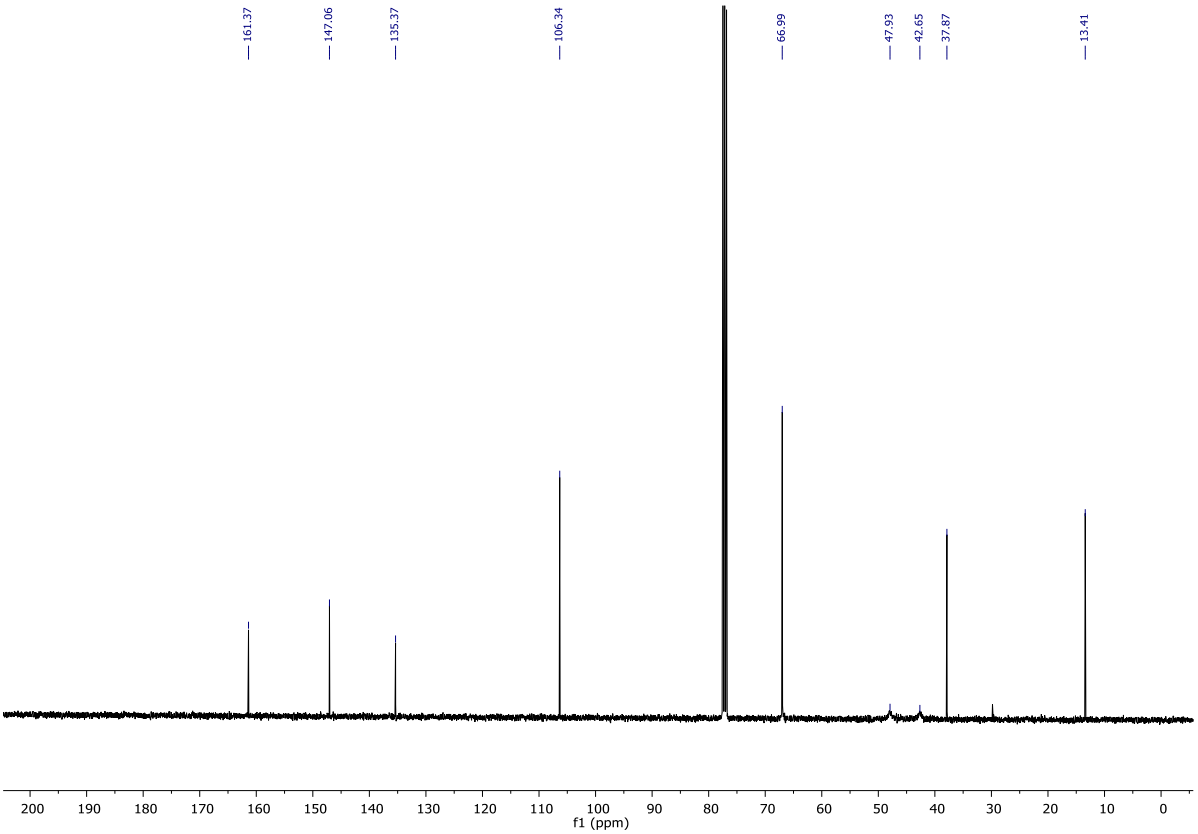

benzofuran-2-yl(morpholino)methanone (**3.24**). $CDCl_3$, 400 MHz:

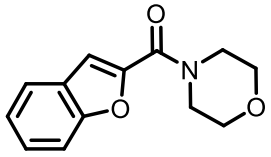

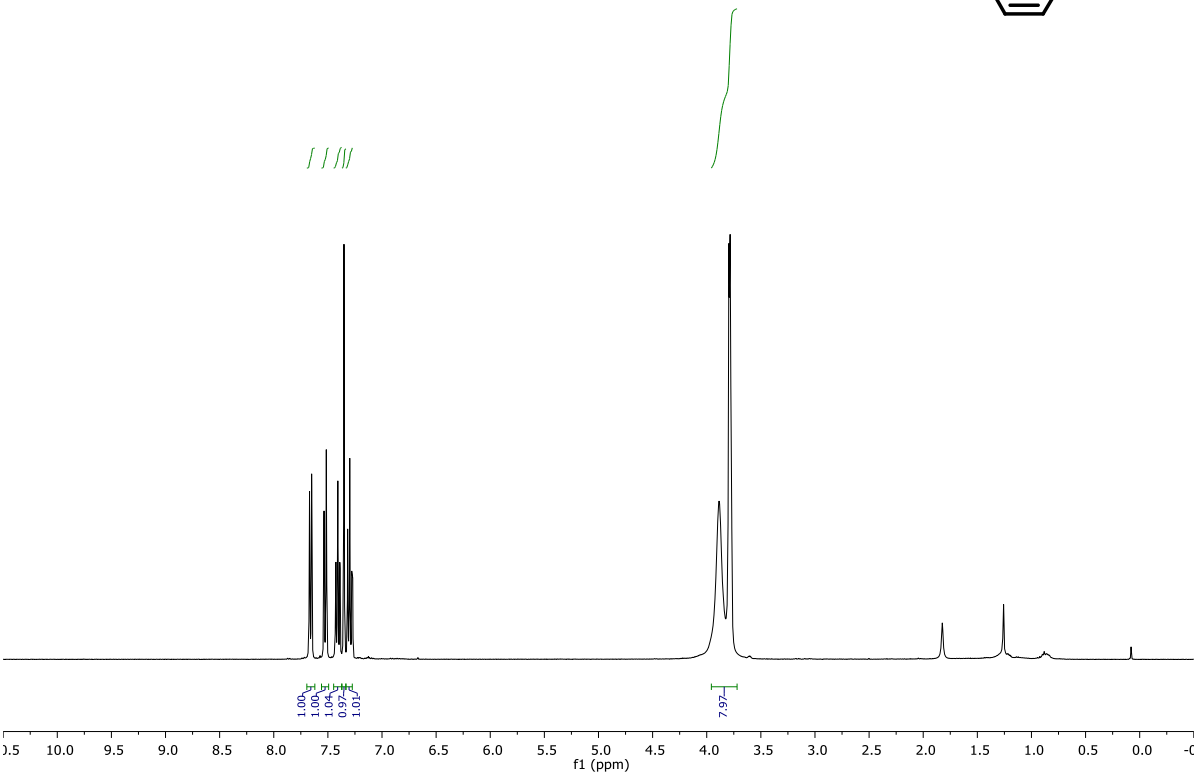

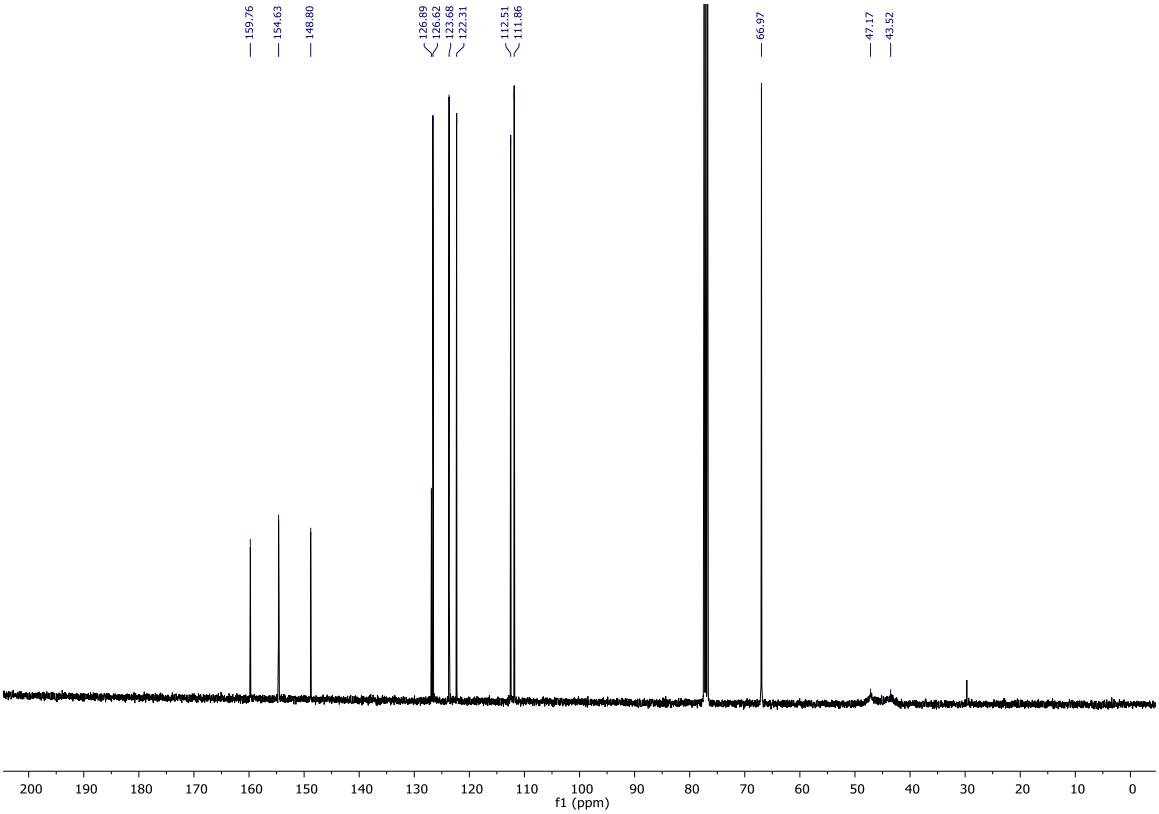

(1-methyl-1H-indol-4-yl)(morpholino)methanone (**3.26**). $CDCl_3$, 400 MHz:

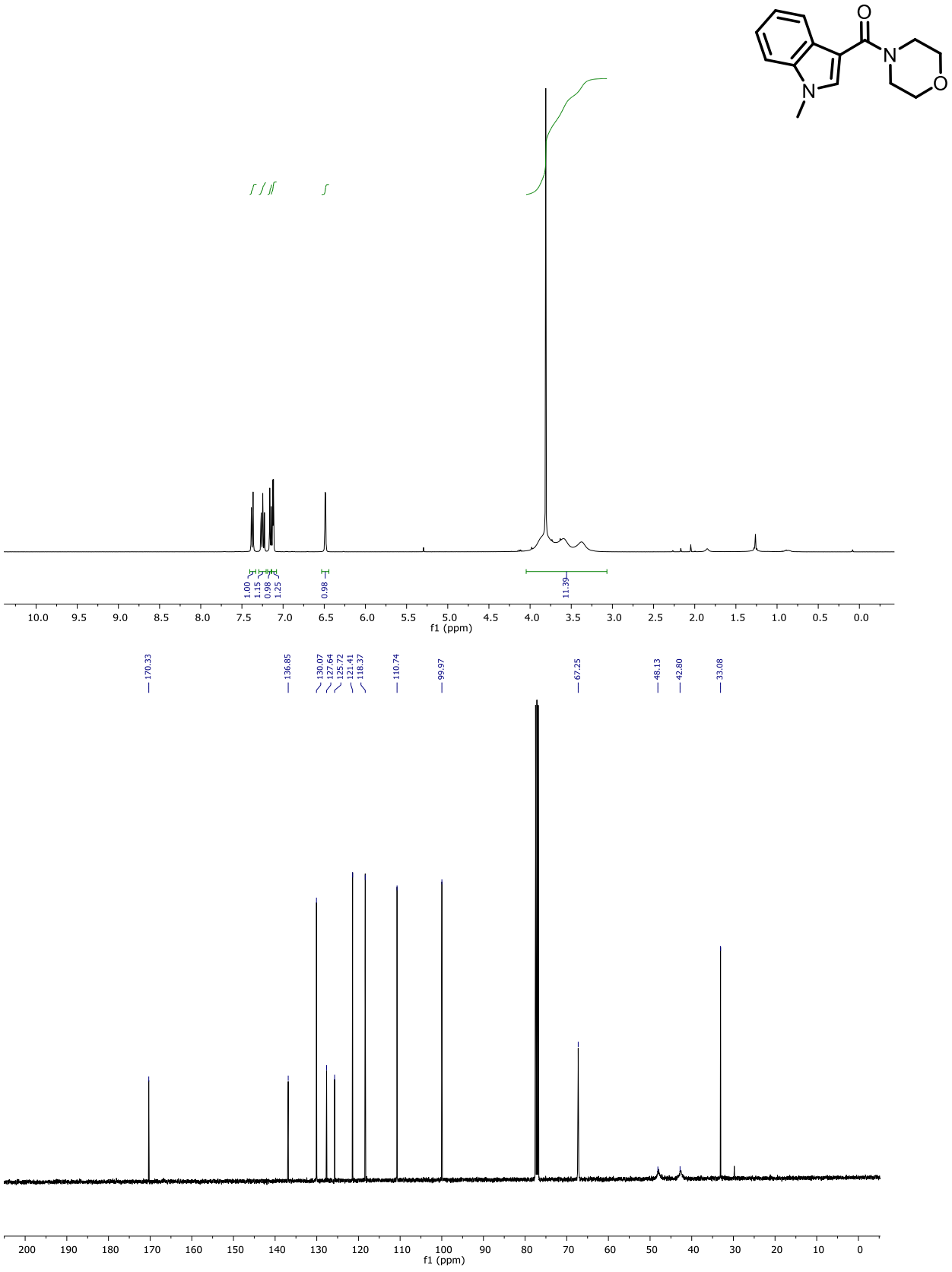

4-(3-phenyl-propionyl)-morpholine (**3.28**). $CDCl_3$, 400 MHz:

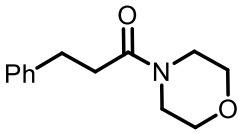

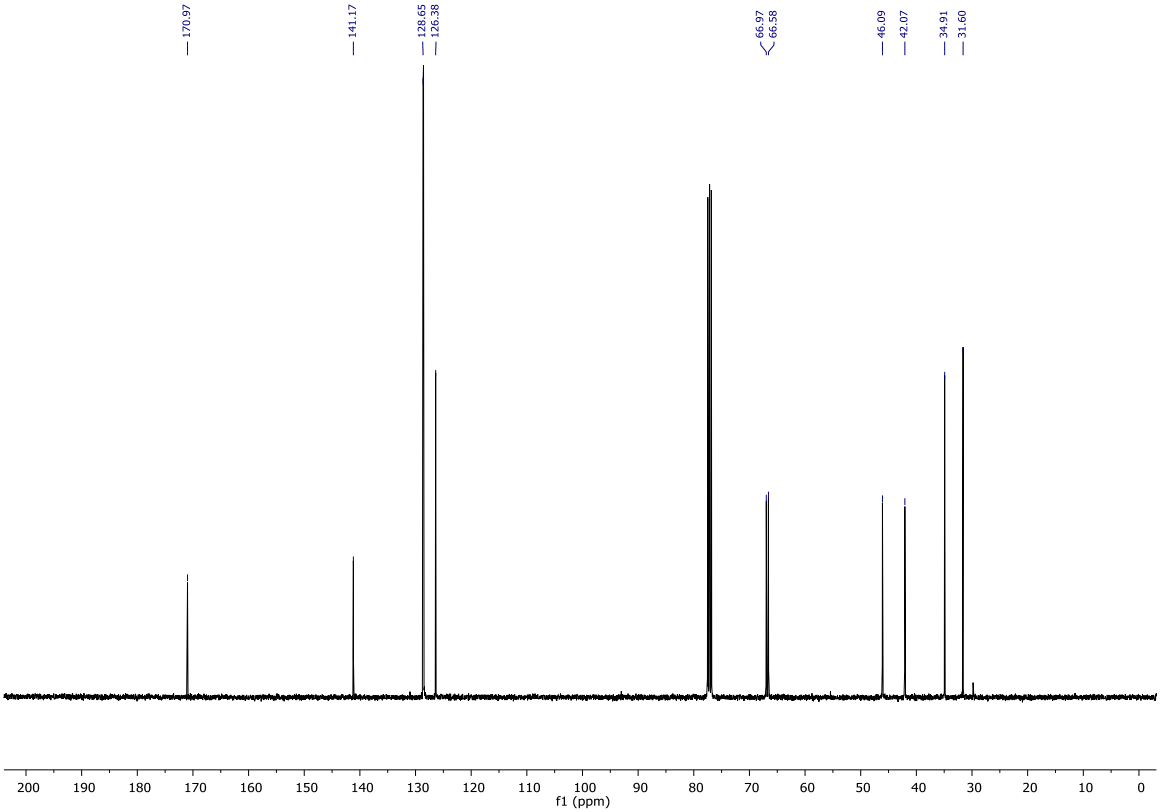

(S)-N-phenyloxolane-2-carboxamide (**3.30**). $CDCl_3$, 400 MHz:

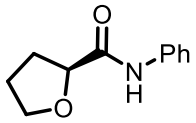

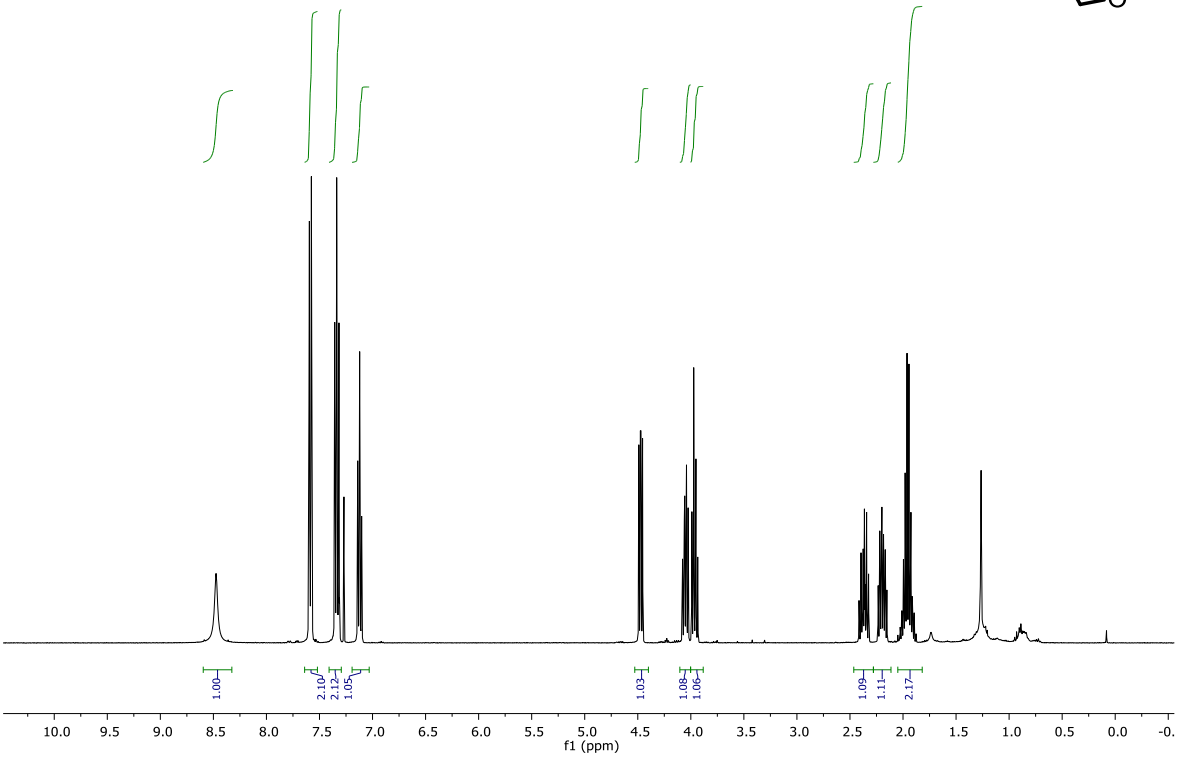

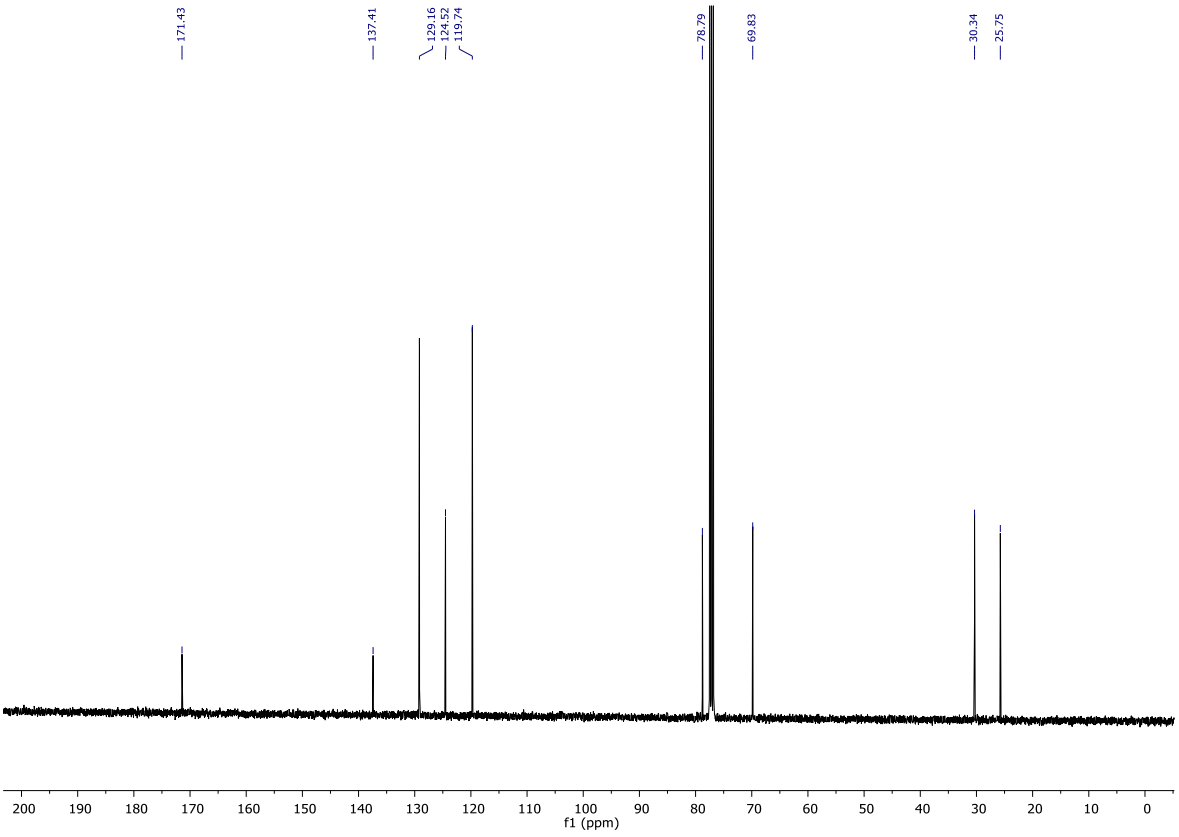

(S)-1-benzyl-N-phenylpyrrolidine-2-carboxamide (**3.32**) $CDCl_3$, 400 MHz:

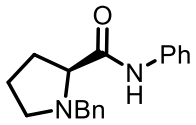

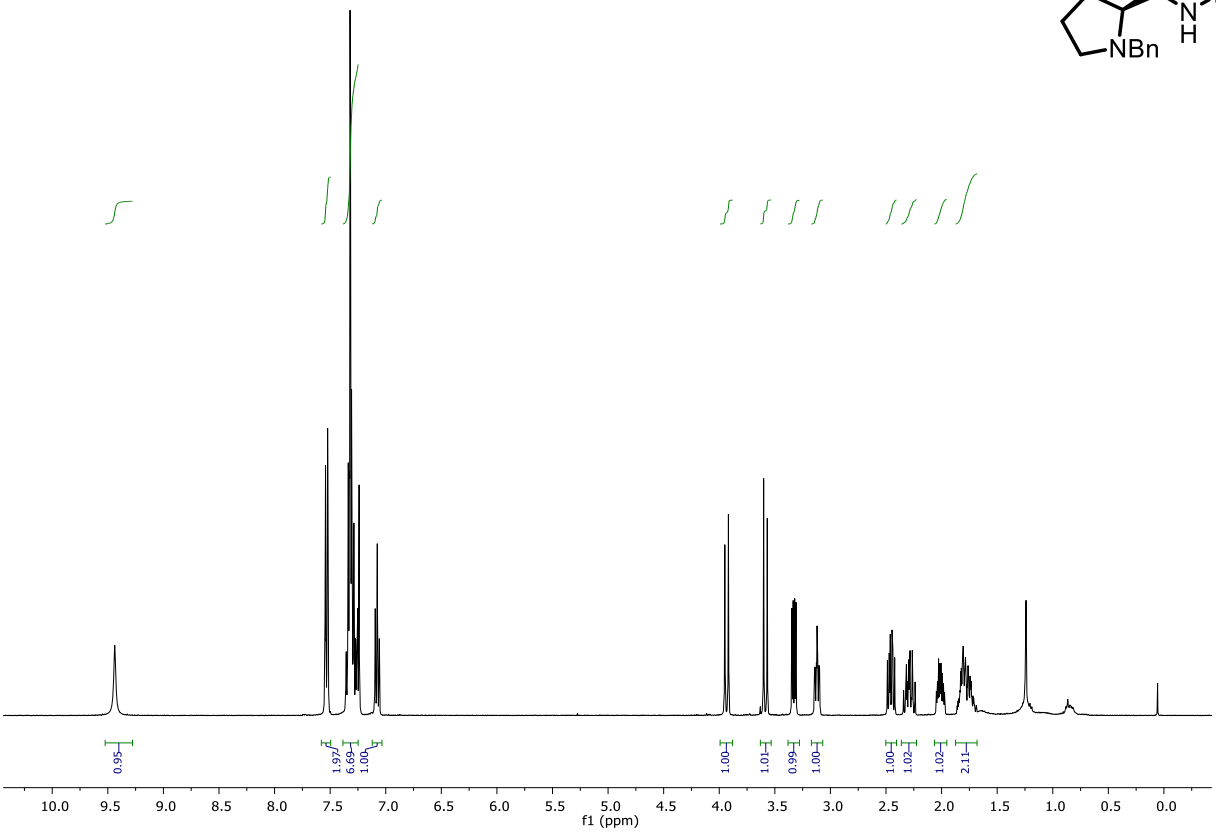

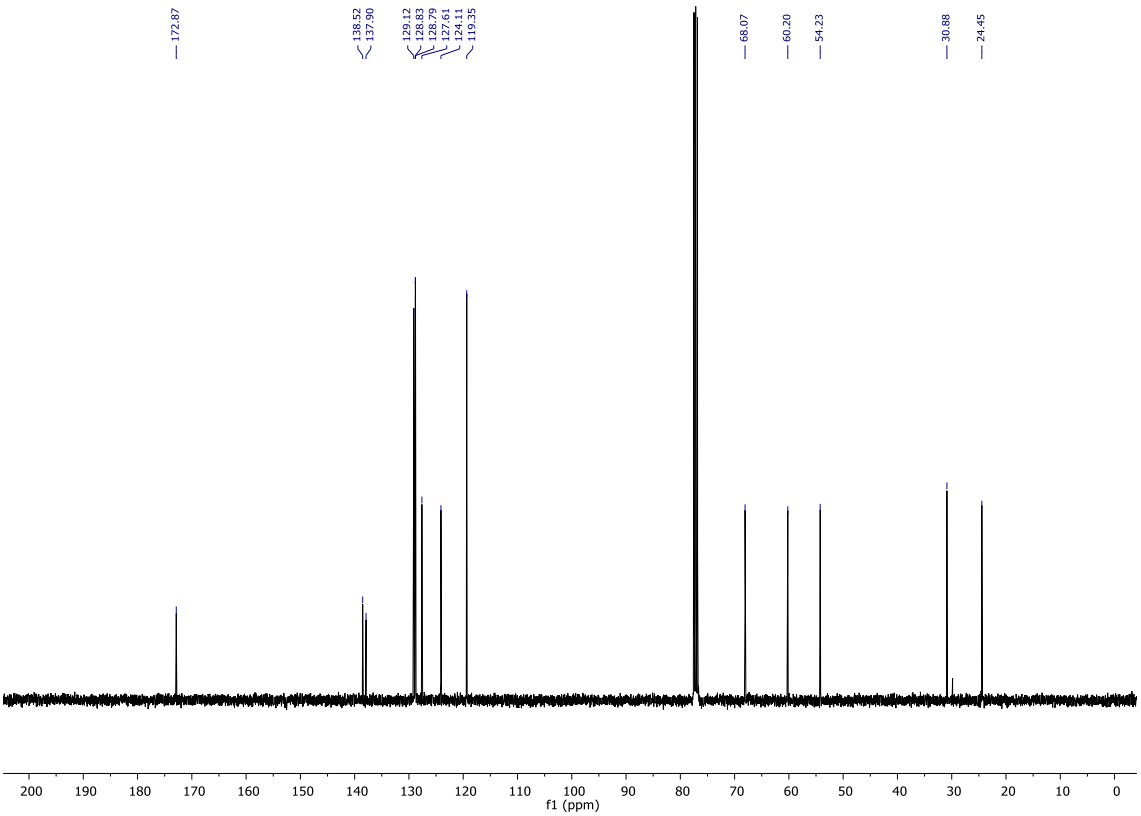

(1,4-dioxa-8-azaspiro[4.5]dec-8-yl)phenylmethanone (**3.35**). $CDCl_3$, 400 MHz:

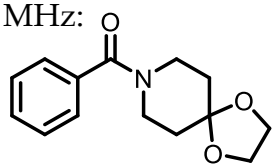

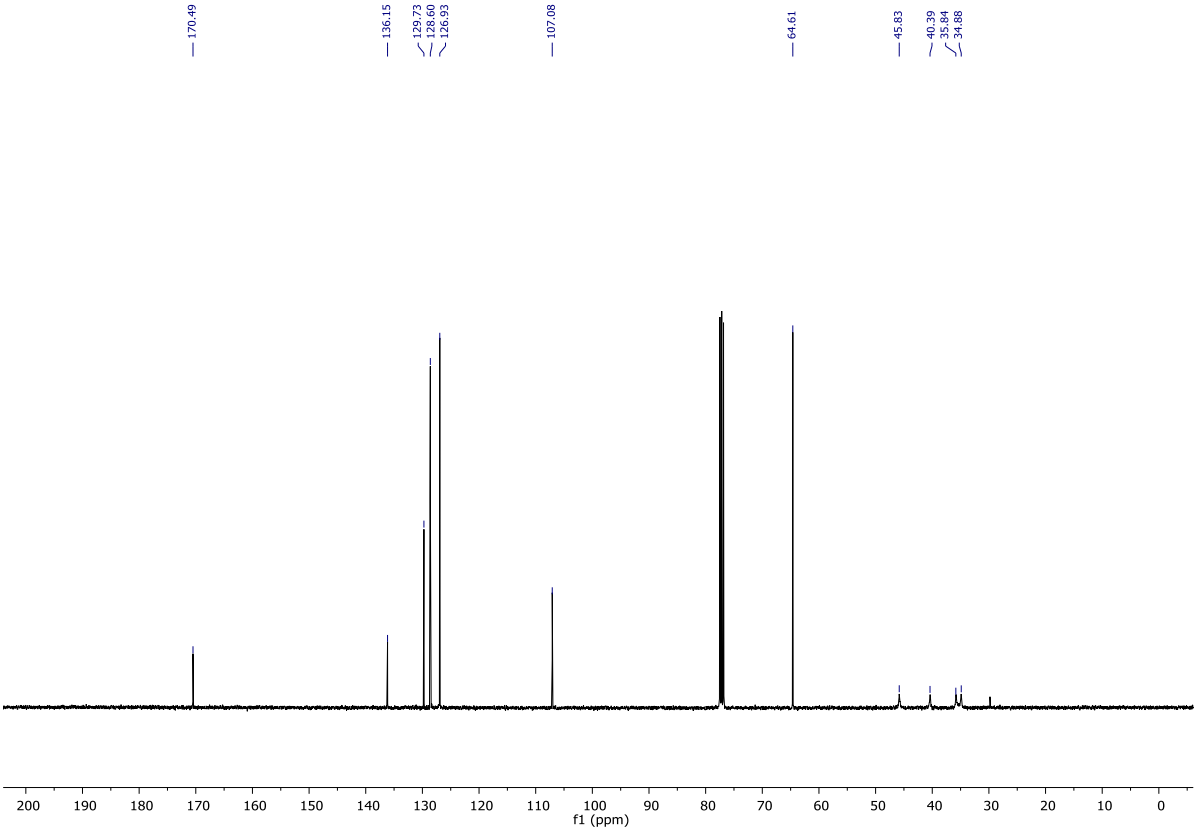

N,N-dibutylbenzamide (**3.37**). $CDCl_3$, 400 MHz:

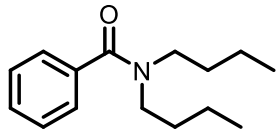

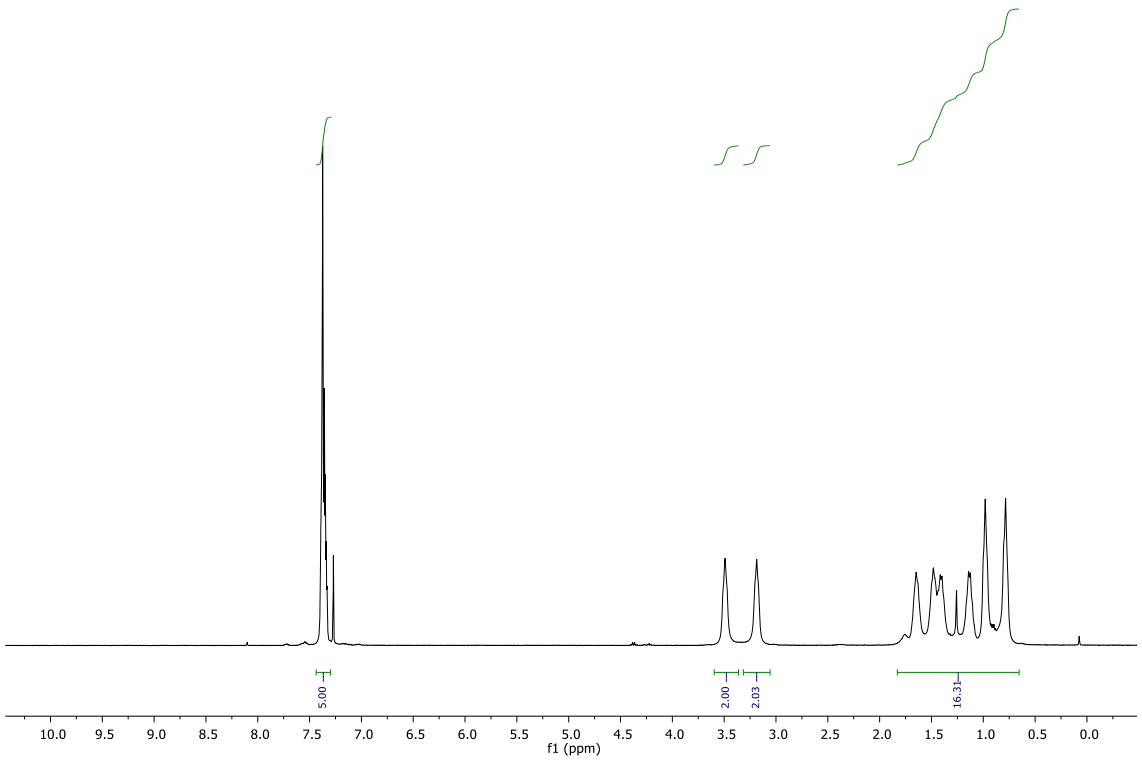

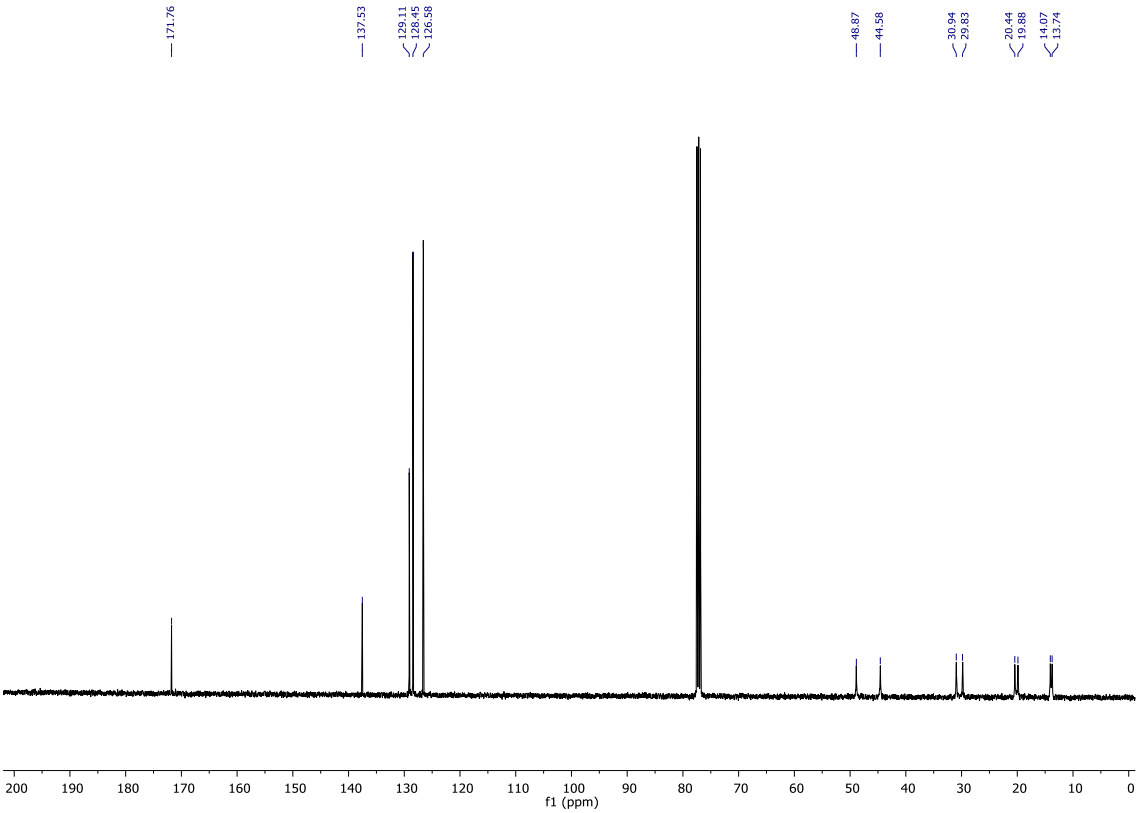

N-benzylbenzamide (**3.39**). $CDCl_3$, 400 MHz:

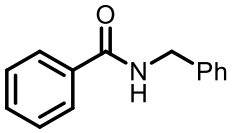

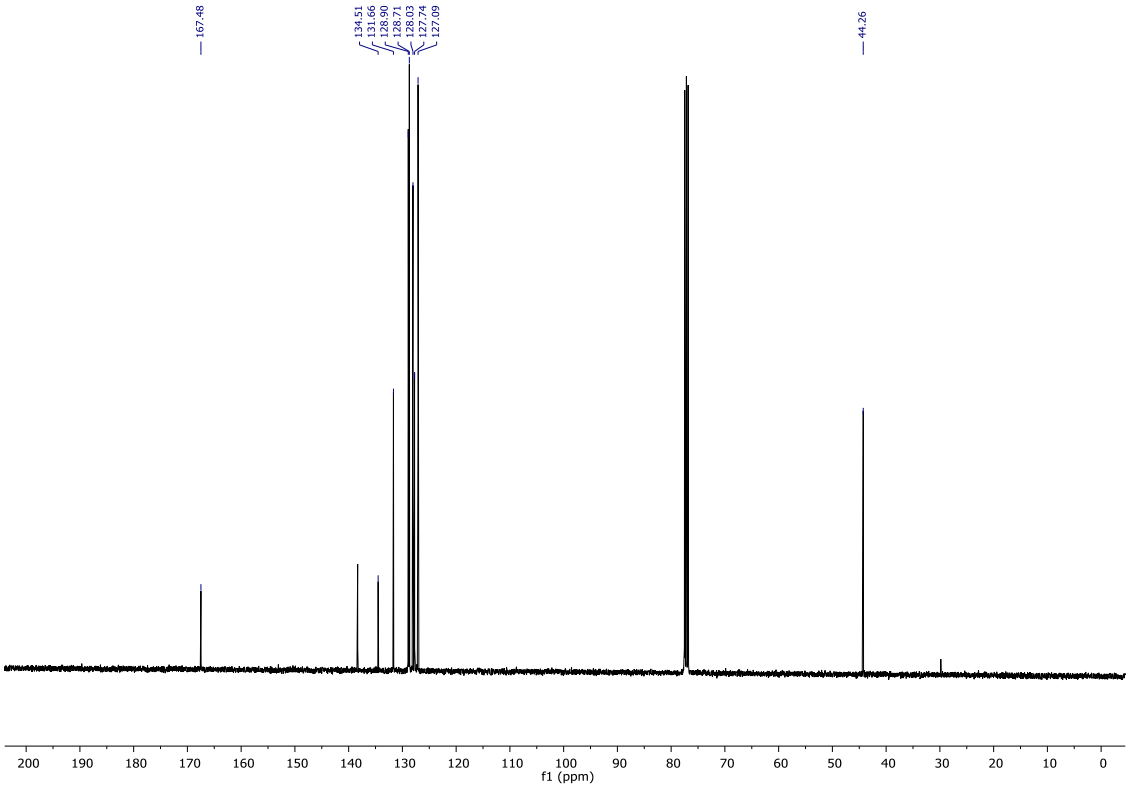

N-cyclopentylbenzamide (**3.41**). $CDCl_3$, 400 MHz:

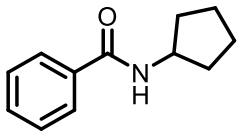

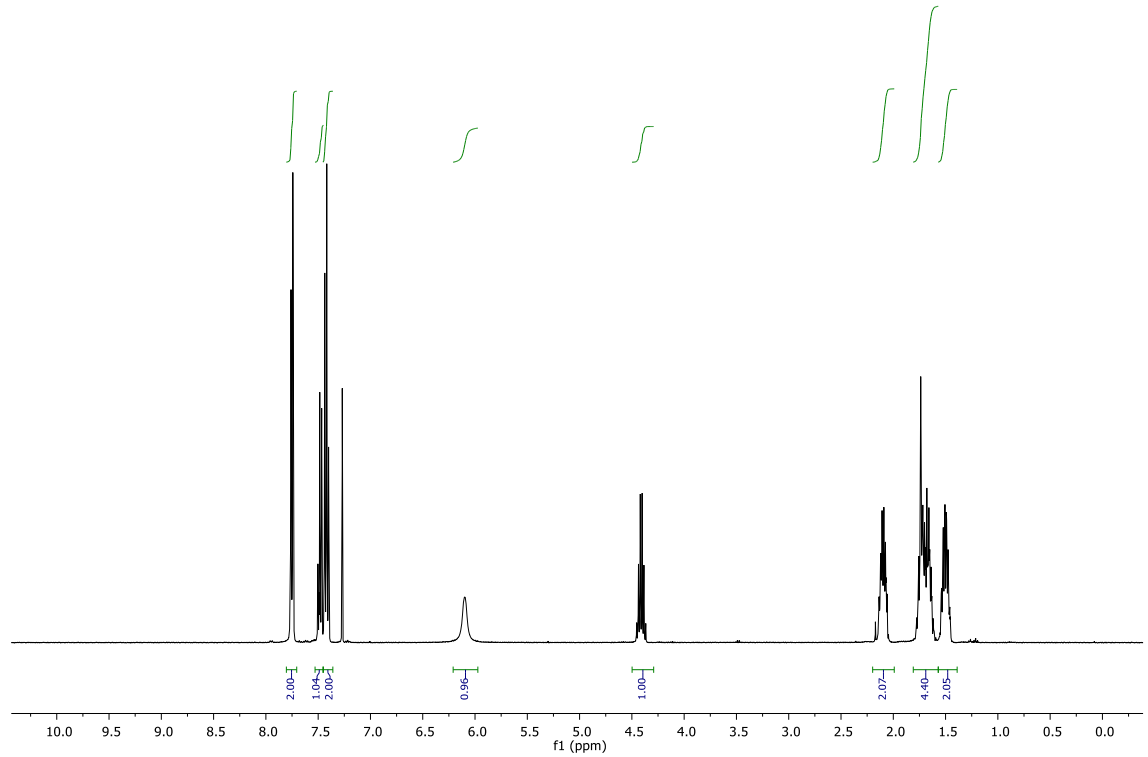

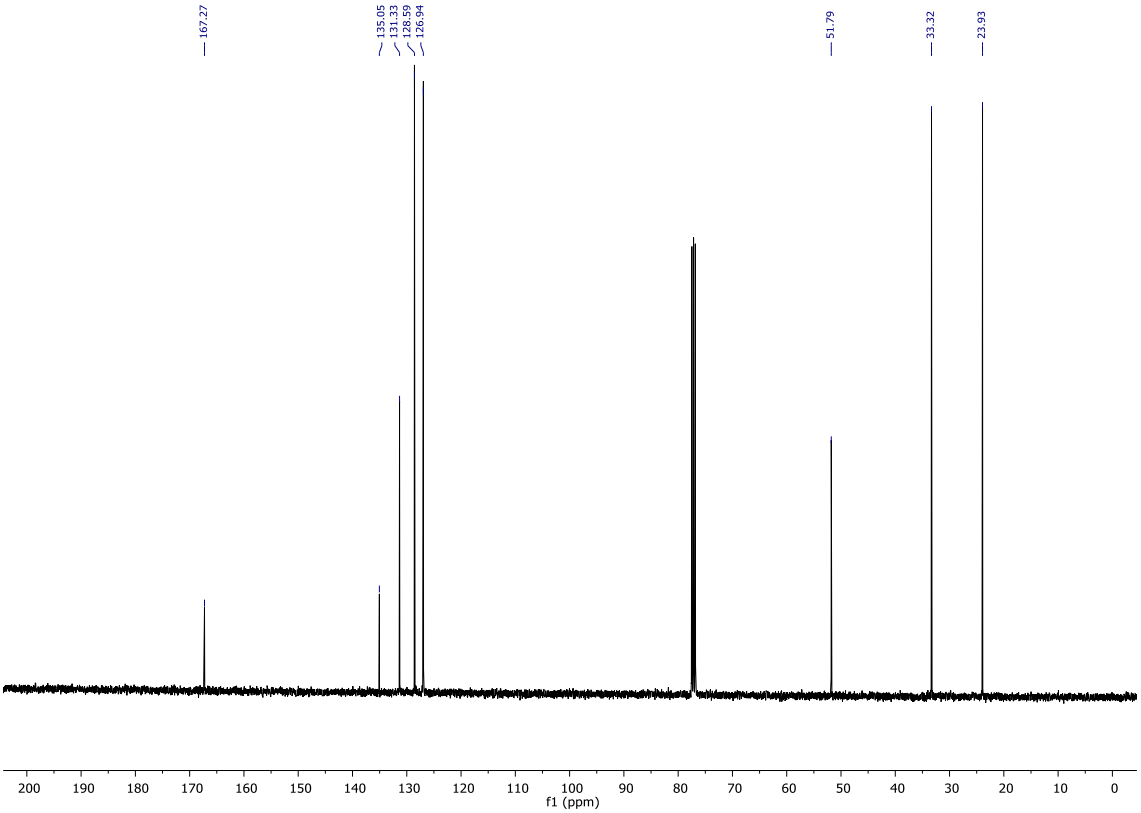

N-((tetrahydrofuran-2-yl)methyl)benzamide (**3.43**). $CDCl_3$, 400 MHz:

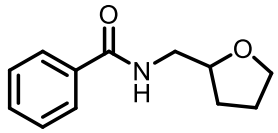

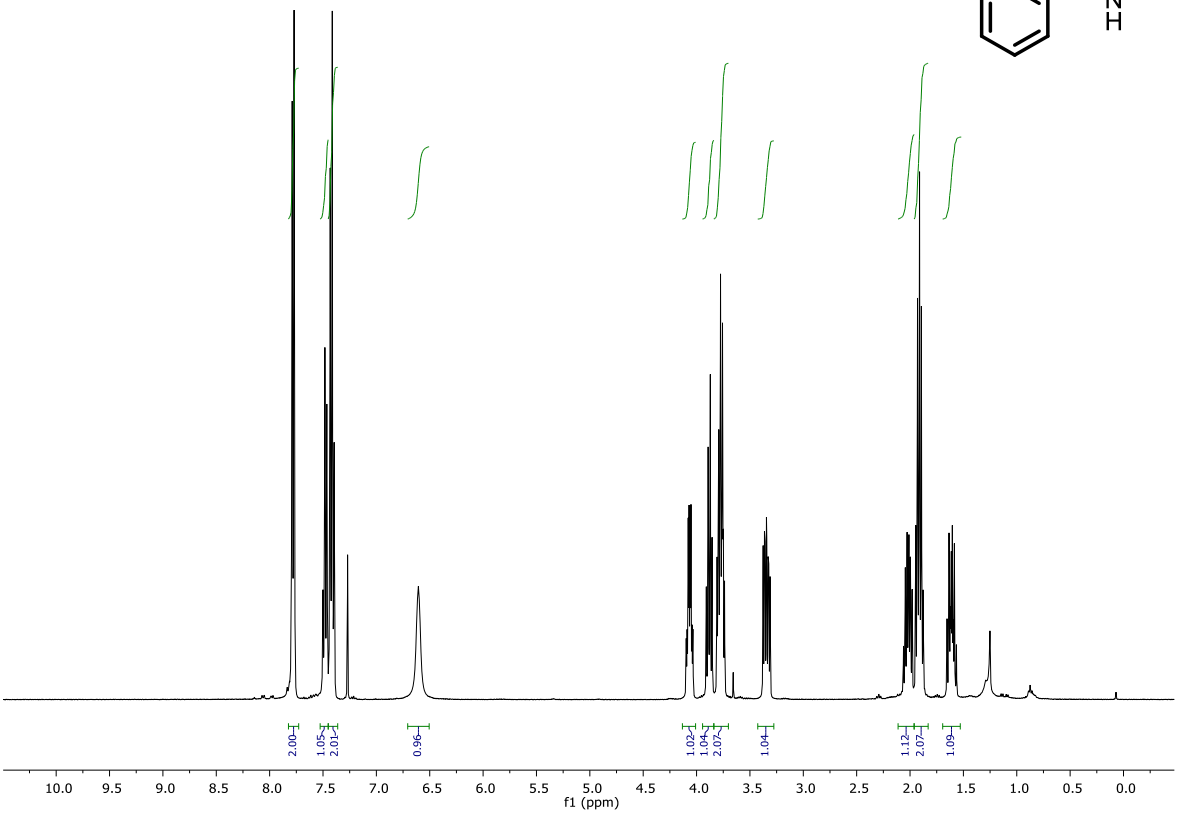

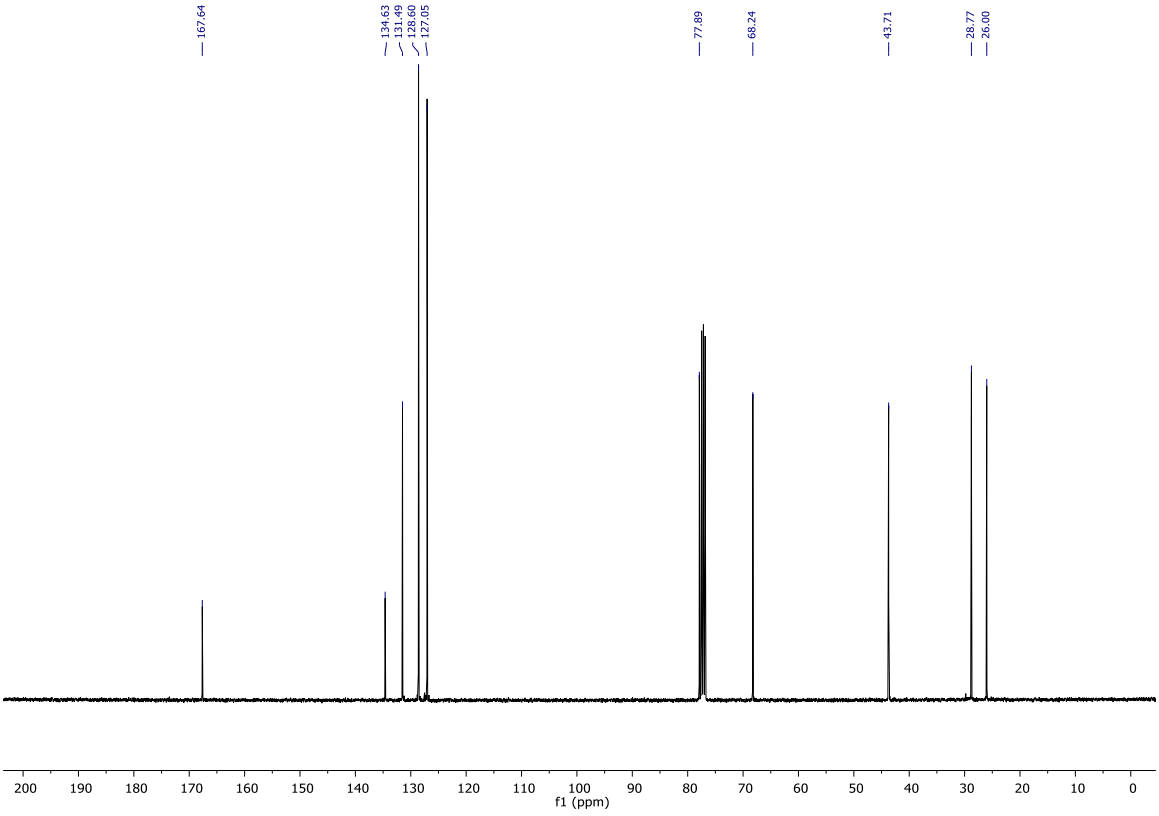

N-phenylbenzamide (**3.45**). $CDCl_3$, 400 MHz:

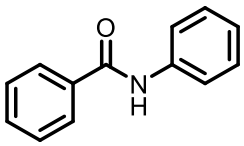

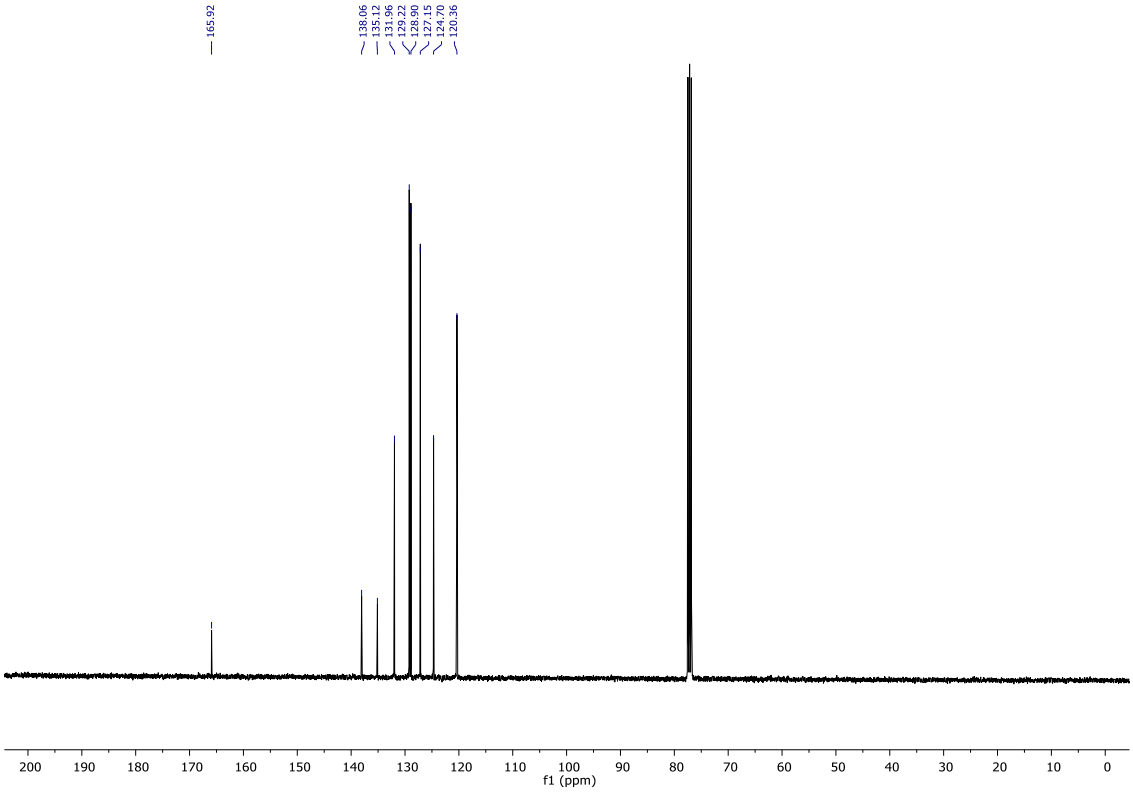

N-([1,1'-biphenyl]-2-yl)benzamide (**3.47**). $CDCl_3$, 400 MHz:

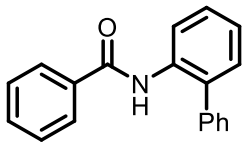

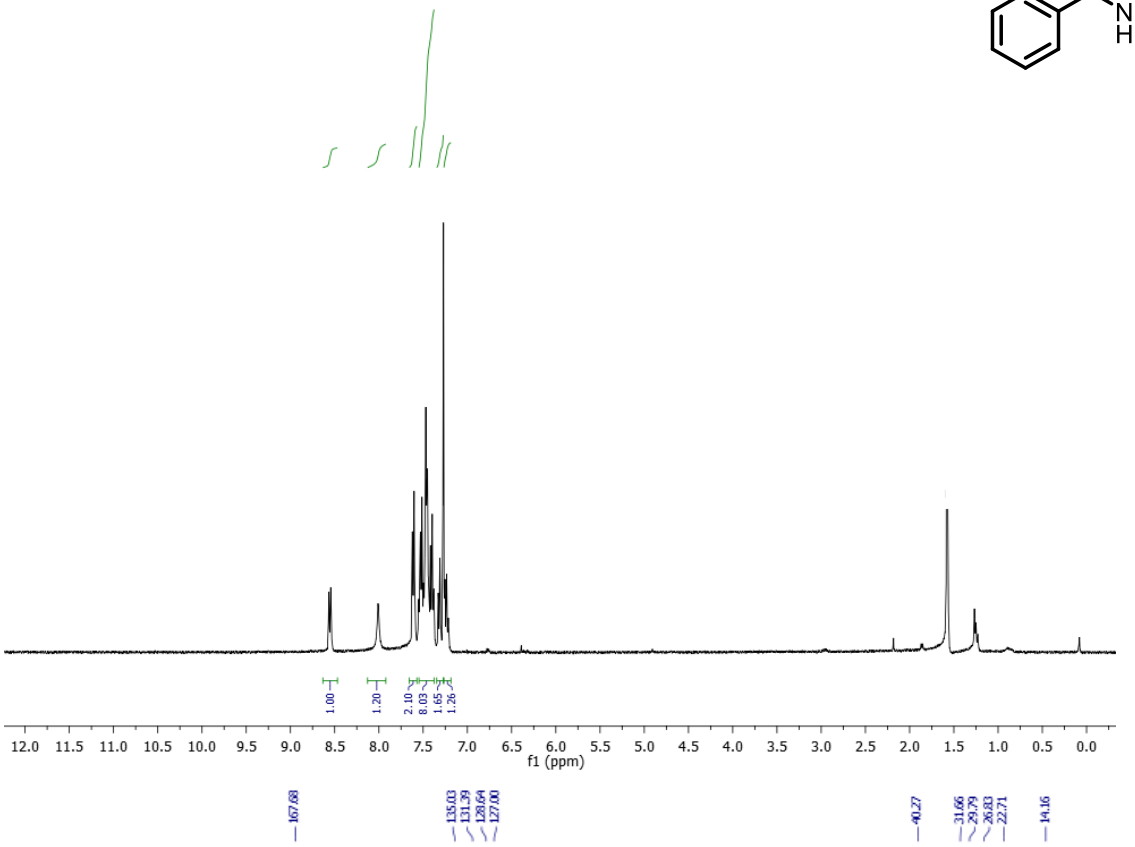

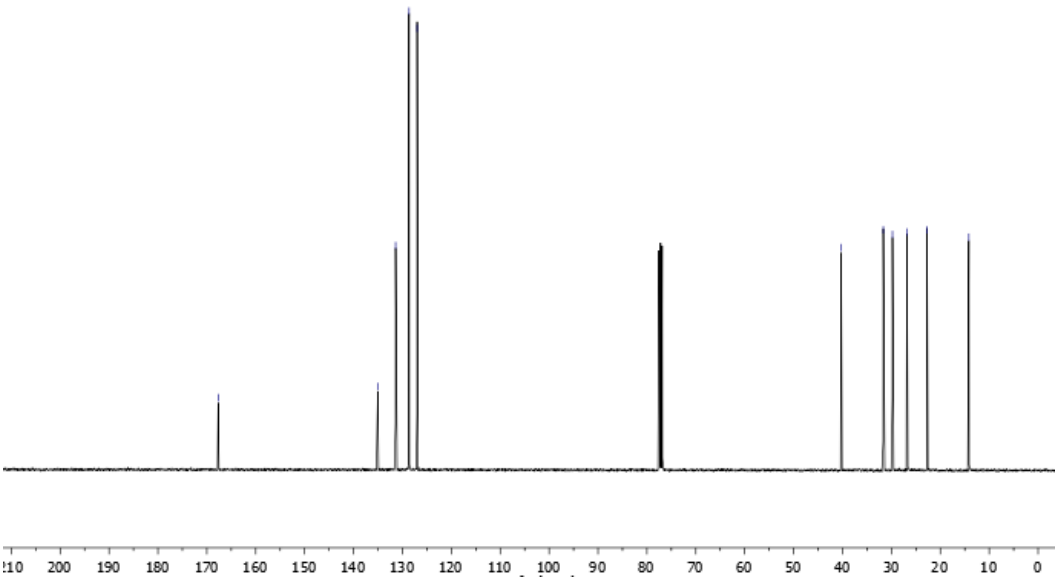

1-(N-benzoyl-sulfanilyl)-piperidine (**3.49**). $CDCl_3$, 400 MHz:

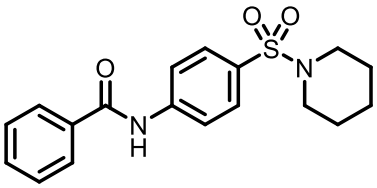

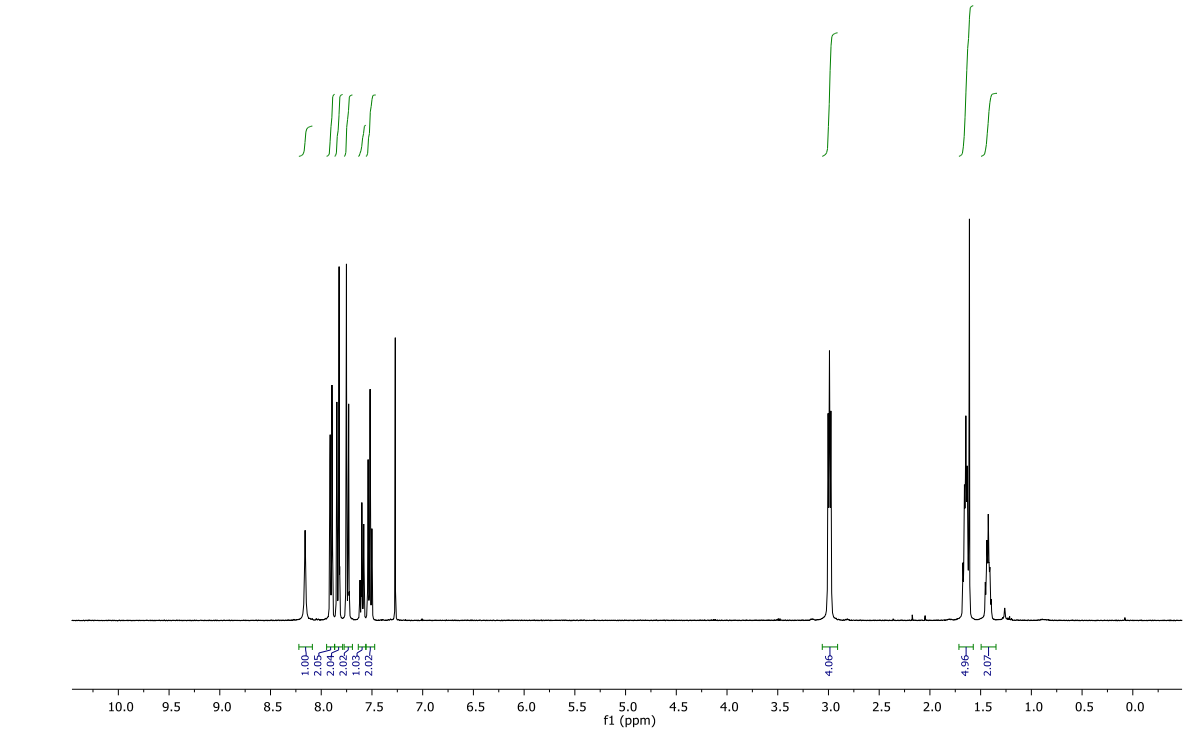

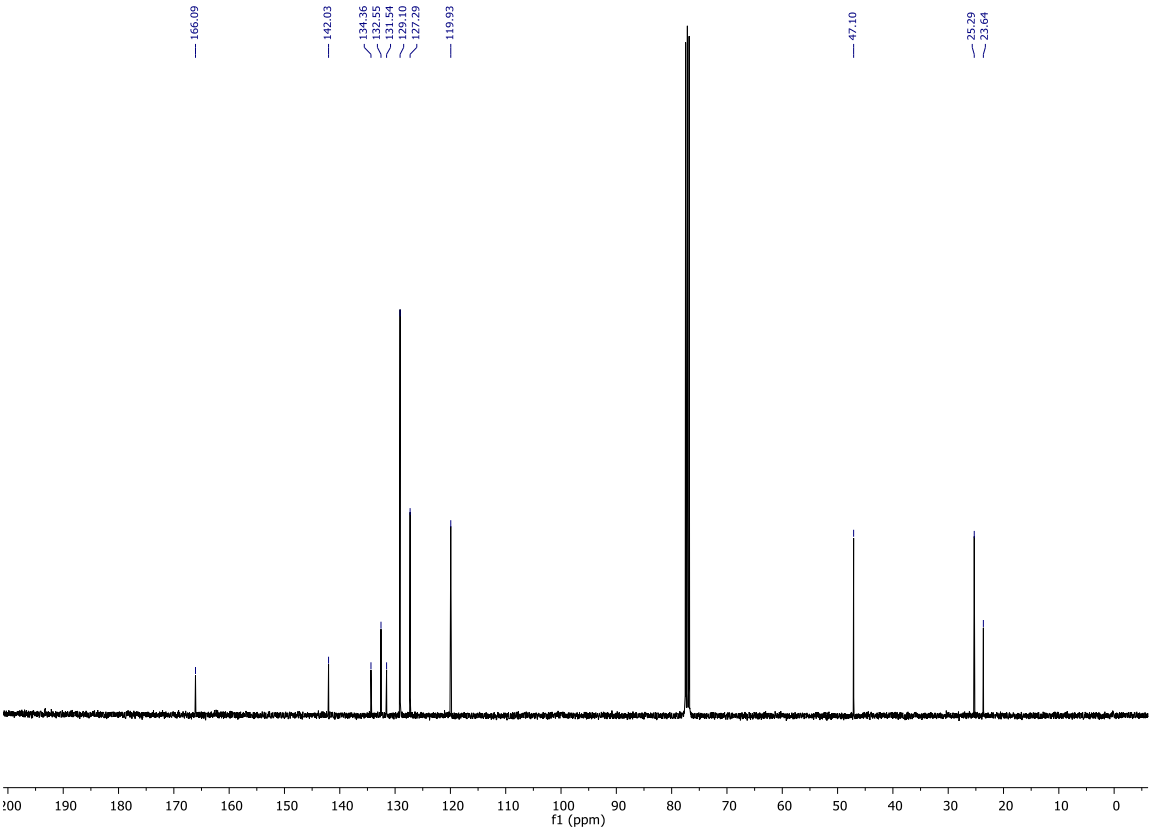

2-diethylamino-N-phenylacetamide (**3.114**) $CDCl_3$, 400 MHz:

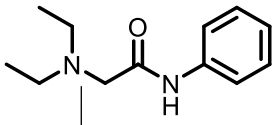

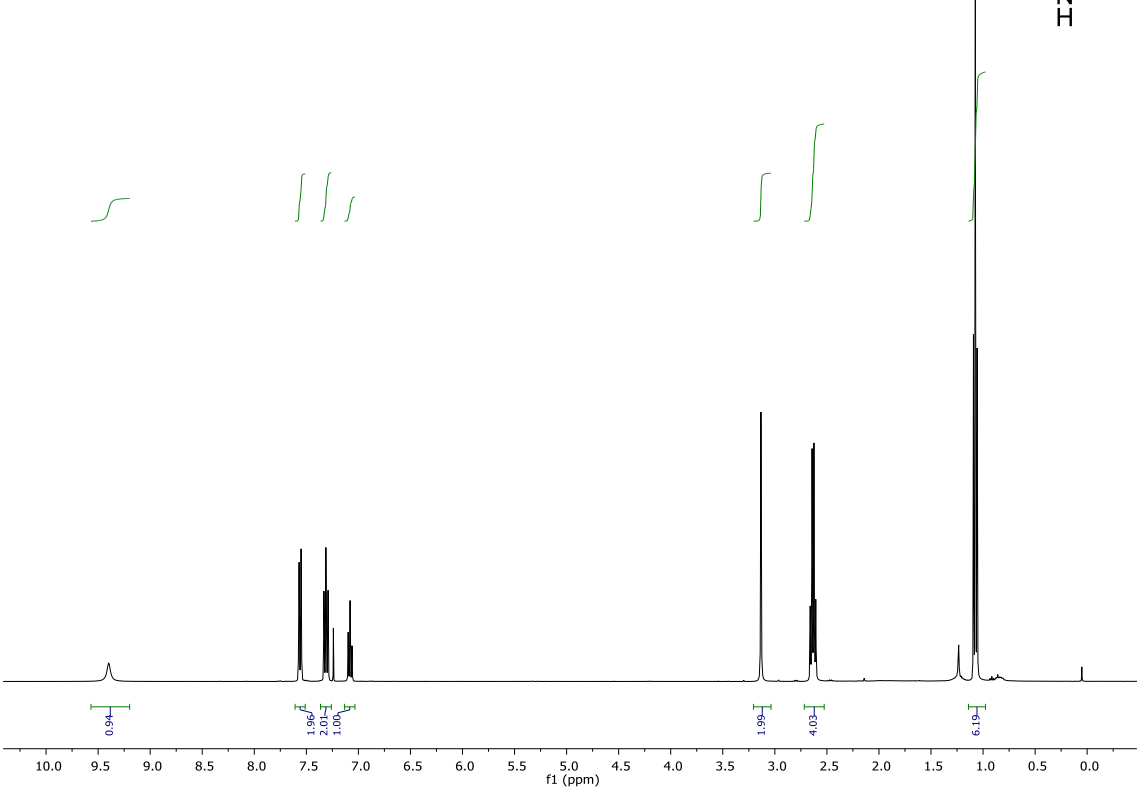

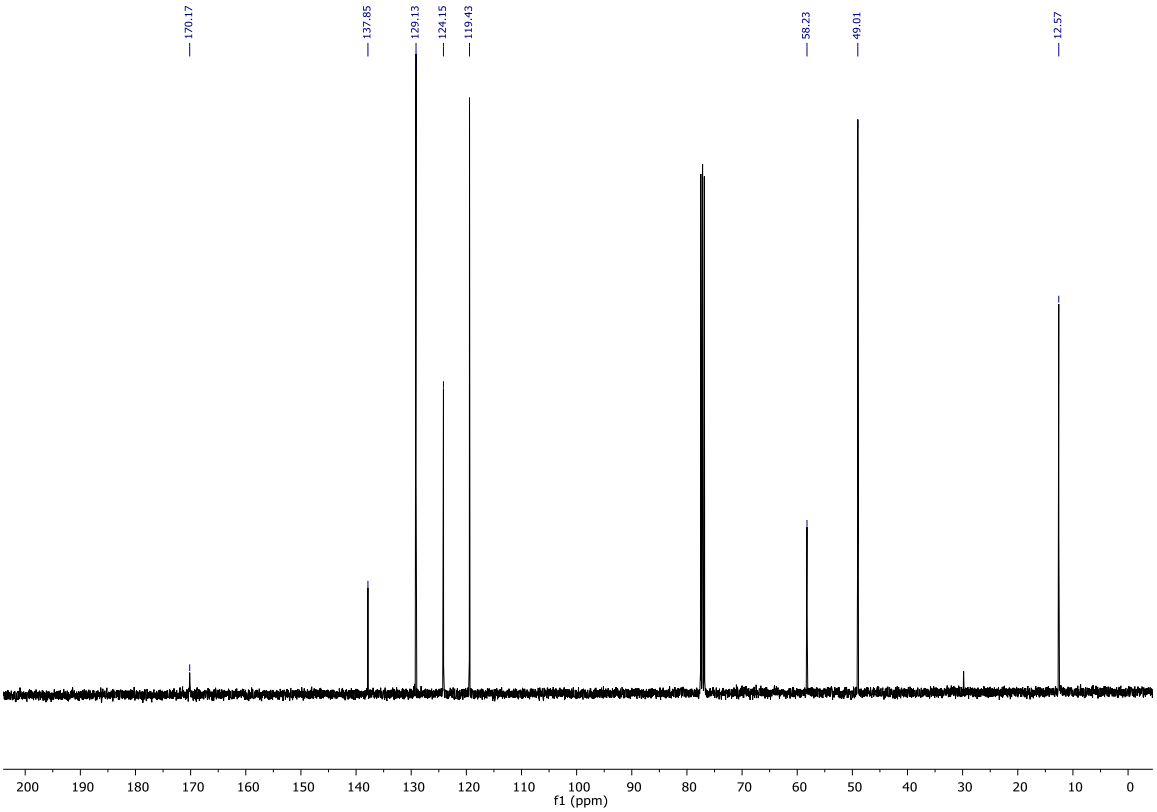

2-(diethylamino)-N-(3,5-dimethyl-phenyl)acetamide (**3.115**) $CDCl_3$, 400 MHz:

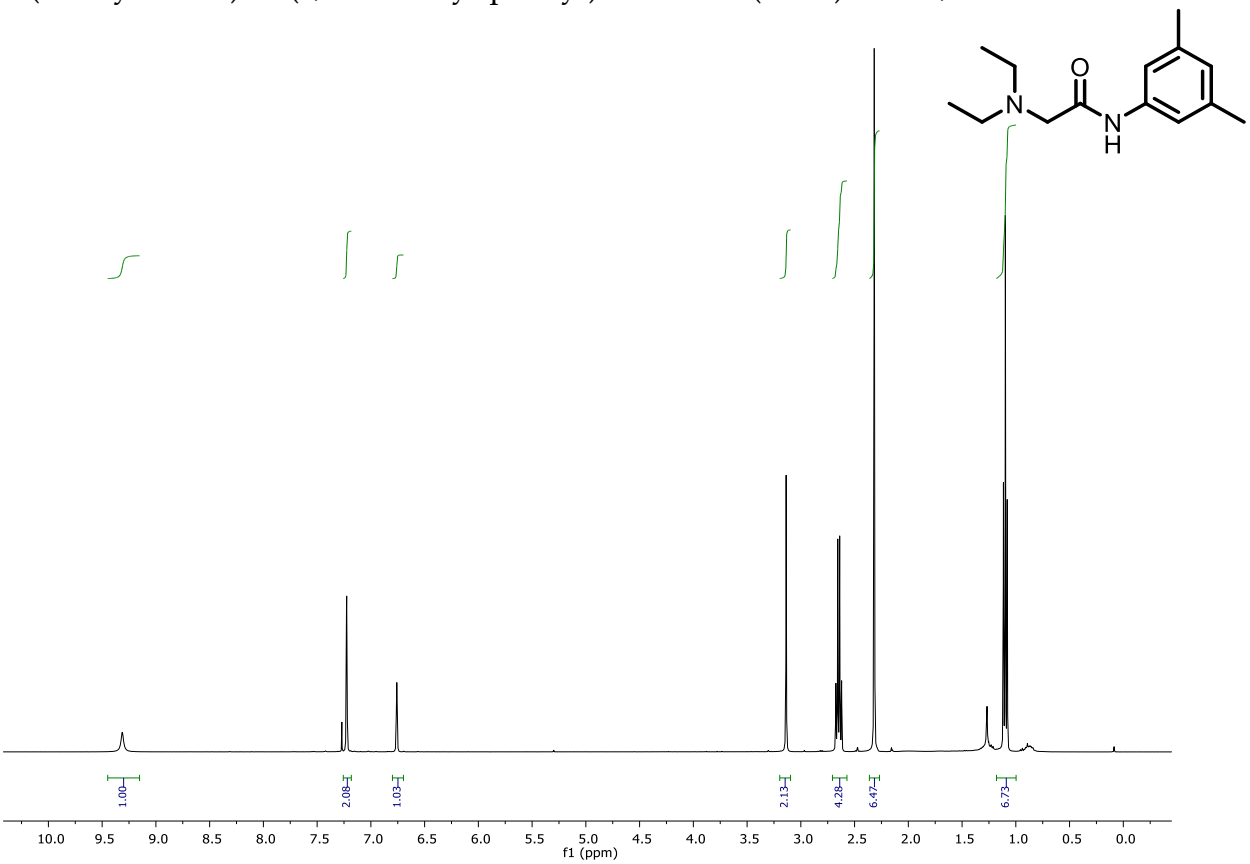

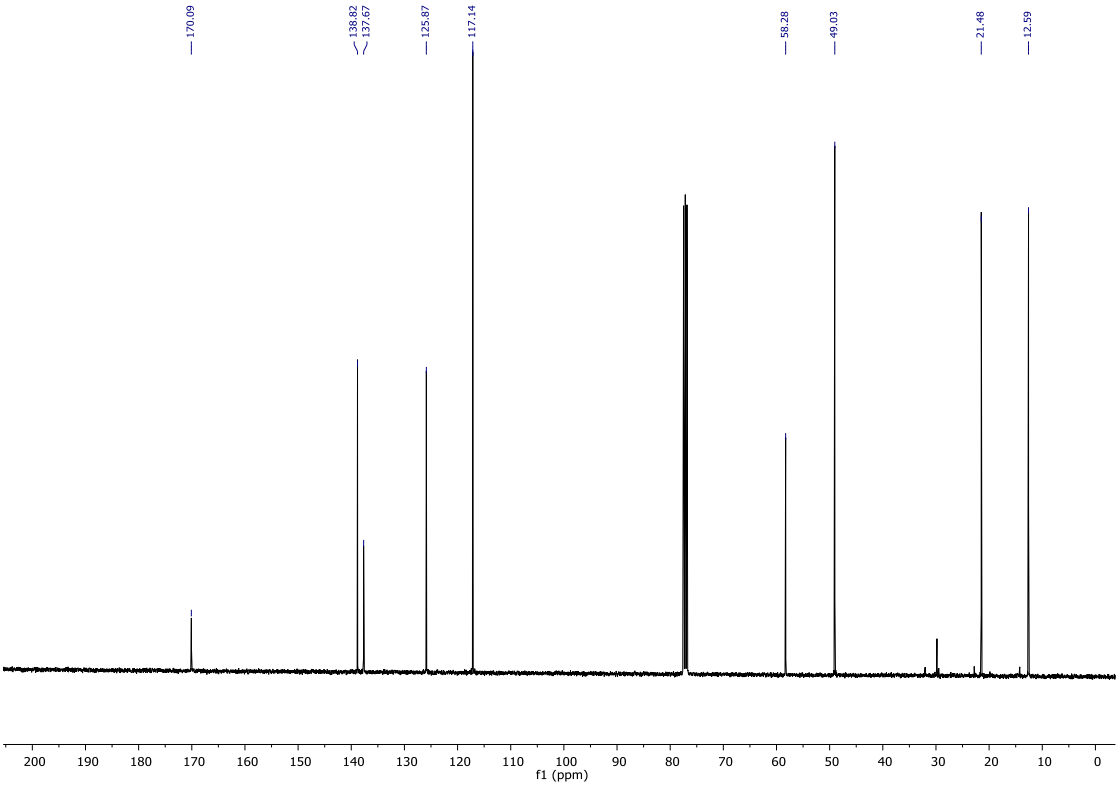

2-(diethylamino)-N-(4-trifluoromethyl-phenyl)acetamide (**3.116**) $CDCl_3$, 400 MHz:

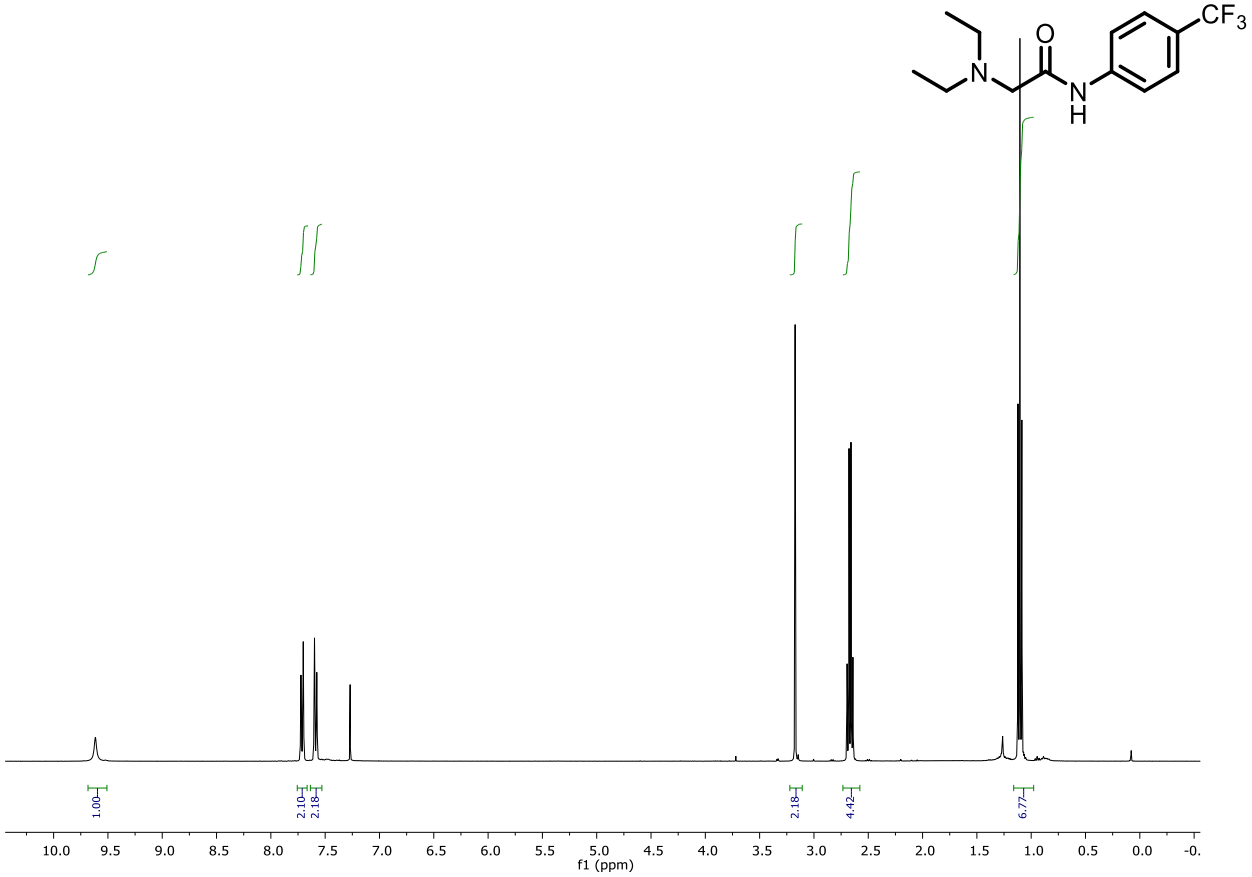

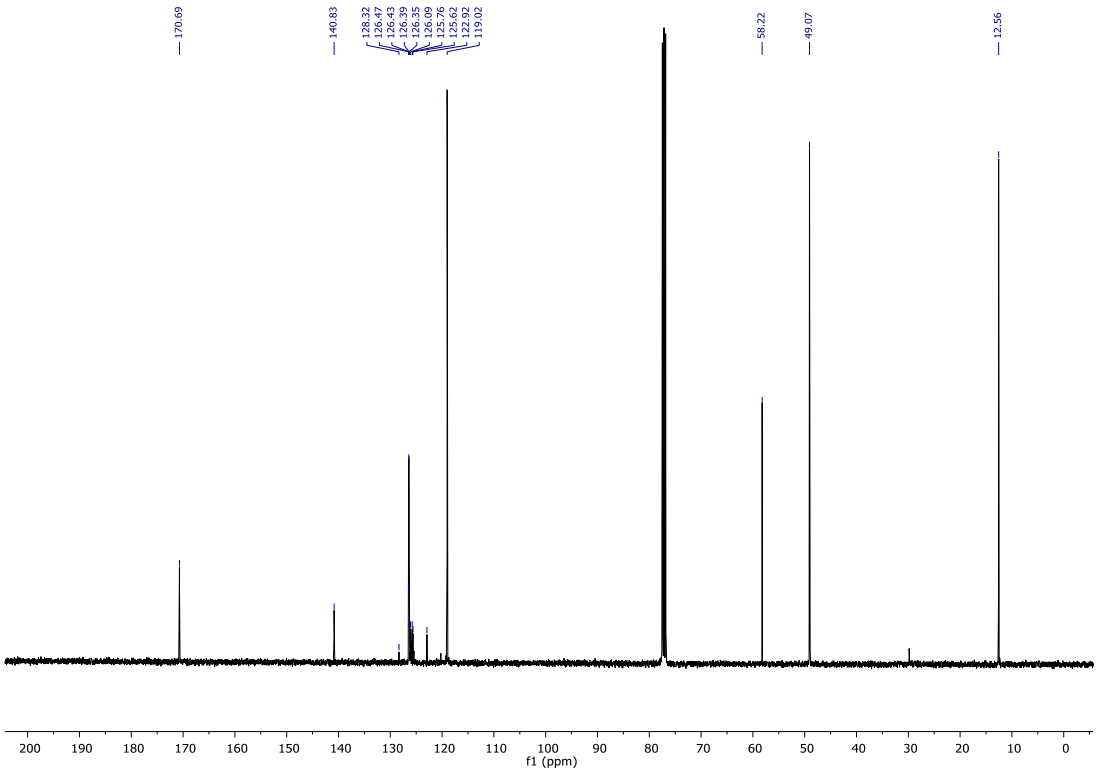

2-(diethylamino)-N-(2,5-dimethyl-phenyl)acetamide (**JM25-1**). $CDCl_3$, 400 MHz:

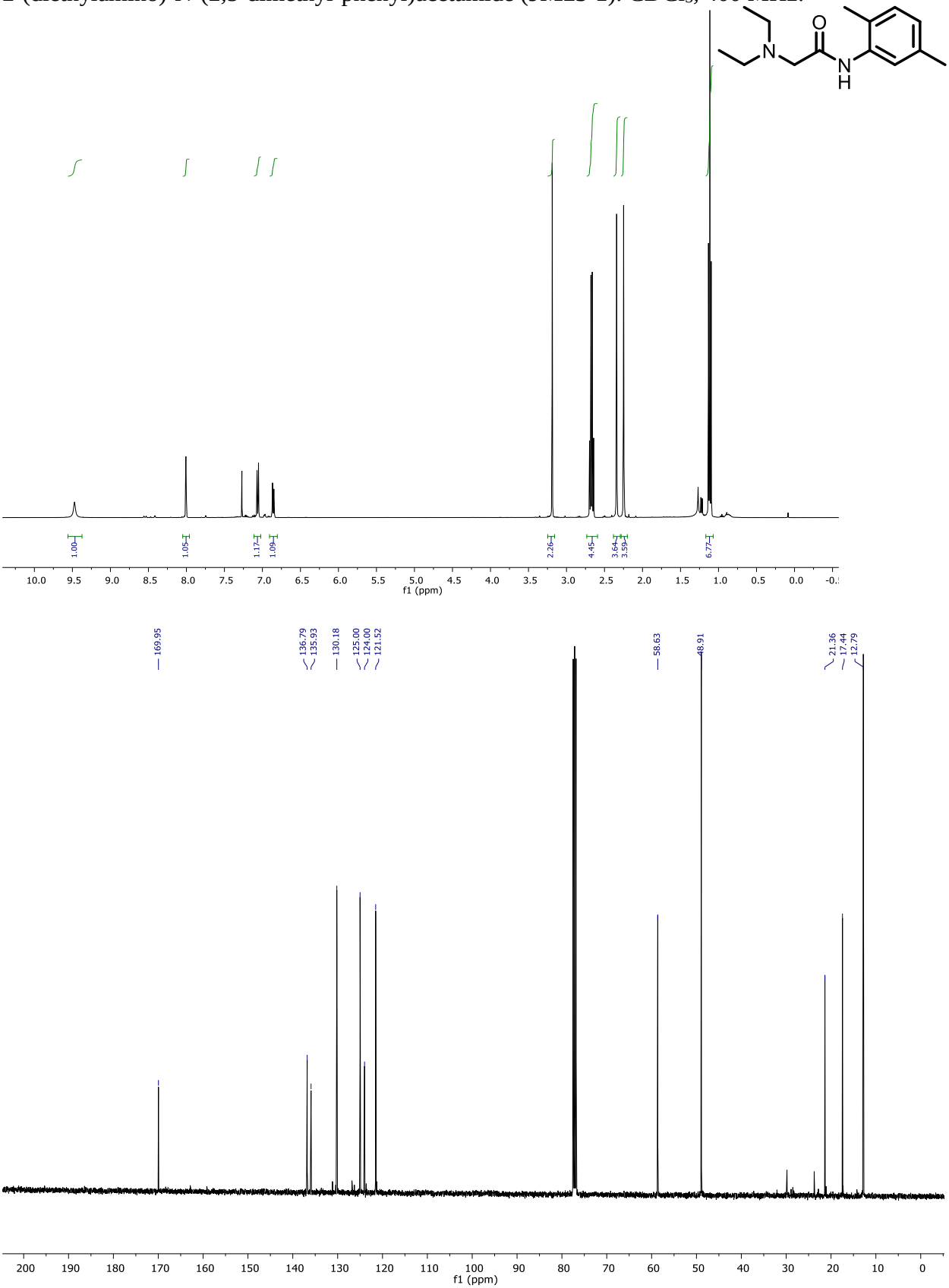

2-(diethylamino)-N-(2,3-dimethyl-phenyl)acetamide (**JM23-1**). $CDCl_3$, 400 MHz:

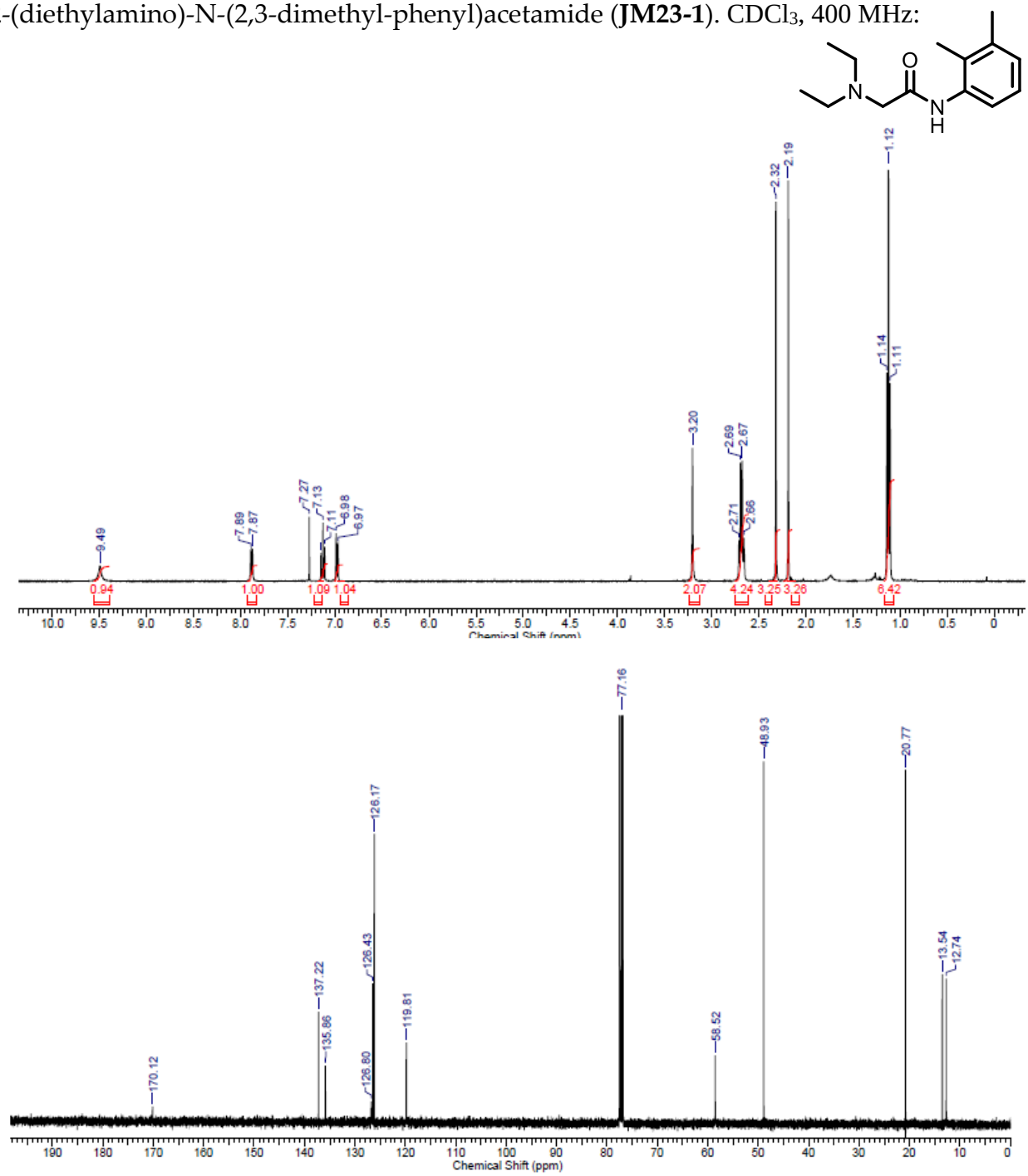

L-menthyl benzoate (**3.132**). $CDCl_3$, 400 MHz:

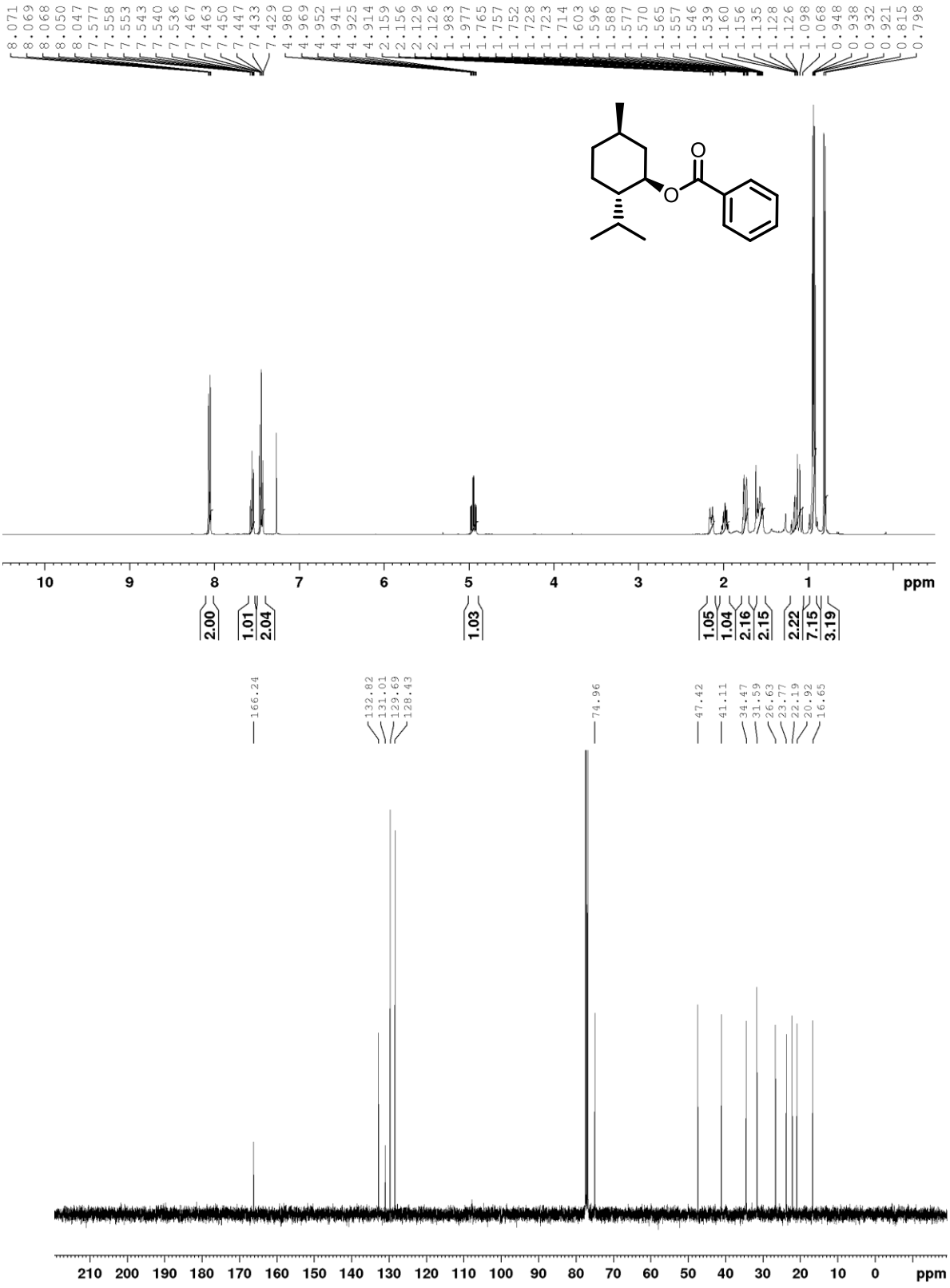

Adamantan-1-ylmethyl 1,5-dimethyl-1H-pyrazole-3-carboxylate (**3.147**). $CDCl_3$, 400 MHz:

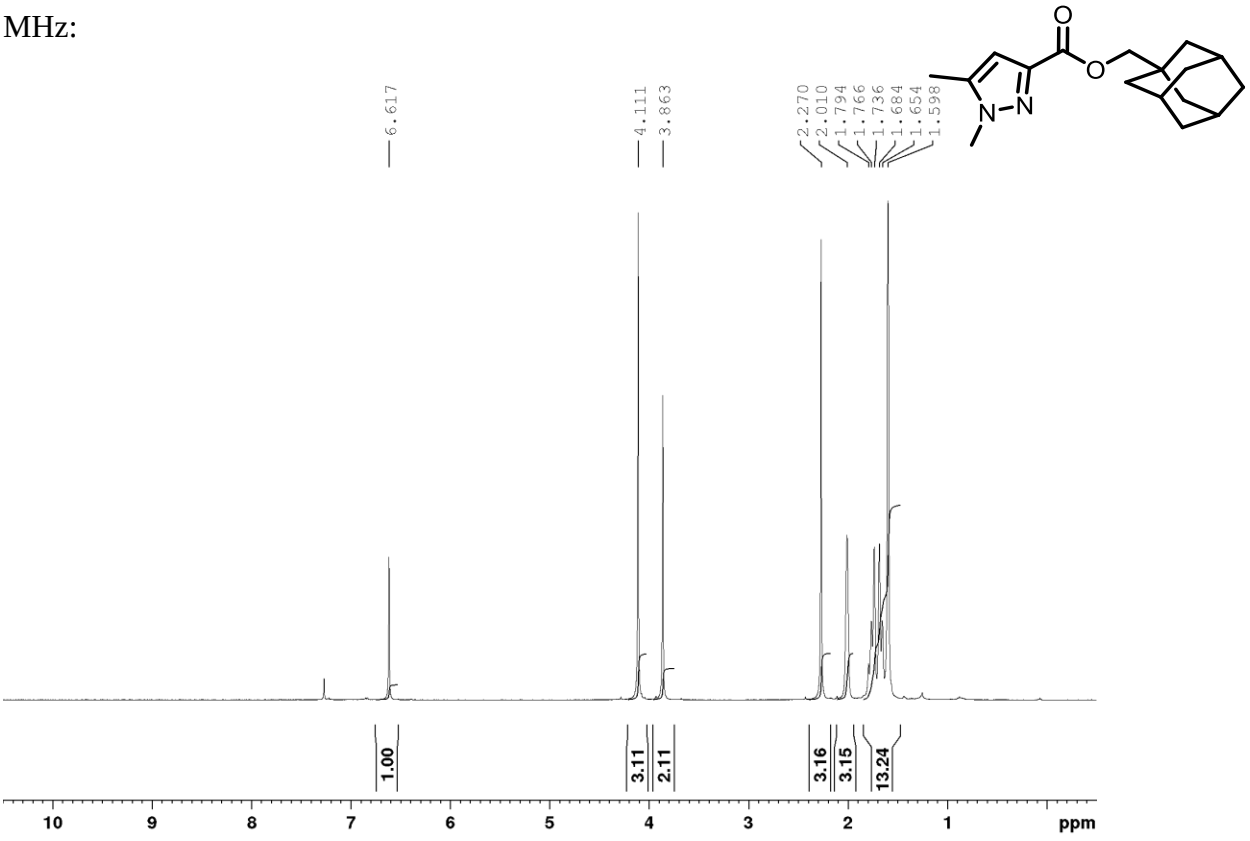

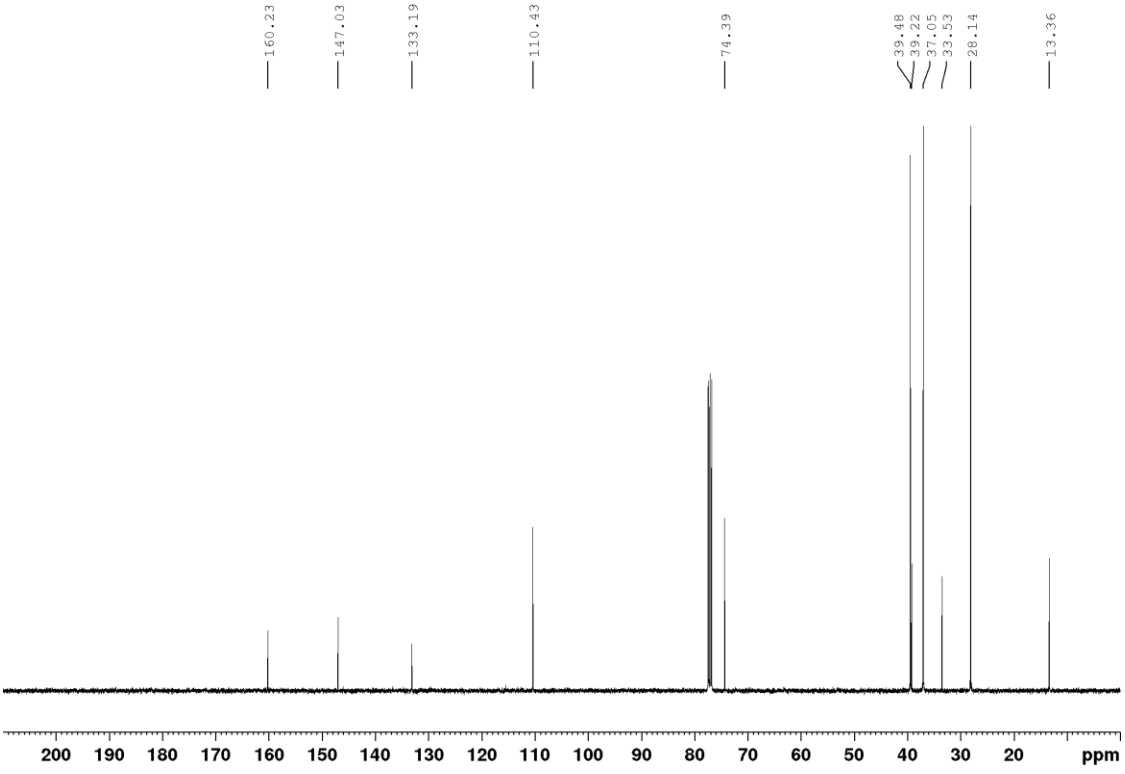

Cyclohexylmethyl 6-methyl-2-oxo-2H-chromene-3-carboxylate (**3.149**). $CDCl_3$, 400 MHz:

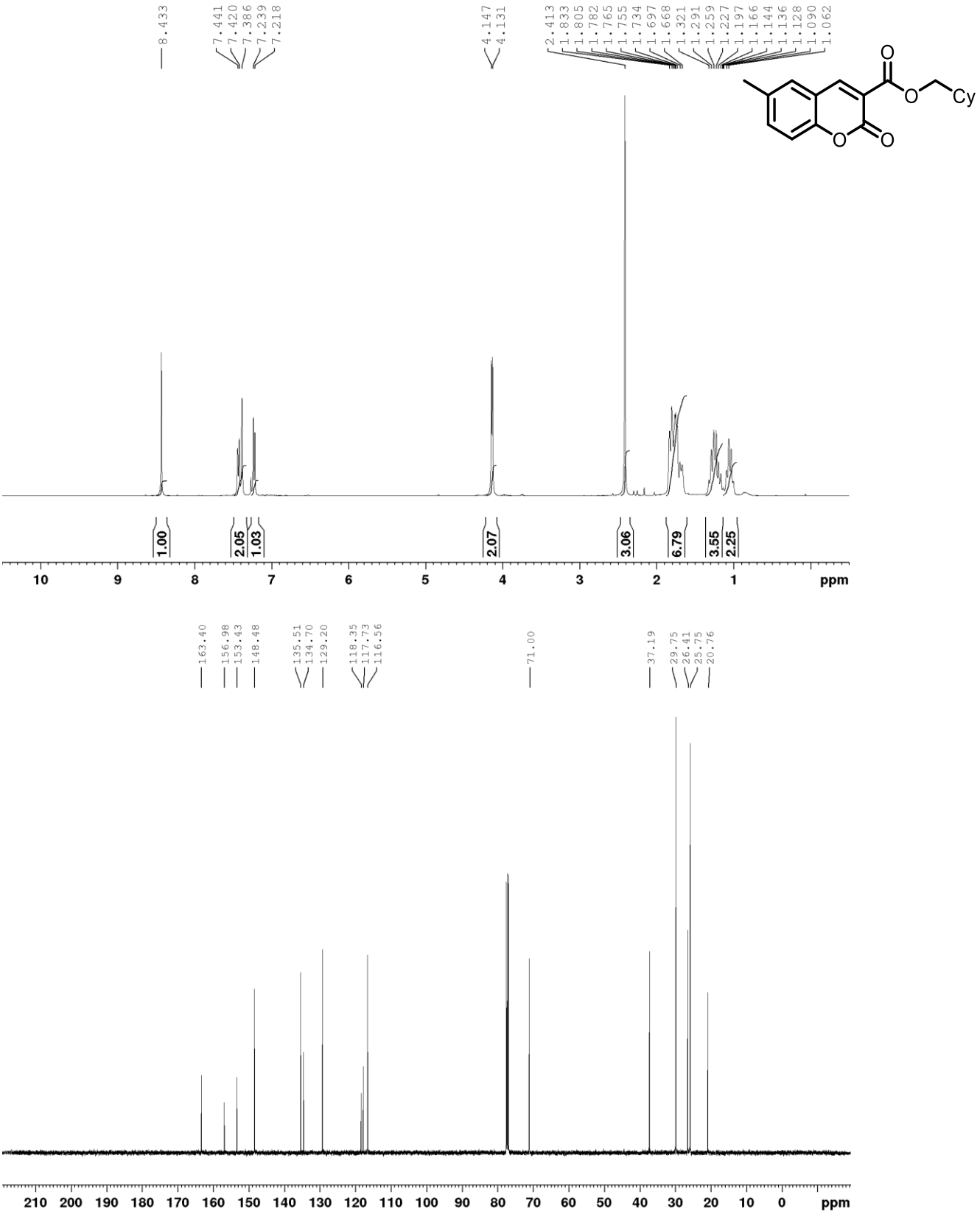

Appendix C: HPLC Traces for Chapter 3

General information: Enantiomeric ratios were determined by separation on a chiral HPLC column. The peaks for major and minor enantiomers were confirmed by comparison with racemic material. The racemate of ester **3.29** was obtained commercially. The racemate of **3.30** was obtained via coupling of aniline with racemic ester **3.29.** A partially racemic sample of **3.32** was obtained via treatment of the corresponding enantiopure material with 3 equivalents of potassium tert-butoxide in THF (0.05 M) for 6 h at 90 °C, followed by quenching with ammonium chloride, extraction with ethyl acetate, and evaporation of the solvent *in vacuo*.

Compound: (S)-methyl tetrahydrofuran-2-carboxylate (**3.29**)
Method: Chiralcel AD-H, 1.5% IPA in hexanes, 0.80 mL/min, 230 nm.

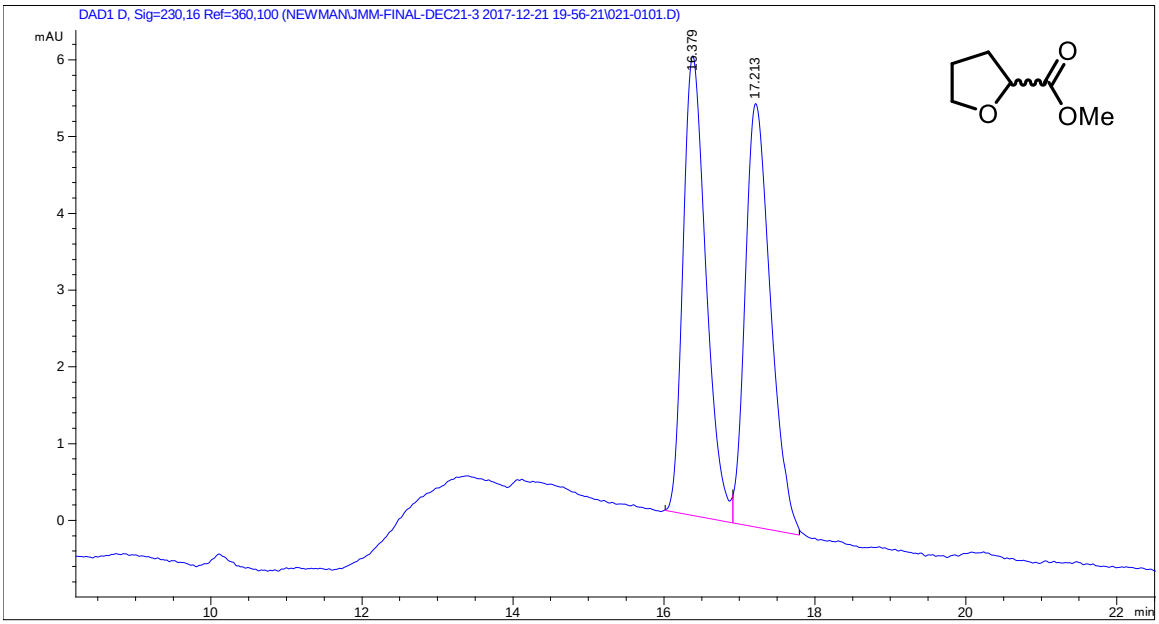

#	Time	Area	Height	Width	Area%	Symmetry
1	16.379	127.4	6	0.3242	49.595	0.683
2	17.213	129.5	5.5	0.3597	50.405	0.663

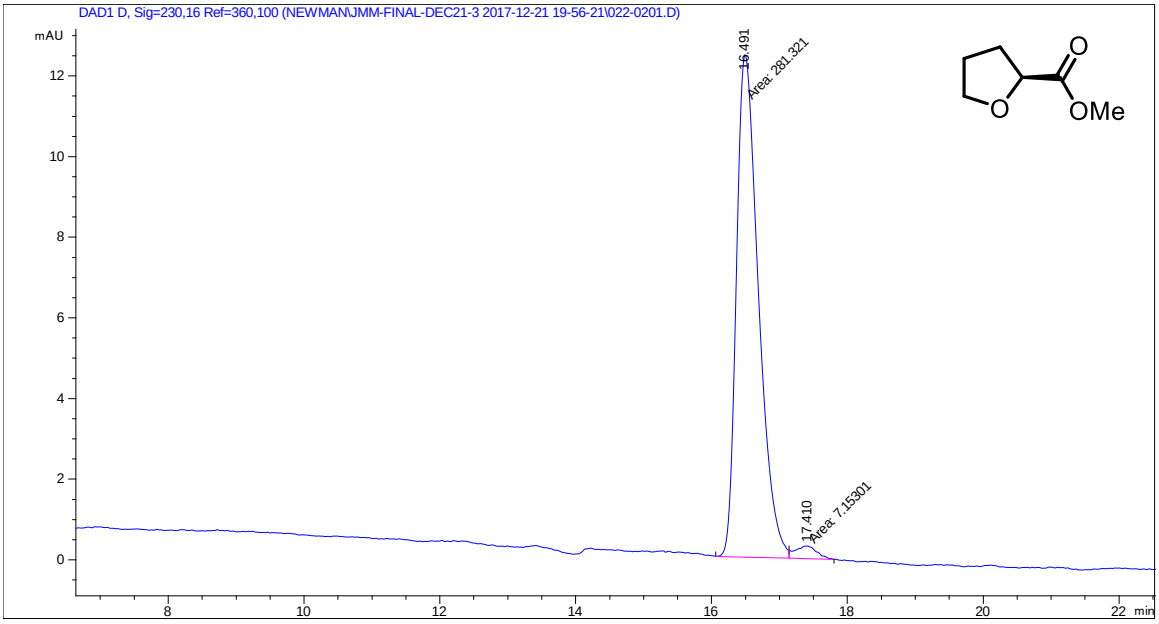

#	Time	Area	Height	Width	Area%	Symmetry
1	16.491	281.3	12.5	0.376	97.520	0.622
2	17.41	7.2	3.2E-1	0.3438	2.480	0.222

Compound: (S)-N-phenyloxolane-2-carboxamide (**3.30**)

Method: Chiracel AD-H, 2% → 5% IPA in hexanes, 1.0 mL/min, 254 nm.

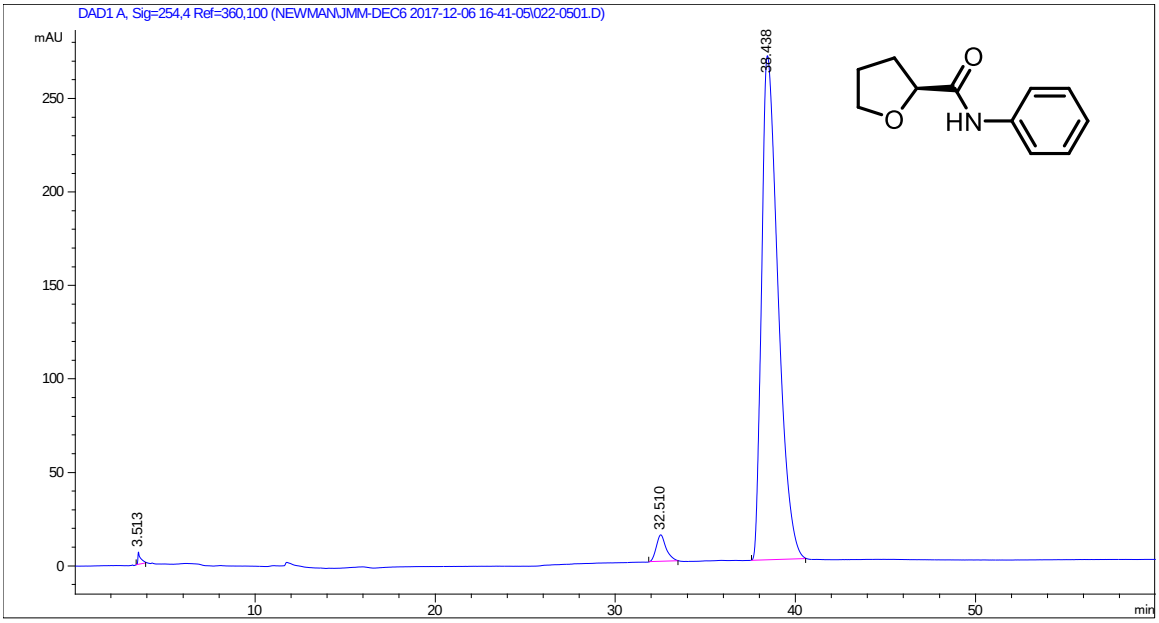

#	Time	Area	Height	Width	Area%	Symmetry
1	32.51	551.7	14.3	0.5585	3.109	0.753
2	38.438	17191.9	269.7	0.9536	96.891	0.51

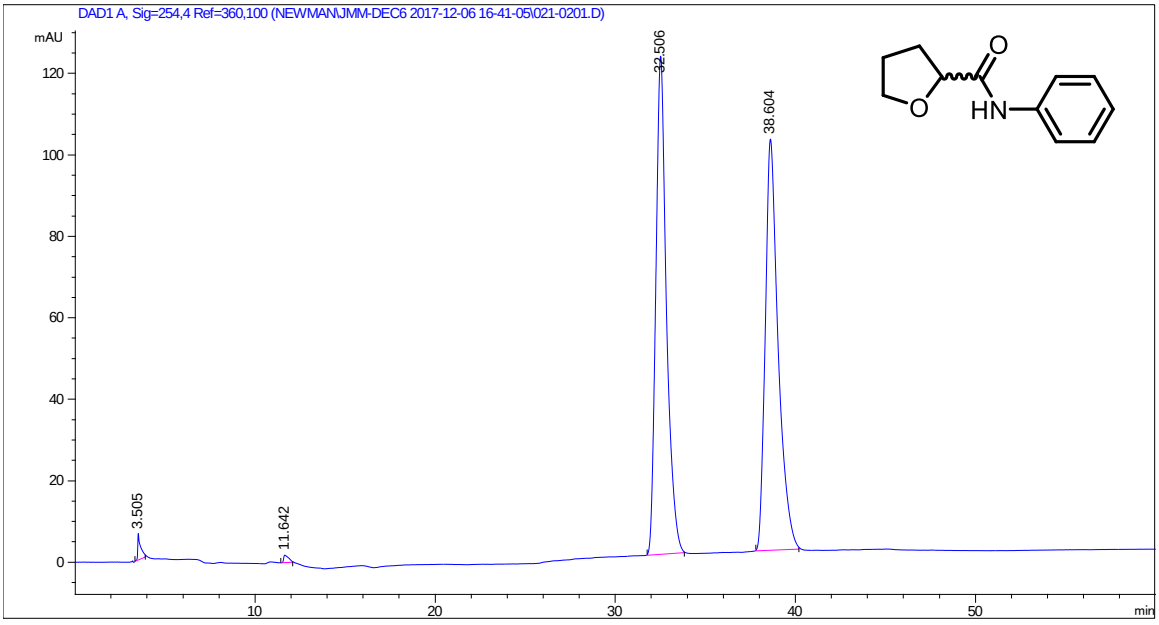

#	Time	Area	Height	Width	Area%	Symmetry
1	32.506	5017.5	122.3	0.6025	50.015	0.752
2	38.604	5014.5	101	0.7134	49.985	0.622

Compound: (S)-1-benzyl-N-phenylpyrrolidine-2-carboxamide (**3.32**)
Method: Chiracel AD-H, 7% IPA in hexanes, 1.0 mL/min flow rate, 254 nm.

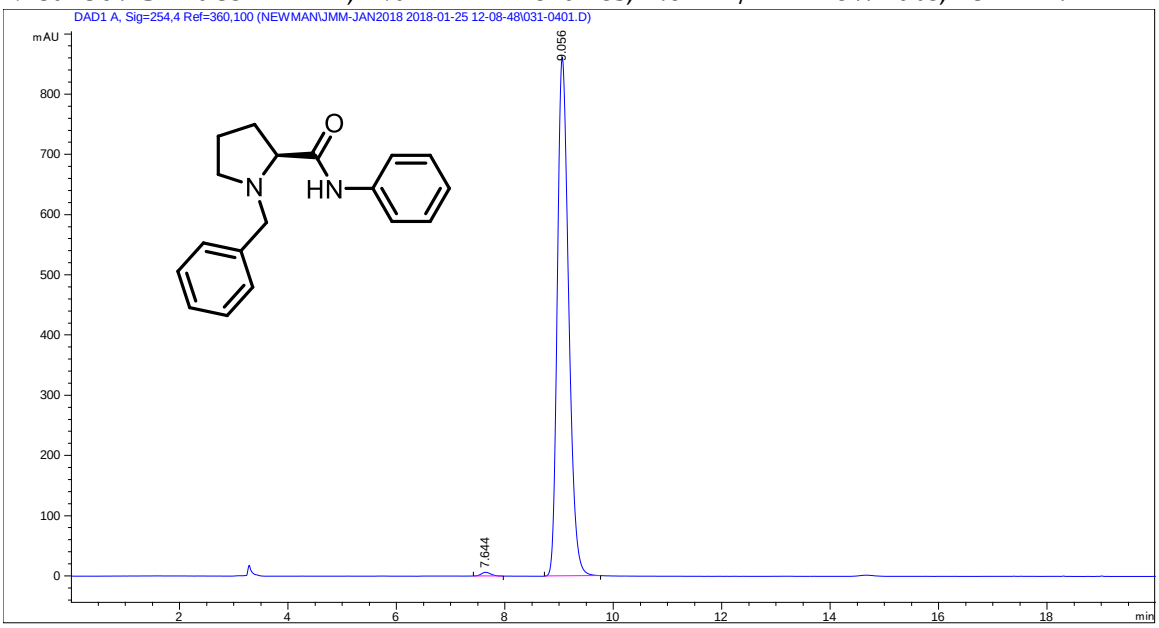

#	Time	Area	Height	Width	Area%	Symmetry
1	7.644	78.8	6.3	0.1899	0.625	0.826
2	9.056	12523.1	861.3	0.2256	99.375	0.718

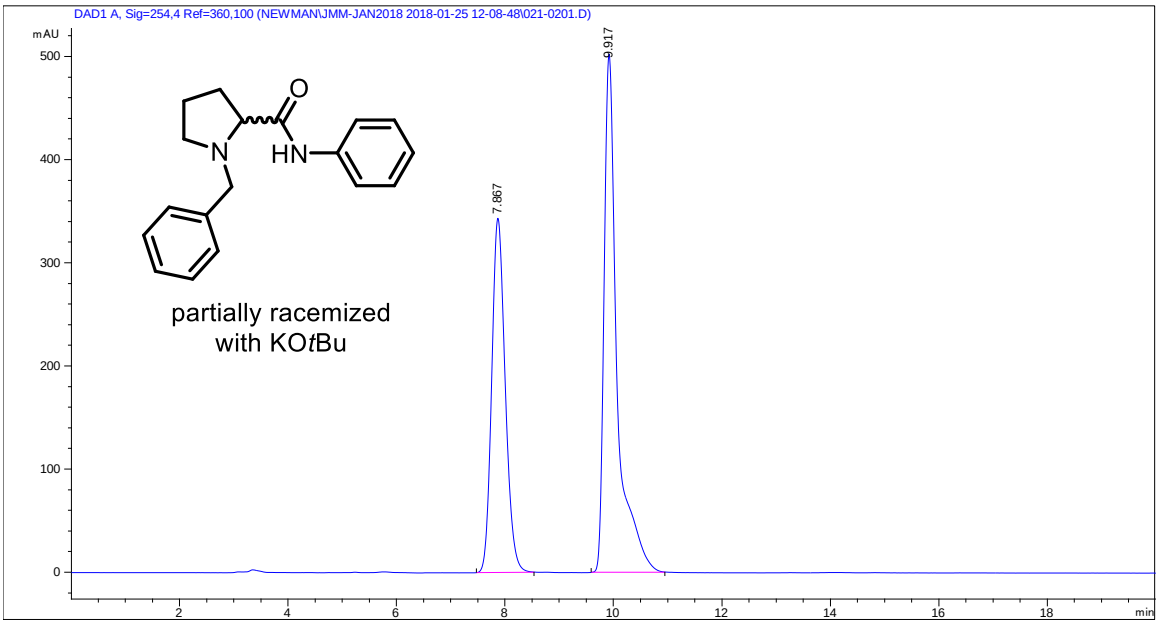

#	Time	Area	Height	Width	Area%	Symmetry
1	7.867	5960.4	343.6	0.2664	41.599	0.801
2	9.917	8367.8	502.6	0.2462	58.401	0.544